INFORMATION TO USERS

University of Alberta

Inhibition of Protein Phosphatase-1
by Endogenous Inhibitor Proteins and
Natural Product Toxins

by

Tara Lyn McCready

©

A thesis submitted to the Faculty of Graduate Studies and Research in partial fulfillment

of the requirements for the degree of Doctor of Philosophy

Department of Biochemistry

Edmonton, Alberta

Fall 1999

Co-author Permission Form

As senior author on all papers listed below, and as supervisor of all of the research presented therein, I, Dr. Charles F. B. Holmes, hereby grant permission to Tara Lyn McCready to use material from:

McCready, T.L., Craig, M., Bagu, J.R., Sykes, B.D., Semchuk, P., Hodges, R.S., and Holmes, C.F.B. Functional Modification of Inhibitor-1 and Identification of Essential Arginine Residues Required for Inhibition of Protein Phosphatase-1. *J. Biol. Chem.* (1999) (submitted).

McCready, T.L., Islam, B.F., Schmitz, F.J., Luu, H.A., Dawson, J.F., and Holmes, C.F.B. Inhibition of Protein Phosphatase-1 by Clavosines A and B; Novel Members of the Calyculin Family of Toxins. *J. Biol. Chem.* (1999). (submitted).

Craig, M., McCready, T.L., Luu, H.A., Smillie, M.A., Dubord, P. and Holmes, C.F.B. Identification and characterization of hydrophobic microcystins in Canadian freshwater cyanobacteria. *Toxicon.* 31:1541-1549 (1993).

in her doctoral thesis.

Signed: _Charles B Holmes_

Name   Dr. Charles F. B. Holmes
           Associate Professor
           Department of Biochemistry
           University of Alberta

Date: _9th August 1999_
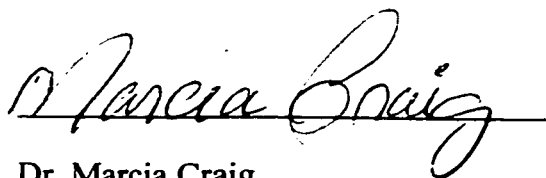
Co-author Permission Form

As senior author of the following paper, I, Dr. Marcia Craig, hereby grant permission to Tara Lyn McCready to use material from:

Craig, M., McCready, T.L., Luu, H.A., Smillie, M.A., Dubord, P. and Holmes, C.F.B. Identification and characterization of hydrophobic microcystins in Canadian freshwater cyanobacteria. *Toxicon.* 31:1541-1549 (1993).

in her doctoral thesis.
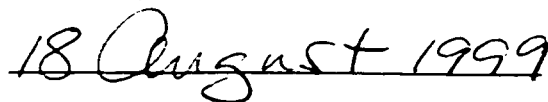
Signed:

Name   Dr. Marcia Craig
Department of Biochemistry
University of Alberta

Date: 18 August 1999

University of Alberta

Library Release Form

Name of Author: Tara Lyn McCready

Title of Thesis: Inhibition of Protein Phosphatase-1 by Endogenous Inhibitor Proteins and Natural Product Toxins.

Degree: Doctor of Philosophy

Year this Degree Granted: 1999

Permission is hereby granted to the University of Alberta Library to reproduce single copies of this thesis and to lend or sell such copies for private, scholarly, or scientific research purposes only.

The author reserves all other publication and other rights in association with the copyright in the thesis, and except as hereinbefore provided, neither the thesis nor any substantial portion thereof may be printed or otherwise reproduced in any material form whatever without the author's prior written permission.

Tara McCready

78 Simcoe Road,
Bond Head, Ontario
L0G 1B0

August 24, 1999

"I can't go on like this."

"That's what you think."

.

Samuel Beckett
Waiting for Godot
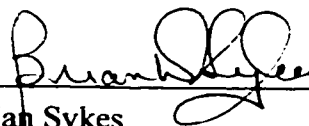
University of Alberta

Faculty of Graduate Studies and Research

The undersigned certify that they have read, and recommend to the Faculty of Graduate Studies and Research for acceptance, a thesis entitled Inhibition of Protein Phosphatase-1 by Endogenous Inhibitor Proteins and Natural Product Toxins submitted by Tara Lyn McCready in partial fulfillment of the requirements for the degree of Doctor of Philosophy.

Dr. Charles Holmes

Dr. Brian Sykes

Dr. Dennis Vance

Dr. Hanne Ostergaard

Dr. Ken Stevenson

16th August 1999

To my mother,
for believing that you can change the world,
one small child at a time.

Acknowledgments

I would like to thank my friends, family, mentors, and coworkers for their support, inspiration, and encouragement throughout my academic career. Other people can make our lives easier, or much more difficult. Thank-you to the people who have made my life (and my PhD) more interesting, more fun, and easier to bear.

I would like to thank my supervisor, Dr. Charles Holmes, as well as the Alberta Heritage Foundation for Medical Research, the Province of Alberta, and the University of Alberta for financial support throughout my PhD.

Dr. Marcia Craig deserves an extra-special thank-you. There is no doubt in my mind that I would not have completed my graduate program without your constant encouragement, helpful advice, unfailing support, 'riotous' friendship, endless conversations, spare bedroom, and sipping sherry. Thanks ever so much for everything.

An extra-special thank-you also to Mom and Larry for their unconditional support, and my beloved Macintosh laptop, both of which got me through my candidacy exam, funding applications, paper writing, and this, my PhD thesis.

And finally, I need to thank Torin, who saved me from UNIX and my difficult thesis figures, supported me through many, many stressful situations, and always made sure I had plenty of chocolate, coffee, and diet coke.

Abstract

Reversible protein phosphorylation is an important mode of regulation of cellular processes. Protein phosphatase-1 (PP1) is one of the major eukaryotic serine/threonine protein phosphatases.

PP1 is potently inhibited by a variety of naturally occurring toxins. These include microcystin-LR, a peptide hepatotoxin produced by cyanobacteria, and the spiroketal marine sponge metabolite calyculin A. Using reversed phase high-performance liquid chromatography (HPLC) guided by a PP1 inhibition assay, we were able to isolate seven novel hydrophobic microcystins. Development of a technique coupling capillary electrophoresis to reversed phase HPLC significantly increased the specificity of microcystin analysis. This technique allowed us to follow the transmission of microcystin up the food chain, from producer microorganism to eukaryotic consumer. Site-directed mutagenesis was used to investigate the interaction between PP1 and novel members of the calyculin family of toxins. We provide evidence that Tyr-134 is important for inhibition of PP1 by the calyculins. A model of calyculin binding is presented that accommodates key structural features of these toxins.

Two of the best-characterized endogenous PP1 inhibitors are the proteins inhibitor-1 (I-1) and inhibitor-2 (I-2). Both are regulated by phosphorylation, which is reversed by phosphatases other than PP1. We identified a 69 residue I-2 peptide that inhibits PP1 at micromolar concentrations. Our competition studies with I-2 and I-1 suggest that these inhibitors have partially overlapping PP1 binding sites.

Two elements in I-1 are required for inhibition of PP1: the region surrounding the Thr-35 phosphorylation site for cAMP-dependent protein kinase (PKA), and a N-terminal PP1 binding motif. We attempted to assess the PP1 binding motif using a library of synthetic peptides in competition assays with an active inhibitor-1 fragment. The results of these experiments indicated that a direct binding assay was needed. Phosphorylation of inhibitor-1 at Thr-35 by PKA converts the protein into a potent inhibitor of PP1. Four sequential arginines preceding Thr-35 were examined in detail. Our results show that Arg-32 is extremely important for I-1 inhibition of PP1. Interestingly, many PP-1 substrates contain a basic amino acid three residues upstream of the phosphorylation site. This has raised the question of binding determinants in PP1 substrates and endogenous inhibitors.

Table of Contents

List of Tables

List of Figures

List of Abbreviations

Adda	[2S, 3S, 8S, 9S]-3-amino-9-methoxy-2,6,8-trimethyl-10-phenyldeca-4,6-dienoic acid
ATP	adenosine 5'-triphosphate
BSA	bovine serum albumin
CaM	calmodulin
cAMP	cyclic- 3',5'- adenosine monophosphate
cDNA	complementary DNA
CE	capillary electrophoresis
CK-II	casein kinase-II
CPI17	C-kinase-activated phosphatase inhibitor of Mr 17,000
CREB	cAMP-response element binding protein
DARPP-32	dopamine and cAMP-regulated phosphoprotein-32, Mr 32,000
DNA	deoxyribonucleic acid
DTT	dithiothreitol
EDTA	ethylenediaminetetraacetic acid
EGTA	ethylglycol-bis-(b-aminoethyl ether)-N,N,N',N'-tetraacetic acid
ELISA	enzyme-linked immunosorbent assay
EOF	electroosmotic flow; influences capillary electrophoresis
ESFF	extensible subset forcefield
FPLC	fast-performance liquid chromatography
G phase	phase of the eukaryotic cell cycle in which growth of the cell occurs
GC/MS	gas chromatography coupled to mass spectrometry
G_L	glycogen-binding subunit of PP-1G from liver
G_M	glycogen-binding subunit of PP-1G from skeletal muscle
GS	glycogen synthase
GSK-3	glycogen synthase kinase-3
HF	hydrogen fluoride
HPLC	high performance liquid chromatography

I-1	inhibitor-1; specific inhibitor of protein phosphatase-1
I-2	inhibitor-2; specific inhibitor of protein phosphatase-1
IC_{50}	concentration of inhibitor causing 50% inhibition of an enzyme activity
ID	internal diameter
IPTG	isopropyl-b-D-thiogalactoside
LD_{50}	50% of the lethal concentration of a toxin in a given organism
ISPK	insulin-stimulated protein kinase
M phase	phase of the eukaryotic cell cycle in which mitosis occurs
M_{110}	myosin-binding subunit of PP-1M
MAPK	mitogen-activated protein kinase
Masp	D-erythro-β-methyl aspartic acid
Mdha	N-methyldehydroalanine
MCLK	myosin light chain kinase
NIPP-1	nuclear inhibitor of protein phosphatase-1
NLD	net-pen liver disease
NMR	nuclear magnetic resonance
OA	okadaic acid
p53BP2	p53 binding protein-2
PCR	polymerase chain reaction
PENCE	Protein engineering network centre of excellence
PhK	Phosphorylase kinase
PKA	cAMP-dependent protein kinase
pNPP	para-nitrophenolphosphate
PP1	catalytic subunit of protein phosphatase-1
PP2A	protein phosphatase type 2A
PP2B	protein phosphatase type 2B, calcineurin
PPP	phosphoprotein phosphatase gene family, including PP1, PP2A and PP 2B
PMSF	phenylmethylsulfonyl fluoride
RB	retinoblastoma protein

RIPP-1	ribosomal inhibitor of protein phosphatase-1
S phase	phase of the eukaryotic cell cycle in which DNA synthesis occurs
SDS-PAGE	polyacrylamide gel electrophoresis performed in the presence of sodium dodecyl sulfate
TFA	trifluoroacetic acid

Standard Amino Acids

Glycine	Gly	G
Alanine	Ala	A
Valine	Val	V
Leucine	Leu	L
Isoleucine	Ile	I
Methionine	Met	M
Proline	Pro	P
Phenylalanine	Phe	F
Tryptophan	Trp	W
Serine	Ser	S
Threonine	Thr	T
Tyrosine	Tyr	Y
Asparagine	Asn	N
Glutamine	Gln	Q
Cysteine	Cys	C
Lysine	Lys	K
Arginine	Arg	R
Histidine	His	H
Aspartic Acid	Asp	D
Glutamic Acid	Glu	E

Units and Constants

Å	Ångstroms (10^{-10} meters)
°C	degrees Celsius
Ci	Curies
cpm	counts per minute
kDa	kiloDaltons
kV	kilovolts
M	molar (moles per liter)
min	minutes
pg	picogram
pH	-log of the concentration of H^+ in solution
U	unit

Chapter One

Introduction

Reversible phosphorylation

The focus of my thesis is inhibition of a serine/threonine protein phosphatase. Reversible protein phosphorylation is an important mode of regulation of cellular processes - proteins can be activated or inhibited by phosphorylation or dephosphorylation. The phosphorylation state of a protein is regulated by two types of enzyme activities: those catalyzed by the protein kinases, which covalently attach a phosphate group to an amino acid side chain, and the reverse activity, removing the phosphate, by protein phosphatases. Traditionally, signal transduction research has focused on protein kinases, but it is now clear that protein phosphatases play an equally important role in the regulation of cellular phosphoproteins. Integrated control of kinases and phosphatases provides the cell with the capacity to rapidly switch proteins from their phosphorylated to dephosphorylated state to meet differing physiological demands.

Most protein phosphatases (recently reviewed in 1,2) are not dedicated to the reversal of the actions of a specific protein kinase. Thus, changes in phosphatase activity have a broad impact on the phosphorylation state of many proteins, which can be substrates for different kinases. Phosphatase regulatory proteins are important components of signal transduction pathways as they provide a mechanism for the control of phosphatase activity and the coordination of multiple signaling pathways. These proteins are often themselves subject to regulation by reversible phosphorylation, creating a link between the activities of various kinases and phosphatases (see glycogen metabolism).

Eukaryotic protein phosphatases are subdivided into two major classes: those that dephosphorylate phosphoserine and phosphothreonine residues and those that dephosphorylate phosphotyrosine residues on their target substrates. In addition, there is also a small family of dual-specificity protein phosphatases that can dephosphorylate both serine/threonine and tyrosine phosphorylated substrates (3). Protein serine/threonine phosphatases share no structural homology with the protein tyrosine phosphatases and are thought to have evolved along separate evolutionary pathways (4).

It has been estimated that one third of cellular proteins undergo reversible phosphorylation (5), and phosphorylation of serine and threonine residues accounts for more than 97% of the protein-bound phosphate in cells (6). Despite this large number, research into the identification and regulation of serine/threonine protein phosphatases lags behind that concerned with tyrosine phosphatases.

Serine/threonine protein phosphatases

Traditionally, protein serine/threonine phosphatases (1,7,8) were classified by their biochemical properties (e.g. substrate specificity, metal requirements and sensitivity to inhibitors) into two broad groups termed type 1 and type 2 serine/threonine protein phosphatases (9). Type 2 phosphatases were further subdivided into three groups, type 2A, calcium-dependent type 2B (or Calcineurin), and type 2C.

Molecular cloning has identified many serine/threonine phosphatases and a re-classification of the enzymes has occurred. Protein phosphatase-1 (PP1), protein

phosphatase-2A (PP2A), and protein phosphatase-2B (PP2B) now comprise the phosphoprotein phosphatase (PPP) family of serine/threonine protein phosphatases (10), which share a common catalytic core domain approximately 35 kDa in size (11). PP2A shares 49% identity with PP1 in its catalytic domain, while PP2B shares 40%. These enzymes are most divergent within their non-catalytic N and C termini and are primarily distinguished from each other by their associated regulatory subunits and sensitivity to inhibitors. The high degree of sequence conservation observed among the eukaryotic members of the PPP family ranks them among the most highly conserved enzymes (12). Mammalian and *Drosophila* PP1 have ~90% sequence identity while mammalian and yeast exhibit >80% identity in the catalytic core domain (13).

PP1 and PP2A make up more than 90% of the serine/threonine phosphatase activity in mammalian cells (7). The PPP family of protein phosphatases exhibits broad and overlapping substrate specificity, with no apparent substrate consensus sequence. Clearly, protein phosphatase activity must be strictly regulated in order to achieve a coordinated intracellular signal transduction system. The work presented in this thesis is concerned with inhibition of protein phosphatase-1 by endogenous inhibitor proteins and natural product toxins.

Protein phosphatase-1

PP1 is a 37 kDa protein that specifically dephosphorylates phospho-serine and phospho-threonine residues. Four mammalian isoforms of the PP1 catalytic subunit are

generated from three distinct genes (Figure 1-1). With the exception of PP1γ2, an alternatively spliced form of the γ isoform expressed only in testes (14), PP1 isoforms, α, β, and γ1 (referred to as γ in this document), are widely expressed in mammalian tissues (15-17). These isoforms are differentiated primarily by their carboxy-terminal sequences. The functional importance of the existence of multiple PP1 isoforms is unknown. It has been speculated that they may associate with distinct regulatory subunits and thereby serve unique physiological functions, but so far there is little evidence to support this idea (7).

PP1 has many *in vivo* substrates which are involved in a diverse range of physiological processes including glycogen metabolism, synaptic plasticity, cell cycle progression, gene expression, muscle contraction, and lipid metabolism (1,7,18-20). These processes are regulated by distinct PP1 holoenzymes in which the catalytic subunit (PP1) is complexed to targeting subunits (21,22). Through interactions with these regulatory proteins, PP1 associates with myosin, glycogen, nuclear chromatin, the sarcoplasmic reticulum and other subcellular compartments.

3-dimensional structure of PP1

The x-ray crystallographic structure of recombinant rabbit muscle PP1α (bound to microcystin-LR, a natural product toxin and inhibitor) was published in 1995 by Goldberg et al. Overall, the phosphatase forms a compact ellipsoidal structure (23) (Figure 1-2, part b). The catalytic domain of PP1 consists of a central β-sandwich of two mixed β-sheets surrounded on one side by seven α-helices and on the other by a

```
               10           20           30           40           50           60
PP1α   MSDSEKLNLD   SIIGRLLEVQ   GSRPGKNVQL   TENEIRGLCL   KSREIFLSQP   ILLELEAPLK
PP1β   MADGE-LNVD   SLITRLLEVR   GCRCGKIVQM   TEAEVRGLCI   KSREIFLSQP   ILLELEAPLK
PP1γ   MADLDKLNID   SIIQRLLEVR   GSKPGKNVQL   QENEIRGLCL   KSREIFLSQP   ILLELEAPLK


               70           80           90          100          110          120
PP1α   ICGDIHGQYY   DLLRLFEYGG   FPPESNYLFL   GDYVDRGKQS   LETICLLLAY   KIKYPENFFL
PP1β   ICGDIHGQYY   DLLRLFEYGG   FPPESNYLFL   GDYVDRGKQS   LETICLLLAY   KIKYPENFFL
PP1γ   ICGDIHGQYY   DLLRLFEYGG   FPPESNYLFL   GDYVDRGKQS   LETICLLLAY   KIKYPENFFL


              130          140          150          160          170          180
PP1α   LRGNHECASI   NRIYGFYDEC   KRRYNIKLWK   TFTDCFNCLP   IAAIVDEKIF   CCHGGLSPDL
PP1β   LRGNHECASI   NRIYGFYDEC   KRRFNIKLWK   TFTDCFNCLP   IAAIVDEKIF   CCHGGLSPDL
PP1γ   LRGNHECASI   NRIYGFYDEC   KRRYNIKLWK   TFTDCFNCLP   IAAIVDEKIF   CCHGGLSPDL


              190          200          210          220          230          240
PP1α   QSMEQIRRIM   RPTDVPDQGL   LCDLLWSDPD   KDVQGWGEND   RGVSFTFGAE   VVAKFLHKHD
PP1β   QSMEQIRRIM   RPTDVPDTGL   LCDLLWSDPD   KDVQGWGEND   RGVSFTFGAD   VVSKFLNRHD
PP1γ   QSMEQIRRIM   RPTDVPDQGL   LCDLLWSDPD   KDVLGWGEND   RGVSFTFGAE   VVAKFLHKHD


              250          260          270          280          290          300
PP1α   LDLICRAHQV   VEDGYEFFAK   RQLVTLFSAP   NYCGEFDNAG   AMMSVDETLM   CSFQILKPAD
PP1β   LDLICRAHQV   VEDGYEFFAK   RQLVTLFSAP   NYCGEFDNAG   GMMSVDETLM   CSFQILKPSE
PP1γ   LDLICRAHQV   VEDGYEFFAK   RQLVTLFSAP   NYCGEFDNAG   AMMSVDETLM   CSFQILKPAE


              310          320
PP1α   KNKGKYGQFS   GLNPGGRPIT   PPRNSA--K-AKK
PP1β   K-KAKY-QYG   GLN-SGRPVT   PPRTANPPK--KR
PP1γ   K-K-K-----   -PNAT-RPVT   PPR-GMITKQAKK
```

Figure 1-1. *Alignment of the primary sequences of the human isoforms of PP1.* Differences among the isoforms of the catalytic subunits of PP1 are found primarily in the carboxy-terminal region of the proteins. In addition to the three predominant isoforms shown here, PP1γ is differentially spliced to produce PP1γ2, a testes-specific isoform.

subdomain comprising three α-helices and a three-stranded β-sheet (Figure 1-4). The interface of the three β-sheets at the top of the β-sandwich creates a shallow catalytic channel. Amino acid side chains present on loops emanating from the β-sandwich coordinate a pair of metal ions to form a binuclear metal centre (1,23).

Three surface grooves emanating from the active site of PP1 are potential binding sites for substrates and inhibitors. The hydrophobic groove consists of a patch of hydrophobic side chains that are conserved in the PPP family. The acidic groove is lined with acidic side chains (Figure 1-6) that are proposed to interact with basic residues in the endogenous inhibitor proteins inhibitor-1 (I-1) and DARPP-32. The C-terminal groove runs from the active site to the C-terminus of the protein and contains a loop between β-strands 12 and 13 that is involved in inhibition of PP1 by natural product toxins.

The identity of the two metal ions in the active site is controversial. An x-ray crystallographic structure of the phosphate analogue tungstate bound in the catalytic site of PP1 expressed in *E. coli* indicated that the metal ions present were Fe^{2}+ and Mn^{2}+ (24). Related PPP family member PP2B has been shown to bind Fe^{2+} and Zn^{2+} (25,26). The structure published by Goldberg et al., 1995, ruled out the presence of Mg, Ni, Cu or Zn in the catalytic site but could not discriminate between Mn, Fe, or Co. PP1α was assumed to contain two Mn^{2+} ions because of the Mn^{2+}-dependency of the recombinant enzyme (discussed later) and the fact that the crystallization solutions contained $MnCl_2$ (23).

Catalytic mechanism (Figure 1-2, panels a,b)

The structure of tungstate-bound PP1 indicated that two oxygens of tungstate coordinate the metal ions in the active site (24). Two water molecules, one of which is a metal-bridging water, also contribute to the coordination of the metal ions. The metal coordinating amino acid residues of PP1 (His-66, Asp-64, His-248, His-273, Asn-124, and Asp-92) are invariant among all the PPP family members (1). Consistent with roles in catalysis, mutation of these residues in PP1 profoundly decreases the activity of the enzyme (27-29).

PP1 is thought to catalyze dephosphorylation of a phosphoprotein substrate in a single step with a metal-activated water molecule or hydroxide ion, without the formation of a phosphoryl-enzyme intermediate (unlike protein tyrosine phosphatases) (1,23,24). Catalytic site arginine residues 96 and 221 appear to stabilize the pentacoordinate transition state, as loss of these residues by site-directed mutagenesis of PP1 dramatically reduces catalytic activity (29). In addition, histidine 125 may donate a proton to the leaving group oxygen atom of the P-O scissile bond, a role consistent with the loss of activity also observed for this PP1 mutant (28,29).

Recombinant PP1

When expressed in *E. coli*, several of the properties of recombinant PP1α, PP1β, and PP1γ resemble those of the native PP1 catalytic subunit purified from mammalian tissues, while others are quite different (30,31). For example, recombinant and native forms of PP1 have similar activities toward glycogen phosphorylase and similar sensitivities to
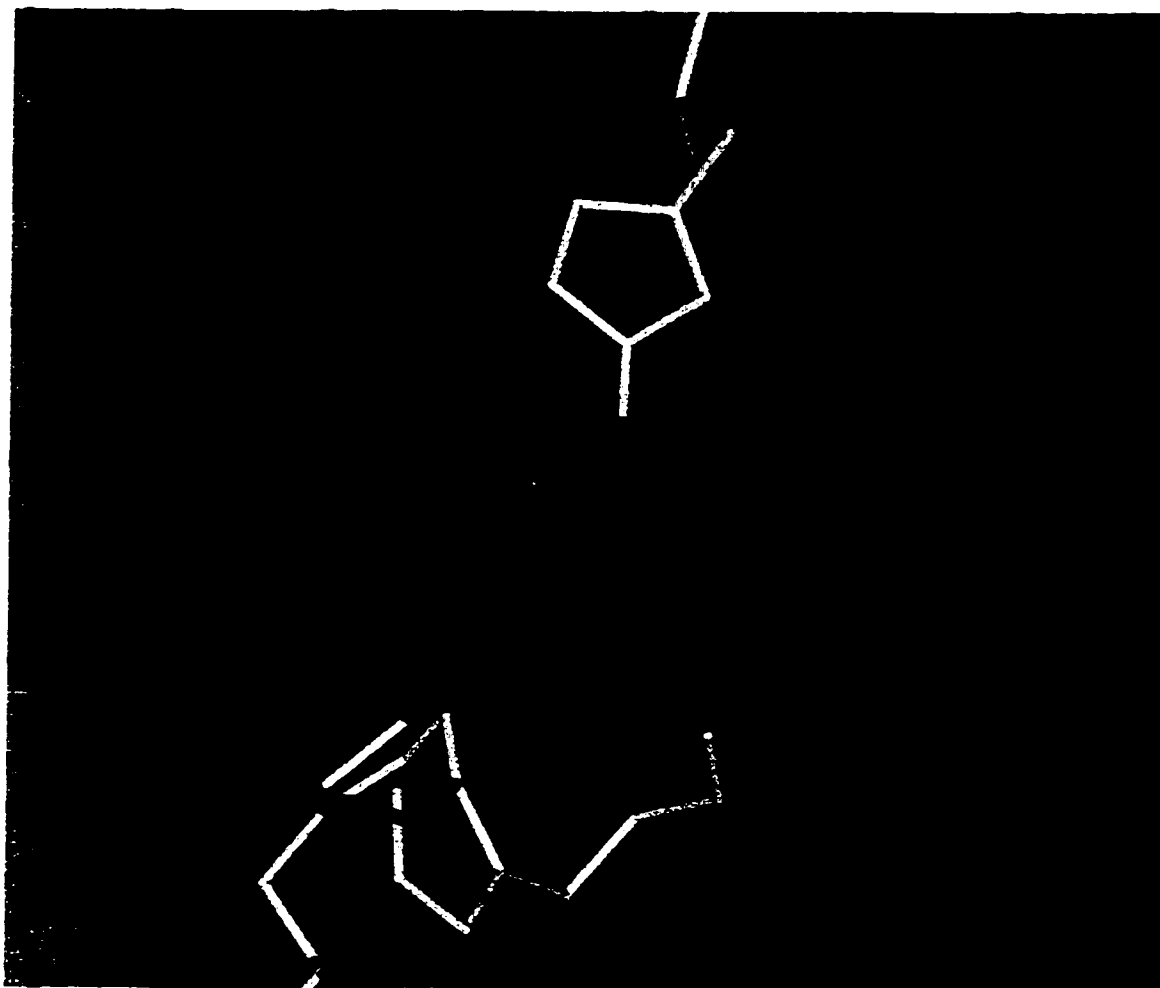
Figure 1-2 (a). *The catalytic domain of PP1.* Residues in PP1 responsible for coordinating a pair of metal ions are shown. Coordination of metal ions (pink spheres) in the active site appears as a solid link between amino acid side chain and metal ion. Two water molecules (blue spheres), one of which is a metal-bridging water molecule, contribute to the coordination of the metal ions. PP1 structures shown throughout this thesis are derived from coordinates of PP1α published by Goldberg et al. 1995, and were created using InsightII software (Biosym/MSI Technologies) on a Silicon Graphics Indigo2 Impact 10000 workstation.
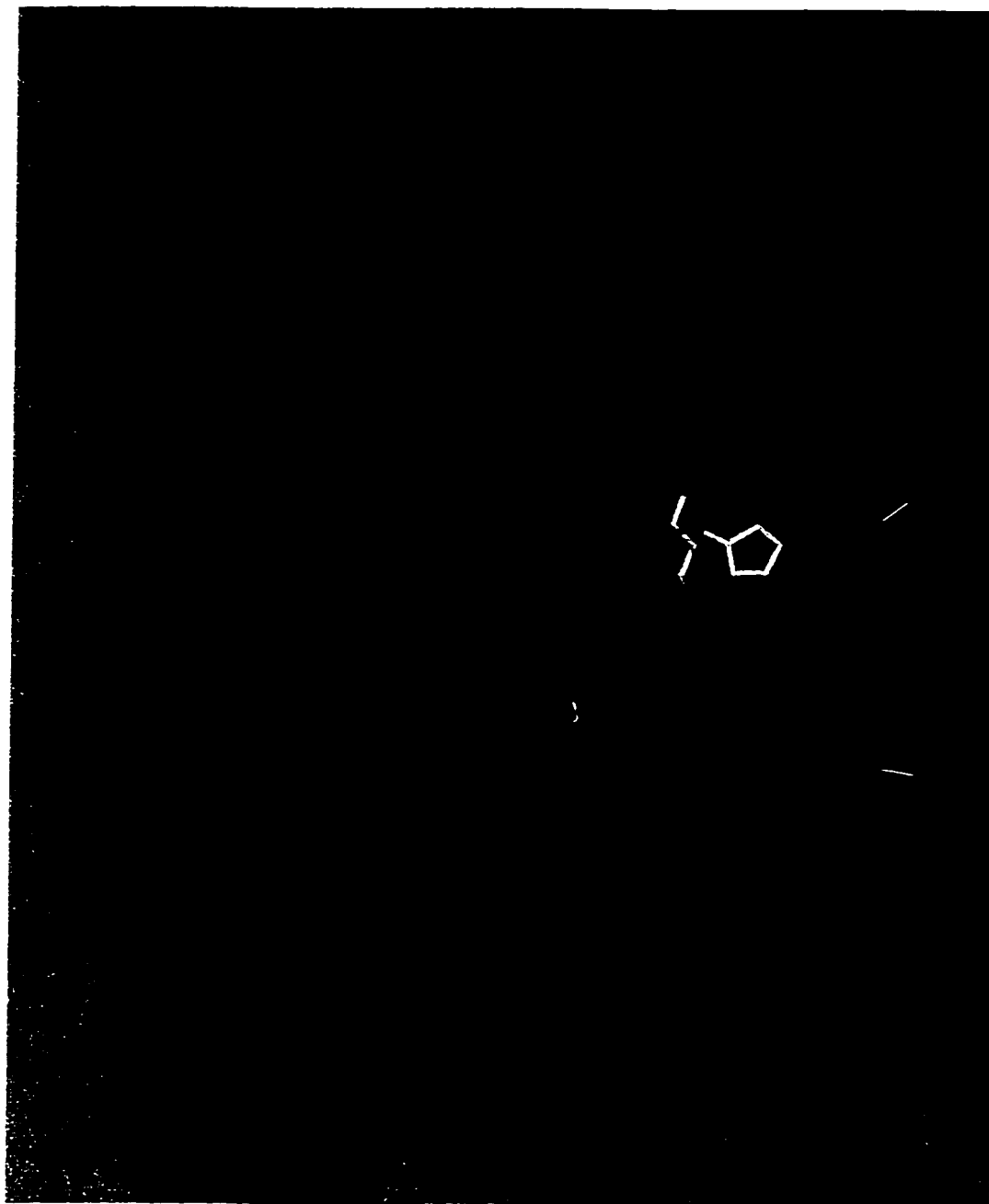
Figure 1-2 (b). *Orientation of the catalytic domain with respect to phosphatase structure.* Residues in PP1 proposed to be involved in binding to a substrate phosphate group (P) are shown. Metal ions (pink spheres) and water molecules (blue spheres) are shown as in Figure 1-3 (a). Inclusion of the phosphate group in this figure is intended to serve only as a general indication of the proposed site of interaction, and has not been experimentally determined. 3-D structures of PP1 suggest that the substrate phosphate oxygens are coordinated by the metal ions and a number of active site residues (23,54). It is proposed that PP1 catalyzes dephosphorylation in a single step with a metal-activated water molecule or hydroxide ion. Catalytic site arginine residues 96 and 221 are thought to stabilize the transition state. His-125 may donate a proton to the leaving group oxygen atom of the P-O scissile bond. (see text for details)

inhibitor-2 (I-2), an endogenous protein inhibitor specific to PP1. However, the activity of recombinant PP1 toward histone H1 and casein (serine/threonine phosphorylated substrates) is much higher than that of native enzyme (30). While native PP1 is devoid of protein tyrosine phosphatase (PTPase) activity, PP1γ expressed in *E. coli* is active toward a variety of phosphotyrosine-containing protein substrates (31). Recombinant forms of PP1 are 100-1000 fold less sensitive than native enzyme to inhibition by inhibitor-1 (I-1), an endogenous phosphoprotein inhibitor specific to PP1. Recombinant PP1α and PP1γ are unable to interact with the PP1 myosin targeting subunit (M_{110}), while PP1β is less sensitive to inhibition by okadaic acid and microcystin-LR than is the native enzyme (30,32). The presence of 1 mM $MnCl_2$ in bacterial culture medium is essential for significant expression of all three isoforms of PP1 in soluble, active forms (30,32). Unlike native enzyme, recombinant PP1 activity is dependent on the presence of manganese in phosphatase activity assays (30).

A possible explanation for the unrestricted substrate specificity of recombinant PP1 is a conformational change in the vicinity of the catalytic site that allows access to bulky phosphotyrosine side chains in addition to phosphoserine and phosphothreonine residues (31). A conformational change in the catalytic region could result in an inability to strongly coordinate metal ions (hence the manganese dependency of the recombinant enzyme) and disruption of an inhibitor-1 binding site (resulting in lack of sensitivity to I-1).

Recombinant PP1 can be converted to a more native-like state ('reactivated') *in vitro* by incubation with inhibitor-2 followed by phosphorylation of I-2 by glycogen

synthase kinase 3 (GSK-3). The PTPase activity of recombinant PP1 is lost after this procedure (31). In addition, reactivated recombinant enzyme regains sensitivity to inhibitor-1 and is no longer dependent on manganese for activity.

It is not known whether 'reactivation' of PP1 by I-2 and GSK-3 occurs *in vivo*. Correct folding of PP1 in the cell may be required to prevent denatured or damaged enzyme from dephosphorylating non-physiological substrates, including phosphotyrosyl-containing proteins. It is also required for effective interaction with important regulatory proteins such as I-1 and PP1 targeting subunits (30).

An important point to remember about all of the crystal structures of PP1 discussed in this thesis is that they are based on the recombinant form of the enzyme which has been expressed in *E. coli*. The structure and catalytic mechanism of the native enzyme has not yet been determined. As discussed (see also Chapter Four), the recombinant form of PP1 is not identical to the native enzyme with respect to several important catalytic and regulatory characteristics.

Regulation of PP1 by targeting subunits

The catalytic subunit of protein phosphatase-1 (PP1) has a broad range of *in vitro* substrates. One important regulatory mechanism in the control of PP1 activity is the subcellular location of the enzyme (22). Targeting subunits confer *in vivo* substrate specificity by directing PP1 holoenzymes (PP1 catalytic subunit plus targeting subunit) to a particular organelle or macromolecular complex (1). Some PP1 targeting subunits also act to enhance or suppress phosphatase activity toward specific substrates. Binding of different targeting subunits to the catalytic subunit of PP1 is mutually exclusive. This suggests that they share one or more common or overlapping binding sites (33-35).

Targeting PP1 to glycogen

The role of PP1 in the control of glycogen metabolism is muscle has been well documented. This system serves as a paradigm for the regulation of PP1 by targeting subunits and thus will be outlined in detail. The activities of enzymes involved in glycogen metabolism are controlled by reversible phosphorylation (reviewed in 21,22,36). In skeletal muscle, PP1 is targeted to glycogen by association with a 124 kDa glycogen-targeting subunit (G_M) (37,38). When complexed to the G_M subunit, PP1 binds to glycogen with high affinity and is more active toward glycogen-associated substrates glycogen synthase, phosphorylase kinase and glycogen phosphorylase (Figure 1-3). Glycogen synthase catalyzes the rate-limiting step in the synthesis of glycogen. In contrast, phosphorylase kinase phosphorylates glycogen phosphorylase, activating its ability to cleave glucose-1-phosphate from glycogen, a preliminary step in ATP

Figure 1-3. *Regulation of the activity and localization of PP1.*

In skeletal muscle, PP1 is targeted to glycogen by association with a glycogen-targeting subunit (G_M). PP1 dephosphorylates and activates glycogen-associated enzyme glycogen synthase (GS). PP1 dephosphorylates and inactivates phosphorylase kinase (PhK) and glycogen phosphorylase (not shown).

An increase in intracellular cAMP (in response to adrenalin) activates cAMP-dependent protein kinase (PKA). Binding of cAMP to the regulatory subunits (R) of the PKA tetramer causes conformational changes in the R subunits that result in the dissociation of two active catalytic subunits (C) from the complex.

PKA catalytic subunits phosphorylate the PP1 binding subunit G_M as well as inhibitor-1 (I-1). PKA phosphorylation of G_M promotes PP1 dissociation from the subunit, reducing the amount of phosphatase activity localized to the glycogen particle. Phosphorylation of I-1 at threonine 35 activates the protein as an inhibitor of PP1. Through these two steps, PKA down-regulates PP1 activity. PKA also phosphorylates and inactivates glycogen synthase (GS) while phosphorylating and activating phosphorylase kinase (PhK). Inhibition of PP1 and inactivation of glycogen synthase reduces glycogen synthesis in muscle tissue. The stimulation of phosphorylase kinase promotes ATP production via the glycolytic pathway.

PP2A and PP2B reverse PKA action by dephosphorylating the PKA site on the G_M subunit as well as inhibitor-1. PP2B activity is dependent on Ca^{2+} binding to its regulatory B-subunit (B) and calmodulin (CaM).

(Adapted from Hubbard and Cohen, *Trends Biochem. Sci.*, 1993)
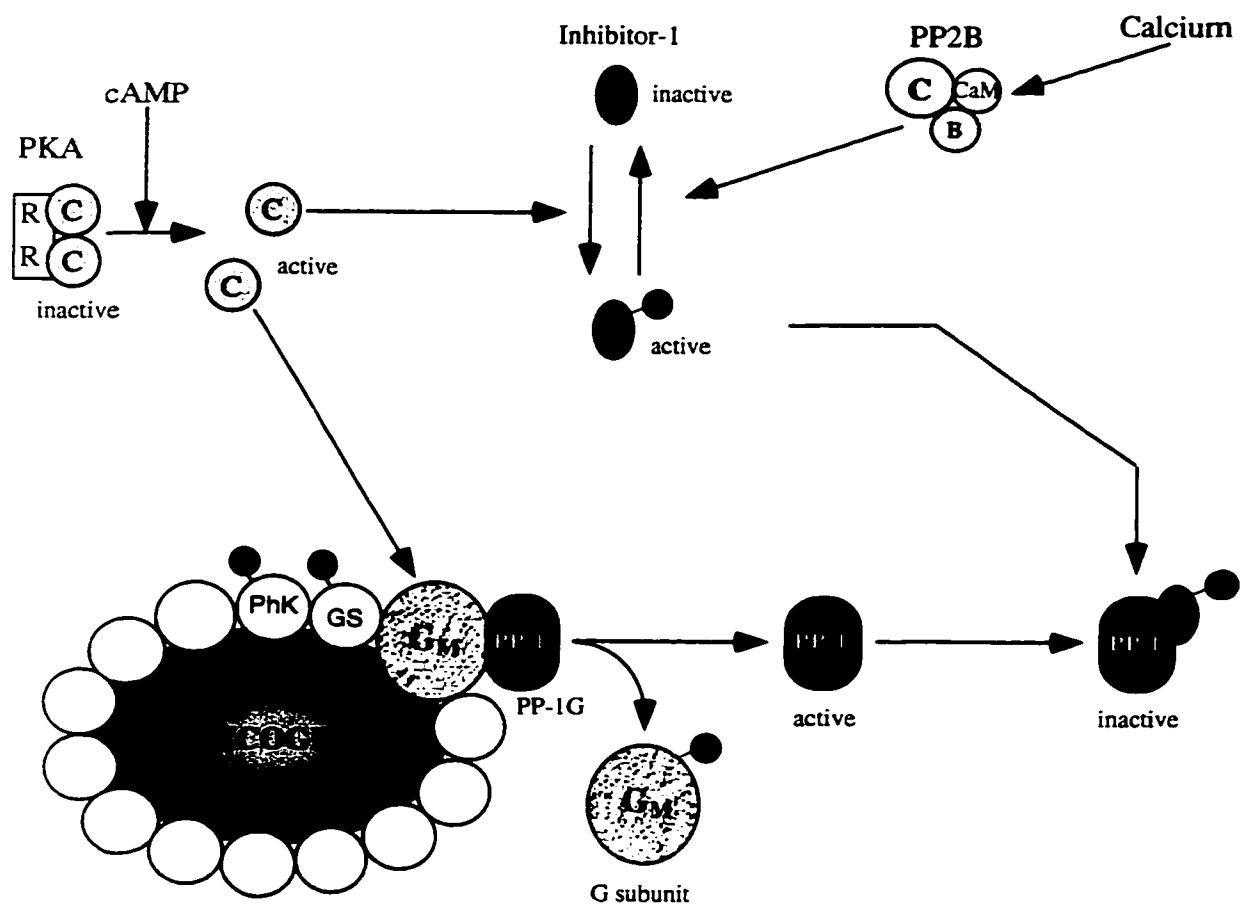
production via the glycolytic pathway. PP1 dephosphorylates and activates glycogen synthase while dephosphorylating and inactivating phosphorylase kinase and glycogen phosphorylase. In this way, PP1 activity promotes glycogen synthesis.

Further regulation of PP1 activity comes from reversible phosphorylation of the G_M subunit. Phosphorylation of G_M by insulin-stimulated protein kinase (ISPK) enhances PP1 activity toward glycogen synthase (21), again resulting in an increase in the rate of glycogen synthesis in muscle. In contrast, phosphorylation of a different site on the G_M subunit by cAMP-dependent protein kinase (PKA) promotes PP1 dissociation from G_M, thus reducing the amount of phosphatase activity localized to the glycogen particle. PKA also phosphorylates a cytosolic inhibitor of PP1, I-1 (39), thereby promoting inhibition of the phosphatase after its release from G_M(21). PKA is activated by increased levels of intracellular cAMP, as produced by the hormone adrenalin. In this pathway, an increase in intracellular cAMP concentration results in a decrease in glycogen-associated PP1 activity, both by reducing the affinity of the G_M subunit for the phosphatase and by activating an inhibitor of PP1. In this way, adrenalin acts through PKA to reduce glycogen synthesis, as required for a typical 'fight or flight' response to stress.

In addition, PKA phosphorylates and inactivates glycogen synthase directly, further reducing glycogen synthesis in muscle tissue. PKA also opposes PP1 activity by phosphorylating and activating phosphorylase kinase, thus ultimately stimulating ATP synthesis through the glycolytic pathway.

Other members of the PPP family are involved in regulation of this system. PP2A and PP2B dephosphorylate PKA substrates G_M (40) and inhibitor-1. This phosphatase activity reverses the effects of adrenalin (via PKA) on glycogen metabolism by inactivating the PP1 inhibitor I-1, and by allowing re-association of G_M and PP1. Once PP1 is active and bound to the G_M subunit, it is free to stimulate glycogen synthesis by dephosphorylating glycogen synthase, phosphorylase kinase, and glycogen phosphorylase. The involvement of calcium-activated PP2B in this pathway links calcium and cAMP, both important second messengers, to a phosphatase activity cascade.

Other examples of PP1 regulation

There is strong evidence to support similar PP1 targeting mechanisms in a variety of cellular processes.

The M_{110} targeting subunit is responsible for association of PP1 with myofibrils of skeletal muscle (41,42) and smooth muscle (41,43). Bound M_{110} enhances the rate at which PP1 dephosphorylates myosin light chain and suppresses PP1 activity toward glycogen phosphorylase (35). Similarly, G_L, a protein which targets PP1 to liver glycogen, suppresses PP1 phosphorylase activity (35,44,45).

PP1 is also involved in control of gene expression. The cAMP-response element binding protein (CREB) must be phosphorylated to be an active transcription factor (7). However, only transient phosphorylation of CREB occurs due to the activity of a nuclear

form of PP1 (46). Several nuclear proteins have been identified - NIPP-1 (47), PNUTS (48) and I-2 (49) -which appear to interact with nuclear forms of PP1.

PP1 may be involved in the regulation of p53, a tumour suppressor in mammalian cells, through its interaction with the p53 binding protein (p53BP2) (50). Phosphorylation is thought to inactivate suppressor proteins such as p53 and the retinoblastoma gene product, RB (51,52). Sustained hyperphosphorylation of various growth suppressor proteins due to inhibition of PP1 may explain the observed tumour-promoting effects of natural product inhibitors of PP1 (as discussed later) (53).

Identification of a conserved PP1-binding motif

Restriction of the substrate specificity of PP1 *in vivo* results from the association of the catalytic subunit with different regulatory or targeting subunits. Co-crystallization of PP1 with a peptide derived from the G_M subunit (residues 63-75) provided structural details regarding subunit binding to PP1 (54). Residues 64-69 of the G_M peptide, [64]RRVSFA[69], bind in an extended conformation to a hydrophobic channel formed at the interface of two β-sheets in the C-terminal region of PP1, removed from the catalytic site (Figure 1-4). Three residues of the G_M peptide (Ser-67 to Ala-69) form a β-strand which is incorporated into β-sheet 1 of PP1 as an additional β-strand parallel to the edge β-strand β-14. Interactions between phosphatase and peptide consist of predominantly hydrophobic contacts with Val-66 and Phe-68, while acidic residues in the phosphatase binding pocket provide a favourable electrostatic environment for Arg-64 and Arg-65 (1).
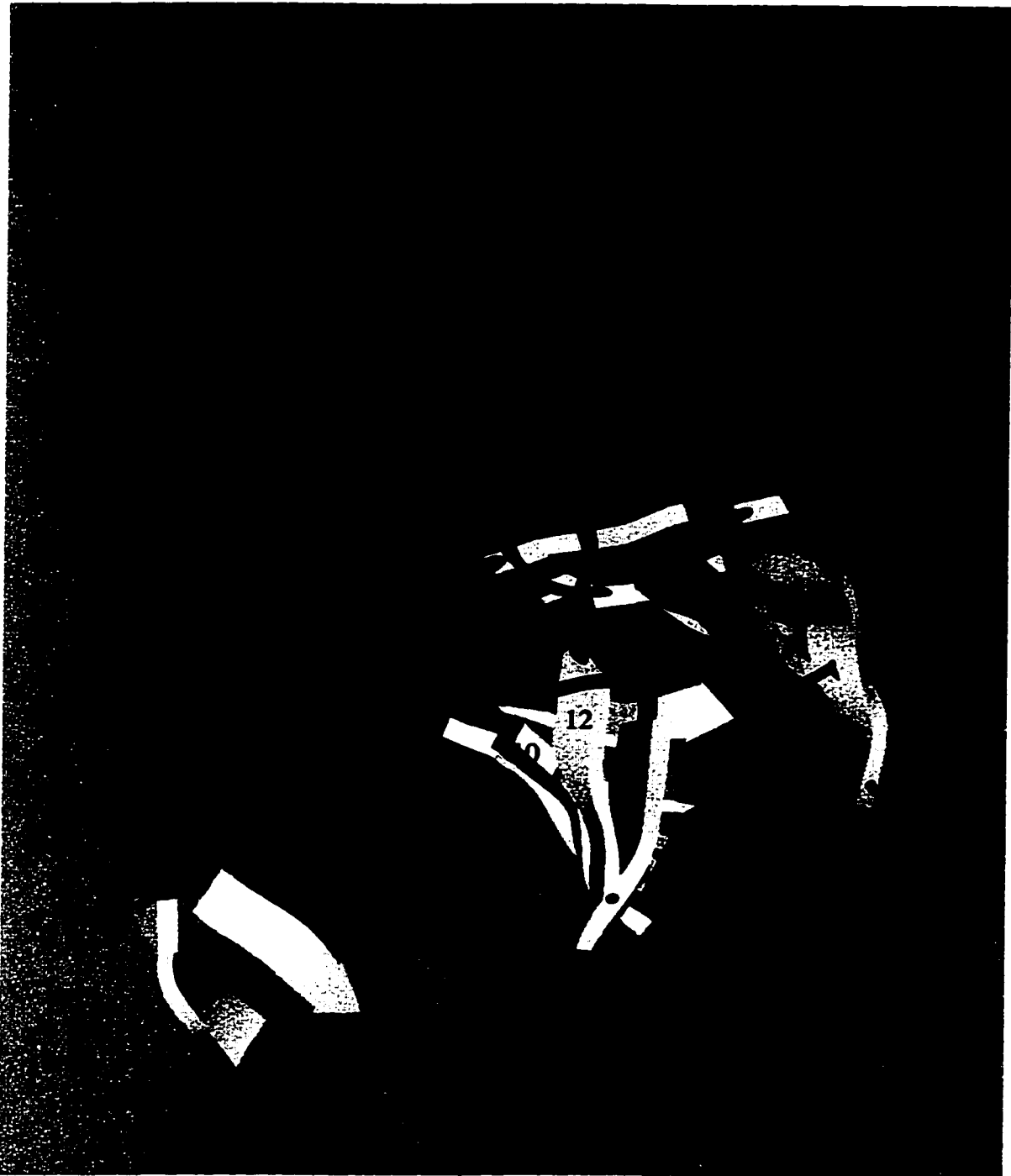
Figure 1-4. *Targeting protein binding channel in PP1.* The G$_M$ subunit peptide binds to PP1 at the interface of two β-sheets (shown in yellow) in the C-terminal region of the protein (54). Residues involved in binding to the G$_M$ peptide are indicated (black sticks, blue sticks). Cys-291 and Phe-257 are shown in blue because are featured in experiments described in Chapters Three and Four. The position of the metal ions (pink spheres) in the active site of the enzyme is shown as a point of reference - this figure represents the opposite face of PP1 displayed in Figure 1-3 (b). (see text for details)

In particular, the binding site for the side chain of Val-66 is formed by PP1 residues Ile-169, Leu-243, Leu-289, and Cys-291. The binding site for the Phe-68 side chain of the peptide is formed by PP1 residues Phe-257, Cys-291, and Phe-293. In addition, Asp-242, Leu-289, and Cys-291 participate in polar interactions with the G_M peptide. Mutagenesis of residues Cys-291 and Phe-257 in PP1 is presented in Chapter Four.

Residues in the phosphatase that interact with the G_M peptide are highly conserved among all isoforms of PP1, from species as diverse as yeast, Drosophila, mammals and higher plants (54). Identification of the RVSF binding sequence in PP1 targeting subunit G_M prompted re-examination of the amino acid sequences of other PP1 regulatory proteins (Chapter Five, Table 5-1). Comparison of regulatory proteins known to bind PP1 in a mutually exclusive manner resulted in identification of a conserved PP1 binding motif (R/K)(V/I)XF (54). This motif is found in PP1 subunits G_M, G_L, M_{110}, inhibitors I-1, DARPP-32, NIPP-1, and in p53BP2. Several related proteins in the yeast *S. cerevisiae* also contain this sequnce. An investigation of residues in the proposed PP1 binding motif found in inhibitor-1 and DARPP-32 is presented in Chapters Five and Six.

There are several important concepts to remember about regulatory proteins, targeting subunits and PP1. First, it is clear that PP1 is not an unregulated enzyme acting indiscriminately throughout the cell. PP1 activity is regulated by an intricate web of inhibitor proteins, kinases, and other phosphatases. Second, the (R/K)(V/I)XF motif is the first defined common PP1 binding sequence - an important step in the identification of other proteins that may interact with the phosphatase. Finally, the binding motif sequence is only one part of the interaction between PP1 and its binding partners. Many

of the motif-containing PP1 targeting subunits enhance or reduce PP1 activity toward specific substrates (e.g. myosin or phosphorylase). These effects cannot be produced by shorter peptide versions of the targeting subunit which contain only the region surrounding the PP1 binding motif (54). Therefore, other regions of the targeting subunits must be involved in alteration of PP1 activity.

Endogenous inhibitors of PP1

One way in which the cell coordinates the activation of kinases with the inhibition of phosphatases is via endogenous phosphatase inhibitor proteins (recently reviewed in 7,55). Many proteins which function as PP1 inhibitors are themselves regulated by phosphorylation. These include inhibitor-1 (I-1), Inhibitor-2 (I-2), dopamine-and cAMP-regulated phosphoprotein of Mr 32,000 (DARPP-32), nuclear inhibitor of PP1 (NIPP-1), C-kinase activated phosphatase inhibitor of Mr 17,000 (CPI17), and a ribosomal inhibitor of PP1 (RIPP-1).

Two of the best-characterized PP1 inhibitor proteins are I-1 and I-2. Both are regulated by phosphorylation, which is reversed by phosphatases other than PP1, namely PP2A and PP2B. This creates a regulatory cascade where one phosphatase, via the dephosphorylation of an inhibitor, modulates the function of another.

Inhibitor-1

The catalytic subunit of PP1 is regulated by the heat-stable protein inhibitors, the 18.7 kDa inhibitor-1 (I-1) and its predominantly neuronal homologue DARPP-32 (dopamine- and cAMP-regulated phosphoprotein, Mr 32,000) (reviewed in 7). Phosphorylation of inhibitor-1 at Thr-35 or DARPP-32 at Thr-34 by PKA converts the protein into a potent inhibitor of PP1. I-1 and DARPP-32 are specific inhibitors of PP1, and have been used extensively *in vitro* to differentiate between PP1 and PP2A activity.

.   The role of I-1 in regulating PP1 function has been investigated in many different physiological settings (7). These include glycogen metabolism (Figure 1-3), synaptic plasticity, tumour cell growth, and the control of muscle contraction. Some but not all hormones that elevate intracellular cAMP activate I-1, presumably through PKA phosphorylation.

DARPP-32 is highly homologous to I-1 near its N-terminus (56) (Figure 1-5). DARPP-32 is found mainly in the brain (57), but it is also expressed in adipose tissue (58) and, to a much lesser extent, in the kidney (59). Some cells in the brain and kidney express both I-1 and DARPP-32. Recent reports suggest that DARPP-32 is myristoylated at its N-terminus, which may allow association with membranes (7). Although originally identified by its enhanced phosphorylation in response to dopamine, DARPP-32 is activated by many hormones and neurotransmitters that elevate cAMP levels (60).

I-1 and DARPP-32 are important regulators of PP1 activity in cellular signaling pathways. They integrate the activities of PP1 and PKA, as well as PP1 and PP2A/PP2B. Despite the high homology among PP1, PP2A and PP2B, phosphorylated I-1 and DARPP-32 are inhibitors of PP1 but substrates of PP2A and PP2B (55). The reasons for these differences are unknown. Replacing phospho-Thr-34 in DARPP-32 or Thr-35 in I-1 with phospho-serine results in a 25 fold and 100 fold decrease in PP1 inhibition, respectively. Dephosphorylation of DARPP-32 by PP2A is decreased less than four-fold by this substitution, and dephosphorylation by PP2B is not decreased at all (61).

a

I-1   1   [sequence]
      : ::::||||:|| ::||| ::|:|||||||| | |::|||
D32   1   [sequence]

I-1 49   [sequence]
      | :|:: :::   :   ::::::: : |:|::|::|:::| || :
D32 48   [sequence]

I-1 97   [sequence]
      : :| :::::|::: |: | | :::|: : ::::::: :|:: :
D32 99   [sequence]

I-1 145   [sequence]
      ::||:: ::: :|: :|:
D32 142   [sequence]

D32 190   [sequence]

b

       9 12 30   ⊕
       | | | ▼36
      KIQF RRRRPTP
       \ /   \ /
1 ■━━━━■━━━━━━━━━━━━━━━━━━━━━━━━ 166   Inhibitor-1

       8 11 29   ▼35
      KIQF RRRRPTP
       \ /   \ /
1 ■━━━━■━━━━━━━━━━━━━━━━━━━━━━━━ 202   DARPP-32

c

       9 12 30   ▼36
      KIQF RRRRPTP
       \ /   \ /
9 ■━━━━■━━━━ 54   Inhibitor-1[9-54] (fully active inhibitor of PP1)

       9 12 30   ▼36
      KIQF RRRRPTP
       \ /   \ /
9 ■━━━━■━━━ 41   Inhibitor-1[9-41] (25% activity of full length inhibitor)

Figure 1-5. *Inhibitor-1 and DARPP-32.* Sequence alignment of the human forms of inhibitor-1 (I-1) and DARPP-32 (D-32) is shown in panel a. Identical residues are highlighted with a solid bar while similar residues are indicated with (:). Panel b shows the subdomains of I-1 and DARPP-32 that are involved in PP1 binding and inhibition. The putative PP1 binding motif sequence (KIQF) (54) and the region surrounding the Thr-34/35 PKA phosphorylation site (↓) are indicated. Four arginine residues preceding the threonine phospho-acceptor site are thought to interact with an acidic region on the surface of PP1 (Figure 1-6) (64,65). Active fragments of inhibitor-1 used in experiments throughout this work are shown in panel c. The peptide fragments contain both subdomains of inhibitor-1 that are required for inhibition of PP1.

DARPP-32 has been extensively studied in the laboratory of Angus Nairn and Paul Greengard. Their studies indicate that two distinct subdomains in DARPP-32 (and I-1) interact with PP1 (Figure 1-5). Subdomain 1 contains phosphorylated threonine 34 and surrounding residues while subdomain 2 includes a short stretch of residues at the amino terminus of the protein which contains a short amino acid sequence (KIQF) that is similar to the (R/K)(V/I)XF binding motif present in many PP1 regulatory subunits (as discussed in the previous section). Disruption of this sequence, especially by loss of the Ile residue, disrupts PP1 binding of both dephosphorylated and phosphorylated forms of the inhibitors (62,63).

In models of I-1 binding to PP1, four sequential arginine residues (Arg-29 to Arg-32) preceding the phosphothreonine residue (Thr-35) of the inhibitor proteins are in a position to interact with acidic amino acids lining a surface groove located near the active site of the phosphatase (Figure 1-6, also Chapter Six). However, recently published studies have determined that Arg-29 and Arg-30 do not make major contributions to the interaction between DARPP-32 and PP1 (64). Mutation of several of the acidic amino acids in PP1, either singly or in combination, did not reduce the inhibitory potency of phospho-DARPP-32 or I-1, with the exception of Asp-208 (29,65). Work is presented in Chapter Six of this thesis which suggests that Arg-32 plays a key role in I-1 inhibition of PP1.
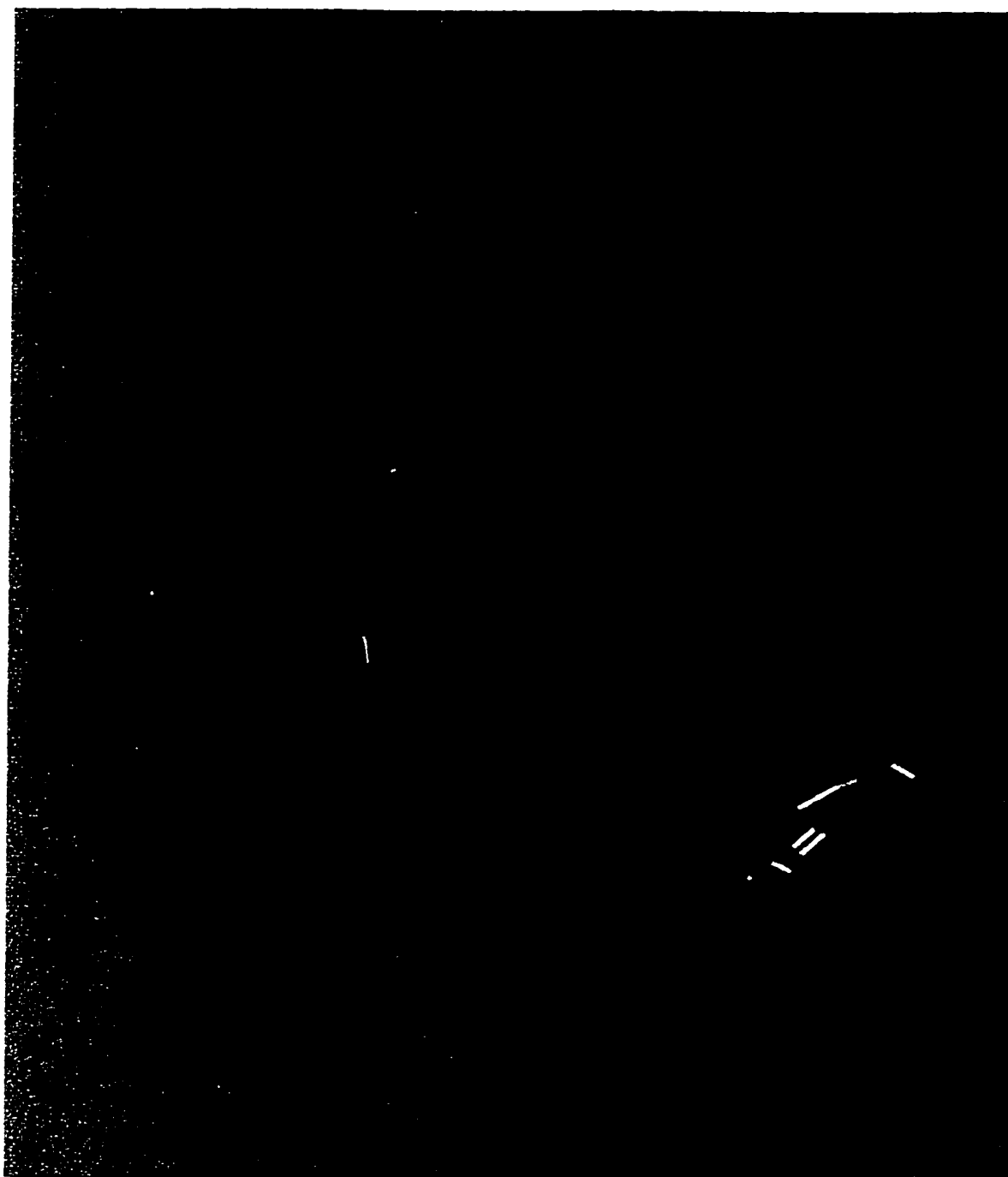
Figure 1-6. *Acidic surface groove of PP1 proposed to interact with inhibitor-1.* Models of I-1 binding propose that phospho-Thr-35 occupies the active site of the enzyme, and that sequential arginines 30-33 interact with Asp and Glu residues within the acidic groove of PP1 (64,65). Acidic residues lining a surface groove of PP1 are indicated in red. Metal ions in the active site of the enzyme (pink spheres) and two of the residues (yellow) involved in PP1 binding to regulatory subunits (Cys-291 and Phe-257, Figure 1-4) are shown as points of reference.

Inhibitor-2

Inhibitor-2 (I-2) is a 23 kDa protein first identified in rabbit skeletal muscle as a specific inhibitor of protein phosphatase-1 (66). I-2 is present in both the cytosol and the nucleus, and its protein and mRNA levels are regulated in a cell cycle-dependent manner (49,67). Inhibitor-2 accumulates in the nucleus during S phase (DNA synthesis phase) of the cell cycle (49).

A cluster of basic residues (residues 140-145) in the C-terminal region of the protein contains a putative nuclear localization sequence (Figure 1-7). Mutation of two lysine residues (143/145) in this sequence prevents I-2 accumulation in the nucleus but does not affect inhibition of PP1 (49). The biological function of the nuclear accumulation of I-2 is unknown but it has been proposed that inhibition of nuclear PP1 prevents dephosphorylation of the retinoblastoma protein RB during S phase (68). Dephospho RB blocks cells in the G_1 phase of the cell cycle, and needs to be phosphorylated in order for cells to pass into S phase.

The phosphorylation of I-2 on threonine 72 by glycogen synthase kinase-3 (GSK-3) reduces its ability to inhibit PP1 (69). I-2 is also phosphorylated on serines 86, 120, and 121 by Casein Kinase II (CKII). This does not affect PP1 inhibition (70) but greatly facilitates subsequent phosphorylation of Thr-72 by GSK-3 (71,72). When Thr-72, Ser-86, or Ser-120/121 were mutated to alanine, inhibitor-2 did not accumulate in the nucleus, indicating that all of these phosphorylation sites are required for translocation (49). The mode of regulation of I-2 accumulation in the nucleus is unknown, but the degree and location of I-2 phosphorylation changes throughout the cell cycle.

a

```
MAASTASHRP  IKGILKNKTS  TTSSMVASAE  QPRGNVDEEL  SKKSQKWDEM
NILATYHPAD  KDYGLMKIDE  PSTPYHSMMG  DDEDACSDTE  ATEAMAPDIL
ARKLAAAEGL  EPKYRIQEQE  SSGEEDSDLS  PEEREKKRQF  EMKRKLHYNE
GLNIKLARQL  ISKDLHDDDE  DEEMLETADG  ESMNTEESNQ  GSTPSDQQQN
KLRSS
```

b
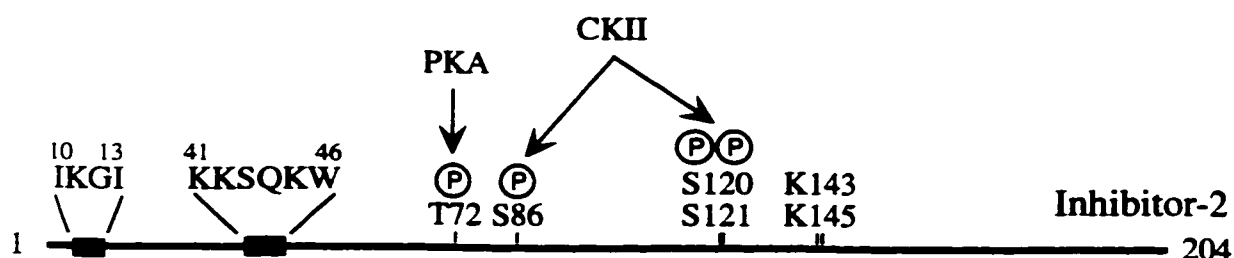
c
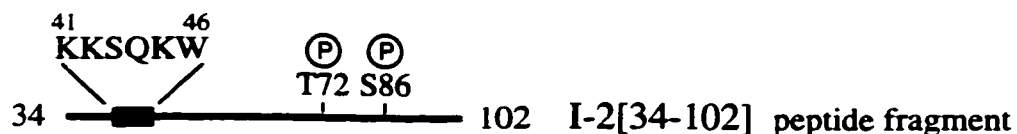
Figure 1-7. *Primary sequence and proposed domain structure of inhibitor-2.* The sequence of human I-2 is shown in panel a. A summary of the regions in I-2 involved in PP1 binding and inhibition, nuclear localization and phosphorylation is presented in panel b. Glycogen Synthase Kinase-3 phosphorylation of Thr-72 is involved in reactivation of PP1 from a stable complex with I-2. Casein Kinase II phosphorylates I-1 at multiple serines. Lysines 143 and 145 are required for nuclear localization of I-2. Conserved sequences IKGI and KKSQKW of inhibitor-2 are proposed to be PP1 binding regions (64,34). Panel c represents a synthetic peptide fragment of inhibitor-2 used throughout this work. This peptide inhibits PP1 at micromolar concentrations instead of the low nanomolar values obtained with full-length inhibitor-2.

There is another suggested physiological function for inhibitor-2. I-2 forms a stable, inactive, 1:1 complex with the PP1 catalytic subunit *in vivo* which is distinct from the rapid and reversible inhibition of PP1 activity which initially occurs (reviewed in 19). *In vitro* activation of PP1 from the complex requires phosphorylation of I-2 with GSK-3 (73). Inhibition of PP1 by I-2 occurs rapidly, is favoured by high concentrations of inhibitor (5-10 fold excess over enzyme) and is not reversed by phosphorylation but is released by proteolytic destruction of the I-2. In contrast, inactivation of PP1 in the stable complex can occur at low concentrations of I-2 (equimolar to PP1), is slow (60 min), and is reversed by phosphorylation of I-2 but not by removal of the inhibitor (74).

The *in vivo* role of the stable I-2/PP1 complex is unknown, and the mechanism of 'reactivation' by GSK-3 phosphorylation is poorly understood. It has been proposed that I-2 phosphorylation promotes a conformational change in the I-2/PP1 complex (75,76). The inactive complex of PP1 and I-2 is postulated to represent a pool of PP1 catalytic subunit, which is maintained inactive and ready to interact with targeting subunits *in vivo* (19,20,30).

An interesting aspect of PP1 complex formation with I-2 is that *in vitro* studies suggest that I-2 can interact with denatured PP1 to promote refolding of the protein to yield an active enzyme, after the complex is phosphorylated by GSK-3 (30). Recombinant PP1 was shown to behave more like native enzyme with respect to substrate specificity, manganese-dependency and inhibitor sensitivity after this procedure (30,31). These observations have led to the proposal that I-2 is a chaperone for PP1 *in vivo*, promoting correct folding of the newly synthesized enzyme into its native

We have very little information regarding the region of PP1 involved in binding to endogenous inhibitor proteins. Much of the evidence supporting common binding sites for I-1 or DARPP-32 and PP1 targeting subunits (via the KIQF sequence) has been determined by competition assays which do not directly measure binding to PP1. In these experiments, PP1 inhibition by I-1 or DARPP-32 is observed in the presence and absence of a competing peptide from a targeting subunit (Chapter Five). In addition, recombinant PP1 is less sensitive than native enzyme to I-1 and DARPP-32. This makes it difficult to assess experiments or computer modelling studies performed with the recombinant enzyme. The nature of the interaction(s) between I-2 and PP1 is also unclear, and will be discussed further in Chapter Four.

Inhibition of PP1 by natural product toxins

PP1 and PP2A are potently inhibited by a variety of naturally occurring toxins. These include: okadaic acid, a polyether fatty acid, diarrhetic shellfish poison and strong tumour promoter produced by single-celled marine organisms; microcystin-LR, a cyclic peptide liver toxin produced by cyanobacteria; and the spiroketal marine sponge metabolite calyculin A (reviewed in 55,78,79) (Figures 1-8, 1-10).

These compounds are important signal transduction research tools because they are small in size (~1000 kDa), cell permeable (okadaic acid and calyculin A), and resistant to proteolysis (microcystin-LR). All are potent inhibitors of PP1 and PP2A, but not PP2B. Okadaic acid can be used to differentiate between PP1 and PP2A because PP1 is 100 fold less responsive to inhibition by this compound.

Microcystins

Toxic cyanobacteria (often called blue-green algae) (reviewed recently in 80-82) are prokaryotes (83) which form colonies of photosynthetic cells that are widely distributed in fresh and marine waters, in soil, and on moist surfaces. Mixed species of cyanobacteria occur in all freshwater, including drinking water reservoirs, and periodically form thick blooms of exponential cell growth on the surface of ponds and lakes.

Over 40 cyanobacteria species of known toxicity have been identified (80) but the factors affecting production of toxins are poorly understood. Cyanobacteria synthesize a variety of neurotoxins and hepatotoxins that are harmful to mammals, birds, and fish (84).

The hepatotoxins have been implicated in poisoning incidents in virtually every corner of the world (83). Livestock and pet deaths due to ingestion of toxic cyanobacteria from water blooms are widely reported in the Northern and Southern Hemispheres (85). Animals die after drinking from ponds or other waters partly covered by 'slimy carpets' of cyanobacteria. Commercial losses to hepatotoxin poisoning are significant. Rural areas where cyanobacterial blooms are endemic suffer yearly losses due to the poisoning of farm animals (81). Cyanobacterial hepatotoxins have been shown to cause severe liver disease associated with high mortality in commercially farmed Atlantic salmon (86). It is not known why cyanobacteria produce toxins.

Microcystins are hepatotoxins produced by cyanobacteria in the genera *Microcystis, Anabaena, Oscillatoria,* and *Nostoc* (reviewed recently in 81,87). These compounds represent a family of cyclic peptides containing a unique C_{20} amino acid Adda ([2S, 3S, 8S, 9S]-3-amino-9-methoxy-2,6,8-trimethyl-10-phenyldeca-4,6-dienoic acid) (88) (Figure 1-8). The general structure of the microcystins is cyclo(-D-Ala-X-D-MAsp-Y-Adda-D-Glu-Mdha) in which X and Y are variable amino acids, Mdha is *N*-methyldehydroalanine and Masp is D-erythro-β-methyl aspartic acid. Most of the variants, which are all cyclic heptapeptides, differ in degree of methylation, configuration of Adda, or in composition of the two variable L-amino acids indicated by suffix letters - L = leucine, R = arginine for microcystin-LR, the most common variant (89). Substitutions in position X and Y are common and lead to minor differences in toxicity. However, changes in amino acid composition can alter the hydrophobicity of the microcystin and thus modify its solubility and cellular permeability (81). Microcystins

a

	Amino Acid	
	X	Y
Microcystin-LR	Leu	Arg
Microcystin-LA	Leu	Ala
Microcystin-LL	Leu	Leu

b

Okadaic Acid
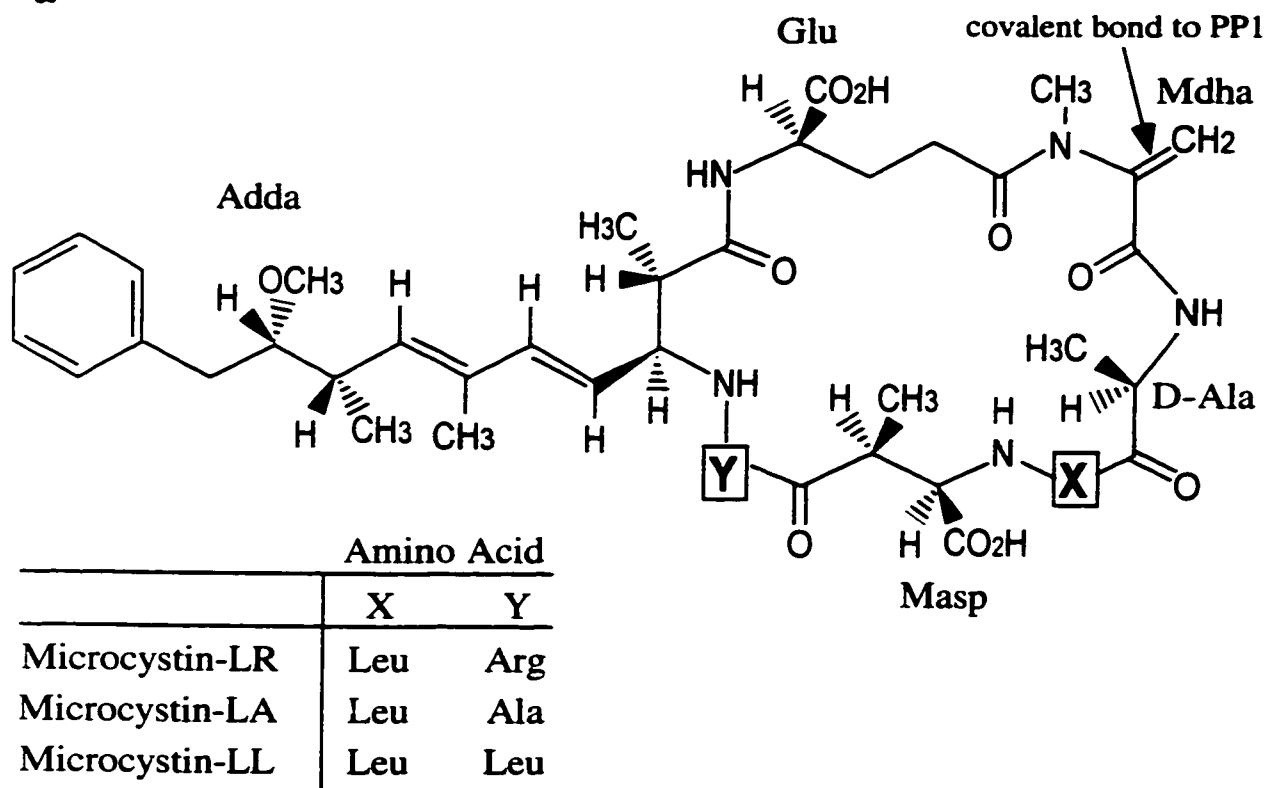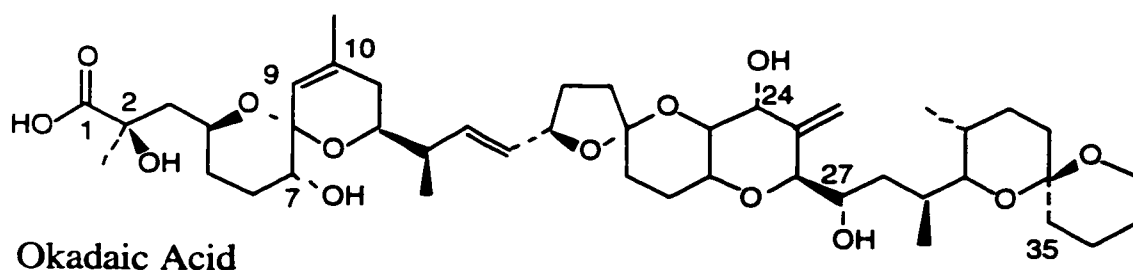
Figure 1-8. *Natural product inhibitors of PP1.* Panel a - cyclic structure of heptapeptide microcystins. Variable L amino acids X and Y are shown in the table. Microcystins contain a unique residue Adda ([2S, 3S, 8S, 9S]-3-amino-9-methoxy-2,6,8-trimethyl-10-phenyldeca-4,6-dienoic acid) as well as N-methyldehydroalanine (Mdha) and D-erythro-β-methyl aspartic acid (Masp). Mdha forms a covalent bond with Cys-273 of PP1 (23). Panel b - linear structure of okadaic acid, a polyether fatty acid.

are not actively secreted, so they may be a defense mechanism of the cyanobacteria (90). As inhibitors of PP1 and PP2A, microcystins damage the phosphorylation networks of organisms (82) (see below).

The intracellular targets of the microcystins are assumed to be the catalytic subunits of PP1 and PP2A. Potent (sub-nanomolar) inhibition of these phosphatases has been well characterized (33,91-93). Given the tight-binding characteristics of the microcystin/PP1 interaction (see below), it is also assumed that inhibition of these enzymes is the molecular basis for the harmful physiological effects of the toxins (81).

Microcystins kill animals by severely damaging the liver. Blood pools in the tissue, leading to fatal circulatory shock within a few hours, or death due to liver failure over the course of several days (83). The mechanism of liver damage is thought to be due to the disruption of the cytoskeletal organization of hepatocytes, which causes the cells to shrink and separate from each other. This in turn forces the sinusoidal capillaries of the liver to separate, allowing blood to accumulate in the tissue (83). Inhibition of PP1 and 2A in liver has been associated with morphological changes in hepatocytes and the breakdown of structural elements such as microfilaments and intermediate filaments (91,94,95).

Numerous studies of mammals injected with microcystins have shown that almost all of the toxin accumulates in the liver (reviewed in 81). In mice, a lethal dose of 65 µg microcystin-LR per kg body weight (intraperitoneal injection) results in death within several hours due to liver hemorrhage and hepatic necrosis (96). Microcystin is considerably less toxic when administered orally - 11 mg/kg. However, the frequency of

animal deaths after drinking water contaminated by cyanobacteria indicates that at sufficiently high doses, the peptide is absorbed through the intestinal tract into the bloodstream (81). Transport into hepatocytes is thought to occur via the bile acid transporter system or a related anion carrier (97,98) although this has not been confirmed.

Microcystin-LR is also a tumour promoter (99). Tumour growth in rat livers and mouse skin is enhanced when mice are pretreated with a tumour initiator and then exposed to microcystin-LR, intraperitoneally or orally (81, and references therein). The mechanism of tumour promotion is unclear, but is possible linked to the increase in protein phosphorylation observed when PP1 is inhibited (80).

Until recently, there were no reported deaths of humans due to cyanobacterial intoxication. In 1996, patients undergoing haemodialysis in Brazil fell ill following the use of water from a reservoir with a massive growth of cyanobacteria (100-102). 60 patients died, out of a total of 126 who were afflicted with muscle pain, weakness, nausea, liver tenderness, and a range of neurological symptoms. Microcystins were detected in water from the reservoir, on dialysis filters, and in the liver tissue of patients who died. Patients are exposed to approximately 360 L of water per week during dialysis treatment, so even low levels of microcystin in the water supply are hazardous in this situation.

The presence of microcystins in drinking water is a growing concern. Extraordinarily high rates of liver cancer in parts of rural China may be tied to microcystin contamination (83), raising concerns about chronic ingestion of the toxin. The World Health Organization and Health Canada have recently established guidelines for levels of microcystins in drinking water of 1.0 and 1.5 µg/L respectively (103). Microfiltration to

remove cyanobacterial cells, coupled with adsorption of microcystin by activated carbon filters, can remove >80% microcystins from the water supply (81). However, high levels of microcystins have been observed in drinking water supplies (even in Western Canada) when blooms of cyanobacteria were killed by treatment with copper sulfate (personal communication, S. Gurney, Manitoba Environment).

Structure of microcystin-LR bound to PP1 (Figure 1-9)

An x-ray crystallographic structure of microcystin-LR bound to PP1 was published by Goldberg et al. in 1995 (23). Microcystin-LR was observed to interact with three distinct regions of PP1. The first involves the carboxyl and adjacent carbonyl group of the microcystin glutamic acid residue. These groups interact with two of the metal-bound water molecules in the catalytic site of the phosphatase. This appears to directly block substrate access to the catalytic site of the enzyme (23). Second, the Adda side chain of microcystin-LR binds in a hydrophobic surface groove near the active site of PP1. Finally, Cys-273 of PP1 forms a covalent bond to the Mdha residue of the toxin.

The 3-D structure also suggests the existence of a hydrogen bond between the D-erythro-β-methyl aspartic acid (Masp) carboxylate group and Tyr-134 of PP1 (23). Tyr-272 of the phosphatase packs against the variable leucine residue of the microcystin. Mutagenesis studies of Tyr-272 in PP1 have shown that mutation or deletion of this residue results in dramatic loss of inhibition by microcystin-LR, okadaic acid, calyculin A and other PP1 inhibitors (104). As seen in Figure 1-9, the variable position arginine
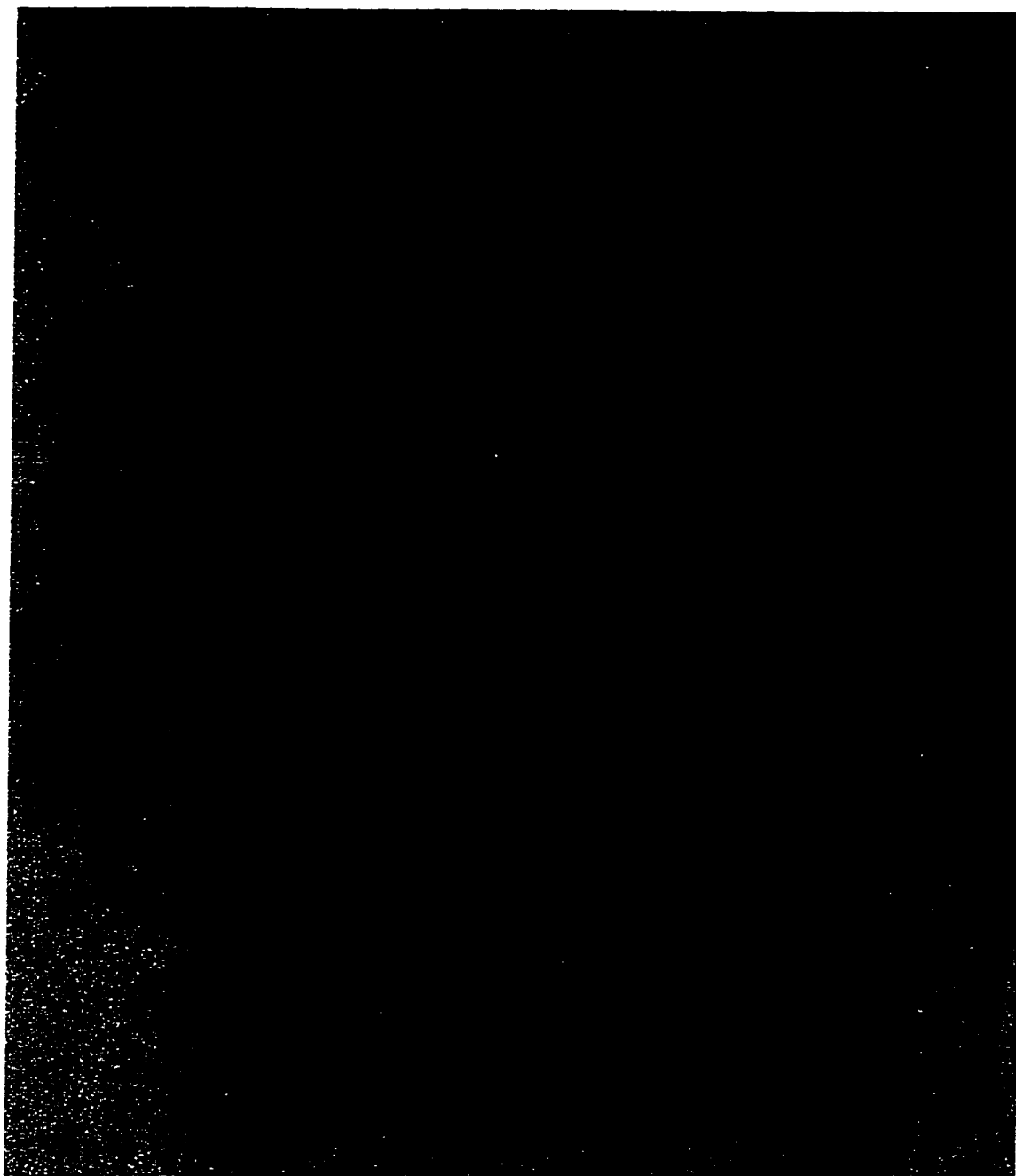
Figure 1-9. *Structure of microcystin-LR bound covalently to Cys-273 of PP1.* Microcystin-LR (in red) blocks substrate access to the active site of PP1. Manganese ions in the catalytic site are shown as pink spheres. Cys-273 of PP1 (shown in green) forms a covalent bond to the Mdha residue of the toxin. As indicated, the variable position arginine and leucine residues of the microcystin are directed away from the catalytic site of the phosphatase, allowing substitutions at these positions in the toxin without affecting inhibitory ability. The PP1α/microcystin-LR structure shown is derived from coordinates published by Goldberg et al., 1995. (see text for details)

residue of the microcystin is directed away from the catalytic site of the phosphatase. This explains why substitutions at this position in the toxin do not affect inhibitory ability (105 and references therein). Variants of microcystin which contain substitutions at the leucine position ('X') are less commonly studied, but often have amino acids (e.g. microcystin-YM) which appear to interact equally well with PP1 (106,107).

The covalent bond between Cys-273 of PP1 and the Mdha group in microcystin-LR forms slowly *in vitro* (108), and has been determined to be a separate event from the initial, rapid inhibition of phosphatase activity (106,107). The effects of covalent complex formation *in vivo* are unknown; microcystin detection and toxicity in light of the covalent interaction is discussed in Chapter Two.

Other natural product phosphatase inhibitors are thought to bind at the catalytic site of the enzyme because inhibition of PP1 by microcystin-LR is prevented by okadaic acid and calyculin A (33,109).

In summary, identification and isolation of microcystins from the aquatic environment will be discussed in Chapter Two. Given the toxicity and tumour-promoting capabilities of these toxins, it is important to develop techniques for the sensitive detection of microcystins in the food-chain.

Calyculins

The first member of the calyculin family of phosphatase inhibitors was identified in 1986 (110). Calyculin A was originally purified from a hydrophobic extract of the marine sponge *Discodermia calyx* because of observed cytotoxicity toward P388 and L1210 leukemia cells (110,111). It was subsequently characterized as a powerful inhibitor of the catalytic subunits of type 1 and 2A protein phosphatases (PP1 and PP2A) (112). Many additional calyculins (113-118), and the structurally related calyculinamides (116,119), have since been identified in *D. calyx* and the New Zealand deep-water sponge *Lamellomorpha strongylata* (Figure 1-10). Marine invertebrates represent an abundant source of naturally, biologically active compounds. The calyculins may be produced as chemical defense mechanisms to protect sponges from environmental dangers such as predation (118).

Calyculins have an interesting polyfunctional structure that includes a novel spiro-ketal with a backbone bearing phosphate, oxazole, and a tetraenic nitrile or amide (Figure 1-10). Calyculin family members B-H differ in the geometry of the tetraene portion of the molecule and the presence/absence of a methyl group on C-32. Calyculinamides have an amide group replacing the terminal nitrile. Despite these differences, calyculins and calyculinamides display similar inhibitory activity against PP2A. Recently, our laboratory (in collaboration with Dr. F. Schmitz, University of Oklahoma) reported the isolation of two novel glycosylated members of the calyculin family, clavosines A and B from the marine sponge *Myriastra clavosa* (120). The clavosines have an unusual trimethoxy rhamnose group at position C-21 but are still able to potently inhibit both

a
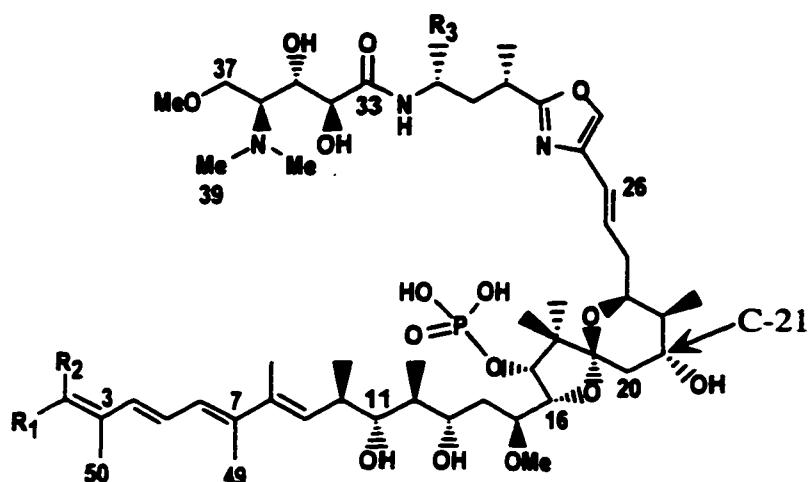
Calyculin A : R1=H, R2=CN, R3=H (0.9 nM)

Clavosine A : R1=H, R2=CONH2, R3=Me C-21=Rhamnose (0.6 nM)
Clavosine B : R1=CONH2, R2=H, R3=Me C-21=Rhamnose (1.2 nM)

Calyculinamide A : R_1=H, R_2=CONH$_2$, R_3=H (0.5 nM)
Calyculinamide B : R_1=CONH$_2$, R_2=H, R_3=H (ND)

Calyculin B : R_1=CN, R_2=H, R_3=H (6.0 nM)
Calyculin C : R_1=H, R_2=CN, R_3=CH$_3$ (1.0 nM)
Calyculin D : R_1=CN, R_2=H, R_3=CH$_3$ (5.2 nM)

b
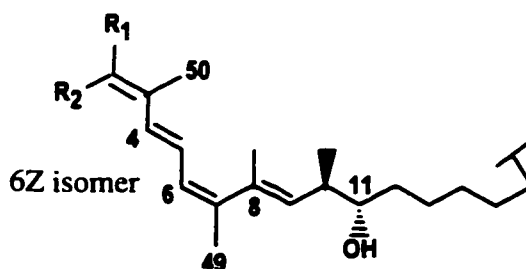
6Z isomer

Calyculin F : 6Z isomer of Calyculin B (2.7 nM)
Calyculin G : 6Z isomer of Calyculin C (3.2 nM)
Calyculin E : 6Z isomer of Calyculin A (5.6 nM)
Calyculin H : 6Z isomer of Calyculin D (6.0 nM)

Figure 1-10. *Structures of the calyculin family of phosphatase inhibitors.* Panel a-Linear diagrams of the calyculins. Calyculins are multifunctional molecules which contain a phosphate monoester, a tetraenic cyanide/amide, an oxazole ring, and a dimethylamine. Family members differ with respect to orientation of the terminal cyanide/amide and methylation of C-32. Clavosines A and B have an unusual C-21 trimethoxy rhamnose group with a corresponding 21(S) configuration. Panel b-Calyculins H-F represent the 6Z isomers of Calyculins A-D. Photochemical isomerization of the C-6 double bond in these compounds converts them to 6E isomers shown in panel a. Numbers in brackets represent IC$_{50}$ values for inhibition of rabbit skeletal muscle PP2A (ND= no data).

PP1 and PP2A. In addition, a naturally-occurring dephospho analogue of calyculin A has also been found to strongly inhibit PP1 and PP2A with IC_{50} concentrations of 3.0 and 8.2 nM, respectively (117).

The phosphate group of calyculin A serves as the centre of an internal hydrogen bonding network which maintains the compact nature of the molecule, as seen in the crystal structure (Chapter Three). Hydrogen-bonding constrains the polar phosphate moiety to the interior of the calyculin, providing resistance to normal hydrolyzing conditions (110). A consequence of the compact structure is that the outer surface of the toxin is hydrophobic in nature. This allows calyculin A to be membrane permeable (121).

In the liver, calyculin A causes cytoskeletal rearrangement, with functional and structural changes similar to those observed with microcystin-LR (122). This is probably a direct consequence of phosphatase inhibition. Calyculin A is as potent as okadaic acid as a tumor promoter on mouse skin (123). Tumour promoters such as okadaic acid, microcystin-LR and calyculin A have been found to induce the clonal expansion of cells that have been mutated (initiated) by treatment with dimethylbenzanthracene (124).

Calyculinamides A and B (Figure 1-10) are potent cell-growth inhibitors with a high degree of differential activity against a range of tumour cell lines in the National Cancer Institute's (NCI) screening system (125). This is in contrast to calyculins A and B, which were potent growth inhibitors but showed markedly less differential effects (119). Therefore, the amide portion of calyculinamides does not significantly affect IC_{50} but does appear to affect cytotoxicity, by an unknown mechanism. Interestingly, the clavosines were found to be more cytotoxic than both the calyculins and the

calyculinamides (119,120) in the NCI's screening panel of tumour cell-lines. A discussion of the role of the rhamnose moiety in clavosine inhibition and toxicity is discussed in Chapter Three.

Interaction of the calyculins with PP1

The mode of interaction of calyculin family members with PP1 is controversial, with many binding models proposed in the literature (Chapter Three) (126-128). The calyculin phosphate group is an important part of an 'extended' model of calyculin binding to PP1, which proposes that the phosphate-containing calyculin is a mimic of the phosphorylated PP1 inhibitor protein I-1. Models of calyculin A binding are often based on models of inhibitor-1 binding, which are themselves based on the crystal structure of tungstate bound to PP1 (24). The importance of more structural work in this area cannot be overstated.

A dephospho analogue of calyculin A has been found to strongly inhibit PP1 (117). This suggests that the phosphate group may not play a major role in the interaction of calyculin A with the phosphatase. Recently, the NMR solution structures of calyculin A and dephosphonocalyculin A were determined (129). The structure of dephosphonocalyculin A was found to be quite similar to that of calyculin A in both methanol and chloroform, implying that the phosphate group is not solely responsible for determining or stabilizing the calyculin structure.

The geometries of the tetraene portion (6Z vs. 6E) of the calyculins, and the presence or absence of a methyl group on C-32, do not affect PP1 inhibition (114). A

synthetic isopropylidene derivative formed between the C-11 and C-13 hydroxyl groups was shown to inhibit PP2A at concentrations greater than 1 micromolar, thus these hydroxyl groups are likely involved in phosphatase inhibition (53). Loss of a methyl group from the C-36 nitrogen also results in reduction of activity (IC_{50}= 49 nM) (116).

Competition studies using unlabelled inhibitors and radiolabelled okadaic acid determined that okadaic acid, calyculin A and microcystin-LR appear bind to PP1 and PP2A in a mutually exclusive manner. These inhibitors may share a common or overlapping binding site on PP1 and 2A, at the active site of the enzyme (109).

In summary, models of calyculin binding to PP1 must address three aspects of the calyculin and clavosine structures: the position of the phosphate group with respect to the phosphatase; correlation of IC_{50} data for the amide/nitrile portion of the tetraene tail and the geometry of the C-6 double bond; and accommodation of the rhamnose moiety in a manner that does not interfere with clavosine binding to PP1. Our models of clavosine and calyculin A binding to PP1 are discussed in Chapter Three.

Technical considerations regarding potent inhibitors of PP1

The natural product toxins discussed in this thesis inhibit PP1 with IC_{50} values in the picomolar to low nanomolar range (Chapters Two and Three). When the steady-state dose-inhibition relationship is analyzed, microcystin-LR, calyculin A, okadaic acid, and other inhibitors act on PP1 as 'tight-binding' inhibitors (130) to which conventional methods of data analysis based on Michaelis-Menten kinetic equations do not apply (109). Standard kinetic analyses are limited by the assumption that the amount of inhibitor bound to the enzyme is negligible compared with the concentration of inhibitor free in solution. This assumption is invalid when the inhibitor binds very tightly to the enzyme and the concentration of the enzyme is relatively high (i.e. similar to that of the inhibitor), because levels of free inhibitor are low (109). In PP1 inhibition assays discussed throughout this work, the concentration of enzyme is typically 0.2 - 0.4 nM. This concentration is similar to the IC_{50} values of many of the natural product and endogenous inhibitors of native PP1.

It has been recognized that the molar concentration of the enzyme is an extremely important parameter in experiments with tight-binding inhibitors (109). The degree of inhibition observed with a specific amount of inhibitor will vary according to the amount of enzyme in the assay, thus care must be taken in order to accurately study the potent inhibition of PP1 (see also Chapter Two, Experimental Procedures).

Prokaryotic protein phosphatases

A brief discussion of prokaryotic phosphatases is relevant to this work, given that many potent inhibitors of eukaryotic protein phosphatases are produced by prokaryotic organisms.

Several examples of protein phosphatases have been characterized in Archaea and Bacteria. They include PP1-like enzymes from the thermophilic archaeon *Sulfolobus solfataricus* (131,132), methanogenic archaeon *Methanosarcina thermophilia* (okadaic acid sensitive (133,134), hyperthermophilic archaeon *Pyrodictium abyssi* (135); the cyanobacteria *Microcystis aeruginosa* (136); and *E. coli* bacteria (137). The physiological roles of the archaeal and cyanobacterial protein phosphatases are unknown (90). In *E. coli*, protein phosphatases form part of a signal transduction pathway that senses protein misfolding caused by heat shock or other stresses (137).

Prokaryotic representatives of the PPP family share several common properties. All can be expressed as active monomers of 25-35 kDa, similar to the catalytic subunit of PP1 from eukaryotes (90,132). The archaeal phosphatases exhibit approximately 30% identity to the catalytic subunit of mammalian PP1 (131,132,134) and cyanobacterial phosphatase PP1-cyano2 exhibits 50% identity to yeast PP1 and 43% to rabbit PP2A in the conserved catalytic domain (136). Most of the archael and cyanobacterial phosphatases are resistant to classic PP1 inhibitors such as microcystin-LR and okadaic acid (90), although two archaeal forms displayed moderate sensitivity to these compounds (133-135). Resistance to the toxins is especially relevant in the case of the

cyanobacterial enzymes, as this may be essential for surviving the effects of their endogenous toxins or those of toxin-producing neighbours (90).

Specific goals and hypotheses of my research

Microcystins (Chapter Two)

<u>Part I</u>

- Our goal for this project was to identify and characterize the hydrophobic phosphatase inhibitors previously detected in cyanobacterial extracts in our laboratory. Our hypothesis was that hydrophobic microcystins exist, and that they could be important, cell permeable, tools for signal transduction research. One of the hydrophobic microcystins identified, microcystin-LL, later proved to be invaluable in the characterization of the mechanism of covalent bond formation with PP1.

<u>Part II</u>

- Our goal for this project was to discover the source of the toxin which had been linked to severe liver disease in commercially farmed Atlantic salmon (Net-pen Liver Disease, NLD). Our hypothesis was that salmon were consuming microcystin-LR in their diet, as opposed to absorption from seawater, and that there must exist an intermediate microcystin-containing zooplankton vector, as no local phytoplankton source of microcystin-LR could be detected. These studies were expected to provide further information concerning the *in vivo* effects of the microcystins, as NLD represents a model system for investigating microcystin toxicity in the food chain.

Calyculins (Chapter Three)

- Our goal for this research was to investigate the interaction between the calyculin family of phosphatase inhibitors and PP1. In collaboration with Dr. F. Schmitz, University of Oklahoma, we determined that marine sponge metabolites clavosine A and B were potent inhibitors of PP1. Publication of the x-ray crystallographic structure of PP1 in 1995 (23) opened up a tremendous number of experimental avenues including rationally designed PP1 mutagenesis and computer modelling of inhibitors bound to the enzyme. Our hypothesis was that calyculin A and the clavosines interacted similarly with the enzyme, and that a structural model of calyculin binding to PP1 could be derived from data generated by experiments with mutant PP1 enzymes and the inhibitors. We were extremely interested in calyculin inhibition and binding because of the presence of a phosphate group in the calyculin structure. It had been previously suggested in the literature that the calyculin phosphate may mimic a phosphorylated endogenous PP1 inhibitor protein, I-1, which was already a focus of my doctoral research (see below).

Inhibitor-2 (Chapter Four)

- Our goal for this work was to find a minimally active fragment of I-2, an endogenous protein inhibitor of PP1. Our hypothesis was that we could further define the specific region of the inhibitor-2 protein that is involved in PP1 binding and inhibition, as had been previously determined for I-1, another endogenous PP1 inhibitor protein. We were also interested in finding out whether a short I-2 fragment could behave

similarly to full-length I-2 with respect to GSK-3 phosphorylation and reactivation of recombinant PP1 to a native-like state.

Inhibitor-1 (Chapters Five and Six)

To investigate distinct regions in inhibitor-1 that are thought to be involved in PP1 binding and inhibition, we undertook two complementary research projects.

- The goal of the first project was to study the putative PP1 binding motif sequence in inhibitor-1. In 1997, the crystal structure of PP1 bound to a peptide from the targeting subunit G_M was published (54). This discovery prompted us to examine whether inhibitor-1 interacted with PP1 through a related binding sequence. Our hypothesis was that we could determine with competition experiments whether inhibitor-1 binds to PP1 through a short, N-terminal sequence ($^9KIQF^{12}$), and also establish the optimal PP1 binding sequence for I-1, using a peptide library produced by Devon Husband (PENCE, University of Alberta).

- The goal of the second project was to determine whether a series of sequential arginine residues preceding the PKA phosphorylation site in inhibitor-1 is involved in PP1 binding and inhibition. Other researchers have created models of I-1 binding which suggest that these arginine residues interact with an acidic groove on the surface of enzyme, but site-directed mutagenesis of PP1 could not confirm this idea. Our hypothesis was that step-wise substitution of the arginines in peptides based on an active I-1 fragment would allow us to determine the role of these residues in PP1 binding and inhibition.

References

1. Barford, D., Das, A. K., and Egloff, M.-P. (1998) *Annu. Rev. Biophys. Biomol. Struct.* **27**, 133-164

2. Jia, Z. (1997) *Biochem. Cell Biol.* **75**, 17-26

3. Guan, K., Broyles, S. S., and Dixon, J. E. (1991) *Nature* **350**, 359-362

4. Charbonneau, H., and Tonks, N. K. (1992) *Annu. Rev. Cell. Biol.* **8**, 463-493

5. DePaoli-Roach, A. A., Park, I.-K., Cerovsky, V., Csortos, C., Durbin, S. D., Kuntz, M. J., Sitikov, A., Tang, P. M., Verin, A., and Zolnierovicz, S. (1994) *Advan. Enzyme Regul.* **34**, 199-224

6. Shenolikar, S. (1994) *Ann. Rev. Cell. Biol.* **10**, 55-86

7. Oliver, C. J., and Shenolikar, S. (1998) *Front Biosci* **3**, d961-972

8. Villafranca, J. E., Kissinger, C. R., and Parge, H. E. (1996) *Curr. Opin. Biotech.* **7**, 397-402

9. Cohen, P. (1991) *Meth. Enzymol.* **201**, 389-398

10. Cohen, P. T. W. (1994) *Adv. Prot. Phosphatases* **8**, 371-376

11. Barton, G. J., Cohen, P. T. W., and Barford, D. (1994) *Eur. J. Biochem.* **220**, 225-237

12. Cohen, P. T. W., Brewis, N. D., Hughes, V., and Mann, D. J. (1990) *FEBS Lett.* **268**, 355-359

13. Orgad, S., Brewis, N. D., Alphey, L., Axton, J. M., Dudai, Y., and Cohen, P. T. W. (1990) *FEBS Lett.* **275**, 44-48

14. Shima, H., Haneji, T., Hatano, Y., Kasugi, I., Sugimura, T., and Nagao, M. (1993) *Biochem. Biophys. Res. Commun.* **194**, 930-937

15. Cohen, P. T. W. (1988) *FEBS Lett.* **232**, 17-23

16. Dombradi, V., Axton, J. M., Barker, H. M., and Cohen, P. T. W. (1990) *FEBS Lett.* **275**, 39-43

17. Sasaki, K., Shima, H., Kitagawa, Y., Irino, S., Sugimura, J., and Nagoa, M. (1990) *Jpn. J. Cancer Res.* **81**, 1272-84

18. Mumby, M. C., and Walter, G. (1993) *Phys. Rev.* **73**, 673-699

19. Bollen, M., and Stalmans, W. (1992) *Crit. Rev. Biochem. Mol. Biol.* **27**, 227-281

20. Cohen, P., and Cohen, P. T. W. (1989) *J. Biol. Chem.* **36**, 21435-38

21. Hubbard, M. J., and Cohen, P. (1993) *Trends Biochem. Sci.* **18**, 172-177

22. Faux, M. C., and Scott, J. D. (1996) *Trends Biochem. Sci.* **21**, 312-315

23. Goldberg, J., Huang, H. B., Kwon, Y. G., Greengard, P., Nairn, A. C., and Kuriyan, J. (1995) *Nature* **376**, 745-753

24. Egloff, M. P., Cohen, P. T. W., Reinemer, P., and Barford, D. (1995) *J. Mol. Biol.* **254**, 942-959

25. King, M. M., and Huang, C. Y. (1984) *J. Biol. Chem.* **259**, 8847-56

26. Yu, L., Haddy, A., and Rusnak, F. (1995) *J. Am. Chem. Soc.* **117**, 10147-48

27. Zhuo, S., Clemens, J. C., Stone, R. L., and Dixon, J. E. (1994) *J. Biol. Chem.* **269**, 26234-38

28. Zhang, L., Zhang, Z., Brew, K., and Lee, E. Y. (1996) *Biochemistry* **35**, 6276-82

29. Huang, H. B., Horiuchi, A., Goldberg, J., Greengard, P., and Nairn, A. C. (1997) *Proc. Natl. Acad. Sci. U.S.A.* **94**, 3530-35

30. Alessi, D. R., Street, A. J., Cohen, P., and Cohen, P. T. W. (1993) *Eur. J. Biochem.* **213**, 1055-66

31. MacKintosh, C., Garton, A. J., McDonnell, A., Barford, D., Cohen, P. T., Tonks, N. K., and Cohen, P. (1996) *FEBS Lett.* **397**, 235-238

32. Zhang, A. J., Bai, G., Deans-Zirattu, S., Browner, M. F., and Lee, E. Y. (1992) *J. Biol. Chem.* **267**, 1484-90

33. MacKintosh, C., Beattie, K. A., Klumpp, S., Cohen, P., and Codd, G. A. (1990) *FEBS Lett.* **264**, 187-192

34. Helps, N. R., Vergidou, C., Gaskell, T., and Cohen, P. T. W. (1998) *FEBS Lett.* **438**, 131-136

35. Johnson, D. F., Moorhead, G., Caudwell, F. B., Cohen, P., Chen, Y. H., Chen, M. X., and Cohen, P. T. (1996) *Eur. J. Biochem.* **239**, 317-325

36. Cohen, P. (1992) *Trends Biochem. Sci.* **17**, 408-413

37. Stralfors, P., Hiraga, A., and Cohen, P. (1985) *Eur. J. Biochem.* **149**, 295-303

38. Tang, P. M., Bondor, J. A., Swiderek, K. M., DePaoli-Roach, A. A. (1991) *J. Biol. Chem.* **266**, 15782-89

39. Nakielny, S., Campbell, D. G., and Cohen, P. (1991) *Eur. J. Biochem.* **199**, 713-722

40. Hubbard, M. J., and Cohen, P. (1989) *Eur. J. Biochem.* **180**, 457-465

41. Alessi, D. R., McDougall, L. K., Sola, M. M., Ikebe, M., and Cohen, P. (1992) *Eur. J. Biochem.* **210**, 1023-35

42. Moorhead, G., MacKintosh, W., Morrice, N., Gallagher, T., and MacKintosh, C. (1994) *FEBS Lett.* **356**, 46-50

43. Chen, Y. H., Chen, M. X., Alessi, D. R., Campbell, D. G., Shanahan, C., Cohen, P., and Cohen, P. T. W. (1994) *FEBS Lett.* **356**, 51-55

44. Doherty, M. J., Moorhead, G., Morrice, N., Cohen, P., and Cohen, P. T. W. (1995) *FEBS Lett.* **375**, 294-298

45. Moorhead, G., MacKintosh, C., Morrice, N., and Cohen, P. (1995) *FEBS Lett.* 101-105

46. Hagiwara, M., Alberts, A., Brindle, P., Meinkoth, J., Feramisco, J., Deng, T., Karin, M., Shenolikar, S., and Montminy, M. (1992) *Cell* **70**, 105-113

47. Van Eynde, A., Wera, S., Beullens, M., Torrekens, S., Van Leuven, F., Stalmans, W., and Bollen, M. (1995) *J. Biol. Chem.* **270**, 28068-74

48. Allen, P. B. (1998) *J. Biol. Chem.* **273**, 4089-95

49. Kakinoki, Y., Somers, J., and Brautigan, D. L. (1997) *J. Biol. Chem.* **272**, 32308-14

50. Helps, N., Barker, M., Elledge, S. J., and Cohen, P. T. W. (1995) *FEBS Lett.* **377**, 295-300

51. Ludlow, J. W., Glendening, C. L., M., L. D., and DeCaprio, J. A. (1993) *Mol. Cell. Biol.* **13**, 367-372

52. Sherr, C. J. (1996) *Science* **274**, 1672-77

53. Fujiki, H., and Suganuma, M. (1993) *Adv. Cancer Res.* **61**, 143-194

54.   Egloff, M. P., Johnson, D. F., Moorhead, G., Cohen, P. T., Cohen, P., and Barford, D. (1997) *EMBO J.* 16, 1876-87

55.   Sheppeck, I. J., Gauss, C. M., and Chamberlin, A. R. (1997) *Bioorg. Med. Chem.* 5, 1739-50

56.   Walaas, S. I., Aswad, D. W., and Greengard, P. (1983) *Nature* 301, 69-71

57.   Hemmings, H. C., Jr., Girault, J. A., Nairn, A. C., Bertuzzi, G., and Greengard, P. (1992) *J. Neurochem.* 59, 1053-61

58.   Stralfors, P., Hemmings, H. C., Jr., and Greengard, P. (1989) *Eur. J. Biochem.* 180, 143-148

59.   Aperia, A., Bertorello, A., and Seri, I. (1987) *Am. J. Physiol.* 252, F39-45

60.   Snyder, G. L., Girault, J. A., Chen, J. Y., Czernik, A. J., Kebabian, J. W., Nathanson, J. A., and Greengard, P. (1992) *J. Neurosci.* 12, 3071-83

61.   Hemmings, H. C., Jr., Nairn, A. C., Elliott, J. I., and Greengard, P. (1990) *J. Biol. Chem.* 265, 20369-76

62.   Desdouits, F., Cohen, D., Nairn, A. C., Greengard, P., and Girault, J. A. (1995) *J Biol Chem* 270, 8772-78

63.   Endo, S., Zhou, X., Connor, J., Wang, B., and Shenolikar, S. (1996) *Biochemistry* 35, 5220-28

64.   Huang, H.-b., Horiuchi, A., Watanabe, T., Shih, S.-R., Tsay, H.-J., Li, H.-C., Greengard, P., and Nairn, A. C. (1999) *J. Biol. Chem.* 274, 7870-78

65.   Connor, J. H., Quan, H. N., Ramaswamy, N. T., Zhang, L., Barik, S., Zheng, J., Cannon, J. F., Lee, E. Y., and Shenolikar, S. (1998) *J. Biol. Chem.* 273, 27716-24

66.   Huang, F. L., and Glinsmann, W. H. (1976) *Eur. J. Biochem.* 70, 419-426

67.   Brautigan, D. L., Sunwoo, J., Labbe, J. C., Fernandez, A., and Lamb, N. J. (1990) *Nature* 344, 74-78

68.   Nelson, D. A., Krucher, N. A., and Ludlow, J. W. (1997) *J. Biol. Chem.* 272, 4528-35

69.   Aitken, A., Holmes, C. F., Campbell, D. G., Resink, T. J., Cohen, P., Leung, C. T., and Williams, D. H. (1984) *Biochim. Biophys. Acta* 790, 288-291

70.   Holmes, C. F., Kuret, J., Chisholm, A. A., and Cohen, P. (1986) *Biochim. Biophys. Acta* 870, 408-416

71.   DePaoli-Roach, A. A. (1984) *J. Biol. Chem.* 259, 12144-52

72.   Park, I. K., Roach, P., Bondor, J., Fox, S. P., and DePaoli-Roach, A. A. (1994) *J. Biol. Chem.* 269, 944-954

73.   Hemmings, B. A., Resink, T. J., and Cohen, P. (1982) *FEBS Lett* 150, 319-324

74.   Park, I. K., and DePaoli-Roach, A. A. (1994) *J. Biol. Chem.* 269, 28919-28

75.   Villa-Moruzzi, E., Ballou, L. M., and Fischer, E. H. (1984) *J. Biol. Chem.* 259, 5857-63

76.   Jurgensen, S., Shacter, E., Huang, C. Y., Chock, P. B., Yang, S. D., Vandenheede, J. R., and Merlevede, W. (1984) *J. Biol. Chem.* 259, 5864-70

77.   Kwon, Y. G., Huang, H. B., Desdouits, F., Girault, J. A., Greengard, P., and Nairn, A. C. (1997) *Proc. Natl. Acad. Sci. U.S.A* 94, 3536-41

78.   MacKintosh, C., and MacKintosh, R. W. (1994) *Trends Biochem. Sci.* 17, 444-447

79. Honkanen, R. E., Codispoti, B. A., Tse, K., Boynton, A. L., and Honkanan, R. E. (1994) *Toxicon* 32, 339-350

80. Falconer, I. R. (1998) in *Quality and Treatment of Drinking Water II* (Hrubec, J., ed.), Springer-Verlag, Berlin, pp. 53-82

81. Craig, M., and Holmes, C. F. B. (1999) in *Toxicity of aquatic organisms: pharmacology, physiology and mode of action* (Botana, L. M., and Dekker, M., eds.), (In press)

82. Carmichael, W. W. (1997) *Adv. Botanical Res.* 27, 211-256

83. Carmichael, W. W. (1994) *Sci. Am.* 270, 78-86

84. Codd, G. A., Ward, C. J., and Bell, S. G. (1997) *Arch. Toxicol.* S19, 399-410

85. Carmichael, W. W., and Falconer, I. R. (1993) In: *Algal toxins in seafood and drinking water*, (Falconer, I. R., ed), Academic Press, London, pp. 187-204

86. Andersen, R. J., Luu, H. A., Chen, D. Z., Holmes, C. F., Kent, M. L., Le Blanc, M., Taylor, F. J., and Williams, D. E. (1993) *Toxicon* 31, 1315-23

87. Dawson, R. M. (1998) *Toxicon* 36, 953-962

88. Botes, D. P., Wessels, P. L., Kruger, H., Runnegar, M. T. C., Santikarn, S., Smith, R. J., Barna, J. C. J., and Williams, D. H. (1985) *J. Chem. Soc. Perkin Trans.* 1, 2747-52

89. Rinehart, K. L., Harada, K. I., Namikoshi, M., Chen, C., Harvis, C. A., Munro, M. H. G., Blunt, J. W., Mulligan, P. E., Beasley, V. R., Dahlem, A. M., and Carmichael, W. W. (1988) *J. Am. Chem. Soc.* 110, 557-558

90. Kennelly, P. J., and Potts, M. (1999) *Front. Biosci.* 4, d372-385

91. Eriksson, J. E., Toivola, D., Meriluoto, J. A., Karaki, H., Han, Y. G., and Hartshorne, D. (1990) *Biochem. Biophys. Res. Commun.* 173, 1347-53

92. Yoshizawa, S., Matsushima, R., Watanabe, M. F., Harada, K. I., Ichihara, K., Carmichael, W. W., and Fujiki, H. (1990) *J. Cancer Res. Clin. Oncol.* 116, 609-614

93. Honkanen, R. E., Zwiller, J., Moore, R. E., Daily, S. L., Khatra, B. S., Dukelow, M., and Boynton, A. L. (1990) *J. Biol. Chem.* 265, 19401-14

94. Wickstrom, M. L., Khan, S. A., Haschek, W. M., Wyman, J. F., Eriksson, J. E., Schaeffer, D. J., and Beasley, V. R. (1995) *Toxicol. Pathol.* 23, 326-337

95. Wickstrom, M., Haschek, W., Henningsen, G., Miller, L. A., Wyman, J., and Beasley, V. (1996) *Nat. Toxins* 4, 195-205

96. Runnegar, M., Berndt, N., and Kaplowitz, N. (1995) *Toxicol. Appl. Pharmacol.* 134, 264-272

97. Dahlem, A. M., Hassan, A. S., Swanson, S. P., Carmichael, W. W., and Beasley, V. R. (1988) *Pharmacol. Toxicol.* 63, 1-

98. Falconer, I. R., Dornbusch, M., Moran, G., and Yeung, S. K. (1992) *Toxicon* 30, 790-793

99. Fujiki, H., and Suganuma, M. (1996) *J. Toxicol.-Toxin Rev.* 15, 129-156

100. Yu, S.-Z. (1995) *J. Gastroenterol. Hepatol.* 10, 674-682

101. Jochimsen, E. M., Carmichael, W. W., An, J.-S., Cardo, D. M., Cookson, S. T., Holmes, C. E. M., de C. Antunes, M. B., de Melo Filho, D. A., Lyra, T. M., Barreto, V. S. T., Azevedo, S. M. F. O., and Jarvis, W. R. (1998) *N. Engl. J. Med.* **338**, 873-878

102. Pouria, S., de Andrade, A., Barbosa, J., Cavalcanti, R. L., Barreto, V. T. S., Ward, C. J., Preiser, W., Poon, G. K., Neild, G. H., and Codd, G. A. (1998) *The Lancet* **352**, 21-26

103. WHO Working group meeting on chemical substances in drinking water (1997) Geneva, Report Section 5.2

104. Zhang, L., Zhang, Z., Long, F., and Lee, E. Y. (1996) *Biochemistry* **35**, 1606-11

105. Sivonen, K. (1996) *Phycologia* **35**, Suppl. 6, 12-24

106. Runnegar, M., Berndt, N., Kong, S. M., Lee, E. Y. C., and Zhang, L. (1995) *Biochem. Biophys. Res. Commun.* **216**, 162-169

107. MacKintosh, R. W., Dalby, K. N., Campbell, D. G., Cohen, P. T. W., Cohen, P., and MacKintosh, C. (1995) *FEBS Lett.* **371**, 236-240

108. Craig, M., Luu, H. A., McCready, T. L., Williams, D., Andersen, R. J., and Holmes, C. F. (1996) *Biochem. Cell. Biol.* **74**, 569-578

109. Takai, A., Sasaki, K., Nagai, H., Mieskes, G., Isobe, M., Isono, K., and Yasumoto, T. (1995) *Biochem. J.* **306**, 657-665

110. Kato, Y., Fusetani, N., Matsunaga, S., Hashimoto, K., Fujita, S., and Furuya, T. (1986) *J. Am. Chem. Soc.* **108**, 2780-81

111. Kato, Y., Fusetani, N., Matsunaga, S., and Hashimoto, K. (1988) *Drugs Exptl. Clin. Res.* **14**, 723-728

112. Ishihara, H., Martin, B. L., Brautigan, D. L., Karaki, H., Ozaki, H., Kato, Y., Fusetani, N., Watabe, S., Hashimoto, K., Uemura, D., and Hartshorne, D. J. (1989) *Biochem. Biophy. Res. Commun.* **159**, 871-877

113. Kato, Y., Fusetani, N., Matsunaga, S., Hashimoto, K., and Koseki, K. (1988) *J. Org. Chem.* **53**, 3930-32

114. Matsunaga, S., Fujiki, H., Sakata, D., and Fusetani, N. (1991) *Tetrahedron* **47**, 2999-3006

115. Okada, A., Watanabe, K., Umeda, K., and Miyakado, M. (1991) *Agric. Biol. Chem.* **55**, 2765-71

116. Matsunaga, S., Wakimoto, T., and Fusetani, N. (1997) *J. Org. Chem.* **62**, 2640-42

117. Matsunaga, S., Wakimoto, T., and Fusetani, N. (1997) *Tetrahedron Lett.* **38**, 3763-64

118. Steube, K. G., Meyer, C., Proksch, P., Supriyono, A., Sumaryono, W., and Drexler, H. G. (1998) *Anticancer Res.* **18**, 129-137

119. Dumdei, E. J., Blunt, J. W., Munro, M. H. G., and Pannell, L. K. (1997) *J. Org. Chem.* **62**, 2636-39

120. Fu, X., Schmitz, F. J., Kelly-Borges, M., McCready, T. L., and Holmes, C. F. B. (1998) *J. Org. Chem.* **63**, 7957-63

121. Namboodiripad, A. N., and Jennings, M. L. (1996) *Am. J. Physiol.* **270**, C449-456

122. Runnegar, M. T., Maddatu, T., Deleve, L. D., Berndt, N., and Govindarajan, S. (1995) *J. Pharmacol. Exp. Therapeut.* **273**, 545-553

123. Suganuma, M., Fujiki, H., Furuya-Suguri, H., Yoshizawa, S., Yasumoto, S., Kato, Y., Fusetani, N., and Sugimura, T. (1990) *Cancer Res.* **50**, 3521-25

124. Fujiki, H., Suganuma, M., Yoshizawa, S., Kanazawa, H., Sugimura, T., Manam, S., Kahn, S. M., Jiang, W., Hoshina, S., and Weinstein, I. B. (1989) *Mol. Carcinogen.* **2**, 184-187

125. Boyd, M. R., and Paull, K. D. (1995) *Drug Dev. Res.* **34**, 91-109

126. Lindvall, M. K., Pihko, P. M., and Koskinen, A. M. (1997) *J. Biol. Chem.* **272**, 23312-16

127. Gauss, C. M., Sheppeck, I. J., Nairn, A. C., and Chamberlain, R. (1997) *Bioorg. Med. Chem.* **5**, 1751-73

128. Gupta, V., Ogawa, A. K., Du, X., Houk, K. N., and Armstrong, R. W. (1997) *J. Med. Chem.* **40**, 3199-3206

129. Volter, K. E., Pierens, G. K., and Quinn, R. J. (1999) *Bioorg. Med. Chem. Lett.* **9**, 717-722

130. Henderson, P. J. F. (1972) *Biochem. J.* **127**, 321-333

131. Kennelly, P. J., Oxenrider, K. A., Leng, J., Cantwell, J. S., and Zhao, N. (1993) *J. Biol. Chem.* **268**, 6505-10

132. Leng, J., Cameron, A. J., Buckel, S., and Kennelly, P. J. (1995) *J. Bacteriol.* **177**, 6510-17

133. Oxenrider, K. A., Rasche, M. E., Thorsteinsson, M. V., and Kennelly, P. J. (1993) *FEBS Lett.* **331**, 291-295

134. Solow, B., Young, J. C., White, R. H., and Kennelly, P. J. (1997) *J. Bacteriol.* **179**, 5072-75

135. Mai, B., Frey, G., Swanson, R. V., Mathur, E. J., and Stetter, K. O. (1998) *J. Bacteriol.* **180**, 4030-35

136. Shi, L., and Carmichael, W. W. (1997) *Arch. Microbiol.* **168**, 528-531

137. Missiakas, D., and Raina, S. (1997) *EMBO J.* **16**, 1670-85

Chapter Two

Identification of Inhibitors of PP1 Throughout the Aquatic Environment:

Techniques for the Isolation of Microcystins from Marine and Freshwater Sources

Part I:
Characterization of Hydrophobic Microcystins from Cyanobacteria*

Part II:
Identification of Microcystin-LR in Marine Organisms

Part I: Characterization of Hydrophobic Microcystins from Cyanobacteria

Introduction

The microcystin peptide hepatotoxins are metabolites of cyanobacteria in the genera *Microcystis, Anabaena, Oscillatoria* and *Nostic* that grow worldwide in fresh and brackish waters (1-4). These toxins are responsible for the deaths of birds, wild animals, and agricultural livestock. In countries where drinking water supplies contain cyanobacteria, adverse effects on human health have also been recognized (5). Recently, it has been shown that microcystin-LR is a tumour promoter as well as a potent (sub-nanomolar) inhibitor of the catalytic subunits of protein phosphatase-1 (PP1) and 2A (PP2A), two of the major eukaryotic (serine/threonine) protein phosphatases (6-10). This is remarkable considering the evolutionary distance between higher eukaryotes and cyanobacteria. The fact that PP1 and PP2A are amongst the most conserved of known proteins suggests that their involvement with the cyanobacterial toxin inhibitors is long-standing (10,11).

An important chemical feature that characterizes microcystins is the presence of the unusual C_{20} β-amino acid Adda ([2S, 3S, 8S, 9S]-3-amino-9-methoxy-2,6,8-trimethyl-10-phenyldeca-4,6-dienoic acid) which is required for inhibition of the protein phosphatases (3,12). To date over 50 different microcystins have been characterized (13-17). Most of these variants, which are all cyclic heptapeptides, differ in the nature of two variable L-amino acids and in the absence of methyl groups on the D-erythro-β-methyl aspartic acid and/or N-methyldehydroalanine residues (Figures 1-8, 2-5). Microcystins are extremely sturdy compounds. They are stable through wide ranges of pH and temperature and are only degraded completely under reflux in the presence of strong acid (18). Unlike other protein phosphatase inhibitors, the microcystins are not

generally cell permeable. This has restricted their application as research tools, except in hepatocytes (which appear have an active uptake mechanism) or in permeabilized or microinjected cells.

The purpose of the study presented here was to identify and characterize a novel group of hydrophobic microcystins derived from a cyanobacteria bloom present in Little Beaver Lake, Alberta, Canada, during the summer of 1991. These compounds were first discovered while testing drinking water from the lake for the presence of microcystin-LR using a HPLC-linked protein phosphatase inhibitor assay procedure. While purifying microcystin-LR, additional PP1 inhibitory activity was detected in a more hydrophobic fraction from the reversed phase HPLC purification. We were interested in identifying the hydrophobic microcystins because of the possibility of discovering a cell-permeable variant. Cell-permeable microcystins would be valuable as research tools to study the activity of PP1 and PP2A *in vivo*. Unlike microcystin-LR, hydrophobic microcystins may be readily absorbed into the bloodstream and distributed throughout the body upon ingestion. This would represent a serious health risk in contaminated water supplies and food.

Experimental Procedures

Materials

Microcystin-LR standard (MW 995) was obtained from Calbiochem (San Diego, CA). Cyanobacteria (containing predominantly *Microcystis aeruginosa*) were collected from a bloom present on Little Beaver Lake, Alberta, Canada (August 1991). Vydac C_{18} columns were purchased from Mandel (Guelph, ON). All other reagents were purchased from Sigma Chemicals or Boehringer Mannheim unless noted.

Cyanobacterial extraction and LH-20 preparative chromatography

Extracts of lyophilized cyanobacteria were prepared using procedures first described in Boland et al., 1993 (19). Cyanobacteria were recovered from the lakewater by centrifugation (4,000 g for 30 min) and lyophilized. Portions (30 g) of this material were extracted four times by Polytron homogenization in methanol and the homogenate was centrifuged at 3,000 g for 30 min at 4°C. Supernatants were extracted with 8 volumes of hexane, then concentrated in a Speed Vac as preparation for LH-20 chromatography (lipophilic sephadex resin used for adsorption and partition chromatography). The samples were fractionated on a Sephadex LH-20 (Pharmacia) column (20 mm x 900 mm), and eluted in methanol with a flow rate of 0.25 mL/min. Fractions from this column separation were tested for inhibitory activity using a protein phosphatase-1 inhibition assay (see below), and active samples were pooled and dried.

HPLC purification of microcystins

Fractions from LH-20 chromatography that were found to be active in a PP1 inhibition assay were purified further by two-step reversed phase HPLC (at pH 6.5 and pH 2). Reversed phase HPLC separates molecules based on their hydrophobicity - separation occurs by differential hydrophobic interactions of sample components with C_{18} functional groups attached to the column matrix. Pooled fractions from the LH-20 separation were lyophilized and dissolved in 20% methanol/80% 10 mM ammonium acetate (pH 6.5) for separation on a C_{18} semi-preparative column (25 cm long, 10 mm internal diameter) in 10 mM ammonium acetate (pH 6.5) at 2.5 mL/min with a linear gradient of 0-75% acetonitrile in 75 min (1.0% increase in acetonitrile per min). Detection was at 238 nm because the Adda side chain in microcystins has a characteristic absorbance at this wavelength. Fractions containing PP1 inhibitory activity from the pH 6.5 HPLC separation step were lyophilized, dissolved in 0.1% trifluoroacetic acid (TFA)/H_2O and chromatographed on a C_{18} analytical column (25 cm x 4.6 mm ID) at 1 mL/min developed with a gradient of acetonitrile/0.1% TFA of 0-20% in 5 min followed by 20-40% in 60 min (0.333% increase in acetonitrile per min). Detection was at 206 nm. Fractions from each chromatographic step were analyzed for their ability to inhibit PP1.

Active fractions isolated by the analytical C_{18} HPLC step were further purified to homogeneity on a narrow bore C_{18} column (25 cm x 2.1 mm ID) at pH 2. These hydrophobic phosphatase inhibitors were dissolved in methanol and diluted to 20% methanol/80% 0.1% TFA/H_2O and chromatographed at 0.2 mL/min with a linear gradient of acetonitrile/0.1% TFA from 0-35% in 20 min followed by 35-100% in 60 min (1.08%

acetonitrile per min). Microcystins were detected by their peptide bond absorbance at 206 nm and by PP1 inhibition assay.

Amino acid analysis

Microcystins were analyzed by amino acid analysis (following hydrolysis in 6N HCL at 110°C for 12 h) by Pierre Dubord on a Beckman 6300 ion-exchange analyzer with ninhydrin detection at 570 nm. The amounts of cyanobacterial protein phosphatase inhibitors (termed CPI) analyzed were as follows; CPI-1 (500 pmol), CPI-2 (600 pmol), CPI-3 (1.3 nmol), CPI-4 (350 pmol), CPI-5 (2.7 nmol), CPI-6 (1.3 nmol) and CPI-7 (500 pmol). When sufficient quantities were available, purified microcystins were analyzed by mass spectrometry.

Purification of PP1 and PP2A from rabbit skeletal muscle

PP1 was purified from rabbit skeletal muscle (by Dawn Chen) as described in Holmes, 1991 (20). Muscle extracts were precipitated with ammonium sulfate and treated with 80% ethanol at room temperature. PP1 was purified to homogeneity on a series of FPLC columns: 16 cm x 5 cm DEAE-Sepharose Fast Flow (weak anion exchange resin, Pharmacia), XK 16 poly-(L-lysine)-Sepharose (Lysine Sepharose 4B affinity resin, Pharmacia), XK 26 Sephadex G-100 (gel filtration resin from Pharmacia) and an HR 5/5 MonoQ (strong anion exchange column, Pharmacia). At each step, fractions from the columns were tested for phosphatase activity using phosphorylase *a* as a substrate. PP1 co-purifies with PP2A on the DEAE-Sepharose column, but is resolved from the type 2A protein phosphatase during the poly-lysine) step (21). Fractions containing the peak of

PP1 activity from the MonoQ chromatographic step were assessed by SDS-PAGE with silver staining to ensure that the preparation was homogeneous. PP1 was dialyzed overnight at 4°C in 25 mM triethanolamine-HCl (pH 7), 0.1 mM EDTA, 0.1% β-mercaptoethanol, and 50% (v/v) glycerol and stored at -20°C.

Protein phosphatase-1 inhibition assays

PP1 assays (30 μL reaction volumes) were performed as described in Holmes, 1991, using [^{32}P]-labelled glycogen phosphorylase *a* as the substrate for PP1. PP1 (10 μL, final concentration 0.36 nM in 30 μL reaction) and microcystin-LR standards or samples to be tested (10 μL), both in assay buffer containing 50 mM Tris-HCl (pH 7), 0.1 mM EDTA, 25 mM β-mercaptoethanol, and 1 mg/mL BSA, were incubated at 30°C for 10 min. The reaction was initiated with the addition of a 10 μL aliquot of ^{32}P-labelled phosphorylase *a* substrate (10 μM final concentration) in Tris-HCl buffer (as above) containing 3.75 mM caffeine. The reaction was stopped by precipitation with 200 μL of cold 20% (v/v) trichloroacetic acid (TCA), and the samples were placed on ice for 2 min. Samples were centrifuged for 2 min at 14000 rpm in a benchtop centrifuge (Eppendorf), and 200 μL of supernatant (containing TCA-soluble free ^{32}P-labelled phosphate) was added to 1 mL of scintillation fluid (ACS) and counted (counts per minute, cpm) on a Pharmacia 1209 Rack β liquid scintillation counter. All reactions were performed in duplicate, and assays were repeated 2-5 times to ensure accuracy. Microcystin-LR standards from Calbiochem were tested for purity by reversed phase HPLC in 0.1% TFA/H$_2$0 (pH 2) with a 0.1% TFA/acetonitrile gradient and the concentration of microcystin was verified by amino acid analysis.

Phosphorylation of glycogen phosphorylase

^{32}P-radiolabelled phosphorylase *a* was prepared by phosphorylation of glycogen phosphorylase b (Boehringer-Mannheim) by phosphorylase kinase (Sigma). 40 mg of phosphorylase b was dissolved in 500 µL H_2O and dialyzed in 50 mM Tris-HCl (pH 7), 1 mM EDTA, 0.1% (v/v) β-mercaptoethanol, and 25 mM NaF (to inhibit endogenous phosphatase activity) at 4°C overnight. 400 U of phosphorylase kinase was dissolved in 500 µL H_2O and dialyzed under identical conditions. After dialysis, phosphorylase b was warmed to room temperature and transferred to a Centricon 30 for concentration at 5000 g at 10-15°C. Phosphorylase b and phosphorylase kinase were added to a 2 mL reaction mixture containing 3 mM magnesium acetate, 0.125 mM calcium chloride, 0.25 mM EDTA, 125 mM sodium glycerolphosphate, 125 mM Tris-HCl (pH 8.6), 1 mM ATP, and 1 mCi ^{32}P-γ-ATP. The reaction was incubated at 30°C for 60 min and terminated by the addition of an equal volume of ice cold saturated ammonium sulfate solution (500 g/L, pH 7). After standing on ice for 30 min, the suspension was centrifuged at 16,000 g for 10 min and the supernatant discarded. The pellet was re-suspended in 2 mL of 50 mM Tris-HCl (pH 7), 1 mM EDTA, and 0.1 % (v/v) β-mercaptoethanol, then dialyzed exhaustively in the same buffer (6-8 changes) to remove ^{32}P-ATP and ^{32}P-inorganic phosphate. Phosphorylase *a* (the phosphorylated form of phosphorylase b) was stored as a crystalline suspension in aliquots at 4°C.

Evaluation of PP1 assay results

The inhibition of PP1 by microcystin-LR has been shown to have a sigmoidal response curve in plots of percent activity PP1 vs. log microcystin-LR concentration (6,8,22,23). The inhibition curve is linear in the 30-60% PP1 activity range (23), and therefore sample microcystin-LR concentrations can be quantified in this range of phosphatase activity. The percent of control phosphatase activity observed in reactions containing unknown inhibitor samples and microcystin-LR standards is calculated with the equation:

$$\% \text{ of control PP1 Activity} = \frac{(\text{sample} - \text{blank})}{(\text{control} - \text{blank})} \times 100$$

where sample is the amount of PP1 activity (in cpm) resulting from adding a test sample or inhibitor standard to the phosphatase reaction, blank is the cpm resulting from free ^{32}P-phosphate and/or ^{32}P-ATP observed in the assay without the addition of phosphatase, and control is the maximum PP1 activity (in cpm) resulting from incubating enzyme and substrate together in the absence of inhibitor.

The amount of inhibition of PP1 observed for a standard concentration of microcystin-LR depends on the concentration of phosphatase in the assay (8). This is due to the tight-binding nature of the interaction between inhibitor and enzyme described in Chapter One. The amount of enzyme in the assay can be related to the amount of ^{32}P-phosphate released from phosphorylase *a* during the reaction, relative to the total amount of ^{32}P-phosphate present.

$$\% \text{ release} = \frac{(\text{control} - \text{blank}) \times 1.15}{(\text{total} - \text{blank})} \times 100$$

where total is the cpm obtained from counting of 10 μL of ^{32}P-labelled phosphorylase a added directly to scintillation fluid, and 1.15 is a dilution factor derived from the volume of the reaction counted (200 μL) divided by the total reaction volume (230 μL) (other terms are defined above).

Protein phosphatase-1 activity is linear in the range of 15-25% percent release, and the PP1 inhibition assay has been shown to be linear from 30-60% enzyme activity (i.e. 70-40% inhibition) (23). In order to accurately compare between assays in this study, control phosphatase activity was standardized to 15% release of total phosphate from the substrate for each assay. Standardizing percent release between assays means that the amount of PP1 activity is the same in each assay, even when different enzyme preparations are used. As long as the specific activity (in units of micromoles of phosphate released per min per mg of substrate) of the phosphatase does not vary inordinately, the enzyme concentration in each assay should be similar. Long-term storage of PP1 (>6 months at -20°C) can result in gradual loss of phosphorylase a activity. If one attempts to use older preparations of enzyme by simply increasing the amount added to the reaction (in order to reach 15% release) it is possible that inactive enzyme in the preparation will still be capable of binding microcystin-LR, thereby removing it from the pool of microcystin available to inhibit active PP1. This will increase the amount of total inhibitor needed in the assay to reach 50% inhibition of enzyme activity, inflating the IC$_{50}$ value obtained. This scenario may also be true for mutant recombinant PP1 enzymes which have higher or lower specific activities than

wild-type phosphatase. If the enzyme concentration in the assay is increased or decreased in order to obtain an activity level of 15% release of phosphate from substrate, IC_{50} values obtained for PP1 inhibitors will likely be affected. On the other hand, if enzyme concentrations are standardized to a certain level, enzyme activity may fall outside of the linear range. In practice, we standardize enzyme activity while remaining aware of the consequences of enzyme concentration, when interpreting IC_{50} values between enzymes with significantly different specific activities.

Results

While developing an effective screen for the detection of microcystins in the freshwater environment, we examined methanolic extracts of cyanobacteria collected from Alberta drinking water lakes for activity in a PP1 inhibition assay (19). We identified a cyanobacteria bloom (containing *Microcystis aeruginosa*) that contained a significant amount of microcystin-LR, a potent inhibitor of PP1 and PP2A (19). At that time we noticed a smaller peak of PP1 inhibitory activity which eluted from the reversed phase HPLC column at a much higher acetonitrile concentration than microcystin-LR (43%, vs. 33% for microcystin-LR). In the present study we have identified the nature of this hydrophobic protein phosphatase inhibitory fraction and purified the active component(s) to homogeneity.

The hydrophobic cyanobacterial phosphatase inhibitors (termed CPI), were isolated by semi-preparative reversed phase HPLC at pH 6.5 (Figure 2-1, panel a). To further purify these inhibitors, the active fractions were combined, dried, and re-chromatographed on a C_{18} analytical column at pH 2.0. The inhibitory activity was separated into several peaks of absorbance corresponding to one major and five minor components (A-F) (Figure 2-1, panel b). Each sample was individually chromatographed on a narrow bore reversed phase HPLC column. This procedure further resolved active fractions A-F into seven inhibitors which were designated CPI 1-7 (Figure 2-2).

The most abundant phosphatase inhibitor (CPI-5) was analyzed by amino acid analysis and found to have an identical amino acid composition to microcystin-LR with the exception of the stoichiometric loss of arginine and presence of two moles of leucine
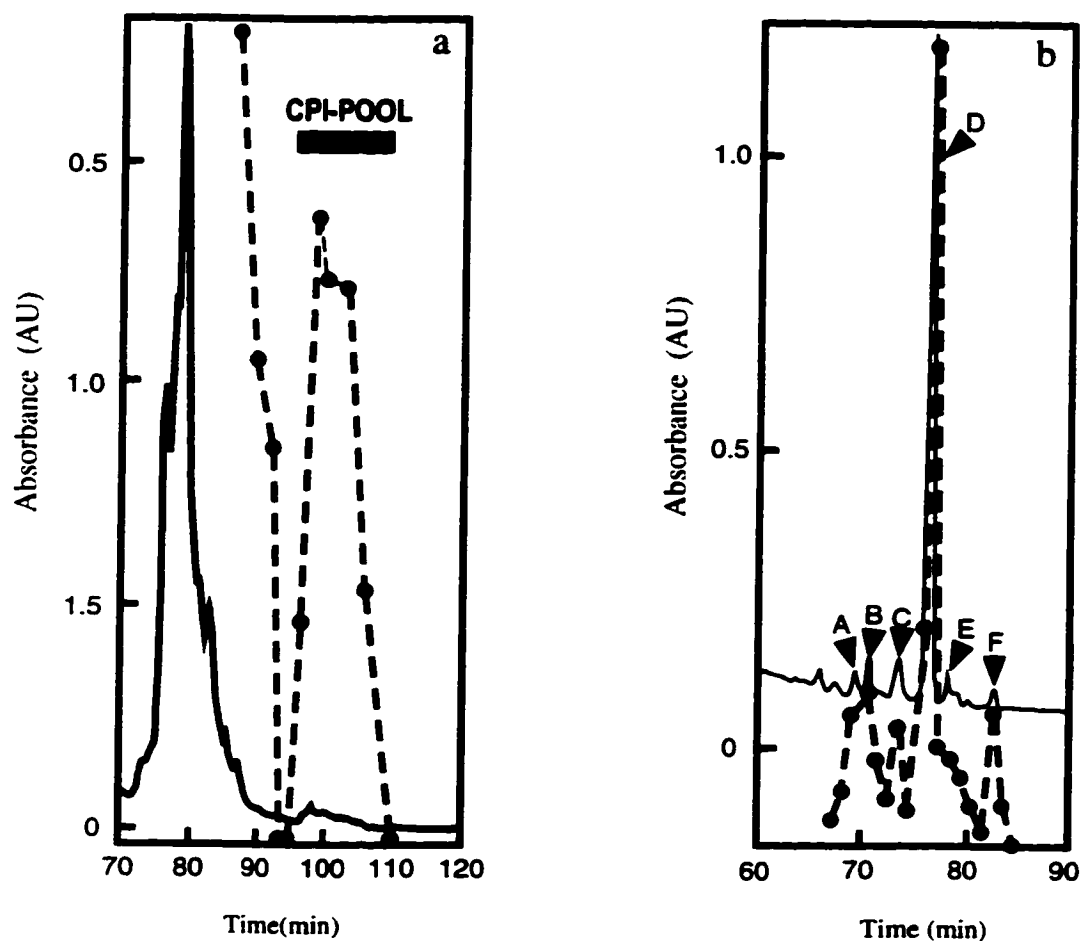
Figure 2-1. *Resolution of hydrophobic protein phosphatase inhibitors by a two-step HPLC-linked inhibition assay procedure.* Panel a represents the identification of several cyanobacterial protein phosphatase inhibitors by reversed phase HPLC at pH 6.5 and by PP1 assay. The dotted line represents activity in a PP1 inhibition assay while the solid line represents absorbance at 230 nm. Panel b represents resolution of the CPI pool (represented by a solid bar) of protein phosphatase inhibitors into six active fractions (labelled A-F) by reversed phase HPLC at pH 2. The dotted line represents activity in a PP1 inhibition assay while the solid line represents absorbance at 206 nm.
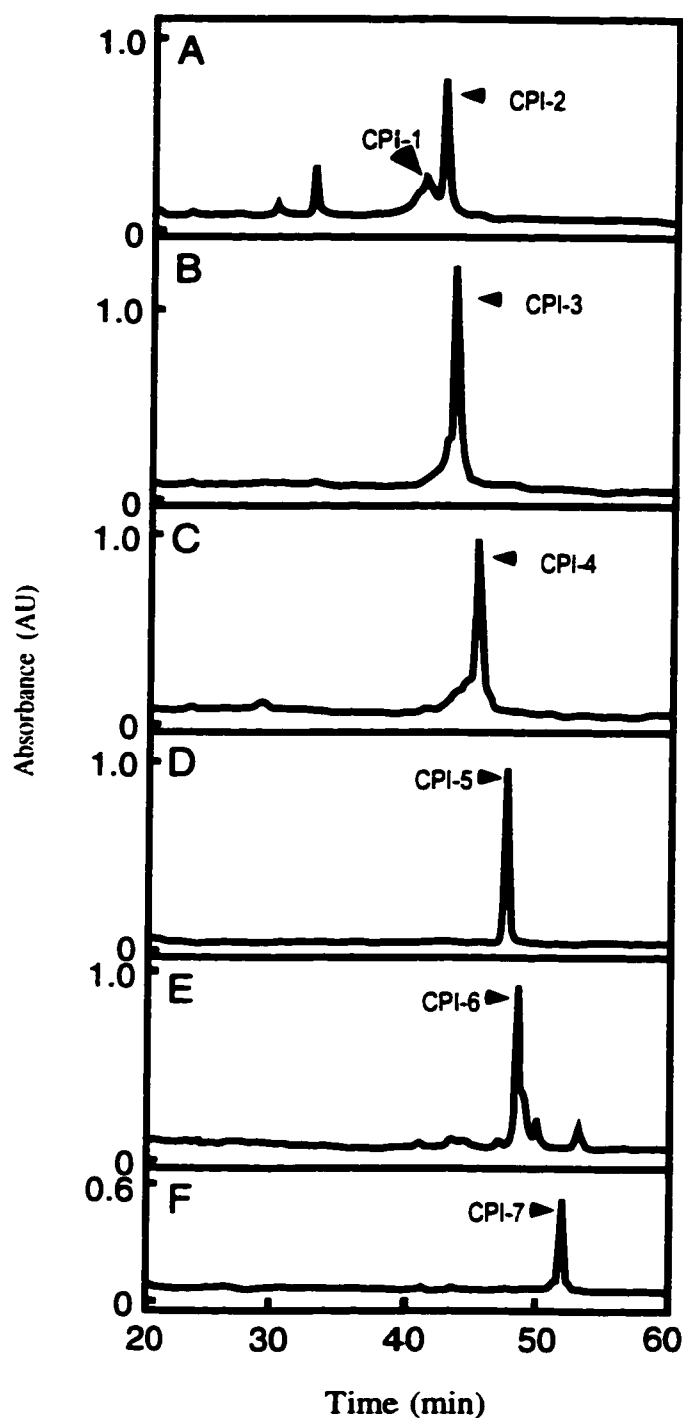
Figure 2-2. *Identification of seven cyanobacterial protein phosphatase inhibitors by reversed phase HPLC.* Panels A-F represent further resolution of active fractions shown in Figure 1(b) into seven cyanobacterial phosphatase inhibitors (CPI 1-7) by narrow bore HPLC at pH 2. CPI 1-7 were detected by absorbance at 206 nm.

per mole of peptide (Figure 2-3). Mass spectrometric analysis of the purified inhibitor showed that it had a mass consistent with microcystin-LL (MW 952). A total of 90 μg microcystin-LL was isolated from 60 g lyophilized cyanobacteria (1.5 ppm). The six other PP1 inhibitors were also analyzed (Figure 2-3). Amino acid analysis indicated the presence of microcystin-LV and -LM in inhibitory fractions CPI-1 and 2; microcystin-LZ (where Z is an unidentified hydrophobic amino acid) in inhibitory fraction CPI-3; microcystin-L (where arginine is missing and apparently not replaced by any amino acid) in inhibitory fraction CPI-4; and microcystin-LF in inhibitory fraction CPI-6. Inhibitory fraction CPI-7 contained a microcystin with identical amino acid composition to microcystin-LL except for the loss of D-Ala and the presence of an unknown but more hydrophobic amino acid.

In order to fully characterize the cyanobacterial phosphatase inhibitors, dose-response inhibition curves were determined for PP1 (Figure 2-4). All seven new microcystins (CPI 1-7) potently inhibited PP1 with IC_{50} values ranging from 0.06-0.4 nM. These values are similar to the IC_{50} value obtained for microcystin-LR (0.15 nM) and agree with previously published data on the inhibition of PP1 by the microcystin peptide family (6-8).
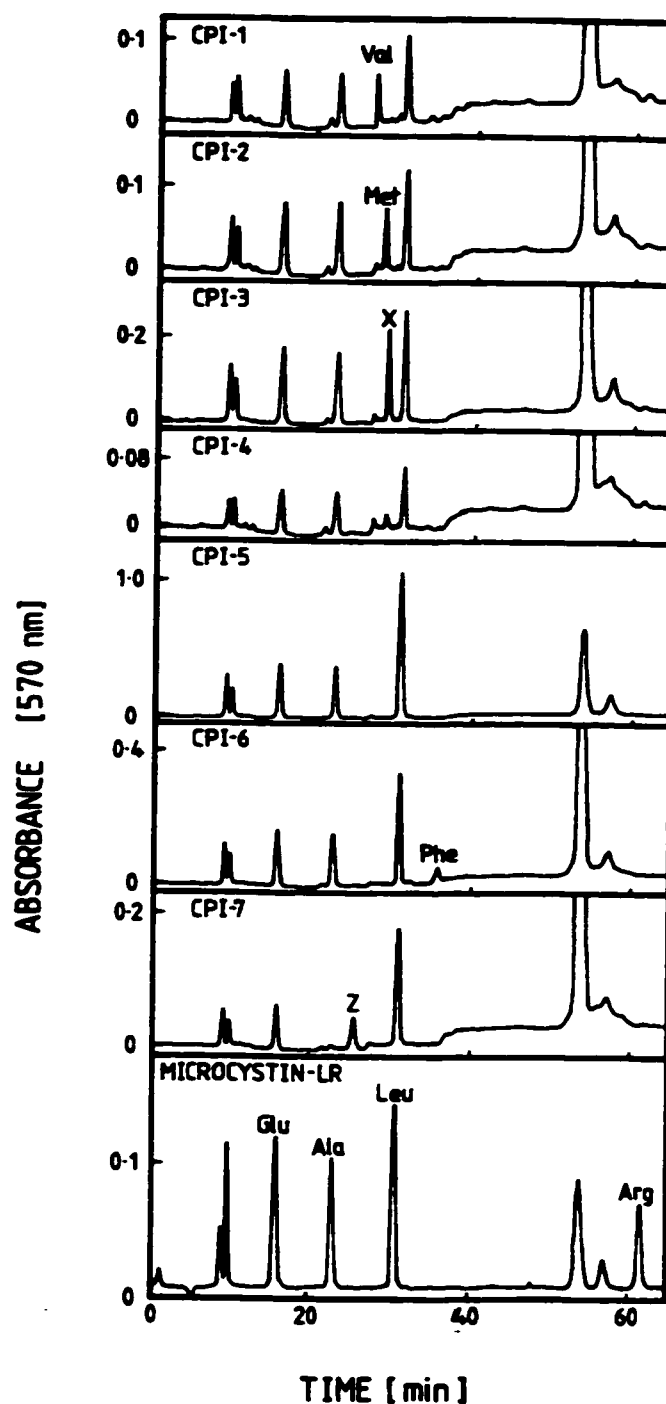
Figure 2-3. *Amino acid analyses of cyanobacterial phosphatase inhibitors 1-7.* Amino acid analysis was carried out as described in Experimental Procedures. Detection was by ninhydrin absorbance of primary amino acids at 570 nm. The elution positions of known amino acids from microcystin-LR are labelled in the bottom panel, with the exception of twin peaks corresponding to possible diastereomers of β-methyl aspartic acid which elute just before 10 min. The elution positions of Val, Met and Phe present in CPI-1, CPI-2 and CPI-6, respectively, are indicated. The unknown amino acids present in CPI-3 and CPI-7 are designated X and Z, respectively.
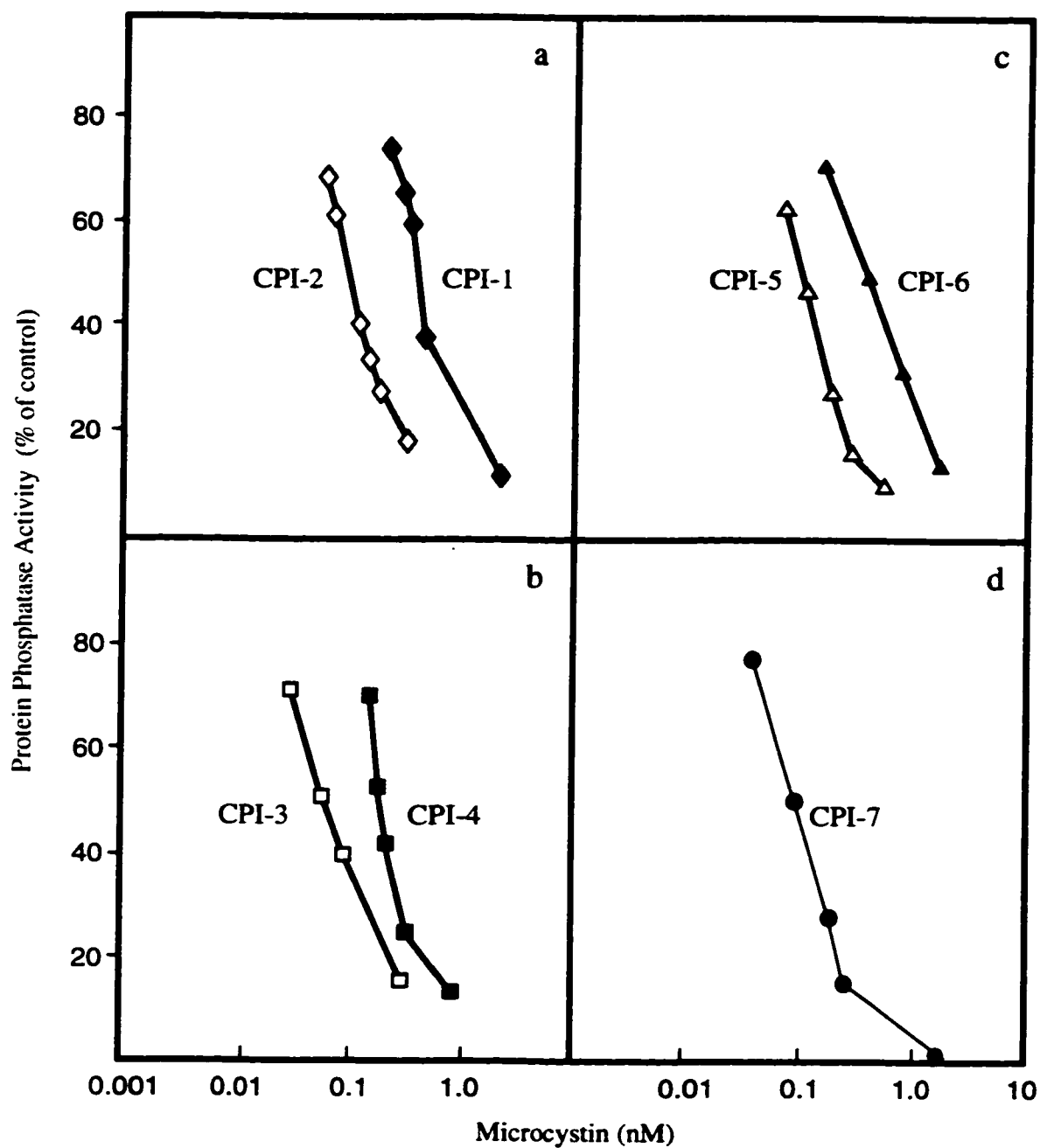
Figure 2-4. *Inhibition of protein phosphatase-1 by hydrophobic microcystins.* Panels a-d represent IC_{50} curves for the inhibition of skeletal muscle PP1 by cyanobacterial protein phosphatase inhibitors (a) CPI-1 (microcystin-LV) and CPI-2 (microcystin-LM), (b) CPI-3 (microcystin-LZ) and CPI-4 (microcystin-L), (c) CPI-5 (microcystin-LL) and CPI-6 (microcystin-LF), and (d) CPI-7 (variant of microcystin-LL without D-Ala residue). PP1 activity was assayed using 10 μM [^{32}P]phosphorylase a substrate. The IC_{50} values for each inhibitor lie between 0.06-0.4 nM.

Discussion

We have described the identification of seven new protein phosphatase inhibitors from a bloom of cyanobacteria collected from a Canadian drinking water lake. One of these compounds was identified as microcystin-LL, a novel hydrophobic inhibitor of PP1. Microcystin-LL is a potent inhibitor of PP1, with an IC_{50} value similar to that of microcystin-LR, the most common microcystin variant. Microcystin-LL may prove to be more useful than microcystin-LR as a research tool, since it is as hydrophobic as the cell-permeable protein phosphatase inhibitor okadaic acid, based on retention time on a reversed phase C_{18} HPLC column. A cell-permeable microcystin could be used in studies of PP1 and PP2A activity *in vivo*.

Although the amounts of hydrophobic PP1 inhibitors found in the cyanobacterial extracts were quite low, the physiological effects of these compound when ingested may be significant. Hydrophobic microcystins could be cell-permeable, and thus present a disproportionate health risk in contaminated drinking water or food.

In addition to microcystin-LL, six other hydrophobic PP1 inhibitors were identified in this study. Three of these were tentatively identified as microcystin-LV, LM, and LF (Figure 2-5). Two of the six inhibitors contained unknown amino acids (microcystin-LZ and microcystin-LL[D-Ala replaced with Z]). A further phosphatase inhibitor (CPI-4) had an similar amino acid composition to microcystin-LR but lacked arginine. When chromatographed by reversed phase HPLC, CPI-4 possessed no appreciable absorbance at 280 nm, ruling out the presence of tryptophan.

We have been able to isolate sufficient quantities of microcystin-LL to undertake determination of the solution structure of this compound by 2-D NMR (24). The

a

IC_{50} Values For Hydrophobic Microcystins vs. PP1

Microcystin	Structure	IC_{50} (nM)
Microcystin-LL	cyclo(D-Ala-L-Leu-D-MAsp-L-Leu-Adda-D-Glu-Mdha)	0.1
Microcystin-LV	cyclo(D-Ala-L-Leu-D-MAsp-L-Val-Adda-D-Glu-Mdha)	0.3
Microcystin-LM	cyclo(D-Ala-L-Leu-D-MAsp-L-Met-Adda-D-Glu-Mdha)	0.1
Microcystin-LF	cyclo(D-Ala-L-Leu-D-MAsp-L-Phe-Adda-D-Glu-Mdha)	0.4
Microcystin-LR	cyclo(D-Ala-L-Leu-D-MAsp-L-Arg-Adda-D-Glu-Mdha)	0.15

b
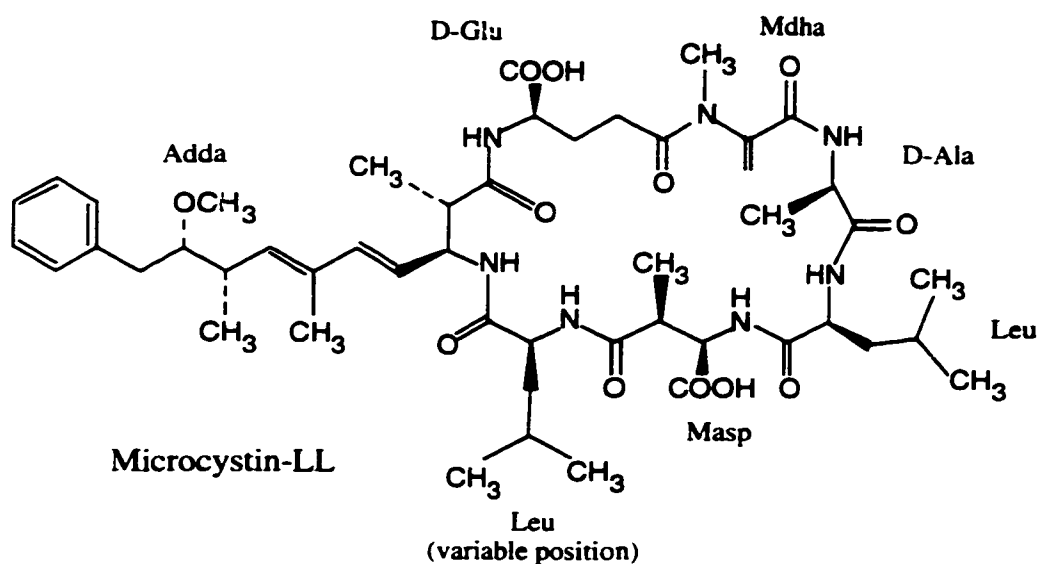
Microcystin-LL

Figure 2-5. *Structures and IC_{50} values of novel hydrophobic microcystins.* Panel a displays the IC_{50} values for the microcystins fully identified in this study determined with native PP1 enzyme. The variable amino acid position is highlighted in bold for each inhibitor. Panel b shows the structure of microcystin-LL, the most abundant hydrophobic microcystin identified in this work. The variable position corresponding to other inhibitors found in panel a is indicated.

extremely low yield of the remaining six microcystins (< 20 ng/g cyanobacteria) precluded detailed structural analysis in this study. Despite these limitations, the biological activity of the seven microcystins was determined in a PP1 inhibition assay. All the compounds strongly inhibited PP1 with IC_{50} values ranging from 0.06-0.4 nM. These values are similar to the value obtained using microcystin-LR ($IC_{50} = 0.15$ nM) in an identical assay (25). All of the novel microcystins contain a hydrophobic amino acid instead of the arginine residue found in microcystin-LR. These results indicate that the amino acid present in the variable arginine position is not essential for microcystin inhibition of PP1.

The findings described in this work demonstrate that the protein phosphatase inhibition assay (linked to reversed phase HPLC) can be applied to identify a wide variety of microcystins in the natural environment. The results presented in this paper may facilitate a routine HPLC-linked phosphatase inhibition assay procedure for the analysis of microcystins in drinking water (23).

Part II: Identification of Microcystin-LR in Marine Organisms

Introduction

Microcystins are hepatotoxic (7), tumour-promoting (26), cyclic peptides produced worldwide by cyanobacteria (reviewed in (27)). Microcystin-LR is the most commonly encountered member of this family, which currently includes more than 50 closely related compounds. These toxins are usually associated with incidents of illness resulting from contamination of freshwater drinking supplies or direct ingestion of toxic strains of freshwater cyanobacteria by animals (28,29). However, our laboratory recently discovered these toxins in saltwater mussels collected from the West Coast of Vancouver Island, providing the first evidence of microcystins in the marine environment (25).

Netpen liver disease (or NLD) is a severe condition associated with high mortality in commercially raised Atlantic salmon. Initial investigations indicated that the disease was caused by chronic exposure to a naturally-occurring toxin (30,31). In collaboration with the laboratories of Dr. M. Kent (Dept. Fisheries and Oceans, Nanaimo, BC) and Dr. R. Andersen (University of British Columbia), our laboratory discovered microcystin-LR in the livers of diseased Atlantic salmon reared in net-pens in the Northeastern Pacific Ocean (32). The predominant symptom of this disease is pronounced alteration of liver architecture - diffuse necrosis and hydropic degeneration (vacuoles of intracellular fluid form in cells), megalocytosis (large cells with intranuclear inclusions of cytosol), pyknotic (collapsed) nuclei, and increased mitotic activity (Figure 2-6). Megalocytosis, the hallmark of NLD, is commonly interpreted as a failure of cell division resulting in the production of polyploid hepatocytes (31). Our study demonstrated that exposure of healthy Atlantic salmon to microcystin-LR generated all of the symptoms of NLD (32).
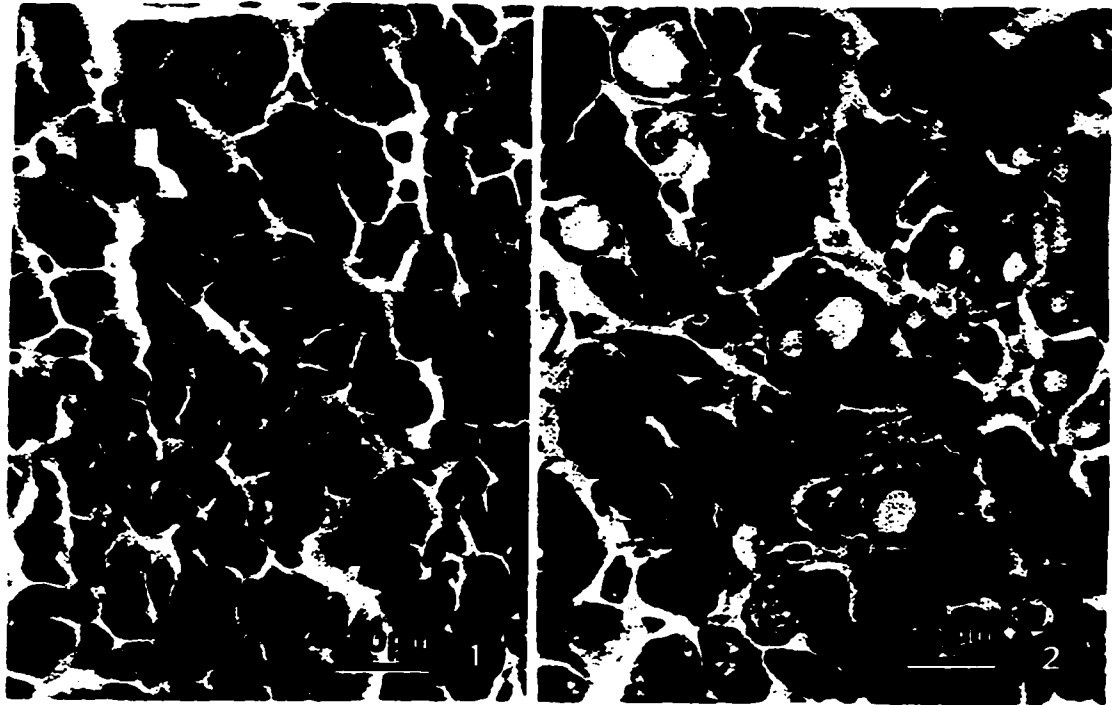
Figure 2-6. *Net-pen liver disease in Atlantic salmon (Salmo salar).* (1) Normal liver of an Atlantic salmon taken from an unaffected net-pen site displaying well-organized hepatic tubules, lack of vacuolation of the hepatocytes, and homogeneous size of hepatocyte nuclei. (2) Liver of an Atlantic salmon reared in a site affected with NLD in Port Townsend Bay , Washington, USA. Diseased liver tissue shows signs of diffuse vacuolar degeneration and necrosis, enlarged nuclei and focal inflammation of the liver with melano-macrophages. Arrows: pyknotic nuclei (dark, collapsed nuclei) Adapted from Kent et al., *Dis. aquat. Org.,* 1988.

It is likely that the liver damage observed after microcystin exposure stems from the fact that microcystins are potent inhibitors of protein phosphatase-1 and 2A, the major serine/threonine protein phosphatases in mammalian cells (6-8). Inhibition of PP1 and 2A in liver has been associated with morphological changes in hepatocytes due to the breakdown of structural elements such as microfilaments, intermediate filaments and microtubules (22,33).

In addition to a commercial diet, farmed Atlantic salmon feed extensively on natural marine biota during plankton blooms. Salmon contained in net-pens are not thought to ingest the toxin directly from a microbial producer of microcystins (unidentified at present), but to instead feed on an intermediate zooplankton 'vector' which has acquired the microcystins from phytoplankton or cyanobacteria in its diet (32). Blooms of copepod and crab larvae zooplankton are common at the affected net-pen sites and NLD invariably occurs during the summer months, when these blooms are the most prevalent. A field observation in which fish feeding on copepods had severe NLD prompted our research group to examine Calanoid copepods and Dungeness crab larvae for microcystins.

We have previously described the application of HPLC-linked protein phosphatase inhibition assay for sensitive detection of microcystin-LR in biological samples (25,29). The present study describes the addition of capillary electrophoresis (CE) to this screening procedure. When used in conjunction with the phosphatase inhibition assay, CE provides a fully-automated method that can rapidly identify microcystins in natural sources.

In capillary electrophoresis (reviewed in 36), a sample is introduced into a capillary that is equilibrated with a buffer solution. An electrical field is applied to the system resulting in electrophoretic separation of compounds past a detector window. There are several advantages to this procedure. First, tiny internal capillary diameters (typically 50 μm) yield high surface-to-volume ratios, resulting in efficient dissipation of Joule heat generated by resistance of the buffer to an electric current. This permits the use of high electrical fields (up to 30 kV) which allow short electrophoretic separation times. Second, sample and buffer volumes are small. The internal volume of the capillary (50 μm x 50 cm) is approximately 1 μL, and a typical analysis can be performed with a sample of 5 μL where as little as 5 nL is actually injected. Finally, all molecules, regardless of charge, are detected at the cathode due to the net movement of the buffer. This phenomenon is known as bulk flow or electroosmotic flow (EOF). When using uncoated fused-silica capillaries, ionized silanol (SiO⁻) groups of the capillary wall attract cations from the buffer, creating an electrical double layer. The pI of fused silica is 1.5; the pH of the separation buffer determines the fraction of silanol groups which are ionized. Under an applied field, cations in the diffuse 'fringes' of the double layer migrate in the direction of the negative electrode, along with associated water molecules. The cohesive nature of the hydrogen bonding between these waters of hydration to the water molecules of the bulk solution is enough to pull the entire buffer solution towards the negative electrode. Therefore, EOF propels all molecules, regardless of charge, toward the cathode and past the detector window. Separation observed in capillaries is the result of both the bulk movement of the solution and the electrophoretic mobility of the individual compounds in the sample.

Experimental Procedures

Materials

Microcystin-LR standard was obtained from Calbiochem (San Diego, CA). Vydac C_{18} columns were purchased from Mandel (Guelph, ON). Expression vector pCW was a generous gift from Dr. Dahlquist, University of Oregon, USA. All other reagents were purchased from Sigma Chemicals.

Zooplankton extraction

Zooplankton samples of copepods (*Calanus marshallae*) and Dungeness crab larvae (*Cancer magister*) were collected from areas surrounding salmon net-pens in British Columbia (by Dr. M. Kent) and prepared as described for cyanobacterial extracts (Chapter Two, Part I). Zooplankton was recovered by centrifugation and pellets were extracted by homogenization in methanol (0.3 g sample/mL methanol). The homogenates were centrifuged at 5000 g for 15 min, and pellets and lipid layers were discarded. An aliquot of each zooplankton sample was diluted in 10 mM Tris-HCl (pH 7) and tested for its ability to inhibit recombinant protein phosphatase-1β in a phosphorylase *a* assay.

Protein phosphatase-1β expression and purification

The catalytic subunit of rabbit skeletal muscle PP1 (β isoform) was cloned (by Hue Anh Luu) and expressed in *E. coli* according to previously published procedures (37-39). The pCW bacterial expression vector has a isopropyl-thio-β-D-galactopyranoside-inducible (IPTG) duplicated trp-lac hybrid promoter (38). *E. coli* DH5α cells were transformed with the pCW-PP1β expression vector and incubated in 200 mL of LB medium

(containing 1 mM $MnCl_2$ to ensure that the recombinant phosphatase has sufficient metal ions to occupy the catalytic site of the enzyme). After overnight growth at 37°C, this culture was used to inoculate 6 -12 L of LB containing 1mM $MnCl_2$. The culture was grown until the absorbance at 600 nm reached 0.3. Protein expression was induced for up to 16 hr at 28°C by the addition of 0.5 mM IPTG. DH5α E. coli cells were harvested by centrifugation for 20 min at 3000 g and suspended in 180 mL ice cold extraction buffer containing Hepes (50 mM, pH 7.5), KCl (100 mM), glycerol (5%), EDTA (1 mM), $MnCl_2$ (2 mM), DTT (2 mM), DNase-1 (5 mg/mL), phenylmethylsulphonyl fluoride (PMSF, 0.1 mM), benzamidine (1 mM) and an additional cocktail of protease inhibitors: Antipain-dihydrochloride, Aprotinin, Bestatin, Chymosatin, E-64, EDTA, Leupeptin, Pefabloc, Pepstatin, Phosphoramidon (Protease Inhibitors Set, Boehringer Mannheim). The suspension was lysed by passage through a French press and centrifuged for 30 min at 13,000 g. The supernatant was filtered, then diluted with an equal volume of buffer A (25 mM triethanolamine/HCl, pH 7.5, 1 mM $MnCl_2$, 0.1 mM EGTA, 0.1% β-mercaptoethanol, 5% glycerol) and loaded on a 16 cm x 5 cm DEAE-Sepharose column (Pharmacia) with a flow rate of 2 mL/min. The column was washed with buffer A, then developed with a 1 L linear gradient from 0-400 mM NaCl in buffer A at a flow rate of 3 mL/min. Fractions were collected at 3 min intervals, assayed for phosphorylase phosphatase activity and active fractions were pooled. PP1 activity typically eluted at 200 mM NaCl. The pool (135 mL) of active fractions was diluted to 150 mL with buffer A and loaded on a 5 mL heparin-Sepharose HiTrap column (affinity resin, Pharmacia). The column was developed with a 200 mL linear gradient from 0-0.5 M NaCl in buffer A at a flow rate of 5 mL/min and 5 mL fractions were collected. Active fractions (5 mL)

were pooled, diluted to 100 mL with buffer A and applied to an HR 5/5 MonoQ column (Pharmacia). The column was developed with a 50 mL linear gradient from 0-0.4 M NaCl in buffer A at a flow rate of 1 mL/min and 1 mL fractions were collected. Active fractions (5 mL) were pooled and concentrated (Centricon-10) to ~ 100 μL at 1000 g, 4 °C. The concentrate was applied to a Superdex-75 gel filtration column equilibrated in buffer A containing 200 mM NaCl at a flow rate of 0.1 mL/min; 0.1 mL fractions were collected. Active fractions were pooled (~ 1.8 mL) and dialyzed overnight at 4 °C against buffer A containing 50% (v/v) glycerol and stored at - 20 °C.

Phosphatase inhibition assay

At each step in the purification process, zooplankton samples were analyzed for their ability to inhibit the dephosphorylation of ^{32}P-labelled glycogen phosphorylase *a* by recombinant protein phosphatase-1. PP1 inhibition assays were carried out as described in Chapter Two, Part 1, with the exception that 0.2 mM $MnCl_2$ was included in the assay buffer. Unlike the native enzyme, recombinant PP1 is almost entirely dependent on Mn^{2+} for activity (38).

HPLC purification of inhibitors

Zooplankton extracts were dissolved in 20% methanol/80% 10 mM ammonium acetate (pH 6.5) in preparation for reversed phase HPLC (Chapter Two, Part I). Samples were separated on a analytical C_{18} column equilibrated in 10 mM ammonium acetate (pH 6.5) using an acetonitrile gradient of 0.333%/min (0-20% in 15 min, 20-45% in 75 min). Detection was at 238 nm. Fractions were collected and assayed for PP1 inhibitory

activity. Active fractions were dried, dissolved in 0.1% TFA/H$_2$0 (pH 2) and chromatographed on a narrow bore C$_{18}$ column equilibrated in water/0.1% TFA at pH 2 using an acetonitrile/0.1% TFA gradient of 0.333%/min (0-20% in 5 min, 20-40% in 60 min). Detection was at 206 nm. A standard of microcystin-LR was chromatographed on the HPLC at both pH 2 and 6.5 in order to determine its retention time on the columns under the same conditions used in the zooplankton purification procedures.

Capillary electrophoresis of microcystin-LR from pH 2-8.3

Detection of a 125 pg microcystin-LR standard (dissolved in 10 mM of the appropriate buffer, see below) was carried out on a Beckman 2100 PACE instrument in a series of buffers covering a range of pH from 2 to 8.3. Buffers used were: 100 mM sodium phosphate buffer (pH 2-3 and 6-7), 100 mM sodium acetate buffer (pH 4-5) and 100 mM sodium borate buffer (pH 8.3). An uncoated silica capillary of 50 μm internal diameter x 50 cm effective length (from point of sample application to detector) was used for the electrophoretic separation, with an applied constant voltage of 20 kV at 25°C. Sample injections (5 nL) employed the pressure mode, and detection was at a wavelength of 200 nm.

Capillary electrophoresis of zooplankton samples

HPLC fractions which eluted with a retention time equivalent to microcystin-LR, and which demonstrated PP1 inhibitory activity, were further analyzed by capillary electrophoresis (CE) as described in Boland et al. 1993 (19). HPLC fractions were dried and dissolved in 10 mM borate buffer (pH 8.3). Separation of the active fractions was

performed in 100 mM sodium borate buffer (pH 8.3) at 20 kV for 10-30 min at 25°C, as

these conditions were previously determined to be optimal for analysis of the

microcystin-LR standard. Sample injections (10-30 nL) employed the pressure mode,

and detection was at a wavelength of 200 nm. Identification of the inhibitors was

confirmed by spiking with 50 picograms of microcystin-LR standard.

Results

HPLC purification of inhibitors

Methanolic extracts of copepods and crab larvae (found to be active by preliminary PP1 inhibition assay) were fractionated by reversed phase HPLC on an analytical column at pH 6.5 and tested for inhibitory activity in a protein phosphatase-1 assay using phosphorylase *a* as a substrate (Figure 2-7, panels a,b). In both samples, a peak of PP1 inhibitory activity was found to elute at a retention time identical to that of a standard of microcystin-LR. The active fractions were pooled, dried, and re-chromatographed on a narrow bore HPLC column at pH 2.0 (Figure 2-7, panels c,d). Further purification and confirmation of the presence of microcystin-LR in the zooplankton samples was found in this HPLC step, where fractions with the greatest activity in a PP1 inhibition assay eluted at the same retention time as a standard of microcystin-LR.

Capillary electrophoresis of microcystin-LR

To determine optimal buffer and pH conditions for microcystin-LR identification with capillary electrophoresis, a series of separations with 125 pg of microcystin-LR standard was performed from pH 2 - 8.3 (Figure 2-8). 100 mM borate buffer, pH 8.3, was chosen for the zooplankton sample analyses because of the rapid migration time of microcystin-LR through the capillary under these conditions. Higher pH buffers tend to produce fast separations because the electroosmotic flow (EOF) is substantial. At high pH, the majority of silanol groups on the capillary are ionized (SiO^-), and therefore able to attract many cations from the buffer. This double layer of ions lining the capillary wall is responsible for creating EOF. When a current is applied, cations in the outer layer
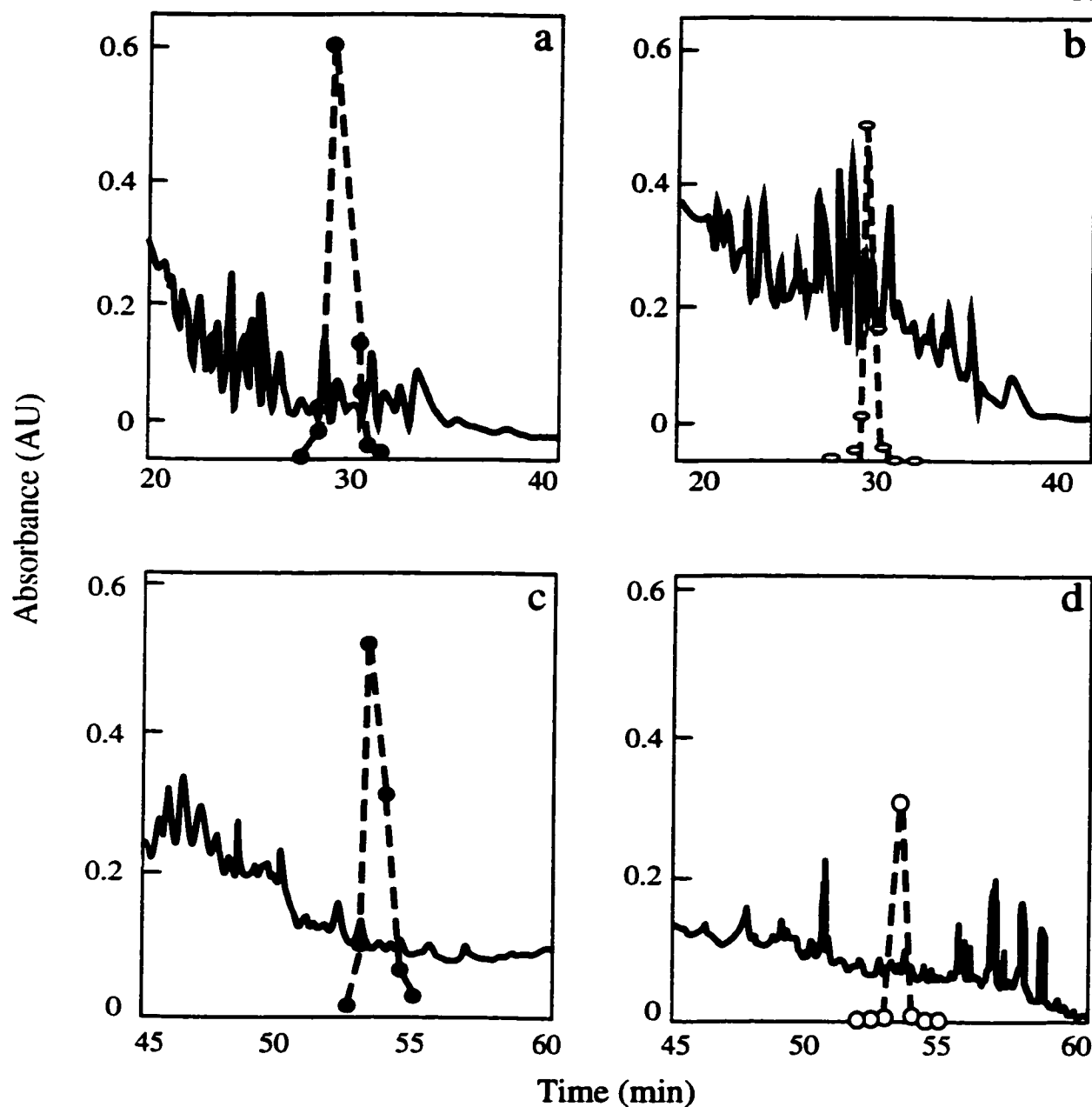
Figure 2-7. *Resolution of protein phosphatase inhibitors by two-step HPLC.* Separation of copepod (panel a) and crab larvae (panel b) extracts by reversed phase liquid chromatography on a C_{18} analytical column at pH 6.5. The dotted line represents inhibitory activity in the PP1 assay using 10 mM [^{32}P]phosphorylase a substrate. The solid line represents absorbance at 230 nm. Panels c (copepod) and d (crab larvae) represent further purification of the active fractions (from panels a and b) by reversed phase HPLC on a C_{18} analytical column at pH 2. The dotted line represents activity in a PP1 inhibition assay. The solid line represents detection at 206 nm. A standard of microcystin-LR eluted at 29 min (pH 6.5, top panels) and 54 min (pH 2, bottom panels) under identical conditions

migrate toward the negative electrode, taking water molecules with them. Hydrogen bonds between these water molecules and others in the buffer pull all of the buffer components, including anions, towards the negative electrode. At pH 8.3, EOF pulls the microcystin-LR toward the negative electrode despite the negatively charged Asp and Glu side chains. Peptide interactions with the capillary wall are also minimized at higher pH as both peptide (aspartic acid and glutamic acid side chains, pKa 3.9-4.8) and silanol groups on the capillary should be negatively charged. At pH 2, microcystin-LR will be positively charged due the to arginine side chain and will therefore migrate toward the negative electrode. However, EOF is significantly diminished at low pH, reducing mobility of the system when compared to the pH 8.3 CE separation. Capillary silanol groups are not completely ionized (SiOH) at pH 2, so cations from the buffer will not interact with the capillary wall to produce EOF (40). In the mid-range pH separations, mobility of the microcystin-LR is reduced compared to pH 8.3 because the negative charge of both the Asp and Glu side chains cannot be overcome by the only moderate EOF generated below pH 6.

Capillary electrophoresis of zooplankton samples

The presence of microcystin-LR was confirmed in copepod samples by capillary electrophoretic analyses (Figure 2-9). The PP1 inhibitor in the copepod extract co-migrated with a microcystin-LR standard. Co-injection of 50 picograms of microcystin-LR with the sample produced an appropriate increase in peak area. Unfortunately, results of the crab larvae sample analyses were not as clear (Figure 2-10). Although a small peak of absorbance did migrate at the same time as a standard of microcystin-LR, it
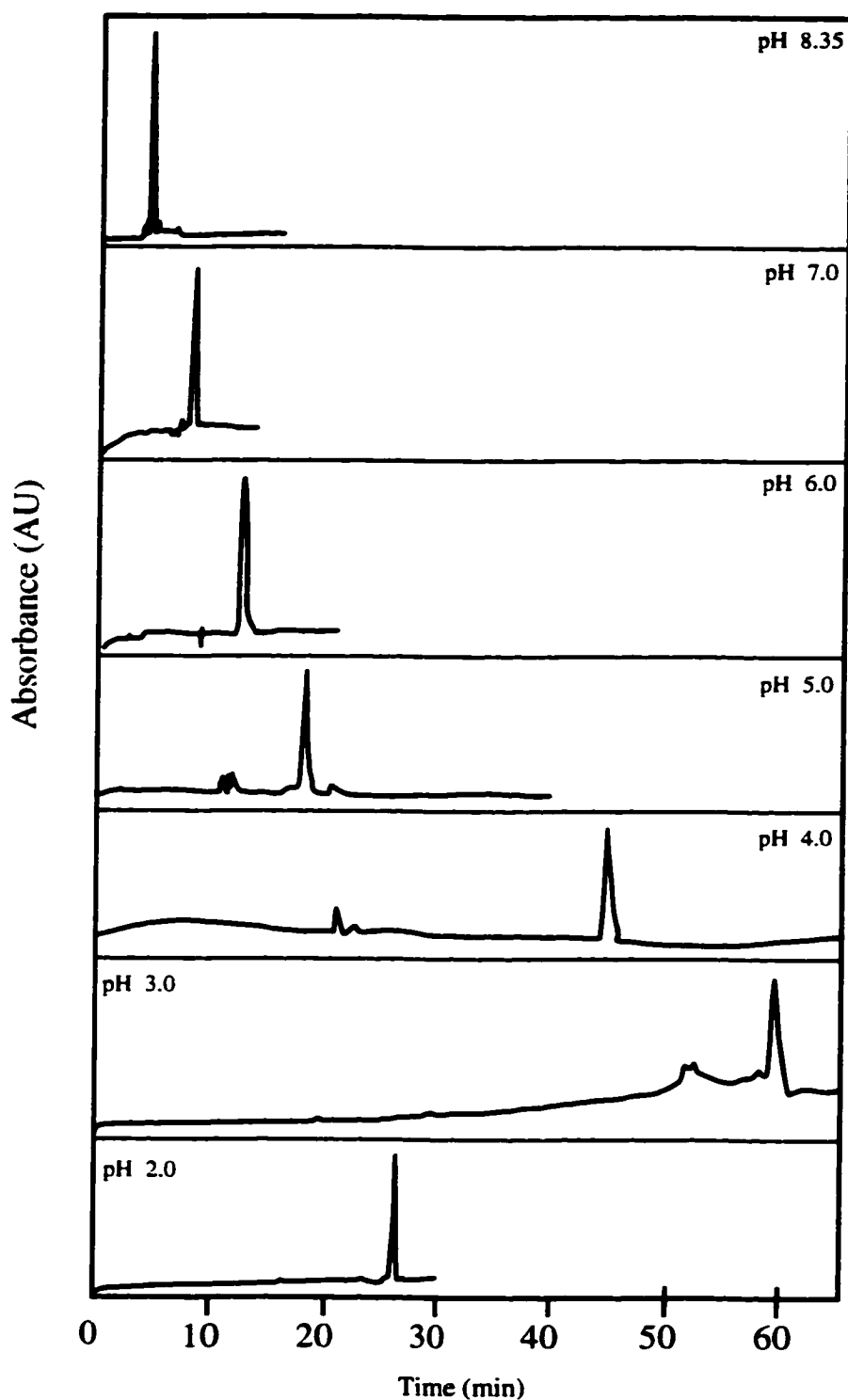
Figure 2-8. *Capillary electrophoresis of a microcystin-LR standard.* Detection of a 125 pg microcystin-LR standard was performed on a Beckman 2100 PACE instrument in a series of buffers covering a range of pH from 2 to 8.3. Buffers used were: 100 mM sodium phosphate buffer (pH 2-3 and 6-7), 100 mM sodium acetate buffer (pH 4-5) and 100 mM sodium borate buffer (pH 8.3). Separations were performed at 25°C with an applied constant voltage of 20 kV. Detection was at a wavelength of 200 nm.

0.005

a

0

b

0.004

0

c

0.004

Absorbance (AU)

0

3   4   5   6

Time (min)
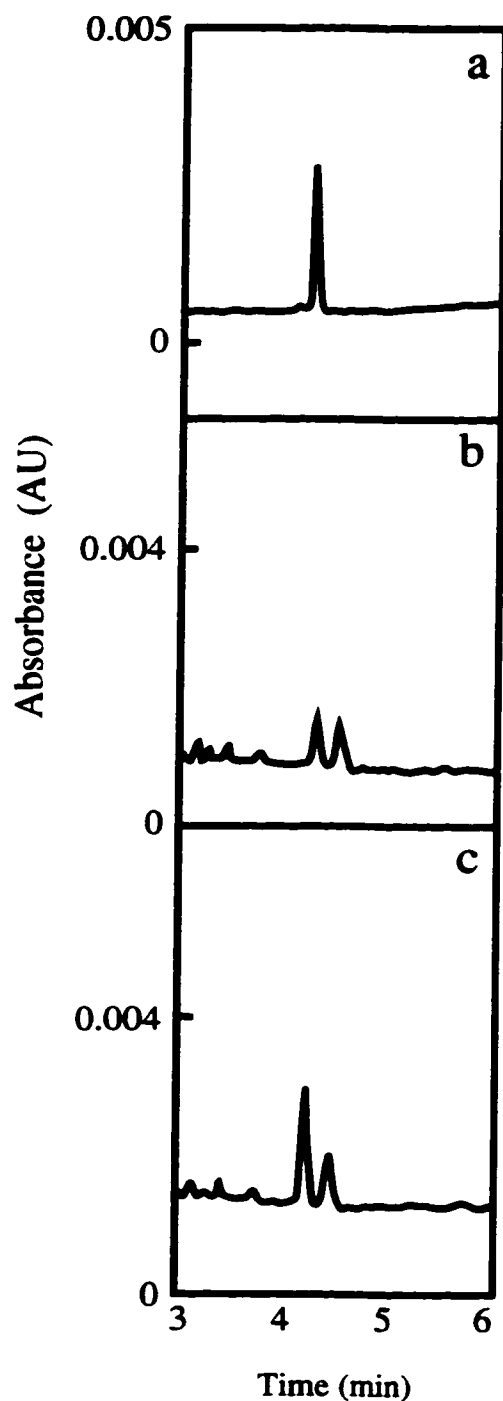
Figure 2-9. *Identification of microcystin-LR in copepod extracts by capillary electrophoresis.* Panel a represents a 100 pg standard of microcystin-LR separated by capillary electrophoresis at pH 8.3. Panel b represents the active PP1 inhibitory fractions from two-step HPLC purification of copepod extract (Figure 2-7, a and c) pooled and separated by capillary electrophoresis. The identity of the protein phosphatase inhibitor in the copepod extract was confirmed by spiking the sample with an internal microcystin-LR standard of 50 pg (panel c). CE detection was at 200 nm.
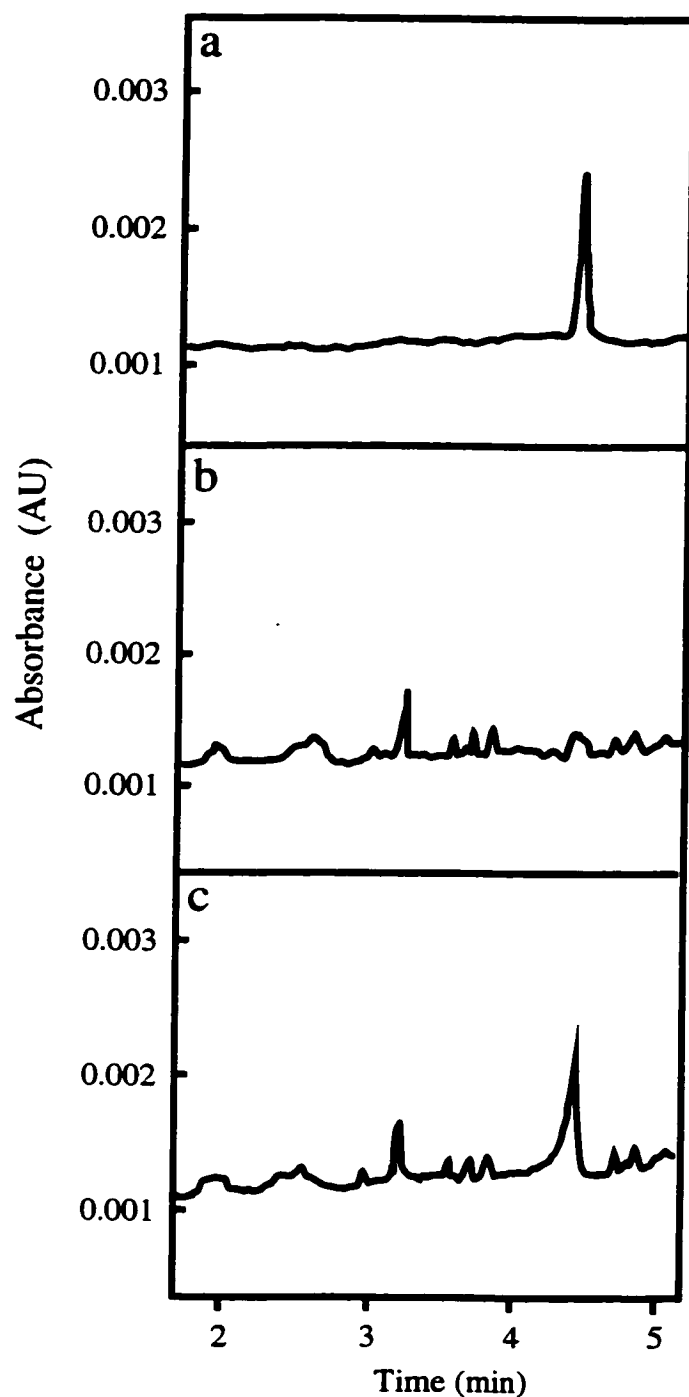
Figure 2-10. *Capillary electrophoretic separation of crab larvae fractions.* Panel a represents a 100 pg standard of microcystin-LR separated by capillary electrophoresis at pH 8.3. Panel b represents the active PP1 inhibitory fractions from two-step HPLC purification of crab larvae extract (Figure 2-7, b and d) pooled and separated by capillary electrophoresis. Panel c represents the results of spiking the sample with an internal microcystin-LR standard of 50 pg. CE detection was at 200 nm.

was not possible to definitively identify the toxin in the sample. As with all purification processes, a small amount of sample is lost at each step in our isolation procedure. This may be one reason that the crab larvae extracts examined in this study contained levels of microcystin-LR too low to unambiguously identify with CE, although the HPLC results certainly suggest that the inhibitor was present in the sample. It is also possible that some of the PP1 inhibition observed in initial phosphatase assays of the larval extracts was contributed by other marine phosphatase inhibitors.

Discussion

This work describes the application of HPLC-linked protein phosphatase inhibition assays followed by capillary electrophoresis for sensitive detection (low picogram levels) of microcystin-LR in marine samples. Testing of zooplankton blooms in the vicinity of salmon net-pens can prevent ingestion of the toxins by the farmed salmon, as net-pens can be towed away from toxic blooms.

Other analytical techniques, including an ELISA method (41) and HPLC/mass spectrometry (42), have been successfully employed for identification of microcystin-LR in biological samples, but are limited in sensitivity to detection of nanogram levels of toxin. Antibody-based methods are often specific to arginine-containing microcystin variants (56) and false positives from non-toxic variants are frequent. Organic solvents (frequently used in extraction protocols) or components of the biological sample often interfere with the ELISA detection system. In addition to requiring considerable animal sacrifice, the standard mouse bioassay (43) is much less sensitive than other methods (detects 1-200 micrograms) and does not allow for identification of toxins.

While many of the problems associated with detection of microcystin toxins were previously overcome by utilizing a protein phosphatase inhibition assay (20), analytical CE applied following reversed phase HPLC allows microcystin-LR to be directly detectable by absorbance at 200 nm. Additionally, it is possible to test samples for inhibitory activity in a phosphatase assay following fraction collection from the capillary (although only tiny amounts of sample are used). Microcystins have proven to be remarkably heterogeneous (13-17) and it is likely that previous methods of detection have underestimated the total number of microcystin variants in marine and freshwater samples

and/or included non-toxic varieties in quantitation. The presence of known analogues, such as microcystin-LA and LL, can be conveniently confirmed by CE using standards of each compound. Used in conjunction with the HPLC-linked PP1 assay, CE provides a valuable analytical technique for the detection of a variety of microcystins. The separation parameters of CE are different from reversed phase HPLC, and can be modified with a wide variety of capillary coatings and buffer additives (e.g. Teflon coating, SDS-gel polymers, surfactants, ion-pairing reagents, organic solvents).

In conclusion, the results presented here provide evidence for the presence of microcystin-LR in zooplankton associated with salmon net-pens. The discovery of microcystins in Calanoid copepods represents the first direct evidence supporting zooplankton as a food chain vector in NLD. Salmon NLD is one of the only easily-studied models of microcystin exposure in higher eukaryotes, and is therefore of interest not only to commercial salmon producers but also to researchers interested in developing possible treatments for acute and chronic microcystin intoxication. There is currently no known antidote to microcystin poisoning. Although several compounds have been shown to protect against microcystin uptake (44,45), they must be administered before exposure to the toxin. The combination of the protein phosphatase inhibition assay and capillary electrophoresis described in this work provides rapid and virtually unambiguous detection of microcystins at picogram levels in complex biological samples. This technique allows us to follow the transmission of microcystin up the food chain, from producer microorganism to eukaryotic, even human, consumer.

In the time since the work presented in this chapter was completed, microcystins have been shown to form a covalent bond with PP1 and PP2A (39,46-48). Inhibition of PP1 catalytic activity by the microcystins is extremely rapid; the phosphatase is fully inhibited by an excess of microcystin after a 10 minute incubation period. In contrast, covalent bond formation between the N-methyldehydroalanine (Mdha) residue of the microcystins and Cys-273 of PP1 is a much slower process - with approximately 65% of the phosphatase bound to microcystin after a 16 hr incubation period. Microcystin-LL played an important role in the identification of the covalent interaction between the microcystins and the phosphatase. Its hydrophobic nature facilitated resolution of the microcystin-PP1 complex from free phosphatase by reversed phase HPLC (39).

The discovery that microcystins can form irreversible bonds with protein phosphatases has important implications for quantitative determinations of the toxins in salmon and other aquatic organisms, as well as for assessments of the health risks of microcystin exposure. A limiting feature in our previous work with microcystins in the marine environment was a lack of correlation between the amount of microcystin detected in the livers of diseased salmon (or zooplankton vector) and the severity of the NLD observed (Charles Holmes, personal communication). This discrepancy has now been resolved, with the discovery of the covalent microcystin/PP1 complex.

It is not clear whether antibody based detection methods or protein phosphatase inhibition assays measure only free or both free and phosphatase-bound microcystins in methanol extracts of biological samples. Reversed phase HPLC separates free microcystin from the phosphatase/microcystin complex (39). This may result in

underestimation of the total amount of inhibitor present if only the fractions containing free microcystin are assayed and quantitated. Dr. D. Williams and Dr. R. Andersen (University of British Columbia), in collaboration with our laboratory, have recently developed a method of microcystin quantitation capable of detecting both free and covalently bound toxin (49). The procedure is based on the chemically unique nature of the C_{20} Adda residue found in all known microcystins. Lemieux oxidation (treatment with $KMnO_4$ + $NaIO_4$ oxidant solution at pH 9) (50-54) of microcystin-LR produces 2-methyl-3-methoxy-4-phenylbutanoic acid, a compound which is not a naturally occurring metabolite (55) and can therefore be used as a marker for the presence of microcystins. The acid can be isolated by ether extraction and detected at low concentrations by GC/MS (49).

The Lemieux oxidation method of microcystin quantitation is still in the development stages. However, an initial comparison between the results of the phosphatase inhibition assay and the Lemieux oxidation found that more microcystin was detected with the latter technique (49). This observation has been taken as direct evidence of the existence of covalently bound microcystins *in vivo*.

While it is possible that differences in sample preparation are responsible for some of the disparity of results between the two methods, the Lemieux oxidation study raises an important issue. We do not have any information about the role of the microcystin/phosphatase complex in the hepatotoxicity of microcystins. Given the tight-binding observed between microcystins and the protein phosphatases, it has been assumed that PP1 and PP2A are the primary target proteins for microcystins in salmon afflicted with net-pen liver disease, although this has yet to be confirmed experimentally.

It is important to determine whether inhibition of protein phosphatases is sufficient, or whether irreversible covalent binding is required, to cause the full pathology of NLD. We also do not know whether the covalent complex itself is toxic when, for example, salmon ingest zooplankton which contain bound microcystin. In practice, if bound microcystin-LR is no longer toxic, quantitation of 'free' microcystin with the HPLC-linked protein phosphatase inhibition assay may be all that is required when determining the health risk associated with any contaminated biological samples.

Chapter Two: References

1. Carmichael, W. W., Beasley, V., Bunner, D. L., Eloff, J. N., Falconer, I., Gorham, P., Harada, K. I., Krishnamurthy, T., Yu, M. J., Moore, R. E., Rinehart, K. L., Runnegar, M., Skulberg, O. M., and Watanabe, M. (1988) *Toxicon* **26**, 971-973

2. Carmichael, W. W. (1988) in *Natural Toxins* (Ownby, C. L., and Odell, G. V., eds), pp. 3-16, Pergamon Press, London

3. Rinehart, K. L., Harada, K. I., Namikoshi, M., Chen, C., Harvis, C. A., Munro, M. H. G., Blunt, J. W., Mulligan, P. E., Beasley, V. R., Dahlem, A. M., and Carmichael, W. W. (1988) *J. Am. Chem. Soc.* **110**, 557-558

4. Krishnamurthy, T., Szafraniec, L., Hunt, D. F., Shabinowitz, J., Yates, J. R., Hauer, C. R., Carmichael, W. W., Skulberg, O., Codd, G. A., and Missler, S. (1989) *Proc. Natl. Acad. Sci. U.S.A.* **86**, 770-774

5. Lawton, L. A., and Codd, G. A. (1991) *J. IWEM* **5**, 460-465

6. Honkanen, R. E., Zwiller, J., Moore, R. E., Daily, S. L., Khatra, B. S., Dukelow, M., and Boynton, A. L. (1990) *J. Biol. Chem.* **265**, 19401-404

7. Yoshizawa, S., Matsushima, R., Watanabe, M. F., Harada, K. I., Ichihara, K., Carmichael, W. W., and Fujiki, H. (1990) *J. Cancer Res. Clin. Oncol.* **116**, 609-614

8. MacKintosh, C., Beattie, K. A., Klumpp, S., Cohen, P., and Codd, G. A. (1990) *FEBS Lett.* **264**, 187-192

9. Nishiwaki-Matsushima, R., Nishiwaki, S., Ohta, T., Yoshizawa, S., Suganuma, M., Harada, K., Watanabe, M. F., and Fujiki, H. (1991) *Jpn. J. Cancer Res.* **82**, 993-996

10. Cohen, P., and Cohen, P. T. W. (1989) *J. Biol. Chem.* **264**, 21435-38

11. Kennelly, P. J., and Potts, M. (1999) *Front. Biosci.* **4**, d372-385

12. Namikoshi, M., Rinehart, K. L., Dahlem, A. M., Beasley, V. R., and Carmichael, W. W. (1989) *Tetrahedron Lett.* **30**, 4349-52

13. Namikoshi, M., Rinehart, K. L., Sakai, R., Stotts, R. R., Dahlem, A. M., Beasley, V. R., Carmichael, W. W., and Evans, W. R. (1992) *J. Org. Chem.* **57**, 866-872

14. Sivonen, K., Namikoshi, M., Evans, W. R., Gromov, B. V., Carmichael, W. W., and Rinehart, K. L. (1992) *Toxicon* **30**, 1481-85

15. Sivonen, K., Skulberg, O. M., Namikoshi, M., Evans, W. R., Carmichael, W. W., and Rinehart, K. L. (1992) *Toxicon* **30**, 1465-71

16. Sivonen, K., Namikoshi, M., Evans, W. R., Carmichael, W. W., Sun, F., Rouhiainen, L., Luukkainen, R., and Rinehart, K. L. (1992) *Appl. Environ. Microbiol.* **58**, 2495-500

17. Sivonen, K., Namikoshi, M., Evans, W. R., Fardig, M., Carmichael, W. W., and Rinehart, K. L. (1992) *Chem. Res. Toxicol.* **5**, 464-469

18. Harada, K.-I., and Tsuji, K. (1998) *J. Toxicol. Rev.* **17**, 385-403

19. Boland, M. P., Smillie, M. A., Chen, D. Z. X., and Holmes, C. F. B. (1993) *Toxicon* **31**, 1393-405

20. Holmes, C. F. B. (1991) *Toxicon* **29**, 469-477

21. Cohen, P., Alemany, S., Hemmings, B. A., Resink, T. J., Stralfors, P., and Tung, H. Y. L. (1988) *Meth. Enzymol.* **159**, 391-408

22. Eriksson, J. E., Toivola, D., Meriluoto, J. A., Karaki, H., Han, Y. G., and Hartshorne, D. (1990) *Biochem. Biophys. Res. Commun.* **173**, 1347-53

23. Lambert, T. W., Boland, M. P., Holmes, C. F. B., and Hrudey, S. E. (1994) *Environ. Sci. Technol.* **28**, 753-755

24. Bagu, J. R., Sykes, B. D., Craig, M. M., and Holmes, C. F. (1997) *J. Biol. Chem.* **272**, 5087-97

25. Chen, D. Z., Boland, M. P., Smillie, M. A., Klix, H., Ptak, C., Andersen, R. J., and Holmes, C. F. (1993) *Toxicon* **31**, 1407-14

26. Nishiwaki-Matsushima, R., Ohta, T., Nishiwaki, S., Suganuma, M., Kohyama, K., Ishiwaka, T., Carmichael, W. W., and Fujiki, H. (1992) *J. Cancer Res. Clin. Oncol.* **118**, 420-424

27. Carmichael, W. W. (1994) *Sci. Am.* **270**, 78-86

28. Yu, S.-Z. (1989) in: *Primary Liver Cancer* (Tang, Z. Y., Wu, M. C., and Xia, S. S., eds), pp. 30-37, Springer-Verlag, Berlin

29. Craig, M., McCready, T. L., Luu, H. A., Smillie, M. A., Dubord, P., and Holmes, C. F. (1993) *Toxicon* **31**, 1541-49

30. Kent, M. L., Myers, M. S., Hinton, D. E., Eaton, W. D., and Elston, R. A. (1988) *Dis. aquat. Organisms* **4**, 91-100

31. Kent, M. L. (1990) *Dis. aquat. Organisms* **8**, 21-28

32. Andersen, R. J., Luu, H. A., Chen, D. Z., Holmes, C. F., Kent, M. L., Le Blanc, M., Taylor, F. J., and Williams, D. E. (1993) *Toxicon* **31**, 1315-23

33. Wickstrom, M. L., Khan, S. A., Haschek, W. M., Wyman, J. F., Eriksson, J. E., Schaeffer, D. J., and Beasley, V. R. (1995) *Toxicol. Pathol.* **23**, 326-337

34. Ohta, T., Nishiwaki, R., Yatsunami, J., Komori, A., Suganuma, M., and Fujiki, H. (1992) *Carcinogenesis* **13**, 2443-47

35. Ghosh, S., Khan, S. A., Wickstrom, M., and Beasley, V. (1995) *Nat. Toxins* **3**, 405-414

36. Oda, R. P., and Landers, J. P. (1997) in *Handbook of Capillary Electrophoresis* (Landers, J. P., ed), pp. 1-48, CRC Press, Boca Raton

37. Alessi, D. R., Street, A. J., Cohen, P., and Cohen, P. T. (1993) *Eur. J. Biochem.* **213**, 1055-66

38. Zhang, A. J., Bai, G., Deans-Zirattu, S., Browner, M. F., and Lee, E. Y. (1992) *J. Biol. Chem.* **267**, 1484-90

39. Craig, M., Luu, H. A., McCready, T. L., Williams, D., Andersen, R. J., and Holmes, C. F. (1996) *Biochem. Cell Biol.* **74**, 569-578

40. Schwartz, H. E., Palmieri, R. H., Nolan, J. A., and Brown, R. (1992) *Separation of Proteins and Peptides by Capillary Electrophoresis: an Introduction*, II, Beckman, Fullerton, CA

41. Chu, F. S., Huang, X., and Wei, R. D. (1990) *J. Off. Assoc. Anal. Chem.* **73**, 451-456

42. Carmichael, W. W. (1992) *J. Appl. Bacteriol.* **72**, 445-459

43. Runnegar, M. T. C., Jackson, A. R. B., and Falconer, I. R. (1988) *Toxicon* **26**, 599-602

44. Kondo, F., Ikai, Y., Oka, H., Okumura, M., Ishikawa, N., Harada, K., Matsuura, K., Murata, H., and Suzuki, M. (1992) *Chem. Res. Toxicol.* **5**, 591-596

45. Runnegar, M., Berndt, N., and Kaplowitz, N. (1995) *Toxicol. Appl. Pharmacol.* **134**, 264-272

46. MacKintosh, R. W., Dalby, K. N., Campbell, D. G., Cohen, P. T. W., Cohen, P., and MacKintosh, C. (1995) *FEBS Lett.* **371**, 236-240

47. Runnegar, M., Berndt, N., Kong, S. M., Lee, E. Y. C., and Zhang, L. (1995) *Biochem. Biophys. Res. Commun.* **216**, 162-169

48. Goldberg, J., Huang, H. B., Kwon, Y. G., Greengard, P., Nairn, A. C., and Kuriyan, J. (1995) *Nature* **376**, 745-753

49. Williams, D. E., Craig, M., McCready, T. L., Dawe, S. C., Kent, M. L., Holmes, C. F., and Andersen, R. J. (1997) *Chem. Res. Toxicol.* **10**, 463-469

50. Lemieux, R. U., and von Rudloff, E. (1955) *Can. J. Chem.* **33**, 1701-709

51. Lemieux, R. U., and von Rudloff, E. (1955) *Can. J. Chem.* **33**, 1710-13

52. von Rudloff, E. (1955) *Can. J. Chem.* **33**, 1714-19

53. von Rudloff, E. (1956) *Can. J. Chem.* **34**, 1413-18

54. von Rudloff, E. (1965) *Can. J. Chem.* **43**, 1784-91

55. Sano, T., Nohara, K., Shiraishi, F., and Kaya, K. (1992) *Int. J. Environ. Anal. Chem.* **49**, 163-170

56. Dawson, R. M. (1998) *Toxicon.* **36**, 953-962

Chapter Three

Inhibition of Protein Phosphatase-1 by Clavosines A and B

Introduction

Serine/threonine protein phosphatases are highly conserved enzymes which have been isolated from numerous eukaryotic and prokaryotic organisms (1,2). Eukaryotic protein phosphatases are inhibited by a structurally diverse array of natural product toxins. These include the polyether okadaic acid from marine dinoflagellates, cyclic peptide microcystins and nodularins from cyanobacteria, and the spiroketal calyculins isolated from marine sponges (3).

The first member of the calyculin family of phosphatase inhibitors was identified in 1986 (4). Calyculin A was originally purified from a hydrophobic extract of the marine sponge *Discodermia calyx*. It was found to be cytotoxic towards P388 and L1210 leukemia cells, and to be a strong inhibitor of starfish egg development (4,5). It was subsequently characterized as a powerful inhibitor of the catalytic subunits of type 1 and 2A protein phosphatases, PP1 and PP2A, two of the major eukaryotic serine/threonine protein phosphatases (6). Calyculin A was also shown to have tumour-promoting activity as potent as that of okadaic acid (7). Many additional calyculins (8-13), and the structurally related calyculinamides (11,14), have since been identified.

Recently we reported the isolation of two novel glycosylated members of the calyculin family, clavosines A and B, from the marine sponge *Myriastra clavosa* (15). Clavosines A and B are potent inhibitors of mammalian PP1 and PP2A, and were found to be more cytotoxic overall than the calyculins and the calyculinamides (14,15) in the National Cancer Institute (NCI) screening panel of tumour cell-lines (16). The polyfunctional structure of clavosines A and B and calyculin A is depicted in linear

diagrams and space filling models in Figure 3-1. The clavosines have structural features in common with the calyculins, but differ markedly from them in having a trimethoxy rhamnose group at position C-21. Like the calyculinamides, the clavosines possess an amide at the end of their tetraene 'tail' instead of the nitrile group found in calyculin A (14). Clavosine A differs from clavosine B in having Z (cis) rather than E (trans) geometry at the C-2/C-3 double bond. Despite the large number of calyculins identified and characterized, we lack a detailed understanding of the mechanisms underlying their interactions with the protein phosphatases.

The mode of interaction of calyculin family members with protein phosphatases is controversial (17-20). Several models found in the literature are based on the assumption that the phosphate-containing calyculins bind in the same fashion as a phosphorylated substrate or inhibitor. However, a dephosphorylated analogue of calyculin A has been found to strongly inhibit PP1 and PP2A (12). This suggests that the phosphate group may not play a major role in the interaction of calyculin A with the protein phosphatases. Recently, the NMR solution structures of calyculin A and dephosphonocalyculin A were determined (21). The structure of dephosphonocalyculin A was found to be quite similar to that of calyculin A in both methanol and chloroform, implying that the phosphate group is not solely responsible for determining or stabilizing the calyculin structure.

a

Clavosine A : R₁=H, R₂=CONH₂, R₃=Me
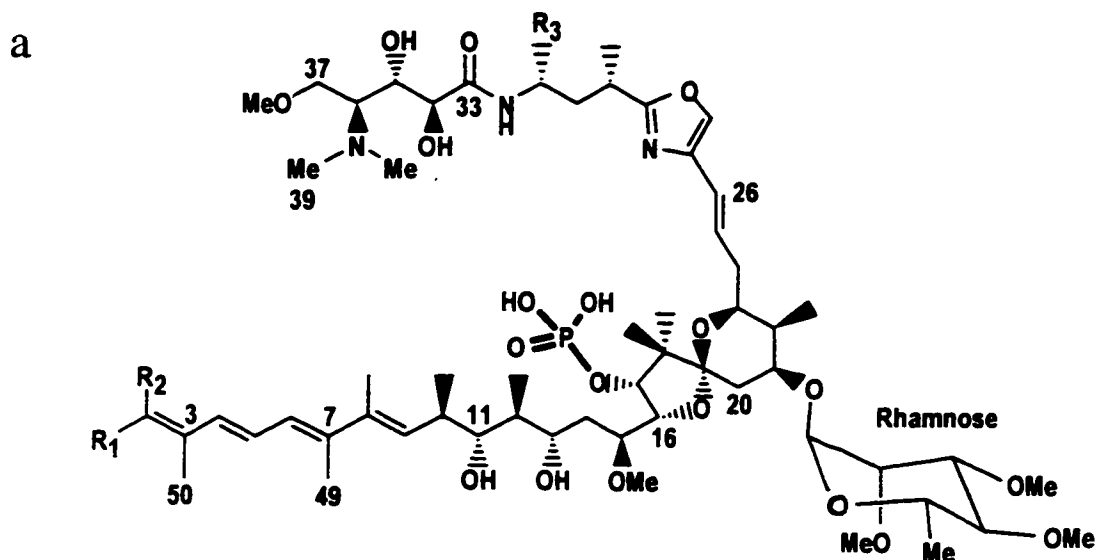
Clavosine A : R_1=H, R_2=CONH$_2$, R_3=Me
Clavosine B : R_1=CONH$_2$, R_2=H, R_3=Me
Calyculin A : R_1=H, R_2=CN, R_3=H, C21=OH

b

Calyculin A   Clavosine A   Clavosine B
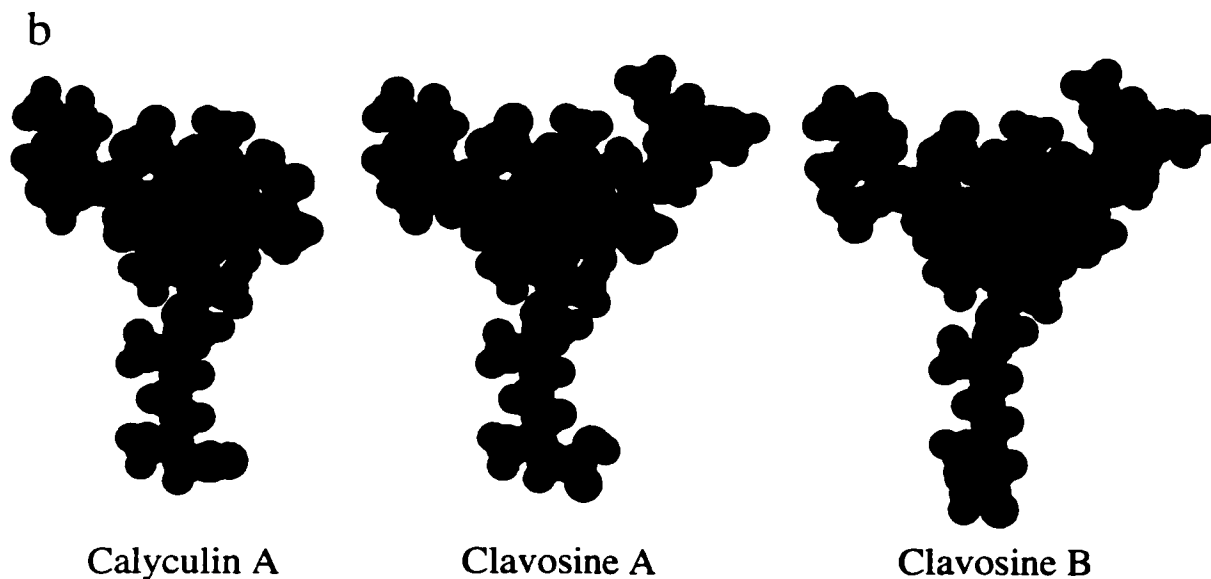
Figure 3-1. *Structures and space-filling models of calyculin A, clavosine A, and clavosine B.* (a) Orientation of the amide in clavosines A and B and the nitrile in calyculin A is indicated. Calyculin A has a C-32 H, C-21 hydroxyl, and 21 (R) configuration instead of the C-32 CH3, methylated rhamnose, and 21 (S) stereochemistry found in the clavosine structures. (b) Computer-generated space-filling models of calyculin A (blue), clavosine A (red), and clavosine B (green) displaying the similarities in inhibitor structure despite the addition of the rhamnose group to the clavosines. Models were generated using Insight II (Biosym/MSI Technologies Inc.) on a Silicon Graphics Indigo2 Impact 10000 workstation.

We have prepared a series of PP1 mutant enzymes to evaluate the roles played by specific amino acids in interactions with the calyculin family of inhibitors. In this study we have characterized the effects of these mutations on the ability of clavosines A and B, and calyculin A to inhibit PP1. Our experimental data gives us a basis for assessing models of calyculin binding found in the literature (Lindvall, M. et al., 1997, *J. Biol. Chem.* 272, 5087-97; Gupta, V. et al., 1997, *J. Med. Chem.* 40, 3199-3206; Gauss, C. et al., 1997, *Bioorg. Med. Chem.* 5, 1751-73). A new model for clavosine and calyculin A binding to PP1 is presented that is consistent with previous structure-function experiments and which accommodates important structural features of the clavosines, including the rhamnose moiety.

Experimental Procedures

Materials

Clavosines were purified by the laboratory of Dr. F. Schmitz (University of Oklahoma) as previously described (15). Calyculin A was obtained from Calbiochem (San Diego). Other reagents were obtained from Sigma Chemicals unless otherwise stated.

Cloning and mutagenesis of PP1γ

The cDNA encoding PP1γ was cloned (by Hue Anh Luu) from a human teratocarcinoma NT2 cDNA library (Stratagene) and sub-cloned into pBluescriptSK (Stratagene). The PP1γ insert was sequenced in its entirety and verified with the published sequence of the gamma isoform (22). PP1γ mutants were generated using the QuikChange Mutagenesis System and native *Pfu* polymerase (Stratagene). All mutant constructs were validated by DNA sequencing. Construction of the Val-223 and Ile-133 mutants was performed by John Dawson; PP1 mutants Phe-257, Cys-291, and Tyr-134 were constructed by Hue Anh Luu. Fragments comprising the wild-type and mutant PP1γ cDNA sequences were cloned into the expression vector pCW (generously provided by Dr. Dahlquist, University of Oregon).

PP1γ expression and purification

The recombinant PP1γ enzymes were expressed and purified to homogeneity as previously described (23,24). Expression of wild-type or mutant PP1γ in vector pCW was performed according to procedures outlined in Chapter Two with the following

exceptions. Cell lysates were produced in 50 mM imidazole, pH 7.5, 0.5 mM EDTA, 0.5 mM EGTA, 2.0 mM $MnCl_2$, protease inhibitor cocktail, 0.1% β-mercaptoethanol, and 10% glycerol. PP1γ was purified using a HiTrap Heparin-sepharose column (Pharmacia) followed by a HR 5/5 MonoQ column (Pharmacia) and fractions were screened by protein phosphatase activity assay after each column. Final phosphatase-containing fractions were pooled and dialyzed in 50 mM Tris-HCl, pH 7.5, 0.1 mM EDTA, 1.0 $MnCl_2$, 0.1% β-mercaptoethanol and 50% (v/v) glycerol for storage at -20°C. Preparations of PP1γ mutants had specific activities comparable to wild-type recombinant PP1γ, with the exception of I133Y, which was 4-fold more active (U/mg) than wild-type enzyme. (see Chapter Two for discussion of enzyme concentration and specific activity).

Protein phosphatase inhibition assays

Protein phosphatase-1 inhibition was assayed using 10 μM [^{32}P]phosphorylase *a* substrate as described in Chapter Two. Control phosphatase activity was standardized to 15% release of total phosphate from the substrate for each enzyme. Inhibitors in competition assays were pre-incubated with the enzyme for 15 minutes at 30°C before addition of dephospho-inhibitor-1 (residues 9-54) peptide or Inhibitor-2 (residues 34-102) peptide (Figures 1-5, 1-7 - see Chapters Four and Five for more information about I-1 and I-2-derived peptides). Reactions were initiated by the addition of substrate and assays were performed in duplicate. Reactions involving the clavosines were performed

under low light conditions to prevent photochemical isomerization of the terminal tetraene unit.

Modelling studies

Structures and binding models were generated on a Silicon Graphics Indigo^2 Impact 10000 workstation using Insight II software (v 95.0.4) developed by Biosym/MSI Technologies Inc. of San Diego. Docking simulations were performed using the extensible subset forcefield (ESFF) with the fixed docking method of Insight II. Energy minimization was performed using the Discover3 (v 3.0) module of Insight II with the ESFF forcefield.

The structure of Calyculin A (4) was obtained from the Cambridge Crystallographic Data Centre (code DUPSUW). In contrast to previous work published in collaboration with our laboratory (26), this calyculin A structure was inverted to obtain the correct, natural enantiomer (27). Although the absolute configurations of the clavosines have not been determined, they are assumed to be the same as those established for calyculins (15), with the exception of the carbon 21(S) configuration where the rhamnose group is linked to the clavosine backbone. Charges were adjusted to -2 for the phosphate group, but the dimethylamine was maintained in the free base form (27). The x-ray crystallographic coordinates of PP1α bound to microcystin-LR (28) were obtained from the Brookhaven Protein Database (PDB#1FJM). Chain B of the structure was deleted, as was microcystin-LR and all water molecules. To complete the structure, 16 amino acid side chains only partially detected by crystallographic methods were added (Arg-23, Pro-24, Lys-41, Glu-54, Gln-181, Met-190, Gln-198, Lys-211, Val-213, Gln-

214, Glu-218, Lys-234, His-237, Lys-260, Asp-300 - see Figure 3-2) as were hydrogens appropriate for pH 7.

Docking was carried out with half of the amino acid residues of PP1 (those comprising the active site 'face' of the protein) designated as the ligand-binding subset. We employed Metropolis docking at a temperature of 300 K with 200 minimization steps between structure evaluations. Several starting positions were investigated for each inhibitor. The lowest energy structures generated were examined and subjected to a more rigorous energy minimization using Discover3. Promising structures were used as the starting position for a second round of docking. During minimization of the docked models, subsets of the protein were defined so that amino acid residues within 10 Å of the inhibitor were allowed to be flexible while the rest of the protein was held fixed. The PP1/inhibitor complex was soaked with water molecules at a thickness of 5 Å and minimized to a convergence of 0.05 kcal/mol/Å using steepest descent and conjugate gradient algorithms.
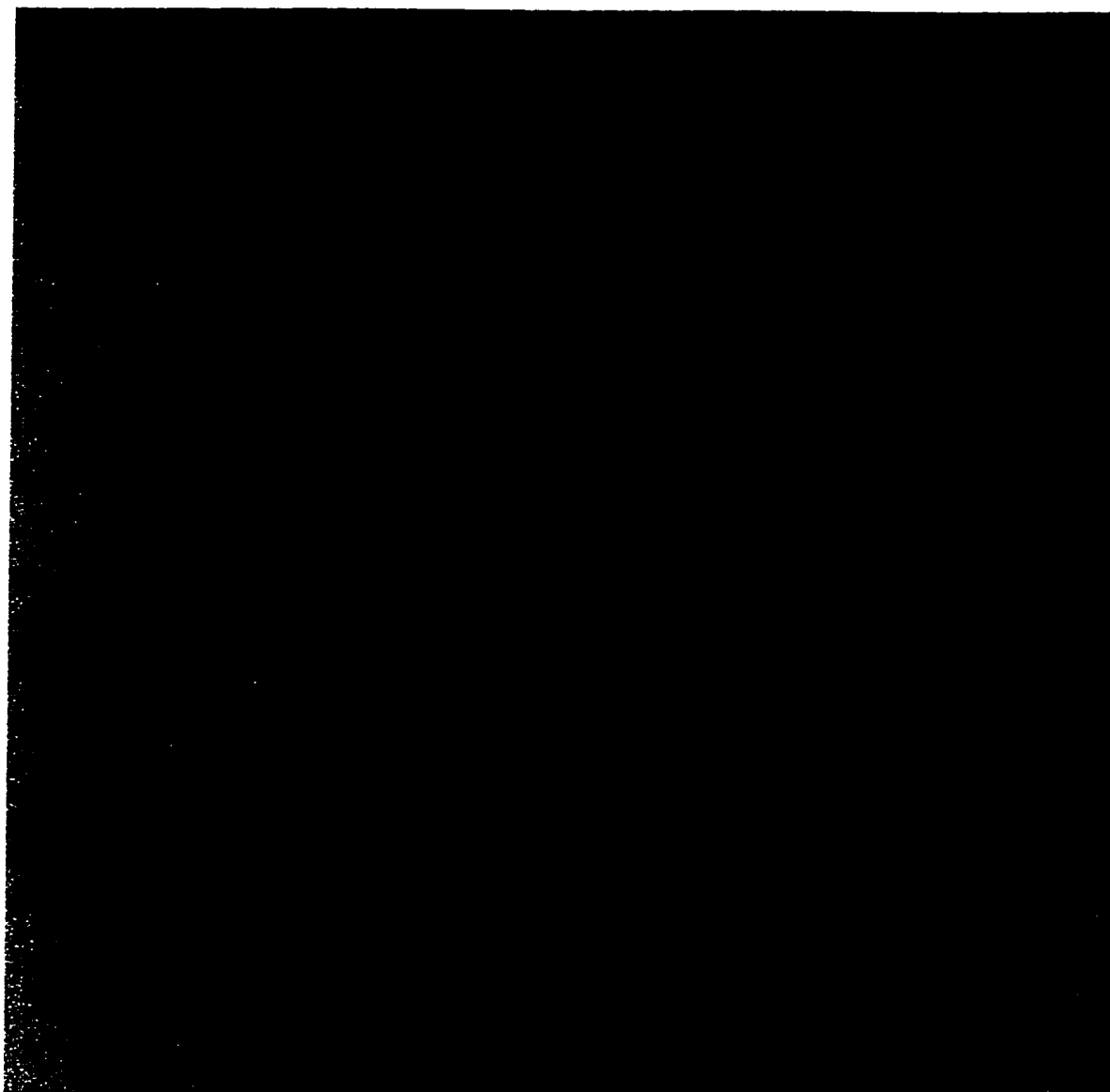
Figure 3-2. *Ribbon structure of PP1α highlighting side chains added for modelling studies.* 16 amino acid side chains only partially detected by x-ray crystallographic methods were added to the structure prior to modelling experiments. Arg-23, Pro-24, Lys-41, Glu-54, Gln-181, Met-190, Gln-198, Lys-211, Val-213, Gln-214, Glu-218, Lys-234, His-237, Lys-260, Asp-300 are shown in red. Lys-211 is labelled because it is proposed to be involved in PP1 binding to clavosine B (see modelling results). Manganese ions found in the catalytic site of the phosphatase are shown as pink balls. The structure shown is derived from the x-ray crystallographic coordinates of PP1α (28).

Results

Inhibition of protein phosphatase-1 and 2A by the clavosines and calyculin A

Clavosine A inhibited PP1γ and PP2A (Figure 3-3, IC_{50}= 0.5 nM and 0.6 nM, respectively) with virtually identical potency to calyculin A (Figure 3-3, IC_{50} = 0.7 nM and 0.5 nM, respectively). These results presumably reflect the similarities in orientation and overall structure of calyculin A and clavosine A. Clavosine B inhibited recombinant PP1γ with decreased potency (IC_{50} = 13 nM), but was almost as effective a PP2A inhibitor (IC_{50} = 1.2 nM) as clavosine A or calyculin A. While the C-2/C-3 E geometry of clavosine B resulted in a >25 fold increase in IC_{50} for this compound against PP1γ, this increase could not be attributed to the presence of a bulky rhamnose group, since clavosine A was as potent a protein phosphatase inhibitor as calyculin A.

Inhibition of PP1γ mutants

To further understand the mechanisms underlying inhibition of PP1γ by the clavosines, we examined the inhibitory effects of these toxins on a number of mutants of PP1γ. The crystal structure of microcystin-LR bound to PP1α (28) and molecular modelling studies of microcystins and okadaic acid bound to PP1 (17,18) suggest that Tyr-134 may be important for interaction with the calyculins. Three Tyr-134 PP1γ mutants allowed us to thoroughly investigate the role this amino acid residue plays in inhibition of phosphorylase *a* phosphatase activity of PP1γ by the clavosines and calyculin A (Figure 3-4). The first mutant tested was PP1γ Y134F, in which the potential for hydrogen
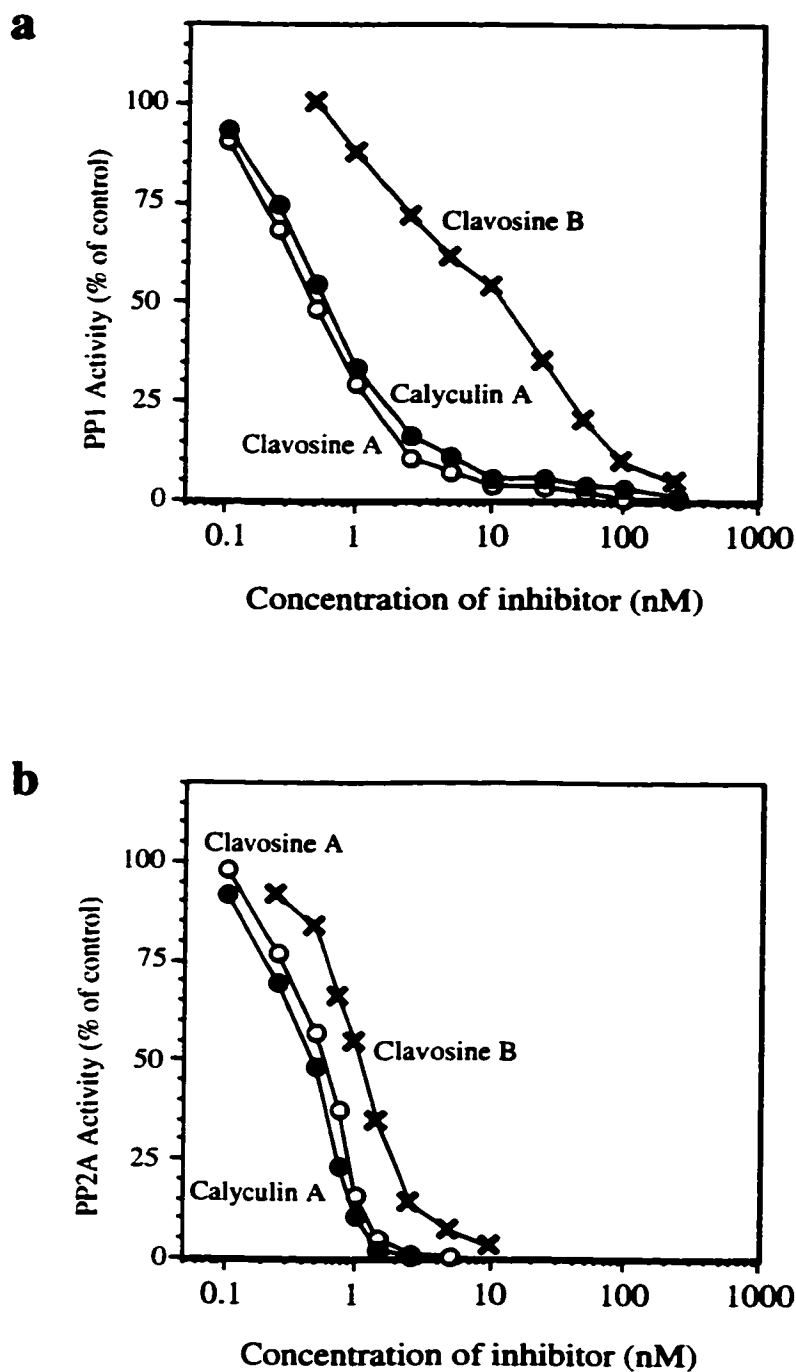
Figure 3-3. *Inhibition of protein phosphatase-1 and 2A by the clavosines and calyculin A.* Recombinant PP1γ was expressed in *E. coli* and PP2A was obtained from bovine cardiac muscle. PP1 and PP2A were assayed for activity using 10 μM [^{32}P]phosphorylase *a* substrate. Dose-response curves for the inhibition of (a) PP1γ and (b) PP2A activity by calyculin A(●), clavosine A(○), and clavosine B(✖) are shown.

bonding with the toxins was abolished with the tyrosine to phenylalanine mutation. The second mutant was Y134A, in which both the hydroxyl and hydrophobic aromatic ring were replaced by an alanine side chain. The third mutant was Y134D, in which an aspartic acid residue was inserted to introduce a negative charge in this region.

PP1γ Y134F was inhibited by clavosine A, clavosine B and calyculin A slightly more strongly (IC_{50} = 0.2 nM, 9.5 nM and 0.3 nM, respectively) than wild-type recombinant PP1γ (IC_{50} = 0.5 nM, 13 nM and 0.7 nM, respectively). In contrast, Y134A was inhibited less potently by all three inhibitors (IC_{50} = 5.5 nM, 145 nM and 2 nM, respectively). Y134D was significantly resistant to inhibition by clavosine A, clavosine B and calyculin A (IC_{50} = 93 nM, 4050 nM and 125 nM respectively).

Calcineurin (protein phosphatase-2B) is a protein phosphatase in the PPP family (with PP1 and PP2A) which is strongly resistant to inhibition by calyculin A (3). The residue corresponding to Val-223 in PP1γ is a cysteine in calcineurin (Cys-256). It was therefore of interest to mutate Val-223 to Ala and Cys in order to determine whether this residue may be involved in clavosine inhibition of PP1γ (Figure 3-5).

PP1γ V223C was inhibited by clavosine A, clavosine B and calyculin A with similar potency (IC_{50} = 0.6 nM, 22 nM and 0.9 nM, respectively) to wild-type PP1γ (IC_{50} = 0.5 nM, 13 nM and 0.7 nM, respectively). Surprisingly, V223A was more strongly inhibited by clavosine A, clavosine B and calyculin A (IC_{50} = <0.1 nM, 1 nM and 0.1 nM, respectively) than the wild-type enzyme. These experiments suggest that replacing the bulky side chain of valine with alanine may allow the calyculins, especially
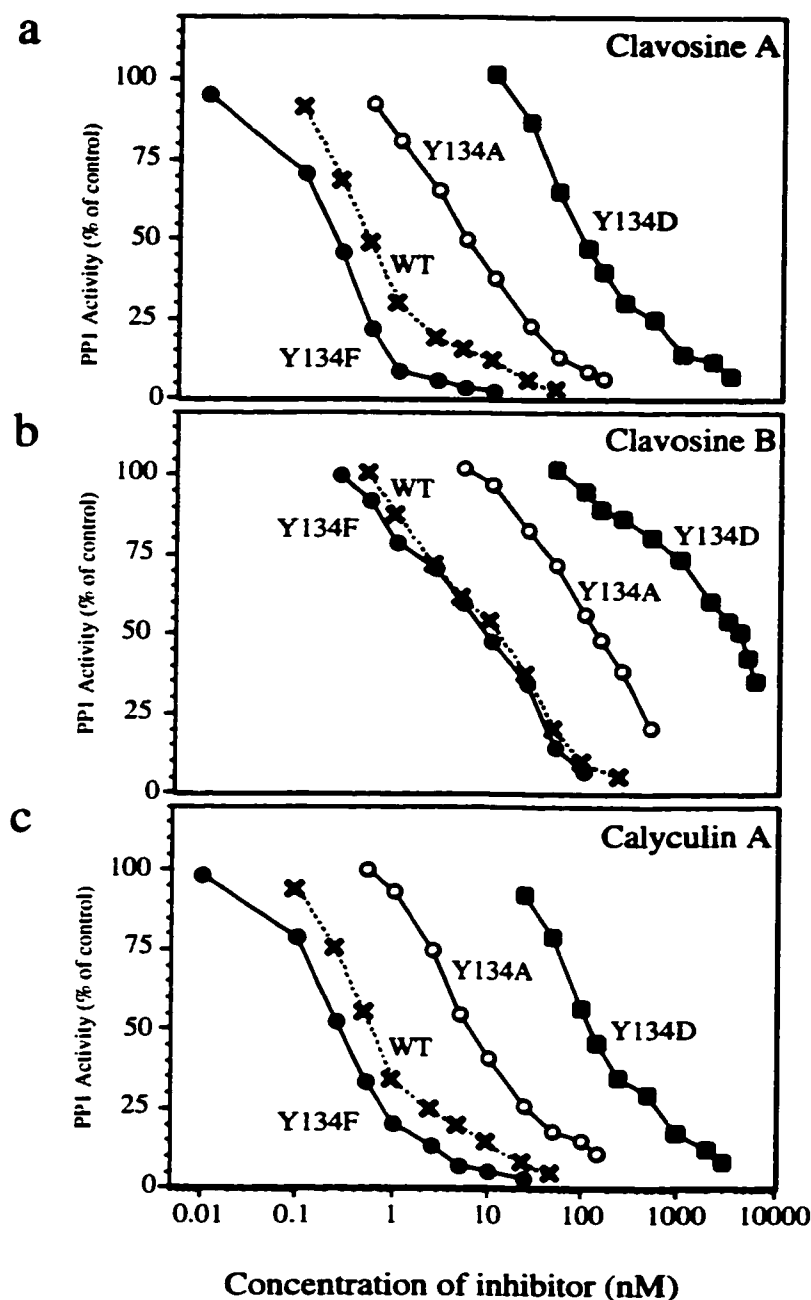
Figure 3-4. *Inhibition of Tyrosine 134 PP1γ mutants.* Site-directed mutagenesis was employed to substitute Phe, Ala and Asp residues in place of Tyr-134 in PP1γ, as described in text. Inhibition of protein phosphatase activity was assayed using 10 μM [^{32}P]phosphorylase *a* substrate. Dose-response curves for the inhibitors (panel a) clavosine A, (panel b) clavosine B, and (panel c) calyculin A, are shown for each of the following enzymes: Tyr134Phe(●), Tyr134Ala(O), Tyr134Asp(■) and wild-type PP1γ(✖).
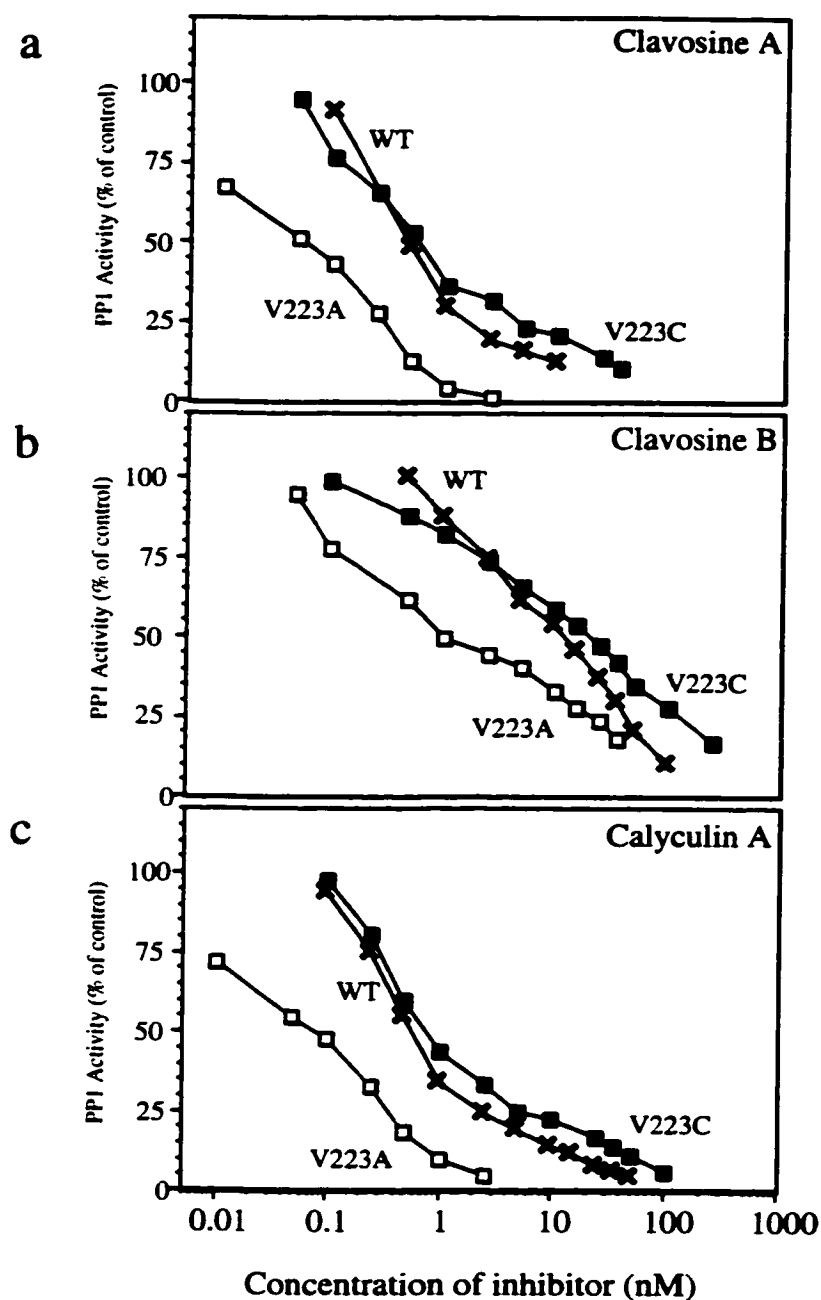
Figure 3-5. *Inhibition of Valine 223 PP1γ mutants.* Site-directed mutagenesis was employed to substitute Ala and Cys residues in place of Val-223 in PP1γ, as described in text. Inhibition of phosphatase activity was assayed using 10 μM [^{32}P]phosphorylase a substrate. Dose-response curves for the inhibitors (panel a) clavosine A, (panel b) clavosine B, and (panel c) calyculin A, are shown for the mutant enzymes Val223Ala(□), Val223Cys(■) and wild-type PP1γ(✗).

clavosine B, to interact more closely with PP1 in this region, thus reducing the IC_{50} values for each inhibitor.

Clavosine inhibition of other PP1γ mutants

The clavosines and calyculin A were additionally tested for inhibitory activity against other PP1γ mutant enzymes. The results from these studies are depicted in Table 3-1. Despite its proximity in sequence to Tyr-134, mutation of Ile-133 to Tyr resulted in no significant change in response to the clavosines or calyculin A. We also examined the effects of mutating Cys-291 and Phe-257 on toxin inhibition of PP1. These residues were chosen for our mutagenesis studies because they have been shown (29) to form part of a binding pocket in the phosphatase that interacts with the PP1 glycogen targeting subunit G_M. The sequence in G_M that binds to PP1 has been proposed to represent a common binding motif found in many PP1 regulatory or targeting proteins, including inhibitor-1 (I-1), a specific phosphoprotein inhibitor of PP1 (This will be discussed further in Chapter Five). PP1γC291A was inhibited by the clavosines and calyculin A with almost identical potency to wild-type recombinant PP1γ. Surprisingly, we found an increase in IC_{50} of approximately ten-fold for each of the calyculins with F257A. We feel that this mutation may have had a global effect on phosphatase structure because an increase in IC_{50} was also observed for the phosphatase inhibitors microcystin-LR, okadaic acid, inhibitor-1 (I-1) and inhibitor-2 (I-2) (Chapter Four, Table 4-2).

Table 3-1

Inhibition of mutant PP1γ enzymes by clavosine A, B and calyculin A

PP1 mutants were generated as described in experimental procedures. PP1γ activity was measured using 10 μM [^{32}P]phosphorylase *a* as a substrate. Each value represents the average of 3-5 independent experiments with a full range of inhibitor concentrations.

PP1γ	IC$_{50}$ (nM)		
	Calyculin A	Clavosine A	Clavosine B
Wild-type	0.7	0.5	13
Tyr134Phe	0.3	0.2	9.5
Tyr134Ala	7.0	5.5	145
Tyr134Asp	125	93	4050
Val223Ala	0.1	<0.1	1.0
Val223Cys	0.9	0.6	22
Ile133Tyr	1.2	0.6	15
Cys291Ala	1.5	0.8	17
Phe257Ala	13	8.0	125

Competition experiments

The addition of dephospho-inhibitor-1[9-54] or inhibitor-2[34-102] peptides did not interfere with inhibition of PP1γ by calyculin A or clavosines A or B (Figure 3-6). Both of these peptides bind PP1, but do not inhibit the enzyme at the concentrations used (Chapter Four). Our results agree with other competition studies using calyculin A and the
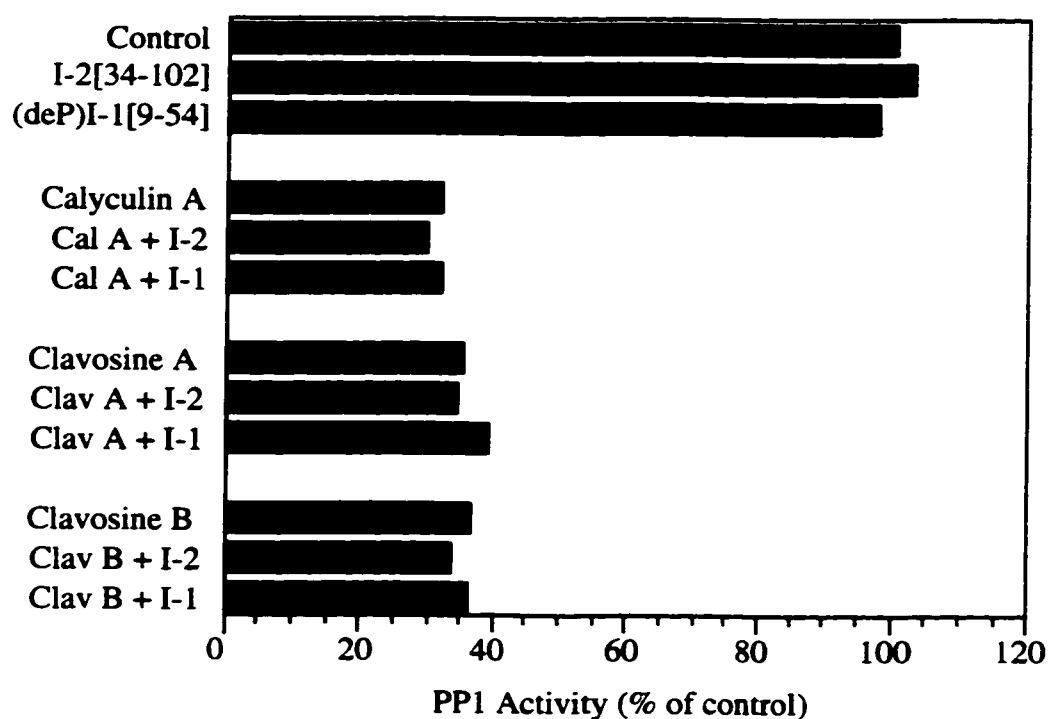
Figure 3-6. *Effect of I-1 and I-2 peptide antagonists on the inhibition of PP1γ by the calyculin family members.* Phosphatase activity was assayed using [^{32}P]phosphorylase as a substrate in the presence of peptide antagonists alone, or in combination with calyculin A, clavosine A or clavosine B. Dephospho I-1[9-54] and I-2[34-102] were added to a final concentration of 5 μM and 100 nM, respectively. Each competition assay was performed in triplicate, bars shown represent the average of 3 independent experiments which varied by <10%.

inhibitor proteins (39), which suggest that the calyculins do not share a common binding site with I-1 and I-2. It must be noted, however, that there are two independent structural elements in I-1 proposed to be required for effective inhibition of PP1: the phosphorylated Thr-35 residue and a PP1 binding motif composed of residues 9-12 (29,30,40). The dephospho-form of the inhibitor used in our competition experiments may only be capable of binding to PP1 via the latter element, which is distinct from the active site of the enzyme where the calyculins are proposed to bind (See Chapters Four through Six for discussion of I-1 and I-2).

Computer modelling studies

We carried out modelling studies on the interaction between the clavosines and PP1 to address three aspects of calyculin and clavosine structure: the position of the phosphate group with respect to the phosphatase, correlation of IC_{50} data with the orientation of the amide/nitrile portion of the tetraene tail, and accommodation of the rhamnose moiety in the PP1/clavosine complex. Using the experimental data generated in our mutagenesis studies and the PP1 structure-function information found in the literature (9,11,12,15,30,31), we generated models of the calyculins bound to PP1 (Figure 3-7).

Use of the extensible subset forcefield (ESFF) allowed us to perform all docking and minimization steps with manganese ions present in the active site of the enzyme. This is an important point. Some of the published structural models of calyculin A bound to PP1 have been created in the absence of metal ions in the catalytic site of the enzyme (19). Standard modelling forcefields (software containing energy parameters for

atoms in proteins) cannot accommodate metal ions in docking simulations. To account for the missing metals, researchers have chosen to fix the phosphate group of calyculin A in the active site of PP1. This is intended to mimic the coordination of metal ions by the phosphate-analogue tungstate, as determined in the crystal structure of tungstate bound to PP1 (2). It has not been experimentally determined that calyculin A binds to the active site of the enzyme. The ESFF forcefield calculates parameters for each atom in the protein structure rather than drawing information from a empirically determined, but limited database. It is capable of accommodating metal ions in modelling simulations. We were therefore able to initiate docking without fixing any portion of the calyculins in the active site of PP1. In this way, our modelling studies were performed without initial bias.

It was necessary to use the coordinates of the alpha isoform of PP1 (28) for our modelling studies, as coordinates for the gamma isoform were not available. The alpha and gamma isoforms of PP1 are nearly identical, with sequence differences located almost exclusively in the first five residues of the amino terminus and the last 29 residues of the carboxy terminus (Figure 1-1).

The inhibitor/phosphatase structures generated in our modelling studies were similar for each inhibitor. Tyrosine 134, one of the PP1 residues mutated in this study, is predicted to lie within 3 Å of the dimethylamine group in all of the inhibitor models. The dimethylamine has been previously determined to be critical for calyculin A inhibition of PP1 (11). Tyr-134 is in close proximity to the amine (Figure 3-1, panel a) in the clavosine A and calyculin A structures and the C-35 hydroxyl in clavosine B. Val-223 is

within 3.5 Å of each inhibitor, residing closer to clavosine B (< 3 Å) than the other two compounds.

From the models, the phosphate group in clavosine A and calyculin A is predicted to form a hydrogen bond with Arg-96 in PP1. All three models suggest a contact between the C-13 hydroxyl of the calyculin or clavosine and Arg-221 in PP1, with the clavosine B predicted to lie the closest to this amino acid. Asn-124 appears to reside within 3 Å of the C-33 carbonyl of each inhibitor. These three residues are proposed to be involved in the catalytic mechanism of the phosphatase (Figure 1-2, panel b). Additionally, the C-13 hydroxyl of calyculin A has been experimentally determined to be important for inhibition of PP1 and 2A (41).

In both clavosine models, the C-1 amide carbonyl group is predicted to form a contact with Lys-211, while the amide NH_2 group in clavosine B may also interact with Asp-210. As a surface residue, Lys-211 is one of the amino acids not fully detected in the original PP1α crystallographic coordinates (Figure 3-2). The Lys-211 side chain was added to the phosphatase structure prior to our docking experiments with the calyculins. It is not clear whether other published modelling studies have supplied the missing side chains; it would obviously be difficult to propose or dispute interactions between Lys-211 and the inhibitors if this residue was not present during docking procedures.

Additional residues in PP1 predicted to reside within 4 Å of the inhibitor in every model include: His-66, Asp-92, His-125, Ile-130, Arg-132, Trp-206, Asp-208, Pro-209, Asp-210, Asn-219, Asp-220, Thr-226, His-248, Gln-249, Val-250, Tyr-272. In addition, the manganese ions in the active site of the enzyme are within 4 Å of the inhibitors in all

of the models. Figure 3-8 displays residues in PP1 mutated in this study, relative to the

active site of the phosphatase. In addition, some of the amino acids proposed to be

involved in calyculin A inhibition of PP1 by other researchers (30,31) are highlighted.

Asp-210 and Lys-211, two residues proposed to be involved in clavosine binding by

computer modelling studies contained in this work, are also indicated.
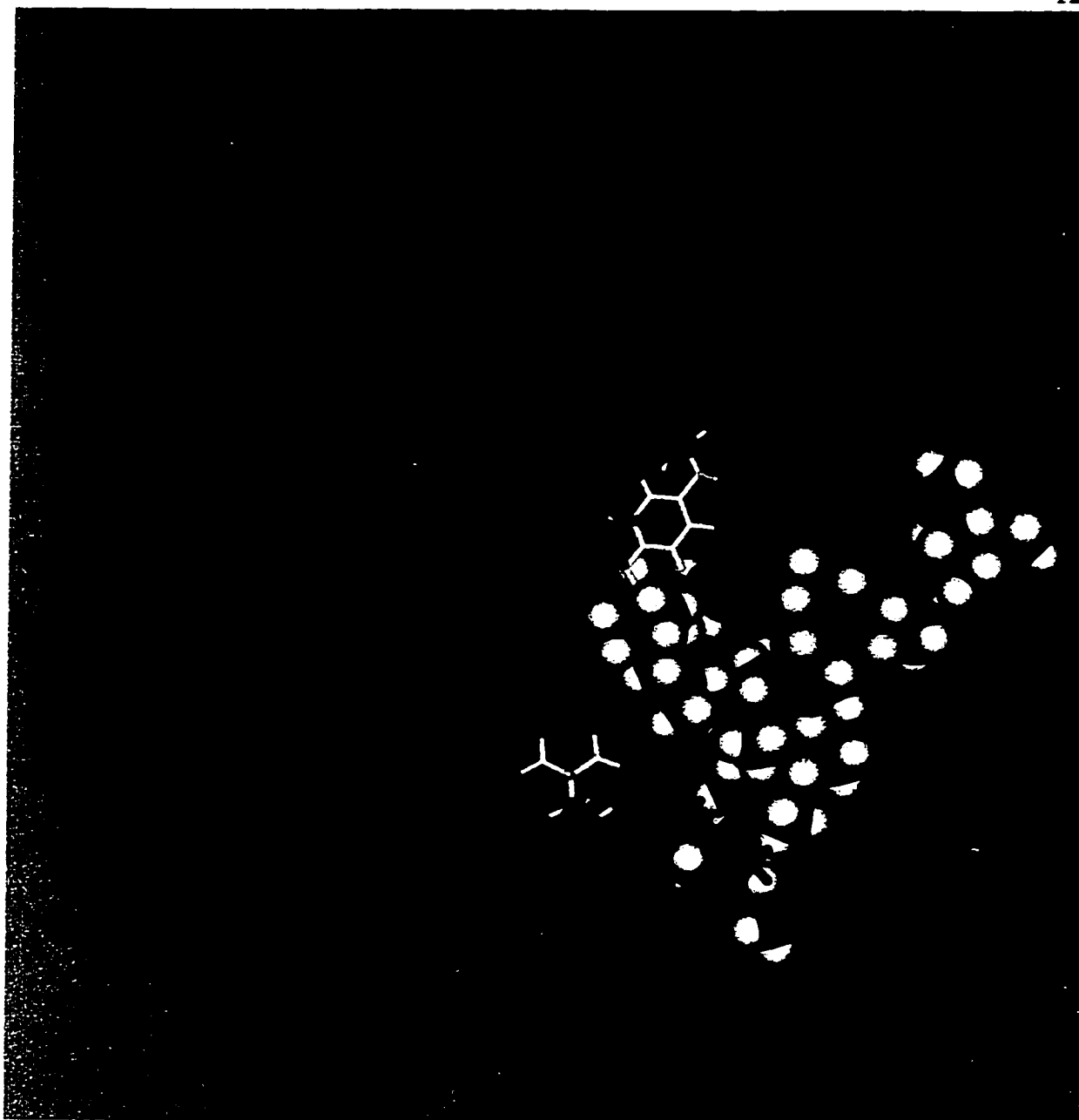
Figure 3-7(a). *Model of clavosine A bound to PP1.* Space-filling molecular model of clavosine A bound to a ribbon model of PP1. Manganese ions (pink balls) and amino acid side chains (blue sticks) in PP1 residing within 4 Å of clavosine A are shown. Key PP1 mutants examined in this study - tyrosine 134 (top) and valine 223 (bottom) - are highlighted in yellow. Atoms in the space-filling inhibitor models are coloured as follows: carbon (green), oxygen (red), nitrogen (blue), phosphorus (pink) and hydrogen (white). All models were generated in docking and energy minimization simulations (described in experimental procedures), using ESFF forcefield and Discover3 module of Insight II, on a Silicon Graphics Indigo2 Impact 10000 workstation.
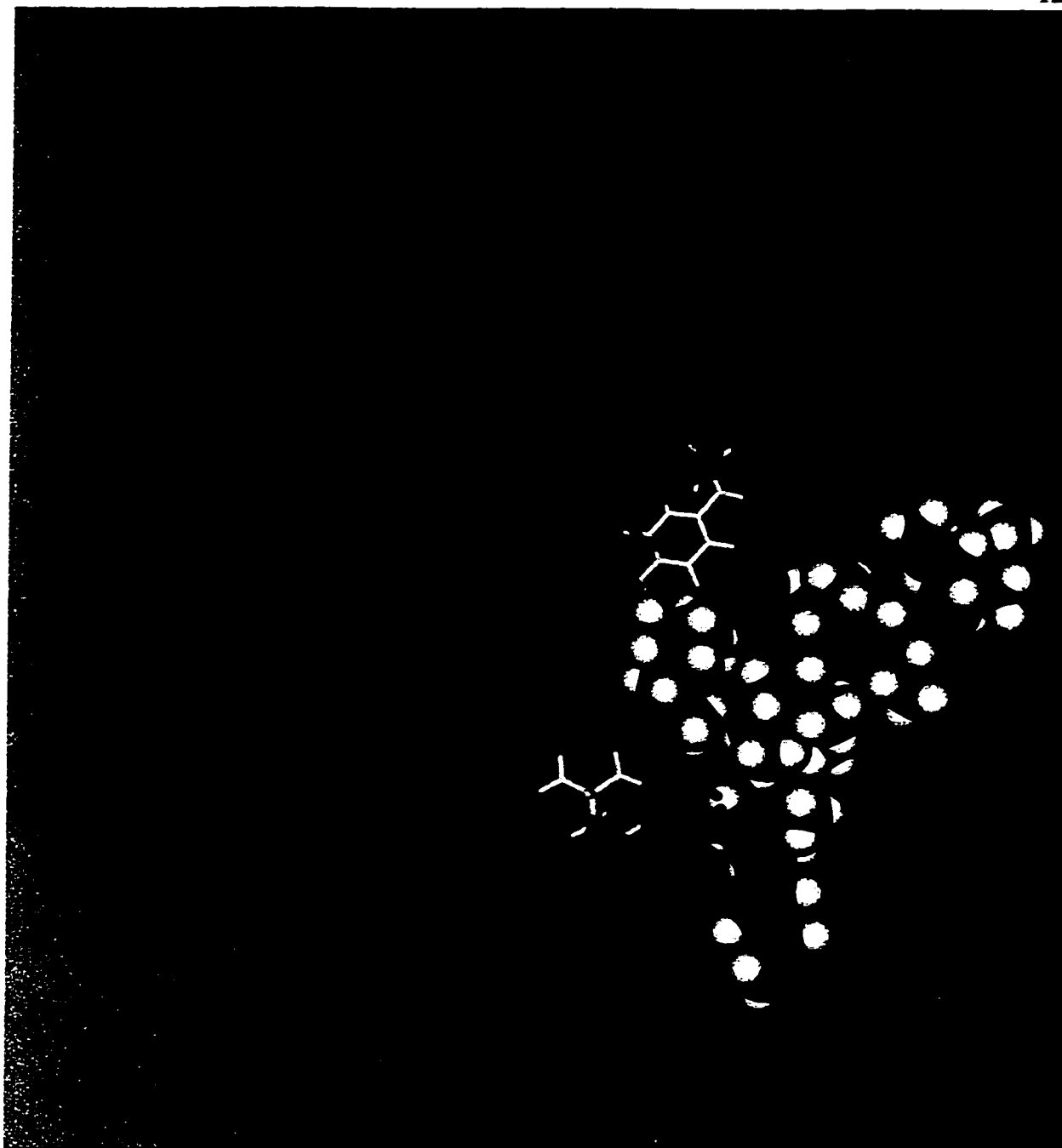
Figure 3-7(b). *Model of clavosine B bound to PP1.* Space-filling molecular model cla-vosine B bound to a ribbon model of PP1. Manganese ions (pink balls) and amino acid side chains (blue sticks) in PP1 residing within 4 Å of clavosine B are shown. Key PP1 mutants examined in this study - tyrosine 134 (top) and valine 223 (bottom) - are highlighted in yellow. Atoms in the space-filling inhibitor models are coloured as follows: carbon (green), oxygen (red), nitrogen (blue), phosphorus (pink) and hydrogen (white). All molecular models were generated in docking and energy minimization simulations (described in experimental procedures), using ESFF forcefield and Discover3 module of Insight II, on a Silicon Graphics Indigo2 Impact 10000 workstation.

Figure 3-7(c). *Model of calyculin A bound to PP1.* Space-filling molecular models of calyculin A bound to a ribbon model of PP1. Manganese ions (pink balls) and amino acid side chains (blue sticks) in PP1 residing within 4 Å of calyculin A are shown. Key PP1 mutants examined in this study - tyrosine 134 (top) and valine 223 (bottom) - are highlighted in yellow. Atoms in the space-filling inhibitor models are coloured as follows: carbon (green), oxygen (red), nitrogen (blue), phosphorus (pink) and hydrogen (white). All molecular models were generated in docking and energy minimization simulations (described in experimental procedures), using ESFF forcefield and Discover3 module of Insight II, on a Silicon Graphics Indigo2 Impact 10000 workstation.
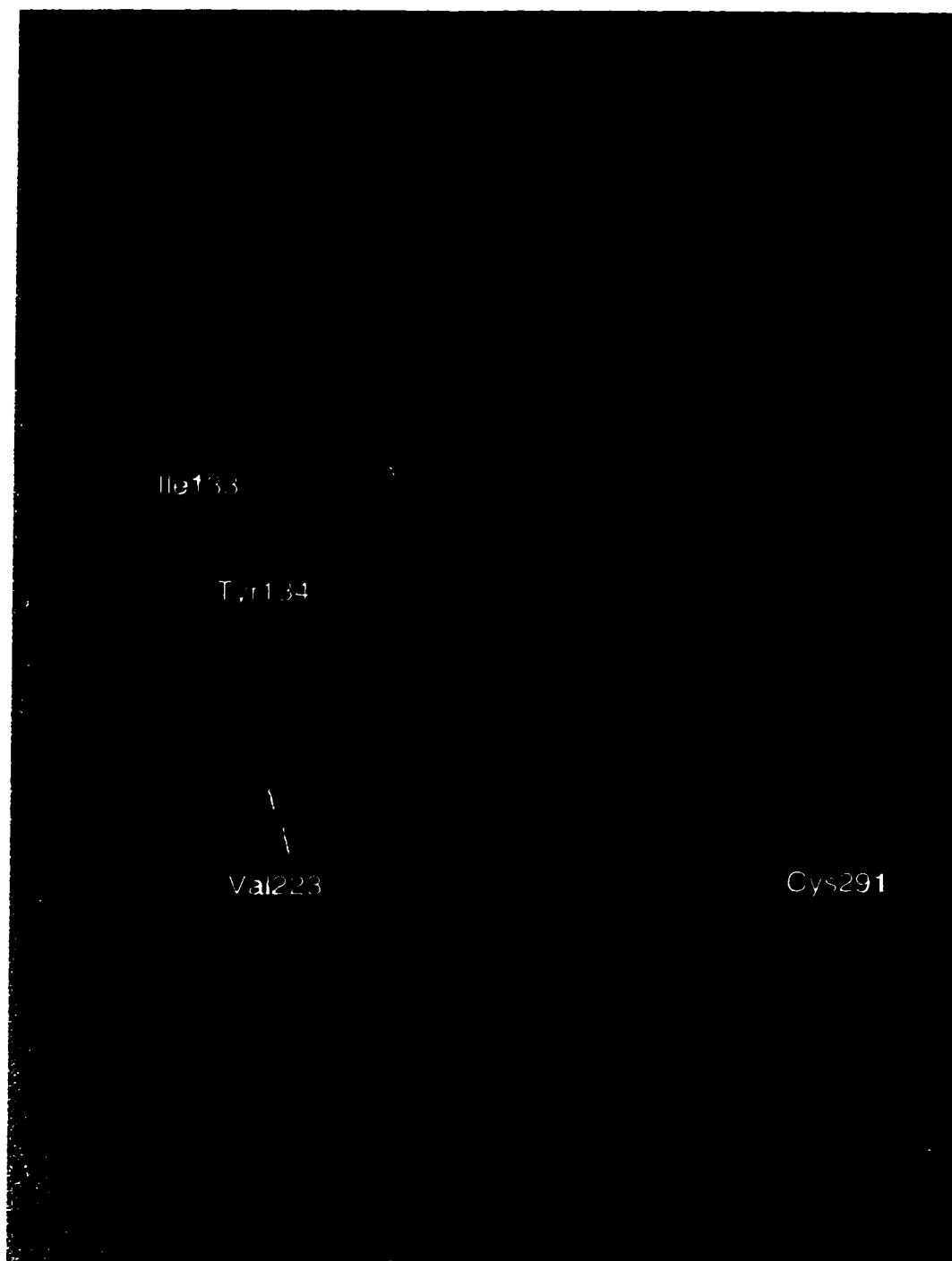
Figure 3-8. *Ribbon structure of PP1 highlighting residues in the phosphatase proposed to be involved in calyculin binding.* Mutations examined in this paper include Tyr-134 and Val-223 (yellow) and Ile-133 and Cys-291 (red). Residues previously shown to be involved in calyculin A inhibition of PP1 are also indicated: Arg-96 and Arg-221 (orange), and Tyr-272 (purple) (refs. 30,31). Amino acids predicted to affect binding of the terminal tetraene portions of the clavosines and calyculins to PP1 - Asp-210 (light blue) and Lys-211 (green) - are also displayed. Manganese ions found in the catalytic site of the phosphatase are shown as pink balls. The structure shown is derived from the X-ray crystallographic coordinates of PP1α (28).

Discussion

Site-directed mutagenesis of Tyr-134

In this study Clavosines A and B have been identified as potent protein phosphatase inhibitors, comparable to the other members of the calyculin family of natural product toxins. We have also shown that the Tyr-134 residue of PP1γ is a mediator of inhibition by these compounds. Mutation of Tyr-134 to Phe resulted in a slight decrease in IC_{50} for all three inhibitors, possibly indicative of an increased hydrophobic interaction with the Phe side chain in the absence of an hydroxyl group. Substitution of the aromatic side chain in this position for alanine significantly increased the IC_{50} values of clavosines A, B and calyculin A. The most dramatic effect on clavosine inhibition of PP1 was found by substituting Asp in place of Tyr-134. Clavosine B inhibited PP1γ Y134D with an approximately 310-fold decrease in potency (i.e. increase in IC_{50}) when compared to its inhibition of the wild-type enzyme. Clavosine A and calyculin A were also poor inhibitors of the Y134D mutant (200-fold and 175-fold worse than wild-type IC_{50} values, respectively). These results clearly show that the presence of a negative charge at residue 134 in PP1 is unfavourable for calyculin or clavosine inhibition.

Examination of existing calyculin A binding models

A recent computer modelling paper (18) has suggested that Tyr-134 may be involved in calyculin binding to PP1. Our mutagenesis data is the first experimental evidence to confirm the importance of this residue for inhibitor binding. The only known 3-D

structure of an inhibitor bound to PP1 is the x-ray structure of a microcystin-LR/PP1α complex determined by Goldberg et al. (28). One of the three areas of interaction between microcystin-LR and the phosphatase involved a possible hydrogen bond between the D-erythro-β-methyl aspartic acid (Masp) carboxylate group and Tyr-134 of PP1 (Chapter One). Therefore, mutagenesis of Tyr-134 served as an important starting point to test proposed models for binding of other toxins to PP1. Our results show that the PP1 Y134F mutant is actually more susceptible to inhibition by clavosine A/B and calyculin A than wild-type enzyme, thus arguing against the importance of hydrogen bonding between this residue and the calyculins .

In addition to the present work, there are three recent modelling papers that address calyculin A binding to PP1: Gauss et al., Gupta et al. and Lindvall et al. (17-19). The Gupta et al. publication proposes a direct role for Tyr-134 in calyculin binding to PP1. Their modelling studies propose hydrogen bonding between 1) the C-17 phosphate and C-35 hydroxyl of calyculin A with Arg-96 and 2) the C-34 hydroxyl and C-37 methoxy group of calyculin A with Tyr-134. We chose to test whether Tyr-134 was likely to make any hydrogen bond contact with the calyculins by mutating this residue to Phe. In view of the data presented here, it is possible that this model is incorrect with respect to hydrogen bond formation between calyculin A and PP1. The calyculin binding models of Gauss et al. and Lindvall et al. make no direct mention of the involvement of Tyr-134 in calyculin A binding. In contrast, our mutagenesis experiments suggest a role

for the aromatic ring of the Tyr-134 side chain in phosphatase inhibition by the calyculins.

Modelling of the interaction between PP1 and the clavosines

It has been widely suggested in the literature (recently in 17,18,30) that many of the natural product inhibitors of PP1 have a common mode of interaction with residues in the active site of the enzyme. Our models of clavosine binding to PP1 are consistent with this idea (Figure 3-7). Other recent mutagenesis studies have determined that Tyr-272 and Arg-96 mutant PP1 enzymes exhibit decreased sensitivity to calyculin A (30,31) (Figure 3-8). The mutants Asn-124, Asp-208, Arg-221 and His-248 also displayed resistance to this inhibitor (30,31). These residues are found within 4 Å of clavosines A, B and calyculin A in the models presented in this study.

The structures generated in our modelling simulations maintain the compact nature of the calyculin A crystal structure (when inverted to obtain the correct enantiomer) (4) and NMR solution structure (21), forming a 'wedge' shape that fits into the active site of the phosphatase (Figure 3-7). Our experiments and modelling studies support the idea that calyculins bind to PP1 in a compact manner, as opposed to the extended calyculin model structures found in the literature (19). Recently, NMR structures of calyculin A and dephosphonocalyculin A in organic solvents were determined (21). In chloroform, the solution structure of calyculin A is very similar to the compact, crystal structure (4).

Clavosine B inhibits recombinant PP1γ with an IC$_{50}$ value 26-fold greater than that observed for clavosine A. This increase in IC$_{50}$ is in agreement with the model shown

in Figure 3-7, panel b. This model suggests that the C-2/C-3 geometry of clavosine B forces the amide portion of the inhibitor towards the phosphatase structure, which results in a slight 'downward' shift away from the active site of PP1. In both clavosine models, the C-1 amide carbonyl appears to form a contact with Lys-211 of PP1. However, the orientation of clavosine B may allow formation of an additional contact between Asp-210 and the amide NH_2 group of the inhibitor, perhaps explaining the shift in the modelled complex. This movement away from the active site of the phosphatase may account for the reduction in effectiveness of clavosine B as an inhibitor of the recombinant enzyme.

The models of clavosine binding to PP1 shown in Figure 3-7 orient the phosphate group of each of the clavosines and calyculin A such that it interacts closely with Arg-96 of the phosphatase. However, given the strong inhibitory activity of a dephospho analogue of calyculin A toward PP1 (12), it is unlikely that this interaction forms the sole driving force for inhibition of the phosphatase. We found that calyculin A does not appear to depend solely on the phosphate group for maintaining its internal structure or its interaction with PP1, as the dephospho form of calyculin A docked similarly to the models in Figure 3-7, despite loss of contact with Arg-96 (Appendix I). During docking and energy minimization, the dephospho analogue exhibited internal structural changes consistent with previously determined experimental and structural observations (12). It will be interesting to compare our model to the recently published NMR structure of the dephospho analogue when the coordinates become available (21). The calyculin phosphate group is an important part of an 'extended' model of calyculin binding to PP1 that has been presented in the literature, which proposes that the phosphate-containing

calyculin is a mimic of the phosphorylated PP1 inhibitor protein I-1 (or the related protein DARPP-32). Several models of calyculin binding (17,19) appear to be based, at least in part, upon models of I-1 binding to PP1. Our computer simulations of clavosine binding suggest that the calyculin family of inhibitors do not bind as linear, phospho-peptidomimetics as has been previously proposed (19).

In our binding models the trimethoxy rhamnose group found in the clavosine structures is positioned so that it cannot interfere with toxin/protein binding. This is in accordance with data from our PP1 inhibition assays (Figure 3-3), which indicate that calyculin A and clavosine A inhibit PP1γ with similar potencies. In both clavosine models the rhamnose resides close to Glu-275 and Phe-276 in PP1 but is clearly oriented away from the enzyme.

Cytotoxicity of the clavosines

The average cytotoxicity of the clavosines was higher than that of calyculin A in the National Cancer Institute tumour cell screens (15). It is possible that the rhamnose group found only in the clavosines may play a role in cytotoxicity. Lectins are a group of proteins which recognize specific carbohydrates and are involved in host-pathogen interactions, targeting of proteins within cells, and cell-cell interactions (32-34). It is possible that a rhamnose-specific lectin could be involved in clavosine binding and uptake by a particular cell type, or in an intracellular targeting mechanism. Rhamnose-specific lectins have been predominantly identified in fish eggs (35-37). Perhaps the clavosines discourage predation of marine sponges and/or associated microorganism(s) which

produce the compounds. Species of fish with rhamnose-specific lectins could be harmed if the clavosines were ingested. Interestingly, some cancer cell types may have receptors that recognize a rhamnose or rhamnose-like residue. Binding of solasodine glycosides (rhamnose-containing sugars) to tumour cells is thought to occur via the rhamnose moiety. These sugars selectively destroy tumour cells *in vivo* (38).

In conclusion, there is a great need for further NMR or x-ray crystallographic work in this area. Determination of the structure of the clavosines or calyculin A bound to PP1 would address many of the controversial questions regarding the specific mode of interaction between the calyculins and the protein phosphatases. Work is currently underway in our laboratory (in collaboration with Dr. M. James, University of Alberta) to crystallize the clavosines bound to recombinant protein phosphatase-1γ.

References

1. Kennelly, P. J., and Potts, M. (1999) *Front. Biosci.* **4**, d372-385

2. Barford, D., Das, A. K., and Egloff, M.-P. (1998) *Annu. Rev. Biophys. Biomol. Struct.* **27**, 133-164

3. MacKintosh, C., and MacKintosh, R. W. (1994) *Trends Biochem. Sci.* **17**, 444-447

4. Kato, Y., Fusetani, N., Matsunaga, S., Hashimoto, K., Fujita, S., and Furuya, T. (1986) *J. Am. Chem. Soc.* **108**, 2780-81

5. Kato, Y., Fusetani, N., Matsunaga, S., and Hashimoto, K. (1988) *Drugs Exptl. Clin. Res.* **14**, 723-728

6. Ishihara, H., Martin, B. L., Brautigan, D. L., Karaki, H., Ozaki, H., Kato, Y., Fusetani, N., Watabe, S., Hashimoto, K., Uemura, D., and Hartshorne, D. J. (1989) *Biochem. Biophy. Res. Commun.* **159**, 871-877

7. Suganuma, M., Fujiki, H., Furuya-Suguri, H., Yoshizawa, S., Yasumoto, S., Kato, Y., Fusetani, N., and Sugimura, T. (1990) *Cancer Res.* **50**, 3521-25

8. Kato, Y., Fusetani, N., Matsunaga, S., Hashimoto, K., and Koseki, K. (1988) *J. Org. Chem.* **53**, 3930-32

9. Matsunaga, S., Fujiki, H., Sakata, D., and Fusetani, N. (1991) *Tetrahedron* **47**, 2999-3006

10. Okada, A., Watanabe, K., Umeda, K., and Miyakado, M. (1991) *Agric. Biol. Chem.* **55**, 2765-71

11. Matsunaga, S., Wakimoto, T., and Fusetani, N. (1997) *J. Org. Chem.* **62**, 2640-42

12. Matsunaga, S., Wakimoto, T., and Fusetani, N. (1997) *Tetrahedron Lett.* **38**, 3763-64

13. Steube, K. G., Meyer, C., Proksch, P., Supriyono, A., Sumaryono, W., and Drexler, H. G. (1998) *Anticancer Res.* **18**, 129-137

14. Dumdei, E. J., Blunt, J. W., Munro, M. H. G., and Pannell, L. K. (1997) *J. Org. Chem.* **62**, 2636-39

15. Fu, X., Schmitz, F. J., Kelly-Borges, M., McCready, T. L., and Holmes, C. F. B. (1998) *J. Org. Chem.* **63**, 7957-63

16. Boyd, M. R., and Paull, K. D. (1995) *Drug Dev. Res.* **34**, 91-109

17. Gauss, C. M., Sheppeck, I. J., Naim, A. C., and Chamberlain, R. (1997) *Bioorg. Med. Chem.* **5**, 1751-73

18. Gupta, V., Ogawa, A. K., Du, X., Houk, K. N., and Armstrong, R. W. (1997) *J. Med. Chem.* **40**, 3199-206

19. Lindvall, M. K., Pihko, P. M., and Koskinen, A. M. (1997) *J. Biol. Chem.* **272**, 23312-16

20. Quinn, R. J., Taylor, C., Suganuma, M., and Fujiki, H. (1993) *Bioorg. Med. Chem. Lett.* **3**, 1029-34

21. Volter, K. E., Pierens, G. K., and Quinn, R. J. (1999) *Bioorg. Med. Chem. Lett.* **9**, 717-722

22. Norman, S. A., and Mott, D. M. (1994) *Mamm. Genome* **5**, 41-45

23. Craig, M., Luu, H. A., McCready, T. L., Williams, D., Andersen, R. J., and Holmes, C. F. B. (1996) *Biochem. Cell Biol.* **74**, 569-578

24. Dawson, J. F. (1998) *Regulation of Protein Phosphatase-1 by Reversible Phosphorylation and Marine Toxins.* Ph.D. Thesis, Dept. Biochemistry, University of Alberta, Edmonton, Alberta

25. Holmes, C. F. B. (1991) *Toxicon* **29**, 469-477

26. Bagu, J. R., Sykes, B. D., Craig, M. M., and Holmes, C. F. (1997) *J. Biol. Chem.* **272**, 5087-97

27. Matsunaga, S., and Fusetani, N. (1991) *Tetrahedron Lett.* **32**, 5605-06

28. Goldberg, J., Huang, H. B., Kwon, Y. G., Greengard, P., Naim, A. C., and Kuriyan, J. (1995) *Nature* **376**, 745-753

29. Egloff, M. P., Johnson, D. F., Moorhead, G., Cohen, P. T., Cohen, P., and Barford, D. (1997) *EMBO J.* **16**, 1876-87

30. Huang, H. B., Horiuchi, A., Goldberg, J., Greengard, P., and Naim, A. C. (1997) *Proc. Natl. Acad. Sci. USA* **94**, 3530-35

31.   Zhang, L., Zhang, Z., Long, F., and Lee, E. Y. (1996) *Biochemistry* **35**, 1606-11

32.   Rini, J. M. (1995) *Annu. Rev. Biophys. Biomol. Struct.* **24**, 551-577

33.   Weis, W. I., and Drickamer, K. (1996) *Annu. Rev. Biochem.* **65**, 441-473

34.   Elgavish, S., and Shaanan, B. (1997) *Trends Biochem. Sci.* **22**, 462-467

35.   Hosono, M., Kawauchi, H., Nitta, K., Takayanagi, Y., Shiokawa, H., Mineki, R., and
       Murayama, K. (1993) *Biol. Pharm. Bull* **16**, 239-243

36.   Gabius, H. J. (1987) *Cancer Invest.* **5**, 39-46

37.   Tateno, H., Saneyoshi, A., Ogawa, T., Muramoto, K., Kamiya, H., and Saneyoshi, M. (1998) *J. Biol. Chem.* **273**, 19190-97

38.   Cham, B. E., and Daunter, B. (1990) *Cancer Lett.* **55**, 221-225

39.   Kwon, Y. G., Huang, H. B., Desdouits, F., Girault, J. A., Greengard, P., and Nairn, A. C.
       (1997) *Proc. Natl. Acad. Sci. U.S.A.* **94**, 3536-41

40.   Connor, J. H., Quan, H. N., Ramaswamy, N. T., Zhang, L., Barik, S., Zheng, J., Cannon, J. F.,
       Lee, E. Y., and Shenolikar, S. (1998) *J. Biol. Chem.* **273**, 27716-24

41.   Fujiki, H., and Suganuma, M. (1991) *Adv. Cancer Res.* **61**, 143-194

Chapter Four

Inhibition of PP1 by Inhibitor-2

Introduction

Inhibitor-2 (I-2) is a 23 kDa protein that was first identified in rabbit skeletal muscle as a heat-stable protein that specifically inhibits protein phosphatase-1 (1). I-2 is present in both the cytosol and the nucleus, and its protein and mRNA levels are regulated in a cell-cycle dependent manner (2,3). *In vitro*, I-2 can be phosphorylated on threonine 72 by glycogen synthase kinase-3 (GSK-3) (4), cyclin B-cdc2 (5), and mitogen-activated protein kinase (MAPK) (6). Thr-72 phosphorylation prevents inhibition of PP1 (4). I-2 is also phosphorylated on serines 85, 120, and 121 by Casein Kinase II (CKII) , which does not alter its activity as an inhibitor of PP1 (7).

The interaction between PP1 and I-2 is complicated and somewhat controversial (8). I-2 forms a stable, inactive, 1:1 complex with the PP1 catalytic subunit which can be purified from the cytosol of many mammalian tissues (9-13). The *in vivo* role of this complex is unclear, but it appears to be distinct from the rapid and reversible initial inhibition of PP1 by the inhibitor protein (reviewed in 14). *In vitro* activation of PP1 from the inactive complex requires phosphorylation of I-2 with GSK-3 (11,15). It has been proposed that phosphorylation of I-2 promotes a conformational change in the I-2/PP1 complex which allows the slow dephosphorylation of I-2 by PP1 (11,16,17). Once I-2 is dephosphorylated, an increase in PP1 activity is observed (13,17,18). The G_M subunit from skeletal muscle or the M_{110} subunit from smooth muscle can displace PP1 from the PP1/I-2 complex only after GSK-3 phosphorylation (19). For this reason, the inactive complex of PP1 and I-2 is postulated to represent a pool of PP1 catalytic subunit

which is maintained inactive and ready to interact with targeting subunits *in vivo* (14,19,20).

In vitro studies suggest that I-2 can interact with denatured PP1 to promote refolding of the protein to yield an active enzyme, after the complex is phosphorylated by GSK-3 (19). Recombinant PP1 was shown to behave more like native enzyme (with respect to inhibitor sensitivity, manganese dependency and substrate specificity) after incubation with I-2 and phosphorylation of I-2 by GSK-3 (19,21). These observations have led to the proposal that I-2 is a chaperone for PP1 *in vivo*, promoting correct folding of newly synthesized enzyme. In addition, maintaining the correct conformation of pre-existing PP1 would prevent the uncontrolled dephosphorylation of phosphotyrosine residues in the cell (19,21) (see Chapter One for discussion of the properties of the recombinant enzyme). No other PP1 binding proteins tested have been able to mimic the behaviour of I-2 (21), which suggests that the ability to correct the conformation and activity of PP1 is one of the physiological roles of inhibitor-2 (21).

The region of PP1 involved in binding to I-2 is unknown, although we do have information about residues in inhibitor-2 which may be involved. Previous truncation studies have indicated that the N-terminal (1-35) region of I-2 is important for inhibition of PP1 (22). The C-terminal acidic region (residues 145-204) is not necessary for inhibition (22), but may be important for re-activation of PP1/I-2 complexes by GSK-3 (22) (Figure 1-7). Recent work by Huang et al. 1999, has determined that residues 9-99 of I-2 are important for PP1 inhibition (23). A conserved region between I-2 and the related proteins Glc8 (*S. cerevisiae*) and inhibitor-t (*D. melangaster*), composed of

residues 140-145 (FEXXRK), has been proposed to be involved in PP1 binding (24) as well as I-2 nuclear localization (3). Conserved residues 10-14 (IKGI) and 41-46 (KKSQKW) of inhibitor-2 have also been suggested to be PP1 binding sequences (23).

A hydrophobic channel in the C-terminal region of PP1 has been shown by x-ray crystallography to form a binding pocket in the phosphatase that interacts with a peptide fragment of the PP1 glycogen targeting subunit G_M (25). The sequence in G_M that binds to PP1 has been proposed to represent a common binding motif - (R/K)(V/I)XF) - found in many PP1 regulatory or targeting proteins, including inhibitor-1 (25) (see Chapter Five). The $^{10}IKGI^{14}$ sequence in inhibitor-2 does not compete with DARPP-32 for binding to PP1, suggesting that this portion of I-2 binds at a region distinct from the (R/K)(V/I)XF binding site (23).

In this study we attempted to find a minimal fragment of inhibitor-2 which could inhibit PP1 and be phosphorylated by GSK-3. We are interested in learning more about the interaction between I-2 and PP1, with the eventual aim of producing 'renatured' PP1 from recombinant enzyme. Compared to the native form of the enzyme, recombinant PP1 is insensitive to inhibitor-1 and more effective at dephosphorylating non-physiological substrates (19,21). Unlike native phosphatase, recombinant PP1 isoforms are Mn^{2+} dependent and are unable to interact with targeting proteins (19,26). When I-2 is complexed with recombinant PP1 and subsequently phosphorylated by GSK-3, the properties of the recombinant PP1 enzyme revert to those of native PP1 (19,21). Creating native-like PP1 may allow us to work more effectively with inhibitor-1 and PP1 in the future (I-1 is discussed fully in Chapters Five and Six).

Experimental Procedures

Materials

Native rabbit skeletal muscle PP1 was obtained from Upstate Biotechnology and recombinant PP1γ was produced as described in Chapter Three. I-1 and I-2 peptide fragments were synthesized by Paul Semchuk (Protein Engineering Network Centre of Excellence, University of Alberta). Recombinant GSK-3β and recombinant rabbit skeletal muscle inhibitor-2 protein were obtained from New England Biolabs (NEB). Phosphocellulose disks were purchased from GIBCO BRL. All other reagents were purchased from Sigma Chemicals unless noted.

Protein phosphatase inhibition and competition assays

Protein phosphatase-1 inhibition was assayed using [^{32}P]phosphorylase a substrate as described in Chapter Two. Assays contained 50 mM Tris-HCl, 25 mM β-mercaptoethanol, 1 mg/mL BSA, 3.75 mM caffeine, 10 μM ^{32}P-phosphorylase a. Control phosphatase activity was standardized to 15% release for each enzyme used. PP1 mutants Phe-257 and Cys-291 were prepared as described in Chapter Three. Competition assays contained 500-750 nM phospho-inhibitor-1$_{[9-54]}$ peptide (see Figure 1-5 or Table 5-3 for sequence) or 2.5-5 nM full-length inhibitor-2 protein (Figure 1-7) with competing peptides I-2$_{[34-102]}$ (100 nM), dephospho-inhibitor-1$_{[9-54]}$ (5 μM), or I-2$_{[72-102]}$ (25 μM). An increase in PP1 activity (which is a decrease in PP1 inhibition) was interpreted to represent competition for PP1 binding between the inhibitor and

competitor peptides present in the assay (see also Chapter Five). Reactions were initiated with the addition of substrate. All reactions were performed in triplicate.

GSK-3 phosphorylation of I-2$_{[34-102]}$

I-2$_{[34-102]}$ peptide was phosphorylated by recombinant rabbit skeletal muscle GSK-3, β isoform, in time-course experiments. 200 μL reactions contained 50 mM Tris-HCl (pH 7.5), 10 mM MgCl$_2$, 0.5 mg/mL BSA, 5% glycerol, 200 μM ATP, 1.5 μL of γ-labelled [^{32}P]ATP (3000 Ci/mmol, Amersham), and 20 μM peptide. Phosphorylations were performed with 20 U of GSK-3β. 1 unit is defined as the amount of GSK-3 required to catalyze the transfer of 1 pmol of phosphate to I-2 per min (27). Reactions were incubated at 30 °C and 15 μL aliquots were removed to 5 μL of 5% acetic acid on ice at time points indicated. Samples were spotted onto phosphocellulose disks, allowed to dry, washed 3 times in 75 mM phosphoric acid, once in distilled H$_2$0 and once in 80% ethanol. Disks were allowed to dry, placed into 2 mL scintillation fluid, and cpm determined in a Pharmacia Rack β counter. Total cpm was determined by adding 15 μL of each reaction directly into 2 mL scintillation fluid. Control reactions without peptide and/or without enzyme were performed. Cpm for each disk was divided by the total cpm/nmol ATP present in the reaction, to obtain the number of moles of ATP incorporated into each peptide.

Results

PP1 inhibition assays with inhibitor-2 fragments

In an attempt to find a short fragment of I-2 capable of binding and inhibiting PP1, we examined the inhibitory activity of two synthetic I-2 peptides (Table 4-1). The first 100 amino acids of inhibitor-2 have been shown to be involved in PP1 inhibition (22,23), so we synthesized fragments representing residues 34-102 and 72-102 to investigate the properties of these shorter I-2 peptides. Full-length I-2 inhibited native PP1 with an IC_{50} of 2.1 nM and recombinant PP1γ with an IC_{50} of 0.9 nM (Figure 4-1). Truncation of the inhibitor-2 sequence to residues 34-102 significantly increased the IC_{50} for both phosphatase enzymes - 14 μM for native PP1 and 8.5 μM for recombinant PP1. A shorter peptide composed of residues 72-102 from inhibitor-2 was unable to fully inhibit native or recombinant PP1, even at extremely high (100 μM) concentrations. These results confirm the importance of I-2 residues 1-33 in PP1 inhibition, although it is interesting that the 69 residue I-2 peptide was able to inhibit PP1, albeit at micromolar concentrations (Table 4-1).

GSK-3 phosphorylation of I-2[34-102]

Inhibitor-2 is phosphorylated on threonine 72 by GSK-3 (4), an event which allows activation of PP1 from an inactive complex with I-2 (11,15,22). In this study, we investigated whether the truncated I-2 peptide[34-102] could be phosphorylated by GSK-3β (Figure 4-2). Although the β isoform of GSK-3 is reported to be a better inhibitor-2 kinase than the α isoform of the enzyme (27), we were unable to incorporate more than

a

b
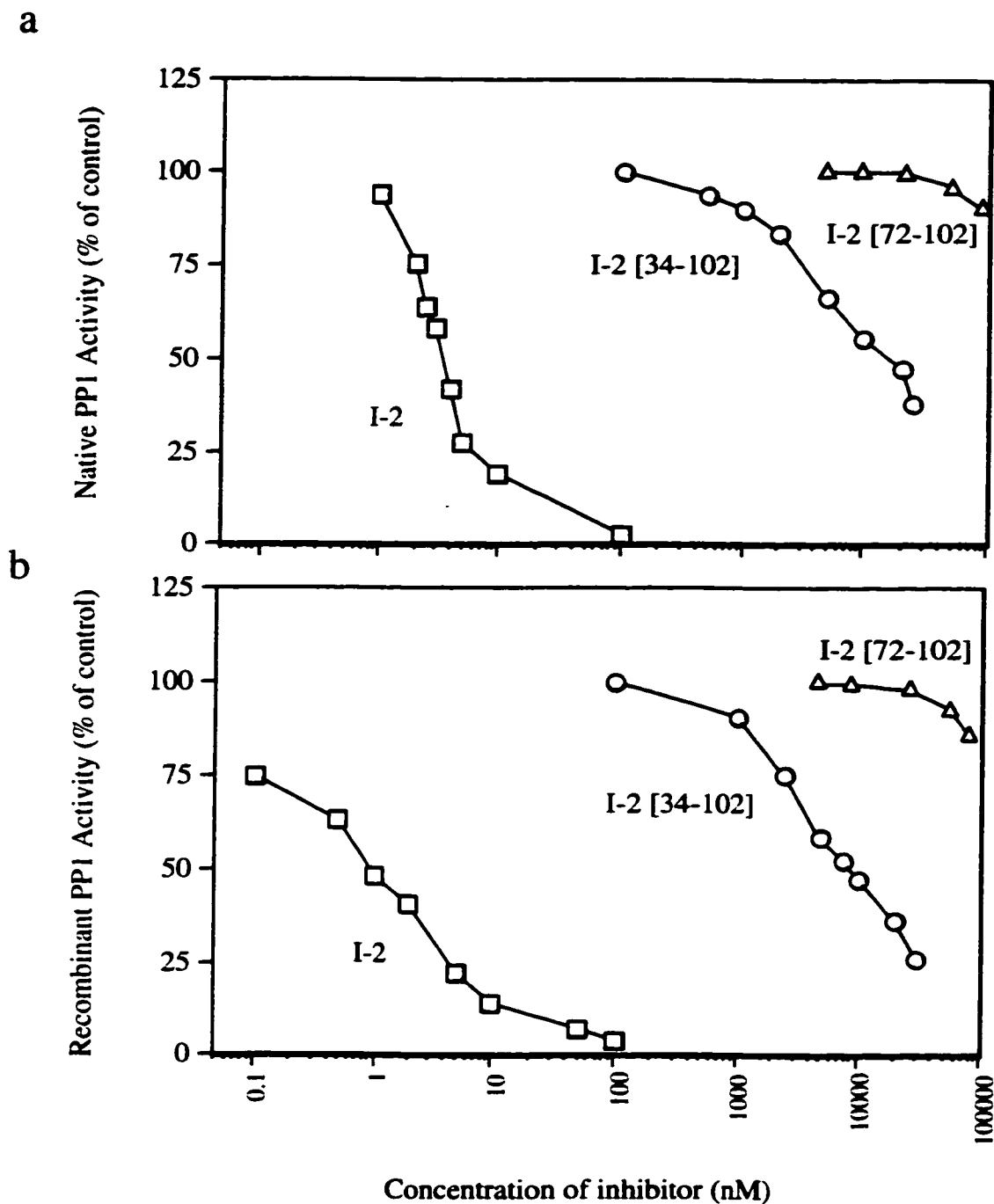
Figure 4-1. *PP1 inhibition assays with inhibitor-2 fragments.* IC_{50} curves for inhibition of native PP1 (panel a) and recombinant $PP1\gamma$ (panel b) by full-length inhibitor-2, I-2[34-102] and I-2[72-102]. Protein phosphatase-1 inhibition was assayed using [^{32}P] a substrate as described in Experimental Procedures.

Table 4-1

Inhibition of protein phosphatase-1 activity by inhibitor-2 fragments

Phosphorylase *a* phosphatase activity was standardized to 15% release for each enzyme. Each inhibitory curve was performed with a full range of inhibitors. No change in inhibition was observed when 0.1 mM $MnCl_2$ was added to the native PP1 assays.
GSK-3 Thr-72 phosphorylation site is indicated ($\downarrow$).

		IC_{50} values	
Inhibitor-2 Fragment		Native PP1	Recombinant PP1
30 mer $\downarrow$ 72▬102		$>>100\ \mu M^*$	$>100\ \mu M^*$
69 mer 34▬▬▬▬102		$14\ \mu M$	$8.5\ \mu M$
wt 1▬▬▬▬▬▬▬▬204		2.1 nM	0.9 nM

* 16.4% (native) and 24% (PP1γ) inhibition was observed at 100 μM

0.2 moles of phosphate per mole of inhibitor-2$_{[34-102]}$ peptide in our reactions. It may be that regions in the full-length inhibitor protein not found in the 34-102 sequence are required for efficient phosphorylation of I-2 by GSK-3β.

I-1 and I-2 competition assays

In order to learn more about the interaction between inhibitor-2 and PP1, we investigated whether I-2 and inhibitor-1, a phosphoprotein inhibitor of PP1 (discussed extensively in Chapters Five and Six), share overlapping PP1 binding sites. Specifically, we tested whether the I-2$_{[34-102]}$ peptide could compete with phosphorylated inhibitor-1$_{[9-54]}$ peptide (Figures 1-5, 1-7) for binding to PP1 (Figure 4-3, panel a). Inhibition of PP1 by

Figure 4-2. *GSK-3 phosphorylation of 1-2[34-102].* 1-2[34-102] peptide was phosphorylated by 20 U of recombinant rabbit skeletal muscle GSK-3β as described in Experimental Procedures.

the I-1[9-54] peptide decreased in the presence of the I-2[34-102] peptide, suggesting some interaction of this region of I-2 with PP1, thereby reducing the ability of I-1 to inhibit the enzyme. Our results are in agreement with other studies which found that residues 15-84 of I-2 compete with DARPP-32, a protein related to inhibitor-1, for binding to PP1 (23,28). The reverse was also found to be true - dephospho-I-1[9-54] competes with full length I-2 for inhibition of PP1 (Figure 4-3, panel b), to a slightly greater degree than the I-2[34-102] peptide could compete with phospho-inhibitor-1[9-54]. The 30 residue inhibitor-2 peptide (72-102) which was not able to inhibit PP1 was also unable to compete for PP1 binding with either phospho-inhibitor-1[9-54] or I-2[34-102] (Figure 4-3, panel c). It seems likely that residues 34-102 in I-2 share a common or overlapping PP1 binding site with residues 9-54 of I-1.

Inhibition of Cys-291 and Phe-257 PP1 mutants by I-1 and I-2

We created mutations of residues Cys-291 and Phe-257 in PP1 in order to investigate the role of these residues in inhibition of the phosphatase by toxins and endogenous inhibitor proteins. These amino acids were chosen for our mutagenesis studies because they have been shown to form part of a binding pocket in the phosphatase that interacts with the PP1 glycogen targeting subunit G_M and other regulatory proteins (25) (Figure 1-4, see Chapter Five for extensive discussion of the PP1 binding motif). Cys-291 and Phe-257 are both involved in hydrophobic contacts to the PP1 binding sequence in G_M. Cys-291 also participates in polar interactions with the G_M peptide.
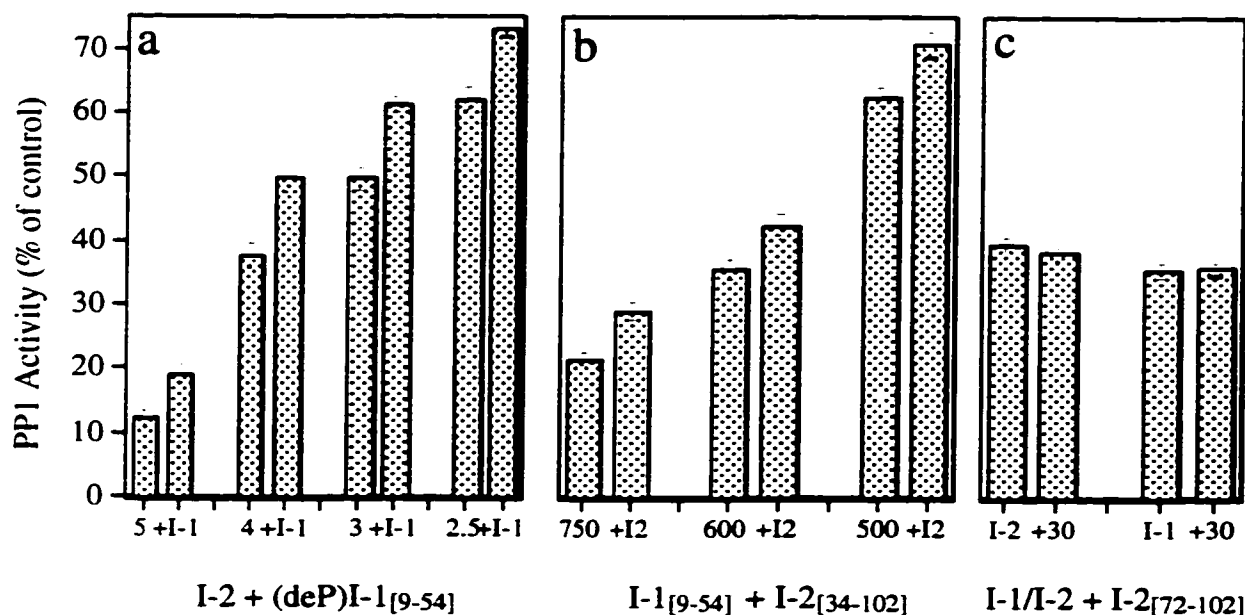
Figure 4-3 *I-1 and I-2 competition assays.* Protein phosphatase-1 activity was assayed using [^{32}P]phosphorylase *a* substrate as described in Experimental Procedures. Panel a depicts a competition assay containing 2.5-5 nM full-length inhibitor-2 protein and 5 µM of dephospho form of inhibitor-1[9-54] peptide. Panel b depicts a competition assay containing 500-750 nM phosphorylated inhibitor-1[9-54] peptide and 100 nM inhibitor-2[34-102] peptide. Panel c depicts competition assays containing either 4 nM full-length inhibitor-2 or 600 nM phosphorylated inhibitor-1[9-54] plus 50 µM inhibitor-2[72-102] peptide. An increase in PP1 activity (which is a decrease in inhibition) is interpreted to represent competition for PP1 binding between the inhibitor and competitor peptides present in the assay.

Recombinant PP1γ C291A was inhibited by all of the inhibitors (including the clavosines and calyculin A - see Table 3-1 in Chapter Three) with IC_{50} values similar to those found for wild type recombinant PP1γ (Table 4-2). We had expected to see an increase in IC_{50} for inhibitor-1[9-54] inhibition of the mutant enzyme. Residues 9-12 of I-1 are thought to bind to the region of PP1 identified in the G_M subunit/PP1 structure (23,25,29), although this has not been experimentally confirmed.

Inhibition assays with the F257A PP1 mutant were also performed with a variety of PP1 inhibitors. All of the inhibitors tested showed increased IC_{50} values in comparison to those found with the wild-type recombinant enzyme. We had expected to see an increase in IC_{50} for I-1 and possibly I-2, given the role that Phe-257 plays in binding to other PP1 regulatory proteins (25). However, we feel that this mutation may have a global effect on phosphatase structure because an increase in IC_{50} was observed for the all of the phosphatase inhibitors tested, including the clavosines and calyculin A (Table 3-1). The increases ranged from five-fold (I-1[9-54]) to seventy-fold (okadaic acid) over wild-type values; an increase of approximately ten-fold was observed for each of the calyculins with F257A.

Table 4-2

Inhibition of PP1γ mutants by I-1, I-2, microcystin-LR, and okadaic acid

Protein phosphatase-1 inhibition was assayed using 10 μM [^{32}P]phosphorylase *a* substrate as described in Chapter Two, Experimental Procedures. Phosphatase activity was standardized to 15% release for each recombinant enzyme and inhibitory curves were performed with a full range of inhibitors.

PP1 Enzyme	IC$_{50}$ values (nM)			
	phospho-I-1 [9-54]	Inhibitor-2 (full-length)	Microcystin-LR	Okadaic Acid
wild-type	550	0.9	1.4	24.5
Phe257Ala	2650	30	42	1700
Cys291Ala	650	4.0	1.2	26.7

Discussion

We initiated this study in an attempt to find a fragment of I-2 which could inhibit PP1 and be phosphorylated by GSK-3, with the eventual aim of producing native-like PP1 from recombinant enzyme. We identified a 69 residue peptide (amino acids 34-102) derived from I-2 that inhibits PP1 at micromolar concentrations. Residues 41-46 (KKSQKW) of inhibitor-2 have been suggested to represent a PP1 binding motif (23). This may explain the ability of I-2$_{[34-102]}$ to inhibit PP1 and the loss of inhibition observed with the shorter 30 residue I-2 peptide$_{[72-102]}$. We have also determined that the 69 residue I-2 fragment can bind to immobilized PP1$_{HIS}$ (see Appendix III) confirming that this peptide can form a complex with the phosphatase. Unfortunately, we have been unable to resolve a I-2$_{[34-102]}$/PP1γ complex from free PP1γ using gel filtration chromatography (personal communication, Marcia Craig). This has prevented us from attempting to convert recombinant PP1 to a more native state using the I-2$_{[34-102]}$ peptide.

We have shown that I-2$_{[34-102]}$ can be phosphorylated to a limited degree by the β isoform of GSK-3. In addition to the GSK-3 phosphorylation of threonine 72, I-2 is phosphorylated on three serines by casein kinase II (CKII) (7). Phosphorylation by CKII on serine 86 does not alter I-2 activity but greatly facilitates the subsequent phosphorylation of Thr-72 by the GSK-3α isoform (30,31). It may be possible to increase the degree of phosphorylation of Thr-72 of the I-2$_{[34-102]}$ peptide by first phosphorylating the peptide at Ser-86 with CKII. Previous studies have demonstrated that this procedure may incorporate more phosphate into Thr-72 than treatment with the GSK-3β isoform alone (27).

Our competition studies with I-2 and I-1 suggest that these inhibitors have at least partially overlapping PP1 binding sites. Although we do not know where I-2 binds to PP1, it seems likely that the overlap between I-2 and I-1 occurs in the region of the phosphatase which interacts with the ^{9}KIQF^{12} motif found in inhibitor-1. When added to a competition assay, dephospho-I-1$_{[9-54]}$ appears to compete for binding to PP1 with full-length I-2, reducing the amount of inhibition observed in the assay (Figure 4-3). The dephosphorylated form of I-1$_{[9-54]}$ may not be able to bind to the active site of the phosphatase via phospho-threonine 35, but it does contain the KIQF PP1 binding motif (residues 9-12), which is thought to contribute most of the interaction of the dephospho-peptide with the phosphatase (Chapter Five). This suggests that it is the KIQF region of inhibitor-1 that is displacing I-2 in our studies.

The results of our PP1 mutagenesis studies of residues Cys-291 and Phe-257 were inconclusive. We were not able to determine whether I-2 or I-1 binds to PP1 at the same region as the (R/K)(V/I)XF binding motif found in PP1 targeting/regulatory proteins (Chapter Five). The alanine side chain in the C291A mutant may have been sufficiently hydrophobic to interact successfully with the KIQF sequence in inhibitor-1, producing similar IC_{50} values for inhibition of the C291A and wild-type PP1 enzymes. We found a slight increase in IC_{50} for C291A inhibition by inhibitor-2 when compared to the wild-type recombinant enzyme. It is possible that I-2 interacts with PP1 in the region of the Cys-291 binding pocket.

Substitution of alanine for phenylalanine in position 257 of PP1 appeared to have a global effect on phosphatase structure because an increase in IC_{50} was observed for the

all of the phosphatase inhibitors tested. We did not expect to see an increase in IC_{50} for the natural product inhibitors of PP1, because Phe-257 does not interact with microcystin-LR in the x-ray crystallographic structure of the toxin-enzyme complex, and it is not predicted to be involved in PP1 binding to okadaic acid or calyculin A. Work is currently underway in our laboratory to investigate the effects of further mutations of residues 257 and 291 in PP1. Substitution of a basic and an acidic amino acid at each of these positions may allow us to determine whether I-2 or I-1 binds in this region of the phosphatase.

In conclusion, this work represents the foundation of a research project designed to investigate the interaction between inhibitor-2 and PP1. Our long-term goal is to attempt to produce 'renatured' recombinant PP1 enzyme by incubation with I-2 followed by GSK-3 phosphorylation. We are currently working on the crystal structure of a complex between recombinant PP1γ and the I-2$_{[34-102]}$ peptide (in collaboration with Dr. M. James). We are also attempting to clone the cDNA for full-length inhibitor-2 from our human teratocarcinoma cDNA library. This will allow us to construct and express truncations and mutations of the I-2 sequence, in order to further investigate I-2 inhibition and regulation of PP1. We will also be able to produce large amounts of the recombinant full-length I-2 protein for renaturation experiments with PP1 and GSK-3. The three-dimensional structures of PP1 that have been reported so far (32,33) describe the recombinant and not the native conformation of the enzyme. We are therefore interested

in investigating the structural differences between the 'renatured' and recombinant forms of the enzyme in the future.

References

1.   Huang, F. L., and Glinsmann, W. H. (1976) *Eur. J. Biochem.* **70**, 419-426

2.   Brautigan, D. L., Sunwoo, J., Labbe, J. C., Fernandez, A., and Lamb, N. J. (1990) *Nature* **344**, 74-78

3.   Kakinoki, Y., Somers, J., and Brautigan, D. L. (1997) *J. Biol. Chem.* **272**, 32308-14

4.   Aitken, A., Holmes, C. F., Campbell, D. G., Resink, T. J., Cohen, P., Leung, C. T., and Williams, D. H. (1984) *Biochim. Biophys. Acta* **790**, 288-291

5.   Puntoni, F., and Villa-Moruzzi, E. (1995) *Biochem. Biophys. Res. Commun.* **207**, 732-739

6.   Wang, Q. M., Guan, K. L., Roach, P. J., and DePaoli-Roach, A. A. (1995) *J. Biol. Chem.* **270**, 18352-58

7.   Holmes, C. F., Kuret, J., Chisholm, A. A., and Cohen, P. (1986) *Biochim. Biophys. Acta* **870**, 408-416

8.   Oliver, C. J., and Shenolikar, S. (1998) *Front. Biosci.* **3**, d961-972

9.   Yang, S.-D., Vandenheede, J. R., Goris, J., and Merlevede, W. (1980) *J. Biol. Chem.* **255**, 11759-67

10. Yang, S. D., Vandenheede, J. R., and Merlevede, W. (1981) *J. Biol. Chem.* **256**, 10231-34

11. Ballou, L. M., Brautigan, D. L., and Fischer, E. H. (1983) *Biochemistry* **22**, 3393-99

12. Tung, H. Y., and Cohen, P. (1984) *Eur. J. Biochem.* **145**, 57-64

13. Li, H. C., Price, D. J., and Tabarini, D. (1985) *J. Biol. Chem.* **260**, 6416-26

14. Bollen, M., and Stalmans, W. (1992) *Crit. Rev. Biochem. Mol. Biol.* **27**, 227-281

15. Hemmings, B. A., Resink, T. J., and Cohen, P. (1982) *FEBS Lett.* **150**, 319-324

16. Villa-Moruzzi, E., Ballou, L. M., and Fischer, E. H. (1984) *J. Biol. Chem.* **259**, 5857-63

17. Jurgensen, S., Shacter, E., Huang, C. Y., Chock, P. B., Yang, S. D., Vandenheede, J. R., and Merlevede, W. (1984) *J. Biol. Chem.* **259**, 5864-70

18. Vandenheede, J. R., Yang, S.-D., Merlevede, W., Jurgensen, S., and Chock, P. B. (1985) *J. Biol. Chem.* **260**, 10512-16

19. Alessi, D. R., Street, A. J., Cohen, P., and Cohen, P. T. W. (1993) *Eur. J. Biochem.* **213**, 1055-66

20. Cohen, P. (1989) *Annu. Rev. Biochem.* **58**, 453-508

21.   MacKintosh, C., Garton, A. J., McDonnell, A., Barford, D., Cohen, P. T., Tonks, N. K., and
       Cohen, P. (1996) *FEBS Lett.* **397**, 235-238

22.   Park, I. K., and DePaoli-Roach, A. A. (1994) *J. Biol. Chem.* **269**, 28919-28

23.   Huang, H.-b., Horiuchi, A., Watanabe, T., Shih, S.-R., Tsay, H.-J., Li, H.-C., Greengard, P.,
       and Nairn, A. C. (1999) *J. Biol. Chem.* **274**, 7870-78

24.   Helps, N. R., Vergidou, C., Gaskell, T., and Cohen, P. T. W. (1998) *FEBS Lett.* **438**, 131-136

25.   Egloff, M. P., Johnson, D. F., Moorhead, G., Cohen, P. T., Cohen, P., and Barford, D. (1997)
       EMBO J. **16**, 1876-87

26.   Zhang, A. J., Bai, G., Deans-Zirattu, S., Browner, M. F., and Lee, E. Y. (1992) *J. Biol. Chem.*
       267, 1484-90

27.   Wang, Q. M., Park, I. K., Fiol, C. J., Roach, P. J., and DePaoli-Roach, A. A. (1994)
       Biochemistry **33**, 143-147

28.   Kwon, Y. G., Huang, H. B., Desdouits, F., Girault, J. A., Greengard, P., and Nairn, A. C.
       (1997) *Proc. Natl. Acad. Sci. U.S.A* **94**, 3536-41

29.   Connor, J. H., Quan, H. N., Ramaswamy, N. T., Zhang, L., Barik, S., Zheng, J., Cannon, J. F.,
       Lee, E. Y., and Shenolikar, S. (1998) *J. Biol. Chem.* **273**, 27716-24

30.   DePaoli-Roach, A. A. (1984) *J. Biol. Chem.* **259**, 12144-52

31.   Park, I. K., Roach, P., Bondor, J., Fox, S. P., and DePaoli-Roach, A. A. (1994) *J. Biol. Chem.*
       269, 944-954

32.   Goldberg, J., Huang, H. B., Kwon, Y. G., Greengard, P., Nairn, A. C., and Kuriyan, J. (1995)
       Nature **376**, 745-753

33.   Egloff, M. P., Cohen, P. T. W., Reinemer, P., and Barford, D. (1995) *J. Mol. Biol.* **254**, 942-959

Chapter Five

*Determination of the Optimal PP1
Binding Motif of Inhibitor-1*

Preface to Chapters Five and Six

Chapters Five and Six represent the results of complementary projects focused on the interaction of inhibitor-1 with PP1. Inhibitor-1, and the related protein DARPP-32, are thought to interact with PP1 via two distinct regions - an N-terminal putative PP1 binding motif and the region surrounding the PKA phosphorylation site. Chapter Five is devoted to an investigation of the PP1 binding motif while Chapter Six presents information regarding residues near the Thr-35 PKA site in I-1 that are critical for inhibition of PP1.

Introduction

Protein phosphatase-1 is one of the major serine/threonine protein phosphatases in eukaryotic cells (1). This enzyme is involved in such diverse cellular functions such as glycogen metabolism, muscle contraction, neurotransmission, and cell cycle progression (2-5). PP1 displays broad substrate specificity, a characteristic which permits a wide range of responses to physiological stimuli (6), but which also requires strict regulation in order to control or limit the response to appropriate substrates. One regulatory mechanism in the control of dephosphorylation events is the subcellular location of PP1 (7). Through interaction with specific targeting subunits, the phosphatase is physically restricted to a particular subcellular environment such as an organelle, membrane, or complex. This may serve to limit access to only a specific substrate, and may even modify the catalytic properties of the enzyme in order to selectively enhance activity toward a specific substrate (8).

Distinct PP1 holoenzymes, composed of a 37 kDa catalytic subunit (PP1) complexed with a regulatory or targeting subunit, appear to be associated with different cellular functions. Examples of mammalian PP1 regulatory subunits include: G_M (glycogen particles and the sarcoplasmic reticulum in muscle) (9), G_L (glycogen in liver) (10), the myofibrillar binding protein M_{110} (skeletal muscle and smooth muscle) (11,12), retinoblastoma protein RB (13), p53 binding protein p53BP2 (14), nuclear proteins NIPP-1 and PNUTS (15,16), and cytosolic inhibitor proteins such as inhibitor-1, DARPP-32, and inhibitor-2 (reviewed in 5,17).

It is likely that over 100 intracellular proteins regulate PP1 *in vivo* (18). Interaction of different regulatory subunits with PP1 is mutually exclusive (19-21), an observation explained by the discovery that a short binding motif present in many of these subunits was sufficient for binding to PP1 (18,22). Co-crystallization of PP1 with a peptide derived from the G_M subunit (residues 63-75) has provided structural details regarding subunit binding to PP1 (18). Residues 64-69 of the G_M peptide, R<u>RVSF</u>A, bind in an extended conformation to a hydrophobic channel formed at the interface of two β-sheets in the C-terminal region of PP1 (Figure 1-4). Interactions between the phosphatase and G_M consist of predominantly hydrophobic contacts between PP1 and Val-66 and Phe-68 in the peptide. Identification of the RVSF binding sequence prompted re-examination of the amino acid sequences of other PP1 regulatory subunits (Table 5-1).

A four residue N-terminal sequence in inhibitor-1 ($^9KIQF^{12}$), and the related protein DARPP-32, has been shown to be necessary for PP1 inhibition by these endogenous inhibitor proteins (23-25). Disruption of the sequence, especially by loss of the Ile residue, disrupts PP1 binding by both dephosphorylated and phosphorylated forms of the inhibitors (24,26). I-1 and DARPP-32 are active as PP1 inhibitors only when phosphorylated by PKA on a single threonine residue (Figure 1-5). It has been proposed that I-1 and DARPP-32 binds to PP1 through two distinct regions: the phosphorylated threonine residue (Chapter Six) and the KIQF motif (21,24). The KIQF sequence in I-1 and DARPP-32 is similar to the (R/K)(V/I)XF binding motif (Table 5-1).

Table 5-1

Sequence alignment of PP1 binding proteins

Mammalian	(R/K)(V/I)XF motif	Residues
G$_M$ subunit	S G G R **R V S F** A D N	61-71
G$_L$ subunit	K V K K **R V S F** A D N	57-67
G$_L$-related protein	Q A K K **R V V F** A D S	80-90
M$_{110}$ subunit	R Q K T **K V K F** D D G	31-41
p53BP2	A H G M **R V K F** D D G	794-804
Inhibitor-1	N S P R **K I Q F** T V P	5-15
DARPP-32	K D R K **K I Q F** S V P	4-14
NIPP-1	R K N S **R V T F** S E D	196-206

Adapted from Egloff et al., 1997 (18).

A structure-function study of the PP1 binding motif provided an opportunity to investigate the potential of a multiple peptide synthesizer designed by Devon Husband (Protein Engineering Network Centre of Excellence, University of Alberta). Our goal was to determine the optimal PP1 binding motif sequence for comparison with motifs in a variety of other possible PP1 regulatory proteins. A set of synthetic peptide analogues was generated by sequence variation of the four positions of the motif shared by inhibitor-1 and DARPP-32.

It is of particular interest to examine variations in the inhibitor-1/DARPP-32 KIQF sequence because it has not been experimentally confirmed that these inhibitors bind to the same region of PP1 as the G$_M$ subunit peptide. When a random peptide library (displayed on the *E. coli* flagellin protein) was screened for PP1 binding sequences,

the most common amino acids found in the four position motif were (R/H)-V-(R/H)-(W/F) (27). Although this sequence is similar to the (R/K)-(V/I)-X-F motif shown in Table 5-1, the isoleucine present in position two of the inhibitor-1 and DARPP-32 motif was not found in any of the 79 sequences isolated from the peptide library screen.

The current study was limited to single substitutions and incorporated all twenty naturally occurring amino acids at each position. The wild type motif-containing fragment and 76 (4 series of 19) analogues were synthesized as explained in Table 5-2. The effect of substitution at each position of the motif was assessed by a competitive [^{32}P]-phosphorylase a phosphatase assay. In this assay phosphorylase a serves as the substrate for PP1, and peptide analogues compete for binding to PP1 with phosphorylated I-1$_{[9-54]}$, an active peptide fragment of inhibitor-1. The ability of a peptide to bind to PP1 was determined by measuring the inhibition of PP1 activity by I-1$_{[9-54]}$ in the absence and presence of the motif peptides. Reduction of PP1 inhibition in the presence of a binding motif peptide was considered to indicate that the peptide competed with I-1 for binding to PP1 (28) (see Table 5-3 for peptide sequences).

Table 5-2

Generation of PP1 binding motif peptides by sequence variation

X represents any one of the 20 naturally occurring amino acids.

Motif position	1 2 3 4	
Parent sequence	K I Q F	
Peptide Analogues		# of peptides
Series 1	**X** I Q F	19
Series 2	K **X** Q F	19
Series 3	K I **X** F	19
Series 4	K I Q **X**	19

Adapted from Husband, 1999 (29).

Table 5-3

Inhibitor-1 and DARPP-32 peptide sequences

Binding motif is highlighted in bold. PKA Thr-35 phosphorylation site is indicated ($\downarrow$).

Peptide	Sequence
I-1[9-54] (active inhibitor)	$\qquad\qquad\qquad\qquad\downarrow$ **KIQF**TVPLLEPHLDPEAAEQIRRRRPTPATLVLTSDQSSPVDEDR
I-1[6-20]	SPR**KIQF**TVPLLEPH
I-1[6-18]	SPR**KIQF**TVPLLE
I-1[7-14]	PR**KIQF**TV
DARPP-32[6-13]	R**KKIQF**SV

Experimental Procedures

Peptide synthesis

I-1$_{[7-14]}$, I-1$_{[6-18]}$, I-1$_{[6-20]}$, and DARPP-32$_{[6-13]}$ peptides were synthesized by Devon Husband (PENCE) as N-acetylated peptide amides for initial development of the competition/screening assay (see Table 5-3 for sequences). Peptides were examined by reversed phase HPLC and molecular weights were verified by mass spectrometry. Peptides were dissolved in 20 mM Tris-HCl, pH 7, and adjusted to pH 7 with NaOH. Peptide concentrations were determined by amino acid analysis (API). The set of 13-residue I-1$_{[6-18]}$ analogues of the binding motif were synthesized simultaneously on the 100-sample reactor model of the multiple peptide synthesizer by Devon Husband (29). Crude analogues were analyzed by reversed phase HPLC (pH 2) and mass spectrometry. Peptides were dissolved in 20 mM Tris-HCl, pH 7, adjusted to pH 7 with NaOH, and peptide concentrations were determined by amino acid analysis (Alberta Peptide Institute, University of Alberta).

Protein Phosphatase Inhibition Assays

Native rabbit skeletal muscle PP1 was obtained from Upstate Biotechnology (10 mU/200 μL). Protein phosphatase-1 inhibition was assayed using [^{32}P]-phosphorylase a substrate as described in Chapter Two. Assays contained 50 mM Tris-HCl, 25 mM β-mercaptoethanol, 1 mg/mL BSA, 3.75 mM caffeine, 10 μM [^{32}P]-phosphorylase a. Control phosphatase activity was standardized to 15% release of ^{32}P-phosphate from substrate. Competition assays also included 50 or 100 nM phospho-inhibitor-1$_{[9-54]}$

peptide and/or 50 µM competition peptide (Table 5-3). 8, 13 or 15 residue competition peptides were pre-incubated with enzyme for 10 minutes at 30°C before addition of phospho-inhibitor-1$_{[9-54]}$. Reactions were initiated with the addition of substrate. All reactions were performed in triplicate.

Results

Inhibitor-1 peptides (8,13,15 residue fragments)

Initially, two 8 residue peptides based on wild type inhibitor-1 (residues 7-14) and DARPP-32 (residues 6-13) were synthesized in order to develop the competition assay between the binding motif peptides and phospho-inhibitor-1$_{[9-54]}$. The I-1 and DARPP-32 sequences differ on either side of the binding motif (Table 5-3), so both peptides were synthesized in order to investigate their solubilities and behaviour in the competition assay. The inhibitor-1 derived peptide was largely insoluble in 10 mM Tris-HCl, and contained an amber-coloured precipitate. The DARPP-32 peptide was tested in a protein phosphatase-1 activity assay (Figure 5-1) and found to activate the enzyme to levels significantly above 100% of control activity. At this point it was decided that both peptides might be contaminated with chemicals from the synthesis process. The inhibitor-1$_{[7-14]}$ peptide was re-synthesized, found to be moderately soluble, and tested in the protein phosphatase-1 inhibition assay (Figure 5-1). Although a small amount of activation was detected, a concentration (50 μM) was chosen for subsequent competition assays at which minimal phosphatase activation was observed.

In an attempt to increase solubility of the inhibitor-1 peptide and improve performance in the competition assay, peptide template lengths were increased to 13 and 15 residues to allow incorporation of polar and ionizable residues (Ser-6, Glu-18, His-20) surrounding the binding motif in the inhibitor-1 sequence (Table 5-3). I-1$_{[7-14]}$, I-1$_{[6-18]}$, and I-1$_{[6-20]}$ peptides were tested for PP1 activation, and for competition with phosphorylated inhibitor-1$_{[9-54]}$ peptide in a PP1 inhibition assay. A slight amount of

Figure 5-1. *Activation of native PP1 by DARPP-32 and inhibitor-1 peptides.* Protein phosphatase-1 activity was assayed using [^{32}P]phosphorylase a substrate as described in Experimental Procedures. 8 residue peptides based on inhibitor-1 (residues 7-14) and DARPP-32 (residues 6-13) were added to a standard phosphatase activity assay at the concentrations indicated to test for changes in enzyme activity in the absence of inhibitor protein.

activation was observed for each peptide (Figure 5-2, panel a), although not as much as

initially found with DARPP-$32_{[6-13]}$. Each peptide produced a significant, consistent,

increase in PP1 activity in the presence of I-$1_{[9-54]}$, over and above the increase in activity

that had been determined for the peptide alone (Figure 5-2, panel b). It was concluded

that reduction of I-$1_{[9-54]}$ inhibition of PP1 in the presence of the 8, 13, or 15 residue

peptides was due to competition between I-$1_{[9-54]}$ and the motif peptides for binding to

PP1. The degree of competition observed appeared to correlate with length of the

competition peptide. Although the 13 residue peptide exhibited only a slight

improvement in solubility (along with a small increase in synthesis purity - Devon

Husband, personal communication) compared to the 8 residue peptide, the 13 mer

template was more effective in the competition assay and was therefore chosen as the

length for the binding motif substituted peptides. The 15 residue peptide was considered

too long for the multi-well synthesizer, as incomplete peptides and other contaminants

would be likely to compromise purity of the final product.

Binding motif peptide synthesis

I-$1_{[6-18]}$ peptide analogues of the binding motif were generated by single substitutions of

all 20 naturally-occurring amino acids in positions 1 through 4 of the motif, denoted by

position and substitution (i.e. 1A refers to the Ala-substituted position 1 analogue AIQF,

Table 5-2). The crude analogues were analyzed by reversed phase HPLC at pH 2 (see

Figure 5-3 for position 1 chromatograms). Purity and yield were lower and more variable

than expected (29). Shorter, incomplete peptides missing one or more amino acids were
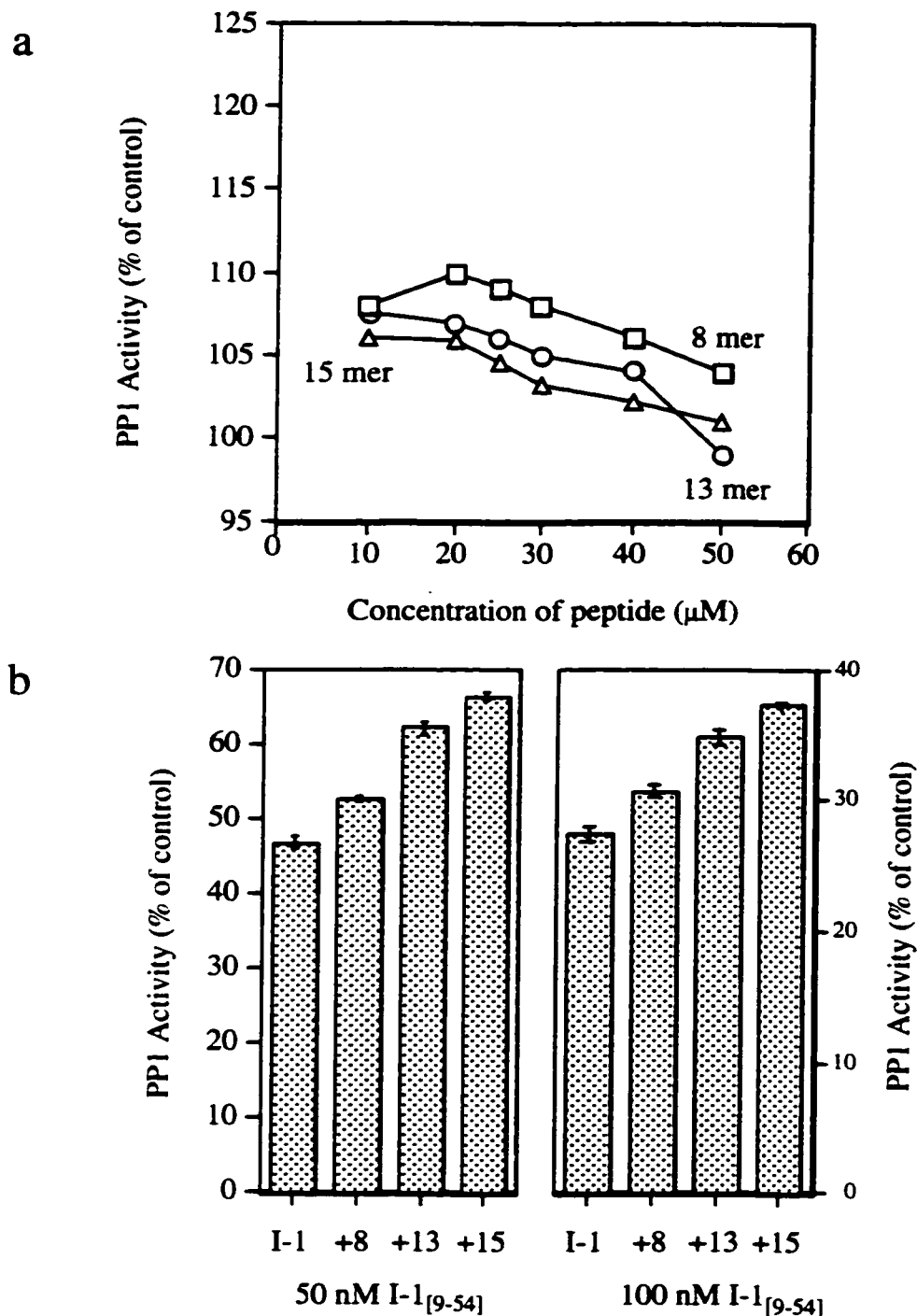
Figure 5-2. *PP1 activity and competition assays with inhibitor-1 peptides.* 8, 13, and 15 residue I-1 peptides were tested for activation of PP1 (panel a) and for competition with phosphorylated inhibitor-1[9-54] peptide in a PP1 inhibition assay (panel b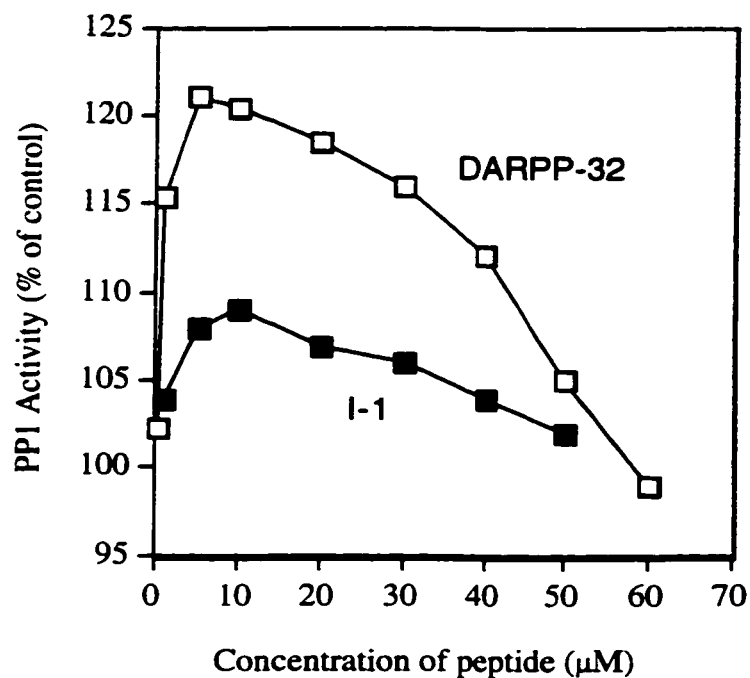). PP1 activity was assayed using $[^{32}P]$phosphorylase a substrate. The 8 residue peptide represents inhibitor-1[7-14], the 13 mer represents inhibitor-1[6-18] and the 15 mer represents inhibitor-1[6-20]. Competition peptides were used at 50 μM in panel b. An increase in PP1 activity (which is a decrease in inhibition) was interpreted to represent competition for PP1 binding between the inhibitor and competitor peptides present in the assay.

common. Other problematic contaminants included side chain protection groups and non-acetylated peptides (29).

Phosphatase assays with binding motif peptides

Preparing the binding motif peptides for competition assays was problematic. Many of the I-1$_{[6-18]}$ peptides were not fully soluble in 20 mM Tris-HCl at pH 7. Peptide solutions contained gel-like insoluble pellets and large amounts of amber-coloured precipitate. There was probable contamination with chemicals from the synthesis procedure, as solutions smelled strongly like reducing agents (thiols). Concentrations obtained from amino acid analyses were deemed unreliable when large amounts of incomplete peptide contaminants were present in the sample.

Peptides from series 1 and 2 (Positions K and I in KIQF) were screened in protein phosphatase-1 assays (at 50 μM) to test for any effects the peptides might have on enzyme activity. Results of these assays were extremely variable (for examples see Figure 5-4) and did not appear to correlate with the amino acid substituted at each position. Activation of PP1 (ranging from 101-120%) was observed in many instances, and inhibitor-1 peptides required varying amounts of dilution to eliminate activation in the assay. It became clear that it would be impossible to interpret the results of competition assays with the binding motif peptides as they would have to be used at different concentrations to avoid activation of the enzyme.
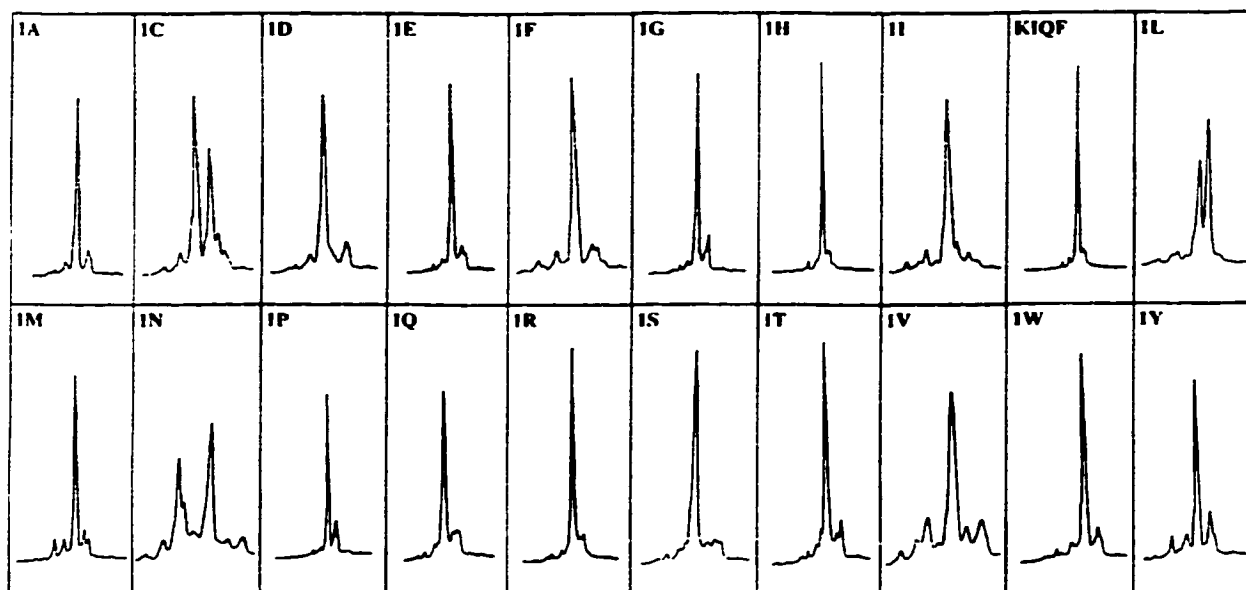
Figure 5-3. *HPLC analysis of position 1 binding motif analogues.* I-1[6-18] peptide analogues of the binding motif were generated by single substitutions of all 20 naturally-occurring amino acids in positions 1 through 4 of the motif, denoted by position and substitution (i.e. 1A refers to the Ala-substituted position 1 analogue AIQF). Peptides were analyzed for purity by reversed phase HPLC at pH 2. Chromatograms from position 1 peptides are shown as typical examples of the results obtained for all of the positions (a total of 80 peptides).
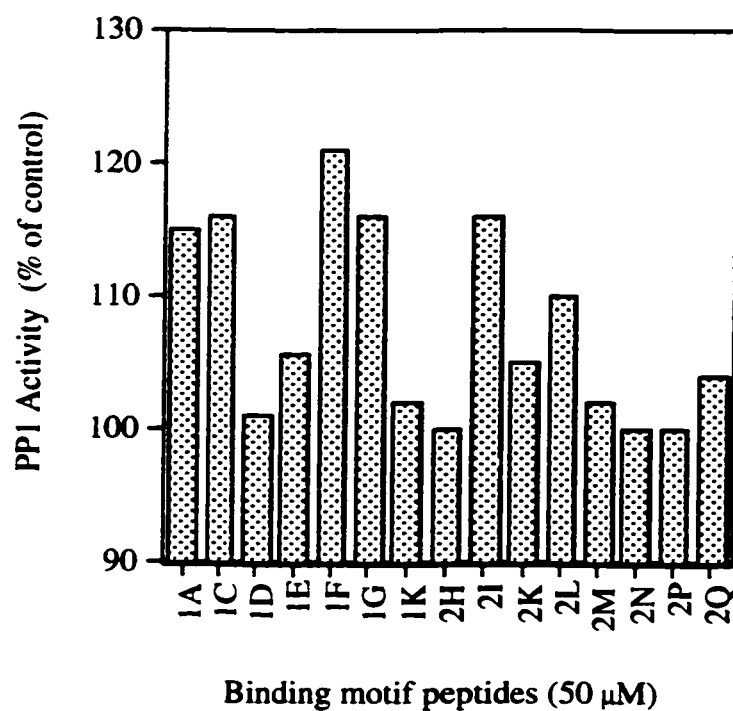
Figure 5-4. *Variable activation of native PP1 by inhibitor-1 binding motif analogues.* Peptides from series 1 and 2 (Positions K and I in KIQF) were screened in protein phosphatase-1 activity assays (at 50 μM) to test for any changes in enzyme activity in the absence of inhibitor protein. PP1 activity was assayed using [^{32}P]phosphorylase *a* substrate as described in Experimental Procedures. Results from position 1 are shown as examples of the variable activation observed for both position 1 and 2 binding motif peptides.

In an attempt to discover whether the activation effects of the inhibitor-1[9-54] peptide analogues were due to a specific interaction with PP1, unrelated peptide sequences (12 and 30 residues long) were tested at similar concentrations (data not shown). These peptides had no effect on enzyme activity, discrediting the possibility that addition of micromolar amounts of any peptide to the PP1 assay could stabilize the phosphatase and produce the observed increase in activity.

Discussion

The results of competition assays with phospho-inhibitor-1[9-54] and the 8, 13, and 15 residue peptides containing the putative PP1 binding motif suggest that inhibitor-1 does indeed bind to PP1 via the ^{9}KIQF^{12} sequence. We interpret the observed reduction in inhibition by phospho-inhibitor-1[9-54] in the presence of the competing motif sequence peptides to mean that that the KIQF sequence is capable of binding to PP1, thereby reducing the amount of inhibitor-1[9-54] binding and inhibition.

However, a combination of problems with the inhibitor-1 binding motif peptides and the phosphatase competition assay has led us to the conclusion that this experimental procedure is not appropriate for further investigation of the PP1 binding motif.

First, the purity of the motif peptides synthesized on the multi-well synthesizer was not suitable for the PP1 assay. This small volume (30 μL) assay requires concentrated stock solutions of peptide and is extremely sensitive to contaminating chemicals from the synthesis procedure. In addition, accurate concentrations of peptide solutions are crucial for quantitative results. In cases where peptide contaminants represent a significant proportion of the sample, it was not clear whether the desired peptide or the contaminant peptide was producing the observed effect.

Second, activation of the phosphatase enzyme is difficult to accommodate in the design of the competition assay. It was initially felt that the activation was non-specific, perhaps due to some contaminant. We now suspect that it might be a specific effect produced by the inhibitor-1 or DARPP-32 sequence. There is a precedent for this behaviour. A 38 residue peptide from the M_{110} targeting subunit which contains the PP1

binding motif (Table 5-1) has been shown to stimulate the myosin light chain phosphatase activity of PP1 up to 3 fold (at 1 μM) (18,22). In addition, a 20 residue G_M subunit peptide containing the binding motif stimulated phosphorylase phosphatase activity by ~25% (at 1 μM) (18,22). In our experiments, the 8 residue DARPP-32 peptide had a more pronounced activating effect than the corresponding I-1 peptide. Although inhibitor-1 and DARPP-32 are often thought of as interchangeable PP1 inhibitors, they do not always behave similarly *in vitro*. Dephosphorylated DARPP-32 has been found to inhibit PP1 activity (1 μM), while dephospho-inhibitor-1 does not (25,28). Phosphorylation of Thr-35 (Thr-34 in DARPP-32) by PKA is required for both proteins to potently inhibit PP1 with nanomolar IC_{50} values (25,28) (Chapter Six). It is possible that short inhibitor-1 and DARPP-32 peptide sequences, encompassing little more than the PP1 binding motif, could stimulate PP1 phosphorylase *a* activity. Other researchers have speculated that peptide sequences containing the binding motif cause a conformational change in the phosphatase upon binding (18). This idea has been rejected (25) because the x-ray crystallographic structure of PP1 bound to the G_M subunit peptide is virtually identical to the structure of the catalytic PP1 subunit bound only to tungstate (18,30).

There are currently two projects underway in our laboratory to address the problems observed in this PP1 binding motif study:

1. Preparation and use of histidine-tagged PP1 for direct binding assays.

We have added a hexahistidine affinity purification sequence to the C-terminus of the beta and gamma isoforms of PP1 (see Appendix III). $PP1_{HIS}$ can be immobilized in a variety

of ways. The histidine tag's affinity for nickel ions allows tagged proteins to bind to a variety of nickel-chelating columns and 96-well plates. It may be possible to assess binding of the I-1$_{[6-18]}$ motif peptides to immobilized PP1$_{HIS}$.

The results presented in this chapter suggest that a physical binding assay may be better suited than an activity-based phosphatase assay to test motif peptides for PP1 binding. A larger scale, less sensitive, direct binding assay could reduce problems with organic contaminants and sample concentrations, and it might be unaffected by peptide contaminants. A binding assay using PP1$_{HIS}$ is currently under development in our laboratory (Appendix III). It was initiated with idea of applying PP1 binding peptides to an FPLC or HPLC nickel-chelating column containing immobilized PP1, and eluting the peptides with a salt gradient. It would then theoretically be possible to assess the strength of the peptide-phosphatase interaction based on the amount of salt required to elute the peptide from the column (Brian Tripet, personal communication). At this point, it is not clear whether a quantitative direct binding assay with the motif peptides is possible, but we hope to further develop this method in the future.

2. 'Renaturation' of recombinant PP1 with I-2 and GSK-3.

The activation effects of binding motif peptides could be due, in part, to the quality of the commercially available native PP1 enzyme (see Appendix II). This enzyme is stored in MnCl$_2$, a situation that may result in the enzyme becoming Mn^{2+}-dependent and losing sensitivity to inhibitor-1, characteristics observed in the recombinant form of PP1 (31). It would be technically advantageous to be able 'renature' recombinant PP1 to a native-like

state. This would allow us to work with mutant PP1 and histidine-tagged PP1 enzymes more effectively, especially with inhibitor-1 peptides. Incubation of recombinant PP1 with I-2, followed by phosphorylation of the complex with glycogen synthase kinase-3 (GSK-3), results in conversion of the phosphatase to a native-like state with respect to sensitivity to inhibitor-1 and manganese dependency (32,33) (Chapter Four).

Work is currently underway in our laboratory to co-crystallize I-1[6-20] and I-1[9-54] with recombinant protein phosphatase-1γ. Structures of the peptides bound to the phosphatase would provide timely and valuable information about the interaction between inhibitor-1 and PP1. We have also investigated the second region of inhibitor-1 involved in PP1 inhibition - the sequence surrounding phospho-Thr-35. These experiments are presented in Chapter Six.

References

1.   Stralfors, P., Hiraga, A., and Cohen, P. (1985) *Eur. J. Biochem.* **149**, 295-303
2.   Cohen, P. (1989) *Annu. Rev. Biochem.* **58**, 453-508
3.   Bollen, M., and Stalmans, W. (1992) *Crit. Rev. Biochem. Mol. Biol.* **27**, 227-281
4.   Wera, S., and Hemmings, B. A. (1995) *Biochem. J.* **311**, 17-29
5.   Oliver, C. J., and Shenolikar, S. (1998) *Front. Biosci.* **3**, d962-972
6.   Cohen, P. (1992) *Trends Biochem. Sci.* **17**, 408-413
7.   Faux, M. C., and Scott, J. D. (1996) *Trends Biochem. Sci.* **21**, 312-315
8.   Hubbard, M. J., and Cohen, P. (1993) *Trends Biochem. Sci.* **18**, 172-177
9.   Tang, P. M., Bondor, J. A., Swiderek, L. M., and dePaoli-Roach, A. A. (1991) *J. Biol. Chem.* **266**, 15782-89

10.   Doherty, M. J., Moorhead, G., Morrice, N., Cohen, P., and Cohen, P. T. W. (1995) *FEBS Lett.* **375**, 294-298

11.   Chen, Y. H., Chen, M. X., Alessi, D. R., Campbell, D. G., Shanahan, C., Cohen, P., and Cohen, P. T. W. (1994) *FEBS Lett.* **356**, 51-55

12.   Moorhead, G., MacKintosh, W., Morrice, N., Gallagher, T., and MacKintosh, C. (1994) *FEBS Lett.* **356**, 46-50

13.   Durfee, T., Becherer, K., Chen, P. L., Yeh, S. H., Yang, Y., Kilburn, A. E., Lee, W. H., and Elledge, S. J. (1993) *Genes Dev.* **7**, 555-569

14.   Helps, N., Barker, M., Elledge, S. J., and Cohen, P. T. W. (1995) *FEBS Lett.* **377**, 295-300

15.   Kreivi, J. P., Trinkle-Mulcahy, L., Lyon, C. E., Morrice, N. A., Cohen, P., and Lamond, A. I. (1997) *FEBS Lett.* **420**, 57-62

16.   Allen, P. B., Kwon, Y. G., Nairn, A. C., and Greengard, P. (1998) *J. Biol. Chem.* **273**, 4089-95

17.   Barford, D., Das, A. K., and Egloff, M.-P. (1998) *Annu. Rev. Biophys. Biomol. Struct.* **27**, 133-164

18.   Egloff, M. P., Johnson, D. F., Moorhead, G., Cohen, P. T., Cohen, P., and Barford, D. (1997) *EMBO J.* **16**, 1876-87

19.   MacKintosh, C., Beattie, K. A., Klumpp, S., Cohen, P., and Codd, G. A. (1990) *FEBS Lett.* **264**, 187-192

20.   Helps, N. R., Vergidou, C., Gaskell, T., and Cohen, P. T. W. (1998) *FEBS Lett.* **438**, 131-136

21.   Huang, H.-b., Horiuchi, A., Watanabe, T., Shih, S.-R., Tsay, H.-J., Li, H.-C., Greengard, P., and Nairn, A. C. (1999) *J. Biol. Chem.* **274**, 7870-78

22.   Johnson, D. F., Moorhead, G., Caudwell, F. B., Cohen, P., Chen, Y.-H., Chen, M. X., and Cohen, P. T. W. (1996) *Eur. J. Biochem.* **239**, 317-325

23.   Hemmings, H. C., Jr., Nairn, A. C., Elliott, J. I., and Greengard, P. (1990) *J. Biol. Chem.* **265**, 20369-76

24.   Endo, S., Zhou, X., Connor, J., Wang, B., and Shenolikar, S. (1996) *Biochemistry* **35**, 5220-28

25.   Connor, J. H., Quan, H. N., Ramaswamy, N. T., Zhang, L., Barik, S., Zheng, J., Cannon, J. F., Lee, E. Y., and Shenolikar, S. (1998) *J. Biol. Chem.* **273**, 27716-24

26.   Desdouits, F., Cohen, D., Nairn, A. C., Greengard, P., and Girault, J. A. (1995) *J. Biol. Chem.* **270**, 8772-78

27.   Zhao, S., and Lee, E. Y. (1997) *J. Biol. Chem.* **272**, 28368-72

28.   Kwon, Y. G., Huang, H. B., Desdouits, F., Girault, J. A., Greengard, P., and Nairn, A. C. (1997) *Proc. Natl. Acad. Sci. U.S.A.* **94**, 3536-41

29.   Husband, D. L. (1999) in: *Development of a multiple peptide synthesizer and complementary multiple peptide purification system*, Ph.D. Thesis, Dept. of Biochemistry, University of Alberta, Edmonton, Alberta

30.   Egloff, M. P., Cohen, P. T. W., Reinemer, P., and Barford, D. (1995) *J. Mol. Biol.* **254**, 942-959

31.   Endo, S., Connor, J. H., Forney, B., Zhang, L., Ingebritsen, T. S., Lee, E. Y., and Shenolikar, S. (1997) *Biochemistry* **36**, 6986-92

32.   Alessi, D. R., Street, A. J., Cohen, P., and Cohen, P. T. W. (1993) *Eur. J. Biochem.* **213**, 1055-66

33.   MacKintosh, C., Garton, A. J., McDonnell, A., Barford, D., Cohen, P. T., Tonks, N. K., and Cohen, P. (1996) *FEBS Lett.* **397**, 235-238

Chapter Six

Inhibitor-1 Arginine Residues Required for Inhibition of PP1

Introduction

Inhibitor-1(I-1) is a 18.7 kDa thermostable protein first described (1) as a specific inhibitor of the catalytic subunit of protein phosphatase-1 (PP1) (2). Many endogenous inhibitors control PP1 activity in mammalian cells including I-1 (3), DARPP-32 (4), inhibitor-2 (5), the ribosomal protein RIPP-1 (6), the smooth muscle PKC substrate CPI17 (7), and the nuclear RNA-binding protein NIPP-1 (8) (reviewed recently in 9).

I-1 is active as a PP1 inhibitor only when phosphorylated by cAMP-dependent protein kinase (PKA) on a single threonine residue (Thr-35) (11). I-1 is dephosphorylated *in vivo* by PP2A and PP2B, other members of the PPP serine/threonine protein phosphatase family (12-14). I-1 is a poor substrate for native PP1, although it is dephosphorylated to a limited extent by the recombinant form of the enzyme (15).

In the early 1980's, Aitken and Cohen (11) isolated a fragment (residues 9-54) of I-1 that retained full inhibitory potency, provided that Thr-35 was phosphorylated. Limited proteolysis of phosphorylated I-1$_{[9-54]}$ showed that peptides composed of residues 22-54 and 13-41 were inactive, which suggested that residues 9-13 were important for I-1 inhibition of PP1. We have now synthesized a 33 amino acid I-1 fragment (residues 9-41) which is active as a PP1 inhibitor when phosphorylated by PKA. This peptide is similar to the 30 residue phosphopeptide fragment of DARPP-32 that has been identified by Hemmings et al. (4) as a potent inhibitor of PP1.

It has been widely proposed that there are two independent structural elements in I-1 (and DARPP-32) required for effective inhibition of PP1. These subdomains consist of the phosphorylated Thr-35 site and a PP1 binding motif composed of residues 9-12

(KIQF) in I-1 (4,15,23). Models of I-1 and DARPP-32 binding to PP1 have proposed that four sequential arginine residues preceding the phosphothreonine residue in the inhibitor interact with acidic amino acids lining a groove located near the active site of the phosphatase (Figure 1-6)(16-19). Recently, Huang et al. (20) used mutagenesis and structure-activity analyses to further characterize the inhibition of PP1 by DARPP-32. This work established that prolines 33 and 35, residues which flank the phosphoacceptor site in DARPP-32, are important for phosphatase inhibition (see Figure 1-5 for sequences).

In this study we have used site specific substitutions in the I-1$_{[9-41]}$ peptide to identify residues critical for PP1 inhibition. In particular, arginines 30-33 in I-1 have been examined in detail by making an Arg to Ala substitution at each position. Our study identifies a new point of interaction between PP1 and inhibitor-1, extending our understanding of this important PP1 regulatory mechanism.

Experimental Procedures

Materials

Native rabbit skeletal muscle PP1 was purchased from Upstate Biotechnology (10 mU/200 μL). PKA used in time-course phosphorylations was obtained from New England Biolabs (NEB). Phosphocellulose disks were purchased from GIBCO BRL. All other reagents were obtained from Sigma Chemicals unless noted.

Preparation of inhibitor-1 peptides

Inhibitor-1 fragments 1-54 (for NMR studies), 9-41 (I-1[9-41]), and Arg to Ala variants of the 9-41 sequence were synthesized by Paul Semchuk (PENCE) on an Applied Biosystems 430A synthesizer using solid phase methodology and standard protocols incorporating t-butyloxycarbonyl amino acids. Peptides were cleaved from the resin with HF and purified by reversed phase HPLC. Peptides were analyzed by amino acid analysis and mass spectrometry.

Phosphorylation and purification of inhibitor-1 peptides

PKA (250 U, bovine heart catalytic subunit) was incubated at 20°C for 10 min in 6 mg/mL DTT, then added to a reaction mixture containing 50 mM Tris-HCl (pH 7.5), 1 mM MgCl₂, 1 mM ATP and 1-3 mg peptide. The reaction was incubated at 30°C for 24 hours. Peptides I-1[9-41] Arg32Ala and Arg33Ala were subjected to a second round of phosphorylation to increase the yield of phosphorylated product. Further experiments

with phospho-Arg32Ala and phospho-Arg33Ala (e.g. testing them as substrates for protein phosphatases or as inhibitors of mutant PP1 enzymes) were not possible because we were only able to obtain extremely small quantities of each peptide. Phospho-peptides were purified by reversed phase HPLC in 10mM ammonium acetate (pH 6.5) with an acetonitrile gradient (20-59% in 26 min = 1.5% increase in acetonitrile/min) (Figure 6-1). R32A and R33A peptides were purified with a shallower gradient (% acetonitrile increases more slowly, 20-45% in 30 min = 0.83% increase in acetonitrile/min) to fully separate phospho-peptide from kinase reaction components and non-phosphorylated peptide.

NMR studies

Phosphorylation of the Inhibitor-1 1-54 residue peptide was performed in a 10 mL reaction containing 10 mM sodium glycerolphosphate, 0.4 mM EDTA, 0.1 mM EGTA, 2mM $MgCl_2$, 1.6 mM ATP, 9 mg peptide, and 500 U of bovine cardiac PKA, and incubated at 30°C for 16 hours. Phosphorylated I-1$_{[1-54]}$ fragment was purified by reversed phase HPLC, verified with mass spectroscopy, and determined to be fully active as an inhibitor in a phosphatase assay using 10 μM [^{32}P] phosphorylase *a* substrate (see below). Sample peptides were dissolved in 10 mM potassium phosphate, 50 mM NaCl, and 10-20% D_2O, at pH 6.5 for NMR. 2,2-dimethyl-2-silapentane-5-sulfonic acid (0.1 mM) was added as a ^{1}H NMR chemical shift standard. ^{1}H NMR spectra were recorded (by John Bagu) on Varian VXR-500 and VXR-600 spectrometers. Proton NMR
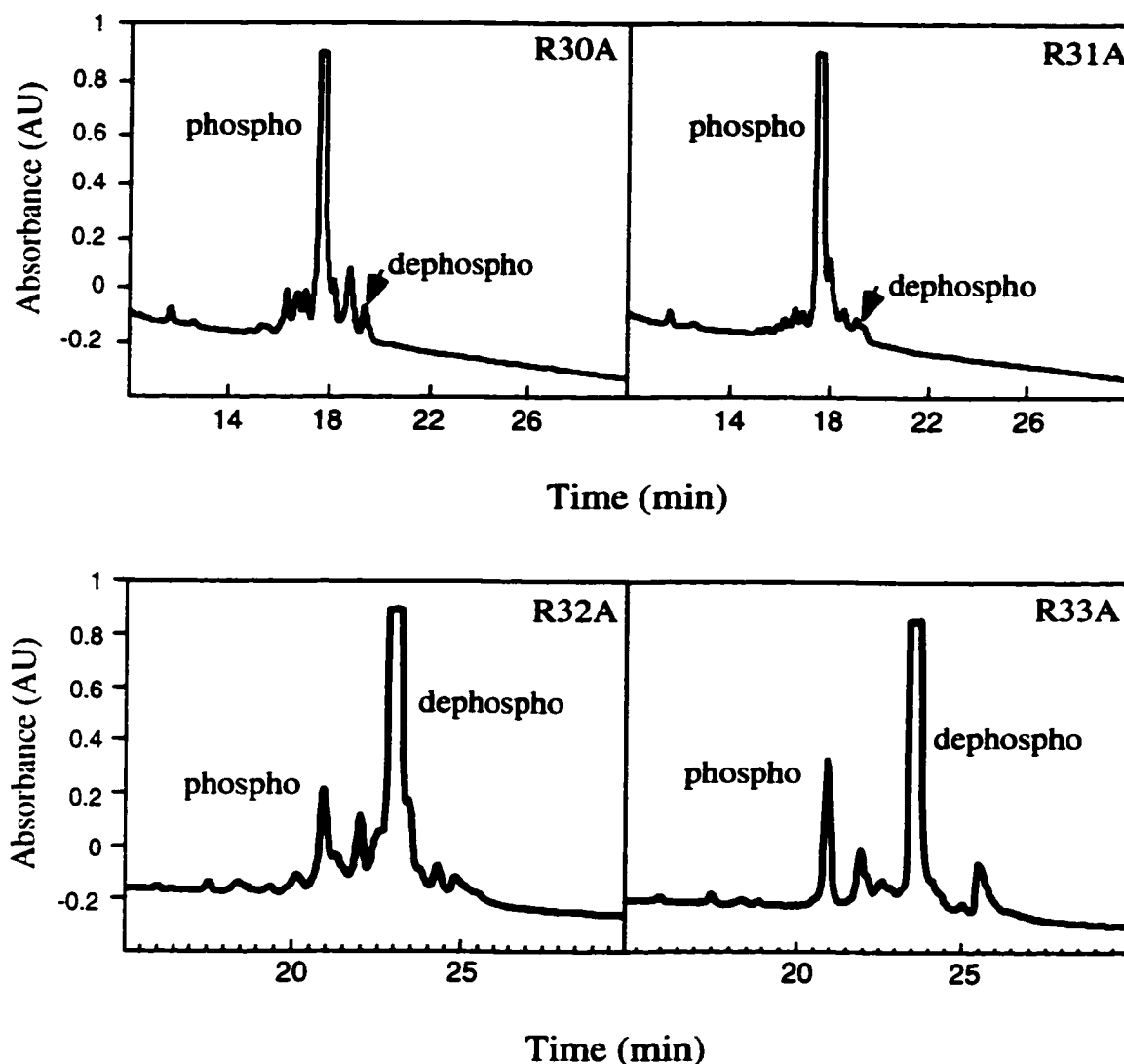
Figure 6-1. *Phosphorylation and purification of inhibitor-1 peptides.* Wild-type and I-1 [9-41] Arg to Ala substituted peptides were phosphorylated by cAMP-dependent protein kinase (250 U, bovine heart catalytic subunit). Peptides I-1[9-41] R32A and R33A were subjected to a second round of phosphorylation to increase the yield of phosphorylated product. Phospho-peptides were purified by reversed phase HPLC in 10 mM ammonium acetate (pH 6.5) with an acetonitrile gradient. R32A and R33A peptides were purified with a shallower gradient (% acetonitrile increases more slowly) to fully separate phospho-peptide from kinase reaction components and non-phosphorylated peptide (see also Experimental Procedures).

resonance assignments of phospho and dephospho-inhibitor-1$_{[1-54]}$ peptides were made using standard sequential assignment methods with double quantum filtered COSY, TOCSY, and NOESY two dimensional ^{1}H NMR spectra. ^{1}H-^{1}H internuclear distance restraints were obtained from 2-D ^{1}H NOESY with a mixing time of 100ms to minimize spin diffusion. Assignments were made at 25°C and 5°C.

Protein phosphatase inhibition assays

Protein phosphatase-1 inhibition was assayed using 10 mM [^{32}P]phosphorylase a substrate phosphorylated by phosphorylase kinase, as previously described in Chapter Two. Control phosphatase activity was standardized to 15% release of total phosphate from the substrate. Assays with native PP1 were performed in the absence of Mn^{2+}, contrary to the manufacturer's instructions (see Appendix II). It has been suggested that the storage and use of native enzyme in Mn^{2+}-containing buffers may promote PP1 conversion to the Mn^{2+} dependent enzyme, which is compromised in its regulation by I-1 (15,22). Inclusion of 0.1 mM MnCl$_2$ in phosphatase assays with native PP1 increased its phosphorylase phosphatase activity 10-fold, with a corresponding reduction in sensitivity of 20-30 fold to inhibitor-1 peptides.

PKA phosphorylation reactions

Wild-type and I-1$_{[9-41]}$ Arg to Ala substituted peptides were phosphorylated by recombinant murine PKA (α isoform, NEB) in time-course experiments. 200 μL reactions

contained 50 mM Tris-HCl (pH 7.5), 10 mM $MgCl_2$, 0.5 mg/mL BSA, 200 µM ATP, 1.5

µL of γ-labelled [^{32}P]ATP (3000 Ci/mmol, Amersham), and 40 µM peptide. Wild-type,

Arg31Ala, and Arg32Ala peptide reactions were performed with 0.5 U PKA (Figure 6-2,

panel a) while Arg33Ala and Arg34Ala reactions each required 25 U of enzyme (Figure 6-

2, panel b). Reactions were incubated at 30 °C and 15 µL aliquots were removed to 5 µL

of 5% acetic acid on ice at time points indicated. Samples were spotted onto

phosphocellulose disks, allowed to dry, washed three times in 75 mM phosphoric acid,

once in distilled H_2O and once in 80% ethanol. Disks were allowed to dry, placed into 2

mL scintillation fluid, and cpm determined in a Pharmacia Rack β counter. Total cpm was

determined by adding 15 µL of each reaction directly into 2 mL scintillation fluid. Control

reactions without peptide and/or without enzyme were performed. The cpm for each disk

was divided by the total cpm/nmol ATP to obtain the number of moles of ATP

incorporated into each peptide.

Results

Ile-10 substitutions in inhibitor-1

To establish our ability to make functional modifications in synthetic I-1 peptides, we carried out substitutions of Ile-10 in a fragment of I-1 comprising residues 9-41 (Table 6-1). This residue has been shown to be important for inhibition of PP1 by I-1 (23,24), and the related protein DARPP-32 (4,20,25). Ile-10 is the hydrophobic second residue in $^9KIQF^{12}$, the I-1 sequence which may be equivalent to the 'RVXF' motif found in many PP1-binding proteins (Chapter Five) (16,26,27). Replacing Ile-10 with threonine (a weakly polar side chain) or phenylalanine (hydrophobic but bulky aromatic side chain) increased the IC_{50} of the altered peptide 5 and 8-fold, respectively. Substitution of Ile-10 with glycine increased the IC_{50} of $I-1_{[9-41]}$ more than 40 fold, from 21 nM to 892 nM, demonstrating the importance of a larger, more hydrophobic, side chain in the Ile10 position. Replacing Ile-10 with the charged amino acids lysine or glutamic acid resulted in a more dramatic increase, with the IC_{50}'s of these substituted peptides increasing to 1420 and 2820 nM respectively. Clearly the presence of a negative charge in position 10 was the most deleterious of the substitutions, confirming that this residue in I-1 is involved in hydrophobic or non-charged interactions with PP1. Models of I-1 binding to PP1 suggest that Ile-10 in the inhibitor forms favourable van der Waals interactions with Leu-243 and Cys-291 of PP1 (26).

Table 6-1

Inhibition of PP1 with inhibitor-1 peptide variants

Phosphatase inhibition assays were performed as described with native PP1 purified from rabbit skeletal muscle using [^{32}P]-labelled phosphorylase *a* as a substrate.

9-41 Inhibitor-1 Peptide		IC$_{50}$ (nM)
wt :	KIQFTVPLLEPHLDPEAAEQIRRRRPTPATLVL	21
I10T:	KTQFTVPLLEPHLDPEAAEQIRRRRPTPATLVL	113
I10F:	KFQFTVPLLEPHLDPEAAEQIRRRRPTPATLVL	178
I10G:	KGQFTVPLLEPHLDPEAAEQIRRRRPTPATLVL	892
I10K:	KKQFTVPLLEPHLDPEAAEQIRRRRPTPATLVL	1420
I10E:	KEQFTVPLLEPHLDPEAAEQIRRRRPTPATLVL	2820

NMR chemical shift analysis of dephospho and phospho inhibitor-1 peptides

Proton NMR resonance assignments of both dephosphorylated and phosphorylated forms of a peptide composed of residues 1-54 of I-1 have been determined (Table 6-2). The chemical shifts are almost identical in both forms, except for residues 28-38. Phosphorylation of the inhibitor peptide causes only a localized change in the area of the Thr-35 phosphorylation site. This observation agrees with earlier circular dichroism studies (23,28,29) in which no major structural differences were observed between phosphorylated and dephosphorylated peptides; in fact, both were found to be largely disordered in solution. Chemical shift differences were most pronounced for residues Arg-32 and Arg-33. Structural change in this region could be caused by partial neutralization of the positive charge on neighbouring arginine residues by the phosphate group present on phospho-Thr-35. While the biological activity of I-1 clearly requires a phosphate on Thr-

35, the three dimensional structure of the inhibitor is not significantly affected by this

phosphorylation event. In order to examine more closely the role of amino acids preceding

threonine 35, we undertook a systematic mutation of each of Arg-30 to Arg-33.

Table 6-2
Chemical shift changes due to phosphorylation of inhibitor-1 (1-54)
(John Bagu, personal communication)

Values are in ppm, only differences greater than 0.05 ppm are shown. Refer to Experimental
Procedures for sample preparation and assignment information.

Atom		Dephospho Peptide	Phospho Peptide	Difference
Gln 28	HN	8.04	8.15	+0.11
	HA	4.10	4.16	+0.06
Ile 29	HN	7.87	7.96	+0.09
	HA	3.86	3.97	+0.11
Arg 30	HN	8.06	8.17	+0.11
	HA	4.15	4.23	+0.08
	HE	7.55	7.44	-0.11
Arg 31	HN	8.08	8.17	+0.09
	HG 1	1.76	1.69	-0.07
	HE	7.51	7.43	-0.08
Arg 32	HN	7.98	8.18	+0.20
Arg 33	HN	8.31	8.57	+0.26
	HE	7.30	7.40	+0.10
Pro 34	HA	4.50	4.40	-0.10
Thr 35	HN	8.55	9.63	+1.08
	HA	4.57	4.38	-0.19
	HB	4.15	4.31	+0.16
	HG	1.28	1.35	+0.07
Pro 36	HD 1	3.90	4.05	+0.15
Ala 37	HN	8.58	8.64	+0.06

Abbreviations used are: HN, amide hydrogens; HA, backbone alpha-carbon hydrogens; HE/HG/HB/HD refer to side chain hydrogens.

PKA Phosphorylation of inhibitor-1 arginine substituted peptides

Protein kinase phosphorylation site recognition is thought to be governed by a common local motif shared by all proteins targeted by a given kinase (reviewed in 30). The consensus sequence for phosphorylation of a protein substrate by PKA is 'RRXS' (31), where X is any residue. PKA is a member of a family of kinases that utilize basic residues as a specificity determinant (30). I-1 is an unusual PKA substrate, because threonine is a relatively poor phosphate acceptor compared with serine. Additionally, Pro-36, the residue immediately C-terminal to the phospho-acceptor residue Thr-35, has a negative effect on PKA phosphorylation in this position (32).

In order to investigate the inhibitory properties of I-1, it was necessary to phosphorylate Thr-35 of each I-1[9-41] Arg to Ala variant peptide with PKA (see Table 6-3 for peptide sequences). Substitution of alanine for arginine in the first two positions (residues 30 and 31) had only a slightly negative effect on the rate of phosphorylation when compared with wild-type I-1 peptide (Figure 6-2, panel a). This is in agreement with previous studies which found that the presence of the first two of four sequential arginine residues in I-1 and DARPP-32 had a slightly positive effect on phosphorylation efficiency by PKA (4,32). As expected, disruption of the standard PKA consensus sequence RRXS with the Arg-32 or Arg-33 substitution greatly reduced the efficiency of phosphorylation by the kinase (Figure 6-2, panel b). The remaining three arginine residues were not able to compensate for the loss of either arginine. I-1[9-41] Arg32Ala was the poorest substrate of all of the peptides tested.
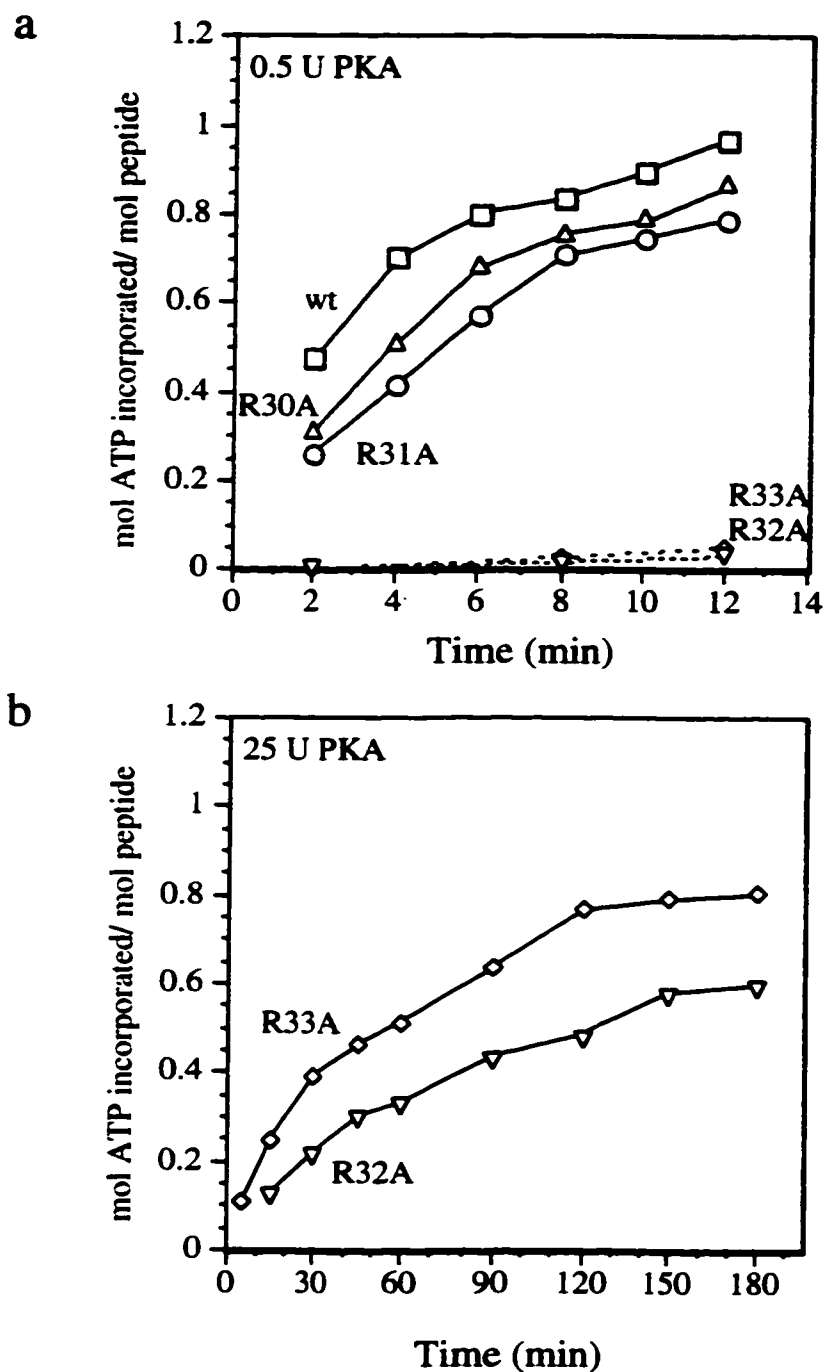
Figure 6-2. *PKA phosphorylation of inhibitor-1 arginine-substituted peptides.* Panel a depicts phosphorylation of wild-type(□), R30A(△), R31A(○), R32A(◊), and R33A(▽) inhibitor-1[9–41] peptides by cAMP-dependent protein kinase (PKA) (see Table 4-3 for peptide sequences). Samples were removed from the reaction mixtures at the time points indicated. Panel b depicts phosphorylation of R32A(▽) and R33A(◊) inhibitor-1 peptides with an increased amount of PKA. Reactions in (a) were performed with 0.5 U PKA while reactions shown in (b) each required 25 U of enzyme.

Inhibition of native PP1 with inhibitor-1 peptides

Models of I-1 bound to PP1 have led to the proposal that the four arginines preceding phosphothreonine-35 play an important part in PP1 binding by interacting with negatively-charged residues in the acidic groove of the enzyme (16-19). However, it has subsequently been determined that the elimination of many of these acidic residues in PP1 (through mutagenesis) had no substantial effect on the sensitivity of PP1 to I-1 (17).

In this study, we investigated the interaction between PP1 and the unusual series of sequential arginine residues in I-1 by making mutations in the inhibitor rather than the phosphatase (Table 6-3). Each of the four substitutions increased the IC_{50} of the I-1 peptide (R30A, 70 nM; R31A, 45 nM; R32A, 1720 nM; R33A, 155 nM) when compared to the wild-type peptide fragment (21 nM). Mutation of Arg-32 to alanine reduced inhibition by greater than 80 fold, clearly demonstrating that the third arginine in the sequence is extremely important for inhibition of PP1 activity by I-1. The increase in IC_{50} that results from substitution of alanine for Arg-32 is of the same order as that found for deletion or mutation of Ile-10 (Table 6-1), a residue widely regarded as essential for I-1 (and DARPP-32) activity (4,20,23-25).

Table 6-3

Inhibition of PP1 by inhibitor-1 arginine-substituted peptides

Phosphatase inhibition assays were performed as described with native PP1 (Upstate) using [^{32}P]-labelled phosphorylase *a* as a substrate.

9-41 Inhibitor-1 Peptide		IC$_{50}$ (nM)
wt :	KIQFTVPLLEPHLDPEAAEQIRRRRPTPATLVL	21
R30A:	KIQFTVPLLEPHLDPEAAEQIARRRPTPATLVL	70
R31A:	KIQFTVPLLEPHLDPEAAEQIRARRPTPATLVL	45
R32A:	KIQFTVPLLEPHLDPEAAEQIRRARPTPATLVL	1720
R33A:	KIQFTVPLLEPHLDPEAAEQIRRRAPTPATLVL	155

Discussion

Previous modelling studies (19) have suggested that basic residues 29-32 in DARPP-32 interact with acidic amino acids present in a surface groove of PP1 (Figure 1-6). These four arginines are analogous to residues 30-33 in inhibitor-1. This model was not supported by a recent publication which found that Arg-29 and Arg-30 do not make major contributions to the interaction between DARPP-32 and PP1 (20). Furthermore, mutation of several acidic amino acids in PP1, either singly or in combination, did not reduce the inhibitory potency of phospho-DARPP-32 (33). Unfortunately, mutation of Arg-31 and Arg-32 in DARPP-32 was omitted from these studies. By extrapolation of our results with Arg-32 in I-1, we hypothesize that the corresponding residue in DARPP-32, Arg-31, is critical for PP1 inhibition.

It is important to make the distinction between inhibition of PP1 activity and actual binding to the phosphatase. NMR solution structure experiments presented in this study suggest that phosphorylation of I-1 causes a small conformational change in the structure in the immediate vicinity of Thr-35. Interaction of Arg-32 with the negatively charged phospho-Thr-35 residue may result in a local structural or electrostatic environment which is critical for inhibition of PP1. It may be that arginines 30-33 do not interact closely with acidic surface residues in PP1 during inhibition of the enzyme, a notion supported by the results of the recent PP1 mutagenesis experiments discussed above.

Further information about I-1 binding to PP1 comes from work currently underway in our laboratory. The gamma isoform of recombinant PP1, tagged with 6 histidine residues, can be immobilized on Ni-NTA silica and used as a matrix to bind the 33 residue fragment of inhibitor-1 (I-1$_{[9-41]}$) (Appendix II). Under identical conditions, similar amounts of dephospho-wild-type peptide, phospho-wild-type peptide, and dephospho-Arg32Ala substituted peptide bound to PP1 (M. Craig, personal communication). While Arg-32 is clearly important for the inhibitory activity of I-1, its contribution to binding is unclear. Additionally, residues in I-1 other than phospho-Thr-35 (for example, ^{9}KIQF^{12}) must play a significant role in binding to the phosphatase. NMR or crystallographic investigations of I-1 bound to PP1 will be necessary to further define the interactions between these two proteins.

Sequence alignment of PP1 substrates

The alignment of PP1 substrates shown in Table 6-4 highlights the presence of basic

amino acids found in each sequence preceding the phosphorylated residue. A basic amino

acid (corresponding to Arg-32 in I-1), is found three residues upstream of the

phosphorylation site in many *in vivo* PP1 substrates. This is not unexpected, because

PKA has an arginine requirement in this position in its RRXS recognition sequence (30).

Table 6-4

Sequence alignment of PP1 substrates highlighting conserved basic residues

Sequences used are of human origin unless otherwise noted. Phosphorylation sites are listed in parentheses and indicated (↓) for each substrate. Key basic residues are shown in bold.

Substrate	Sequence	Kinase	Source
Phos kinase β (Ser-26)	↓ TKRSGSVYE	PKA	liver (35)
Glycogen Phosphorylase (Ser-15)	KRRQISIRG	PhK	liver (36)
Myosin Regulatory Light Chain (Ser-19)	PQRATSNVF	MLCK	rat sm. muscle (37)
CREB (Ser-133)	LSRRPSYRK	PKA	placenta (38)
Phospholamban (Ser-16)	AIRRASTIE	PKA	cardiac (39)
Glycogen synthase site 1a (Ser-698)	WPRRASCTS	PKA	muscle (40)
Glycogen synthase site 1b (Ser-710)	GSKRNSVDT	PKA	"
Glycogen synthase site 2 (Ser-8)	LNRTLSMSL ↓	PhK,PKA	"
Glycogen synthase site 3a (Ser-641) and (Ser-653)	YPRPASVPPSPSLSRHSS	GSK-3	"

Abbreviations used are: Phos kinaseβ, phosphorylase kinase (β-subunit); PhK, phosphorylase kinase; MCLK, myosin light chain kinase; sm. muscle, smooth muscle; CREB, cAMP-response element binding protein; GSK-3, glycogen synthase kinase-3.

Huang et al. (20) recently proposed that the region of I-1 and DARPP-32 surrounding Thr-35 binds near the active site of PP1. In this model Thr-35 binds in such a way that it is not dephosphorylated but instead blocks access of the catalytic site in PP1 to phosphoprotein substrates. The work carried out in our study is consistent with this idea. Indeed, if this model for I-1 binding is correct, our prediction is that a positively charged residue three residues upstream of the phosphorylation site may similarly play a role in substrate binding to PP1.

The status of I-1 as a phosphoprotein inhibitor, rather than a substrate for PP1, leads to many interesting questions related to PP1 binding. A truncated 'core' recombinant PP1 enzyme was found to recognize I-1 as a substrate, retaining interactions with I-1 at or near the phospho-threonine residue, even though loss of the $\beta12$-$\beta13$ loop (Figure 1-4) in this truncated PP1 renders it insensitive to inhibition by I-1 (17). Modelling studies with DARPP-32 have shown that the phospho-threonine residue could be accommodated in or near the active site of the enzyme in several different conformations (33). PP1 does not appear to have a preference for phospho-serine or phospho-threonine substrates in synthetic phosphopeptides (4,34). It is possible that I-1 possesses a threonine instead of a serine in the phospho-acceptor position because threonine is less easily dephosphorylated by PP1 in intact proteins (see Table 6-4). This would be a desirable trait for an inhibitor which binds with an orientation similar to that of a substrate.

The results presented in this chapter have opened up several future research projects. We are interested in synthesizing alanine-substituted peptides derived from the PP1 substrates listed in Table 6-4 in order to determine whether basic residues associated with the phospho-acceptor site are important for dephosphorylation by PP1.

Interestingly, PP1 itself may shed some light on this situation. PP1 is directly regulated by phosphorylation. Cell cycle-dependent kinase CDK-2 phosphorylates a C-terminal threonine residue in PP1 (Thr-320) (see Figure 1-1 for sequence). This results in inhibition of the phosphatase, possibly due to interaction of the region surrounding Thr-320 with the active site of PP1, in a manner analogous to inhibitor-1 (41). PP1 is thought to slowly auto-dephosphorylate Thr-320, allowing the phosphatase to become active again. We plan to synthesize a peptide based on the Thr-320 region to determine whether mutation of the basic arginine residue (Arg-317) which precedes Thr-320 will prevent either inhibition of PP1 by this region or the slow dephosphorylation of Thr-320 by PP1. In conjunction with these experiments, we will create an Arg-317 mutant of full-length PP1 to further investigate the inhibitory properties of the phospho-Thr-320 region.

As mentioned in Chapter Five, we are collaborating with Dr. M. James (University of Alberta) to co-crystallize I-1[9-54] with recombinant protein phosphatase-1γ. If the line of experimentation outlined above is successful, we will also attempt to crystallize the CDK-2 phosphorylated form of PP1, in order to determine the exact nature of the auto-inhibition.

References

1. Huang, F. L., and Glinsmann, W. H. (1976) *Eur. J. Biochem.* **70**, 419-426

2. Cohen, P. (1978) *Curr. Top. Cell. Reg.* **14**, 117-196

3. Nimmo, G. A., and Cohen, P. (1978) *Eur. J. Biochem.* **87**, 341-351

4. Hemmings, H. C., Jr., Nairn, A. C., Elliott, J. I., and Greengard, P. (1990) *J. Biol. Chem.* **265**, 20369-76

5. Park, I. K., and DePaoli-Roach, A. A. (1994) *J. Biol. Chem.* **269**, 28919-28

6. Beullens, M., Stalmans, W., and Bollen, M. (1996) *Eur. J. Biochem.* **239**, 183-189

7. Eto, M., Ohmori, T., Suzuki, M., Furuya, K., and Morita, F. (1995) *J. Biochem.* **118**, 1104-107

8. Van Eynde, A., Wera, S., Beullens, M., Torrekens, S., Van Leuven, F., Stalmans, W., and Bollen, M. (1995) *J. Biol. Chem.* **270**, 28068-74

9. Oliver, C. J., and Shenolikar, S. (1998) *Front. Biosci.* **3**, d961-972

10. Cohen, P., and Cohen, P. T. W. (1989) *J. Biol. Chem.* **36**, 21435-38

11. Aitken, A., Bilham, T., and Cohen, P. (1982) *Eur. J. Biochem.* **126**, 235-246

12. Cohen, P. (1989) *Annu. Rev. Biochem.* **58**, 453-508

13. Hubbard, M. J., and Cohen, P. (1989) *Eur. J. Biochem.* **186**, 711-720

14. Shenolikar, S., and Nairn, A. C. (1991) *Adv. Second Messenger Phosphoprotein Res.* **23**, 1-21

15. Endo, S., Connor, J. H., Forney, B., Zhang, L., Ingebritsen, T. S., Lee, E. Y., and Shenolikar, S. (1997) *Biochemistry* **36**, 6986-92

16. Kwon, Y. G., Huang, H. B., Desdouits, F., Girault, J. A., Greengard, P., and Nairn, A. C. (1997) *Proc. Natl. Acad. Sci. U.S.A.* **94**, 3536-41

17. Connor, J. H., Quan, H. N., Ramaswamy, N. T., Zhang, L., Barik, S., Zheng, J., Cannon, J. F., Lee, E. Y., and Shenolikar, S. (1998) *J. Biol. Chem.* **273**, 27716-24

18. Goldberg, J., Huang, H. B., Kwon, Y. G., Greengard, P., Nairn, A. C., and Kuriyan, J. (1995) *Nature* **376**, 745-753

19. Barford, D., Das, A. K., and Egloff, M.-P. (1998) *Annu. Rev. Biophys. Biomol. Struct.* **27**, 133-164

20. Huang, H.-b., Horiuchi, A., Watanabe, T., Shih, S.-R., Tsay, H.-J., Li, H.-C., Greengard, P., and Nairn, A. C. (1999) *J. Biol. Chem.* **274**, 7870-78

21. Holmes, C. F. (1991) *Toxicon* **29**, 469-477

22. Alessi, D. R., Street, A. J., Cohen, P., and Cohen, P. T. W. (1993) *Eur. J. Biochem.* **213**, 1055-66

23. Endo, S., Zhou, X., Connor, J., Wang, B., and Shenolikar, S. (1996) *Biochemistry* **35**, 5220-28

24. Aitken, A., and Cohen, P. (1982) *FEBS Lett.* **147**, 54-58

25. Desdouits, F., Cheetham, J. J., Huang, H.-B., Kwon, Y.-G., da Cruz e Silva, E. F., Denefle, P., Ehrlich, M. E., Nairn, A. C., Greengard, P., and Girault, J.-A. (1995) *Biochem. Biophys. Res. Commun.* **206**, 653-658

26. Egloff, M. P., Johnson, D. F., Moorhead, G., Cohen, P. T., Cohen, P., and Barford, D. (1997) *EMBO J.* **16**, 1876-87

27. Zhao, S., and Lee, E. Y. (1997) *J. Biol. Chem.* **272**, 28368-72

28. Cohen, P., Nimmo, G. A., Shenolikar, S., and Foulkes, J. G. (1979) *FEBS Symp.* **76**, 161-169

29. Neyroz, P., Desdouits, F., Benfenati, F., Knutson, J. R., Greengard, P., and Girault, J. A. (1993) *J. Biol. Chem.* **268**, 24022-31

30. Pinna, L. A., and Ruzzene, M. (1996) *Biochim. Biophys. Acta* **1314**, 191-225

31. Kemp, B. E., and Pearson, R. B. (1990) *Trends Biochem. Sci.* **15**, 342-346

32. Chessa, G., Borin, G., Marchiori, F., Meggio, F., Brunati, A. M., and Pinna, L. A. (1983) *Eur. J. Biochem.* **135**, 609-614

33. Huang, H. B., Horiuchi, A., Goldberg, J., Greengard, P., and Nairn, A. C. (1997) *Proc. Natl. Acad. Sci. U.S.A.* **94**, 3530-35

34. Agostinis, P., Goris, J., Waelkens, E., Pinna, L. A., Marchiori, F., and Merlevede, W. (1987) *J. Biol. Chem.* **262**, 1060-64

35. Wuellrich-Schmoll, A., and Kilimann, M. F. (1996) *Eur. J. Biochem.* **238**, 374-380

36. Newgard, C. B., Nakano, K., Hwang, P. K., and Fletterick, R. J. (1986) *Proc. Natl. Acad. Sci. U.S.A.* **83**, 8132-36

37. Taubman, M. B., Grant, J. W., and Nadal-Ginard, B. (1987) *J. Cell Biol.* **104**, 1505-13

38. Hoeffler, J. P., Meyer, T. E., Yun, Y., Jameson, J. L., and Habener, J. F. (1988) *Science* **242**, 1430-33

39. Fujii, J., Zarain-Herzberg, A., Willard, H. F., Tada, M., and Maclennan, D. H. (1991) *J. Biol. Chem.* **266**, 11669-75

40. Browner, M. F., Nakano, K., Bang, A. G., and Fletterick, R. J. (1989) *Proc. Natl. Acad. Sci. U.S.A.* **86**, 1445-47

41. Dohadwala, M., Da Cruz e Silva, E. F., Hall, F. L., Williams, R. T., Carbonara-Hall, D. A., Nairn, A. C., Greengard, P., and Berndt, N. (1994) *Proc. Natl. Acad. Sci. U.S.A.* **91**, 6408-12

Chapter Seven

General Conclusions and Future Experiments

General conclusions

At the beginning of my doctoral research, the serine/threonine protein phosphatase field had just started to explore production of recombinant PP1 isoforms. We didn't know where the catalytic site of the enzyme was or why the recombinant forms required manganese for activity. We could only imagine the mode of interaction between PP1 and its endogenous inhibitors, and the number of natural product toxins that inhibited PP1 was starting to explode. At that time, it was difficult to convince other biochemists that serine/threonine protein phosphatases were not unregulated housekeeping enzymes.

Determination of the x-ray crystallographic structure of PP1 in 1995 by Goldberg et al. opened up exciting new research possibilities. For the first time, we could see the active site, and imagine how substrates might bind to the phosphatase. More importantly, we were now able to design PP1 site-directed mutagenesis experiments guided by the structure. Computer modelling of inhibitors bound to the enzyme was possible because the Goldberg et al. coordinates were made available in the protein structural database. In 1997, publication of the crystal structure of a targeting subunit peptide bound to PP1 (Egloff et al. 1997) gave us new insights into the interactions between regulatory proteins and the enzyme.

A major challenge for the next decade in serine/threonine protein phosphatase research will be to understand how PP1 interacts with its many substrates. We also need to definitively establish how the endogenous inhibitor proteins I-1 and I-2 bind to the enzyme. Discovery of a common PP1 binding motif sequence has identified hundreds of proteins that may be capable of interacting with the phosphatase, providing many

avenues of future study. The serine/threonine phosphatase field needs to build upon *in vitro* research by investigating the regulation of PP1 activity *in vivo*.

Future Work

This section contains a brief summary of the essential findings of my thesis work and a discussion of areas of future study that have evolved from this research.

Exogenous Natural Product Inhibitors of PP1

Chapter Two: Microcystins

Using reversed phase HPLC guided by a PP1 inhibition assay, we were able to isolate seven novel hydrophobic microcystins. The hydrophobic nature of microcystin-LL was essential to the identification and purification of a covalent complex of PP1 bound to the toxin. This work provided a foundation for important future studies in which we will attempt to investigate the fate of the covalent complex *in vivo*, and to determine whether the complex itself is toxic when consumed by organisms in the food chain. At the time of the experiments presented in Chapter Two, we were unable to produce sufficient quantities of recombinant PP1 to perform *in vivo* work with the covalent complex. Cloning and expression of the gamma isoform of the enzyme now allows us to obtain enough enzyme to proceed with experiments in salmon with microcystin-LL and PP1γ.

Development of a technique coupling capillary electrophoresis to reversed phase HPLC significantly increased the specificity of microcystin analysis. As contaminated drinking water and blue-green algae health food products come increasingly to the

attention of the public, we need assays that are capable of unambiguously identifying small amounts of toxic microcystins.

Chapter Three: Calyculins

The models of calyculin binding to PP1 presented in this work were based on experimental data. While this is an improvement upon models of calyculin binding which are based on models of inhibitor-1 binding to PP1, we need to directly determine the nature of the interactions between each of these inhibitors and PP1. In order to move beyond computer models, we are currently collaborating with Dr. Francis Schmitz (University of Oklahoma) and Dr. Michael James (University of Alberta) to produce x-ray structures of clavosine A and B bound to the phosphatase.

We would like to know if the rhamnose group found in clavosine A and B can bind rhamnose-specific lectins, and if so, if this is a viable method of immobilizing the clavosines on an affinity column. Intracellular targets of the toxin might then be isolated from cell extracts by binding to immobilized clavosine. A clavosine affinity column could also be used to immobilize PP1. A similar technique using the affinity of microcystin for PP1 is well-established (Moorhead et al., 1994, *FEBS Lett.* **356**, 46-50). Immobilization of PP1 via a histidine tag (see Appendix III) or a clavosine affinity column would allow us to search for additional PP1 binding proteins in cell extracts.

Endogenous inhibitor proteins

Chapter Four: Inhibitor-2

In collaboration with Dr. M. James, we are attempting to co-crystallize PP1 with the 69 residue fragment of I-2 found to be a micromolar inhibitor of PP1 in Chapter Four. We would like to learn more about the interactions between inhibitor-2 and PP1 because our long-term goal is to produce native-like recombinant PP1 enzyme by incubation with I-2 followed by GSK-3 phosphorylation (Chapter Four). This procedure will be facilitated by expression of full-length I-2 protein, therefore work is currently underway in our laboratory to clone inhibitor-2 from a cDNA library. Obtaining I-2 cDNA will allow us to construct and express truncations and mutations of the I-2 sequence, in order to further study I-2 inhibition and regulation of PP1. It would be interesting to determine the structure of PP1 after reactivation, in view of the behavioural differences between native and recombinant enzyme.

Chapter Five: Inhibitor-1 binding motif

We attempted to assess the I-1 PP1 binding motif using a library of synthetic peptides in competition assays with an active inhibitor-1 fragment. The results of these experiments indicated that a direct binding assay was needed. A binding assay rather than an activity-based assay would avoid problems such as activation of the enzyme by the binding motif analogues and impurities in the peptide preparations. Histidine-tagged PP1 (PP1$_{HIS}$) is suitable for this work, as it can be immobilized on nickel-chelating resin (see Appendix III

for construction of histidine-tagged PP1). Experiments are currently underway in our laboratory with the library of binding motif peptides and PP1$_{HIS}$.

Chapter Six: Inhibition of PP1 by Inhibitor-1

The discovery that arginine 32 of inhibitor-1 is crucial for inhibition of PP1 has raised the question of binding determinants in PP1 substrates and endogenous inhibitors. It is generally accepted in the protein phosphatase-1 field that inhibitor-1 binds to PP1 in a manner similar to that of a substrate protein. The proline residues which flank Thr-35 in inhibitor-1 (Figure 1-5) are thought to interfere with I-1 dephosphorylation by PP1. Our laboratory plans to investigate the requirements for a basic residue preceding the phosphorylated residue in a variety of PP1 substrates (Table 6-2). Synthetic peptides containing alanine substitutions for the basic residues in these PP1 substrates will allow us to determine whether this position is critical for PP1 dephosphorylation. Consensus sequences have been determined for many protein kinases, but little is known about recognition sequences in protein phosphatase substrates.

As discussed in Chapter Six, we are specifically interested in the auto-inhibitory C-terminal region of PP1 surrounding Thr-320 (Figure 1-1). Phosphorylation of PP1 at this site by CDK2 results in inhibition of phosphatase activity, possibly due to interaction of Thr-320 with the catalytic site of PP1 (see Chapter Six, Discussion). We plan to make peptides based on the Thr-320 region to determine whether mutation of the basic arginine residue (Arg-317) which precedes Thr-320 will prevent either inhibition of PP1 upon CDK2 phosphorylation or the subsequent slow dephosphorylation of Thr-320

by PP1. Similar experiments can also be performed with Arg-317 mutations in the full-length phosphatase. This research may help us to better understand binding of phosphoprotein inhibitors and substrates to PP1.

Conclusion

Three dimensional structures of protein phosphatase-1 have allowed us to ask many new questions about serine/threonine protein phosphatases. It is my hope that research in this field will continue to be guided by structural work, and that fruitful biochemical experiments will continue to develop from structural determinations. It will be interesting to discover whether my *in vitro* experiments and computer modelling studies are confirmed or discredited by structures published in the future. I remain astonished that such a biochemically diverse array of natural product toxins and endogenous proteins are potent inhibitors of protein phosphatase-1.
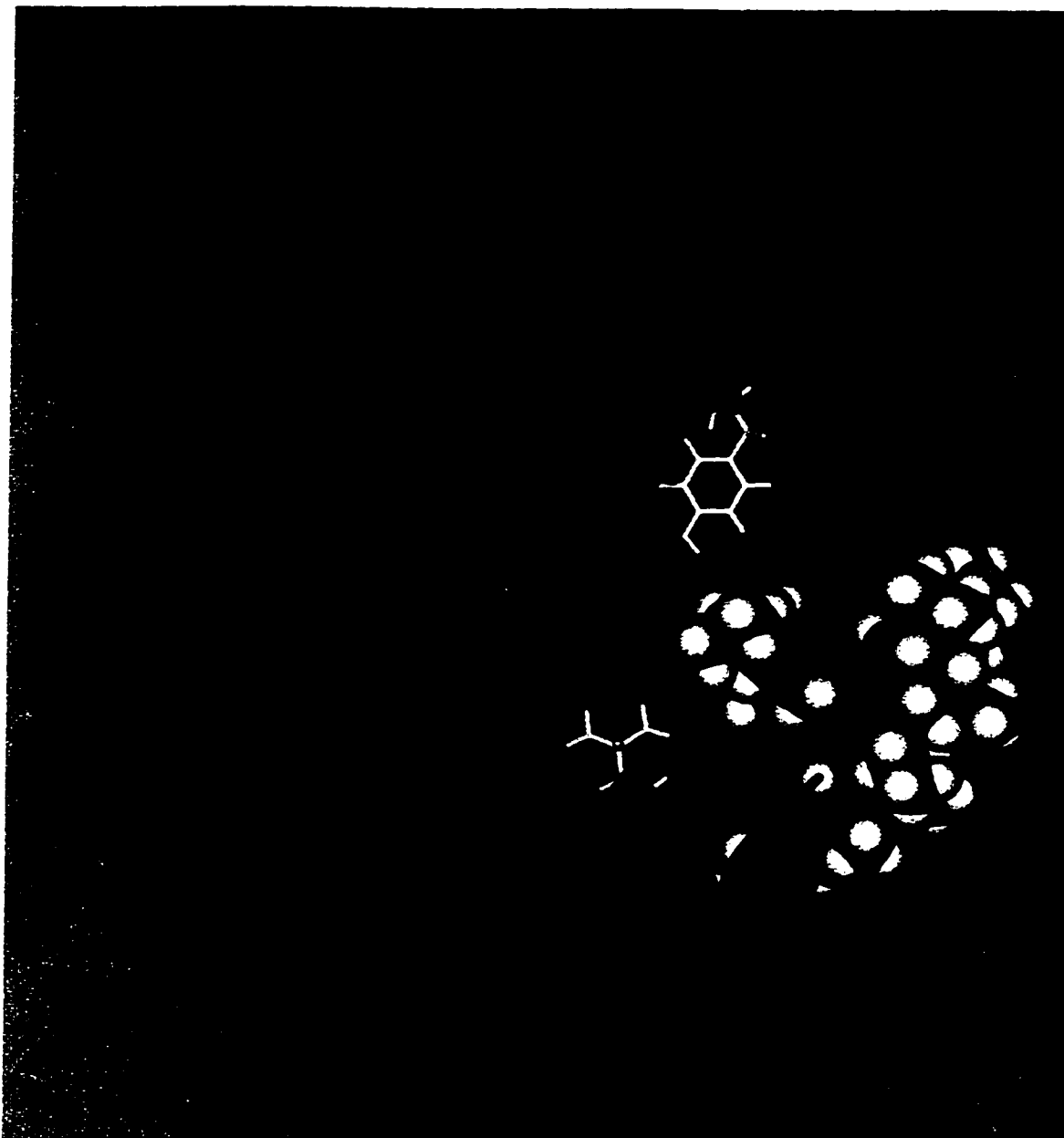
Appendices

Figure A1-1. *Model of dephosphonocalyculin A bound to PP1.* Space-filling molecular model of dephosphonocalyculin A bound to a ribbon model of PP1. Manganese ions (pink balls) and amino acid side chains (blue sticks) in PP1 residing within 4 Å of cla-vosines A,B, and calyculin A in models discussed in Chapter Three are shown. Tyrosine 134 (top) and valine 223 (bottom) - are highlighted in yellow. Atoms in the space-filling inhibitor models are coloured as follows: carbon (green), oxygen (red), nitrogen (blue), phosphorus (pink) and hydrogen (white). The model was generated with docking and energy minimization simulations using the ESFF forcefield and Discover3 module of Insight II, on a Silicon Graphics Indigo2 Impact 10000 workstation (as described in Chapter Three, experimental procedures). Dephosphonocalyculin A was created by removing the C-17 phosphate ester (leaving a hydroxyl) from the crystal structure of calyculin A (natural enantiomer), followed by energy minimization.

Appendix II

Table A2-1
Effects of manganese on the inhibition of PP1 by inhibitor-1 peptides

Native PP1 activity was standardized to 15% release in the presence or absence of 0.1 mM $MnCl_2$ by dilution in assay buffer.

Inhibitor-1 (9-41) Peptide	IC_{50} values (nM)	
	PP1 (1/125 dil.)	PP1 + Mn^{2+} (1/1000 dil.)
wt: KIQFTVPLLEPHLDPEAAEQIRRRRPTPATLVL	21	630
A1: KIQFTVPLLEPHLDPEAAEQIARRRPTPATLVL	70	1785
A2: KIQFTVPLLEPHLDPEAAEQIRARRPTPATLVL	45	970
A3: KIQFTVPLLEPHLDPEAAEQIRRARPTPATLVL	1720	>3300 *
A4: KIQFTVPLLEPHLDPEAAEQIRRRAPTPATLVL	155	2800

*30% inhibition was observed at 3300 nM

Protein phosphatase-1 inhibition was assayed using 10 mM [^{32}P]phosphorylase a substrate, as described in Chapter One, Experiment Procedures. Control phosphatase activity was standardized to 15% release of total phosphate from the substrate. Assays with native PP1 (1/125 dilution) were performed in the absence of Mn^{2+} (see Results, Chapter Six) It has been suggested that the storage and use of native enzyme in Mn^{2+}-containing buffers may promote PP1 conversion to the Mn^{2+} dependent enzyme, which is compromised in its regulation by I-1 (1,2), similar to recombinant forms of the enzyme. Inclusion of 0.1 mM $MnCl_2$ in phosphatase assays with native PP1 (as recommended by the manufacturers, Upstate Biotechnology) increased its phosphorylase phosphatase activity ~10-fold (to 1/1000 dilution), with a corresponding reduction in sensitivity of 20-30 fold to inhibitor-1 peptides.

Unlike PP1 purified from mammalian tissues, recombinant PP1 catalytic subunits are inactive in the absence of divalent cations (3). Following activation by Mn^{2+}, recombinant PP1 enzymes show higher activity toward some substrates (including p-nitrophenylphosphate and histone H1) than native PP1 (2,4). Native PP1 is inhibited by Mn^{2+} concentrations above 0.1 mM, and after extended incubation with Mn^{2+} native enzyme becomes capable of dephosphorylating non-physiological substrates (5). During prolonged storage at -20°C (and/or treatment with nonspecific phosphatase inhibitors ATP or NaF) native PP1 is converted into a manganese-dependent enzyme with altered substrate specificities and inhibitor sensitivities (6-8). This may be due to loss of metals from the active site or changes in the metal chelating properties of the active site. Native and recombinant PP1 show similar sensitivity to microcystin-LR, calyculin A, and I-2 (Table A1-1). In contrast, recombinant PP1 is 100-600 fold less sensitive to inhibition by I-1 (2). Conversion of native PP1 to a manganese-dependent enzyme is also accompanied by a 500-fold reduction in its sensitivity to I-I (1,2). The molecular basis for this phenomenon is unknown.

It is unclear why the manufacturers of native PP1 at Upstate Biotechnology would include 0.1 mM $MnCl_2$ in native PP1 enzyme storage solutions and recommend its use in phosphatase activity assays. Long-term storage of native or recombinant PP1 at -20°C results in gradual loss of phosphatase activity and sensitivity to inhibitor-1, possibly due to loss of manganese ions from the active site of the enzyme. Mn^{2+} would presumably increase the shelf-life of commercial enzyme by stimulating older enzyme.
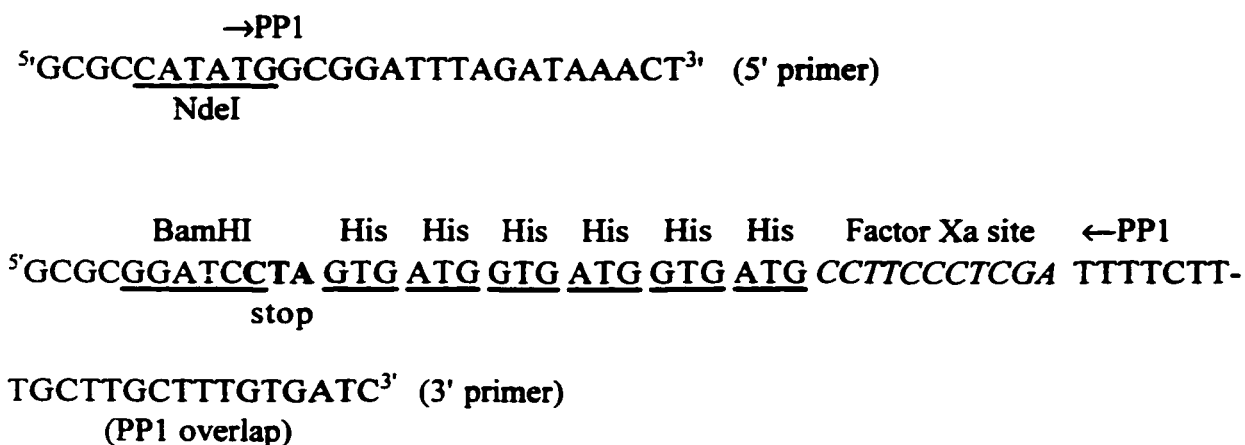
However, activation of older enzyme present in the commercial preparation also results in a loss of sensitivity to inhibitor-1 when a mixture of 'old' and 'native' enzymes is used in phosphatase inhibition assays. In addition, the inclusion of Mn^{2+} in enzyme storage buffer, like other nonspecific PP1 inhibitors, may actually promote conversion from native to Mn^{2+}-dependent phosphatase over time (1).

In summary, it appears that the ideal solution to PP1 manganese-dependency and insensitivity to I-1 is to use only freshly purified native enzyme for experiments involving inhibitor-1 and PP1. This is not practical in all circumstances, as the native enzyme purification procedure requires animal sacrifice, an arduous series of chromatography columns and a small yield of phosphatase enzyme which consists of a mixture of PP1 isoforms. Experiments with mutant PP1 enzymes would not be possible in this scenario. Another solution could be the 'renaturation' of recombinant PP1 by incubation with inhibitor-2 protein followed by phosphorylation (of I-2) by Glycogen Synthase Kinase-3. This procedure has been previously demonstrated to revert recombinant PP1 to a more native state with respect to manganese dependency, substrate specificity, and sensitivity to inhibitor-1 (2,8). Current work in our laboratory to address this situation is discussed in Chapter Four.

Generation of His₆ tag

The cDNA encoding PP1γ cloned from a human teratocarcinoma NT2 cDNA library (see

Chapter Three, Experimental Procedures) was modified to contain a C-terminal

hexahistidine tag for metal-chelating affinity purification (PP1ₕᵢₛ). The six histidine

residues (and intervening Factor Xa protease cleavage site) were added to the 3' end of the

PP1γ cDNA sequence in a PCR reaction using native *Pfu* DNA polymerase (Stratagene)

and the primers:

```
                    →PP1
⁵'GCGCCATATGGCGGATTTAGATAAACT³'   (5' primer)
        NdeI
```

```
        BamHI       His  His  His  His  His  His    Factor Xa site   ←PP1
⁵'GCGCGGATCCTA GTG ATG GTG ATG GTG ATG CCTTCCCTCGA TTTTCTT-
            stop
```

```
TGCTTGCTTTGTGATC³'   (3' primer)
    (PP1 overlap)
```

The 3' primer encodes six histidine codons, a Factor Xa protease site and a 3' overhang of

the PP1γ sequence. PCR products were cloned into pBluescriptSK using the NdeI and

BamHI restriction enzyme sites encoded in the PCR primers. Complete DNA sequencing

of the PP1ₕᵢₛ construct was performed to ensure sequence fidelity. A NdeI-XbaI

fragment containing the PP1ₕᵢₛ sequence was cloned into protein expression vector pCW,

17 bases downstream of the promoter. The construct was transformed into *E. coli* strain

DH5α using a modified Hanahan procedure as described (3).

Generation of nickel column

A 5 mL HiTrap Chelating affinity column (Pharmacia), containing the metal chelating

group iminodiacetic acid (IDA), was charged with 25 mL of 0.1 M $NiCl_2$ using a

Pharmacia FPLC system (1 mL/min). The column was washed with 25 mL deionized

H_2O (2 mL/min) to remove excess $NiCl_2$. It was necessary to saturate the nickel column

with 500 mM imidazole prior to the PP1$_{HIS}$ purification procedure in order to allow

accurate imidazole concentrations during wash and elution steps (without this, the

unoccupied Ni^{2+} sites in the column act as an imidazole 'sink'). This step also prevents

the formation of insoluble β-mercaptoethanol/nickel ion complexes when running buffer is

first applied to the column (β-mercaptoethanol cannot displace imidazole). The column

was equilibrated with 25 mL of running buffer (50 mM Hepes pH 7.5, 100 mM KCl, 10

mM β-mercaptoethanol, 2 mM $MnCl_2$, 1 mM imidazole) before use. 25 mL of 50 mM

EDTA was used to strip and clean the affinity column of nickel ions and any remaining

associated protein after the purification procedure was completed.

PP1$_{HIS}$ purification

DH5α *E. coli* cells containing PP1$_{HIS}$ in vector pCW were grown and harvested as

outlined in Experimental Procedures, Chapter Two. Cell pellets were resuspended (0.2

g/mL) in ice-cold extraction buffer (50 mM Hepes pH 7.5, 100 mM KCl, 10 mM β-

mercaptoethanol, 2 mM MnCl₂, 1mM imidazole) and disrupted with passage through a French Press. The resulting extracts were centrifuged at 16 000 g for 30 min at 4°C. The supernatant was loaded on the affinity column at 0.2 mL/min and the column run-through recycled back through the column approximately 4 times. Running buffer was used to wash the nickel column (1 mL/min) until the absorbance (280 nm) returned to baseline levels. A step gradient program was used to wash the column with 15 mL of 50 mM imidazole in running buffer followed by 15 mL of 100 mM imidazole. This washing procedure removed non-specifically bound proteins and those containing 1-2 adjacent transition metal-binding amino acids (histidine, tryptophan, cysteine). PP1$_{HIS}$ was eluted with 400 mM imidazole in running buffer at a flow rate of 2 mL/min with 1 mL fractions. All wash steps and eluent fractions were tested for PP1 activity using phosphorylase a as a substrate (Chapter Two, Experimental Procedures). Active fractions were pooled and dialyzed in buffer containing 50 mM Tris-HCl, pH 7.5, 0.1 mM EDTA, 1.0 MnCl₂, 0.1% β-mercaptoethanol and 50% (v/v) glycerol for storage at -20°C. The high level of expression of the PP1γ isoform in DH5α cells combined with the selective affinity purification step resulted in very few contaminating proteins in the PP1$_{HIS}$ preparation after HiTrap metal chelating chromatography. If the phosphatase preparation needed to be extremely pure (>85%), the nickel column was either preceded by a heparin HiTrap affinity column or followed by a Superdex 75 gel filtration column (see Chapter Two, Experimental Procedures).

Spin-column experiments

As mentioned in Chapter Six, further information about I-1 binding to PP1 comes from PP1$_{HIS}$ work currently underway in our laboratory. The gamma isoform of recombinant PP1, tagged with 6 histidine residues, can be immobilized on Ni-NTA silica and used as a matrix to bind a 33 residue fragment of inhibitor-1 (I-1$_{[9-41]}$). Under identical conditions, similar amounts of dephosphorylated wild type I-1$_{[9-41]}$ peptide, phosphorylated wild type I-1$_{[9-41]}$ peptide, and dephosphorylated Arg32Ala I-1$_{[9-41]}$ peptide bound to PP1 (Marcia Craig, personal communication). This information is extremely interesting because both the Arg32Ala inhibitor-1 peptide is a poor inhibitor of PP1 (Chapter Six). The fact that these three peptides bind equally well to PP1 reinforces the distinction between binding and inhibition, and suggests that phospho-Thr-35 and surrounding residues are not critical for I-1 binding to PP1.

Spin-column procedures

PP1$_{HIS}$, in a total volume of 200 µl buffer A (10 mM imidazole, 50 mM HEPES, pH 7.5, 0.1 mM MnCl$_2$, 0.1% β-mercaptoethanol), was injected on a column of Ni-NTA silica (Qiagen) equilibrated in buffer A. The column was centrifuged at 2000 rpm until the applied volume eluted. Eluent was chromatographed by reversed phase HPLC with detection at 206 nm. The quantity of protein applied to the column (4.2 nmol) was slightly more than sufficient to saturate all active chelated-nickel sites, as specified by the manufacturer. Column saturation was further verified by the appearance of a small peak of PP1$_{HIS}$ in the chromatogram of the load eluent. To remove excess protein, the column

was washed with buffer A and fractions were examined by HPLC until no PP1$_{HIS}$ appeared in the chromatographs of the eluents. 4.2 nmol inhibitor-1$_{[9-41]}$ (wild type or Arg32Ala mutant) was applied and the column was centrifuged at low speed (500 rpm) to allow the peptide to move slowly through the PP1-bound matrix. An incubation time of 10 minutes is necessary for maximum inhibition of PP1 by phosphorylated I-1 peptides (C.F.B. Holmes, unpublished). Peptide eluent was reloaded and centrifuged slowly again; the total time for peptide to pass through the column was not less than 15 minutes. The column was washed with buffer at pH 7.5 until all of the excess inhibitor-1$_{[9-41]}$ had eluted, as determined by HPLC. Protein and peptide were eluted with buffer A adjusted to pH 2. Similar amounts (~1 nmol) of inhibitor-1$_{[9-41]}$ (wild type) and inhibitor-1$_{[9-41]}$ (Arg32Ala) peptides eluted when 4 nmol peptide was initially applied to 4 nmol PP1$_{HIS}$ bound on Ni-NTA silica columns (Marcia Craig, personal communication)

References for Appendices I-III

1. Endo, S., Connor, J. H., Forney, B., Zhang, L., Ingebritsen, T. S., Lee, E. Y., and Shenolikar, S. (1997) *Biochemistry* **36**, 6986-92

2. Alessi, D. R., Street, A. J., Cohen, P., and Cohen, P. T. W. (1993) *Eur. J. Biochem.* **213**, 1055-66

3. Zhang, A. J., Bai, G., Deans-Zirattu, S., Browner, M. F., and Lee, E. Y. (1992) *J. Biol. Chem.* **267**, 1484-90

4. Zhao, S., Zhang, Z., and Lee, E. Y. C. (1994) *Biochem. Mol. Biol. Int.* **34**, 1027-33

5. Silberman, S. R., Speth, M., Nemani, R., Ganapathi, M. K., Dombradi, V., Paris, H., and Lee, E. Y. (1984) *J. Biol. Chem.* **259**, 2913-22

6. Burchell, A., and Cohen, P. (1978) *Biochem. Soc. Trans.* **6**, 220-222

7. Egloff, M. P., Cohen, P. T. W., Reinemer, P., and Barford, D. (1995) *J. Mol. Biol.* **254**, 942-959

8. MacKintosh, C., Garton, A. J., McDonnell, A., Barford, D., Cohen, P. T., Tonks, N. K., and Cohen, P. (1996) *FEBS Lett.* **397**, 235-238